

# **Unlocking the DOR to the Surface: Regulated Surface Trafficking of the $\delta$ - Opioid Receptor**

by

Daniel Shiwarski

A thesis submitted in partial fulfillment of the requirements for the degree of  
Doctor of Philosophy in the field of Biological Sciences

Department of Biological Sciences  
Carnegie Mellon University  
Pittsburgh, Pennsylvania

*For my wife, Cary, her unrelenting patience and support, both emotionally and scientifically is unmatched. For my daughter, Piper, her willingness to assist in weekend microscopy experiments and desire to use the computer while I write grants and papers is something I will always cherish. To my friends and family, their unconditional interest and support throughout my career, has pushed me to always be the very best version of myself.*

## **Acknowledgements**

I would like to begin by thanking my thesis advisor, Dr. Manojkumar Puthenveedu. He has been a constant source of guidance, support, and friendship over the past 5 years. Manoj has a remarkable ability to stay positive, believing every experiment will work, even when we are unsure, and it is this optimism that keeps us all moving forward. Additionally, his ability to push me to think critically, and ask the right questions has allowed me to become a better and more efficient scientist. I could not have imaged a better mentor to guide me through this journey.

To my thesis committee members: Drs. Nathan Urban, Adam Linstedt, and Gerry Hammond, who have all helped to guide aspects of my project and career through feedback on manuscripts and during committee meetings. Having a committee with diverse views and expertise across different disciplines has been instrumental in my success during my time at CMU. Apart from my committee, I would like to thank Drs. Peter Friedman and Michael Gold. Their mentorship and willingness to provide scientific support and constructive feedback on grant applications and manuscripts allowed me to become a better writer and understand the importance of interdisciplinary collaboration. Additionally, I thank Dr. Shoba Subramanian for her professional help and career guidance, as well as her constant support for all members of our lab.

I would like to thank all my past and present lab members: Drs. Rachel Vistein, Amanda Soohoo, and Shanna Bowman, as well as Zara Weinberg, Elena Shuveuva, Stephanie Crilly, Maneesha Sakhuja, Isaac Shamie, Preethy Sridharan, Ashita Vadlumudi, Marlana Daar, Andrew Dates, and Tiffany Phan for all of their assistance, support, lively conversation, eclectic music libraries, and creative ideas over the years. I will truly miss our early morning philosophical conversations over coffee and Friday happy hours with this awesome group of people.

To all of the members of our joint lab meetings at both Carnegie Mellon University and the University of Pittsburgh, specifically the Lee and Linstedt labs at CMU, and the Friedman, Vilardaga, Romero, and Bisello Labs at Pitt, for providing guidance and suggestions that were integral in the successful completion of my thesis and personal development as a scientist. I would also like to thank my previous advisor and mentor Dr. Umamaheswar Duvvuri. His support and guidance early in my career was a critical driving force in my pursuit of an academic career.

Finally, I would like to thank my friends and family for their continued love and support. To my wife, Cary, and daughter, Piper. You make it all worthwhile. To my parents, you have been incredibly generous and supportive to me throughout my education and I couldn't have done it without you. To my friends, for constantly asking when I am going to be finished with school, and my fellow graduate students at CMU, you have all helped and supported me over the past 5 years to make this journey fun and memorable.

**Abstract:**

Pain is a major global health problem affecting 1.5 billion people. More Americans suffer from chronic pain than from diabetes, heart disease, and cancer combined (Institute on Medicine Report, 2011). Opioid analgesics that target the  $\mu$ -Opioid Receptor (MOR), such as morphine or oxycodone, are the primary treatment options for chronic pain. These MOR agonists are initially effective, but have extreme adverse effects, lose their efficacy over time, and lead to dependence and addiction. Therefore, identifying alternative targets for pain remediation is of extreme significance. The  $\delta$ -Opioid Receptor (DOR) is a highly attractive alternate target. DOR activates similar cellular pathways as MOR, and can mediate attenuation of pain under specific experimental conditions. However, in the clinical context, DOR agonists have been minimally effective as an analgesic target, and the precise reason for this is not clear. I hypothesize that DOR agonists have limited analgesic efficacy because of the decreased delivery of DOR to the plasma membrane in neurons. In neurons, newly synthesized DOR is retained in intracellular compartments, and may require specific signals for release from intracellular stores and insertion into the cell membrane. Recent data have localized DOR within subsets of neurons that mediate modalities of pain similarly to MOR, increasing the potential impact of targeting DOR agonists. However, the clinical inefficacy of DOR agonists, and the significance of DOR's regulated surface trafficking, are topics of debate.

This thesis will investigate the mechanism controlling the regulated surface trafficking of DOR in neuronal cells in order to determine the mechanism of DOR retention, and subsequently reverse the retention to induce DOR trafficking to the surface. Chapter 2 studies the mechanism controlling surface trafficking of DOR, and shows that a phosphoinositide-regulated Golgi checkpoint regulates the bioavailability of  $\delta$ -opioid receptors. Chapter 3 elaborates on the phosphoinositide-regulated Golgi checkpoint controlling DOR trafficking, and demonstrates that optogenetic recruitment of PI3K C2 $\alpha$  to the *trans*-Golgi network is sufficient to promote surface trafficking of the  $\delta$ -opioid receptor. Chapter 4 explores the amino acid sequence required for Golgi retention of DOR, and reveals that NGF-induced golgi retention of  $\delta$ -Opioid receptors requires dual RXR retention/retrieval motifs. Chapter 5 investigates the role of the Rho-associated GTPase TC10 in DOR surface trafficking, and shows that TC10 GTP is sufficient to drive constitutive surface trafficking of the  $\delta$ -Opioid receptor. Together, the data presented in this thesis reveal a novel mechanism for the regulated delivery of  $\delta$ -opioid receptors to the cell surface, and demonstrate a proof of principle for induced trafficking of DOR to provide analgesic benefits under circumstances of chronic pain.

## Table of Contents

<b>Chapter 1: Introduction</b> .....	1
<b>Chapter 2: A Phosphoinositide-regulated Golgi Checkpoint Regulates the Bioavailability of <math>\delta</math>-Opioid Receptors</b>	
Abstract.....	7
Introduction.....	8
Results.....	10
Discussion.....	16
Methods.....	20
Figures.....	28
References.....	45
<b>Chapter 3: Optogenetic Recruitment of PI3K C2<math>\alpha</math> to the <i>trans</i>-Golgi Network is Sufficient to Promote Surface Trafficking of the <math>\delta</math>-Opioid Receptor</b>	
Abstract.....	50
Introduction.....	51
Results.....	53
Discussion.....	60
Methods.....	65
Figures.....	73
References.....	84
<b>Chapter 4: NGF-induced Golgi Retention of <math>\delta</math>-Opioid Receptors Requires Dual RXR Retention/Retrieval Motifs</b>	
Abstract.....	89
Introduction.....	90
Results.....	92
Discussion.....	98
Methods.....	104
Figures.....	107
References.....	119
<b>Chapter 5: TC10 GTP is Sufficient to Drive Constitutive Surface Trafficking of the <math>\delta</math>-Opioid Receptor</b>	
Abstract.....	122
Introduction.....	123
Results.....	125
Discussion.....	131
Methods.....	136
Figures.....	142
References.....	150
<b>Chapter 6: Conclusion</b> .....	152

## List of Figures

<b>Chapter 1: Introduction</b> .....	1
Figure 1: The $\delta$ -Opioid Receptor is a Single-Use Receptor that Undergoes Regulated Trafficking to the Cell Surface.....	4
<b>Chapter 2: A Phosphoinositide-regulated Golgi Checkpoint Regulates the Bioavailability of <math>\delta</math>-Opioid Receptors</b>	
<b>Figure 1:</b> PI3K is required for DOR delivery to the surface from intracellular pools that overlap with the Golgi.....	28
<b>Figure 2:</b> PI3K inhibition does not induce MOR retention.....	30
<b>Figure 3:</b> NGF treatment or PI3K inhibition do not cause endocytosis of surface DOR.....	31
<b>Figure 4:</b> PTEN inhibition releases Golgi-retained DOR and promotes surface delivery in PC12 cells and TG neurons.....	32
<b>Figure 5:</b> SHIP2 inhibition causes intracellular accumulation of DOR, similar to NGF.....	34
<b>Figure 6:</b> The pool of DOR delivered to the surface by phosphoinositide conversion is functional.....	35
<b>Figure 7:</b> Phosphoinositide conversion delivers a functional pool of endogenous DOR in TG neurons.....	37
<b>Figure 8:</b> Stimulated DOR delivery enhances the antinociceptive efficacy of the DOR agonist SNC80.....	38
<b>Figure 1 S1:</b> Workflow of quantitative image analysis for determining the percentage of total DOR retained in intracellular pools.....	39
<b>Figure 1 S2:</b> Inhibition of PKC, Akt, or Src do not cause DOR retention in intracellular pools.....	40
<b>Figure 5 S1:</b> Schematic of phosphoinositide conversion and summary of results of manipulation.....	41
<b>Figure 6 S1:</b> Validation of live-cell Epac sensor imaging assay for evaluating DOR activity following agonist administration.....	42
<b>Chapter 3: Optogenetic Recruitment of PI3K C2<math>\alpha</math> to the <i>trans</i>-Golgi Network is Sufficient to Promote Surface Trafficking of the <math>\delta</math>-Opioid Receptor</b>	
<b>Figure 1:</b> Activation of PI3K by 740Y-PDGFR is sufficient to reduce the PI3K-inhibition induced retention of DOR.....	73
<b>Figure 2:</b> Class I PI3K is not required for Golgi retention of DOR.....	75
<b>Figure 3:</b> Class II PI3K C2 $\alpha$ is required for surface trafficking of DOR.....	77
<b>Figure 4:</b> Optogenetic recruitment of the PI3K C2 $\alpha$ kinase domain to the <i>trans</i> -Golgi network is sufficient to induce DOR surface trafficking.....	79
<b>Figure S1:</b> Activation of PI3K by 740Y-PDGFR is sufficient to reduce the PI3K-inhibition induced retention of DOR.....	81
<b>Figure S2:</b> Class I PI3K is not required for Golgi retention of DOR.....	83

## **Chapter 4: NGF-induced Golgi Retention of $\delta$ -Opioid Receptors Requires Dual RXR Retention/Retrieval Motifs**

<b>Figure 1:</b> The C-terminal tail of DOR regulates delivery of the receptor to the cell surface.....	107
<b>Figure 2:</b> Mutating the potential phosphorylation sites within the C-terminal tail of DOR to alanine does not significantly affect the basal or NGF-regulated Golgi retention of DOR.....	109
<b>Figure 3:</b> Eliminating the potential post-translational modification site C360 within the C-terminal tail of DOR to alanine minimally decreases the NGF-induced Golgi retention of DOR.....	111
<b>Figure 4:</b> Alanine mutations of di-arginine containing motifs within the third intracellular loop and C-terminal tail of DOR do not significantly inhibit the NGF-induced retention of DOR.....	113
<b>Figure 5:</b> Two RXR motifs within the C-terminal tail of DOR are required for NGF-induced Golgi retention.....	115
<b>Figure S1:</b> The DOR C-terminal tail deletions $\Delta$ 345-352 and $\Delta$ 353-359 exhibit a reduction in Golgi retention following PI3K inhibition.....	117

## **Chapter 5: TC10 GTP is Sufficient to Drive Constitutive Surface Trafficking of the $\delta$ -Opioid Receptor**

<b>Figure 1:</b> DOR and TC10 co-localize following NGF treatment.....	142
<b>Figure 2:</b> Following NGF treatment, PTEN inhibition drives DOR and TC10 trafficking to the cell surface .....	144
<b>Figure 3:</b> TC10 co-immunoprecipitates with DOR, and PTEN inhibition increases their interaction.....	145
<b>Figure 4:</b> The dominant-active TC10 Q75L is sufficient for DOR surface trafficking in the presence of NGF treatment.....	146
<b>Figure 5:</b> The dominant-active TC10 Q75L is sufficient for DOR surface trafficking in the presence of PI3K inhibition.....	148
<b>Figure S1:</b> Dominant-active TC10 Q75L strongly co-immunoprecipitates with DOR, while the dominant-negative TC10 T31N decreases co-immunoprecipitation.....	149

## **Chapter 6: Conclusion.....**

156

# Chapter 1: Introduction

## Introduction:

Physiological responses of cells to changes in the extracellular environment rely on the precise localization of transmembrane receptors on the cell surface. Due to the amount of energy required for synthesis and trafficking of new membrane proteins from the endoplasmic reticulum to the surface, one might intuit that the cell would re-use transmembrane receptors multiple times; however, this is not always the case. Nature has engineered many receptors to undergo one-time activation on the surface followed by immediate destruction. Further response to signals requires delivery of newly synthesized receptors. At first glance, such a "single-use" strategy seems wasteful, so why might this system have evolved?

Re-using receptors requires their endocytosis, re-sensitization, and recycling, taking several minutes<sup>1,2</sup>. This would not permit the rapid sub-second receptor responses required to detect repeated bursts of chemical signals like those observed in many neuronal and endocrine cells. Single-use signaling, because it relies on a separate pre-sensitized pool of receptors for recovery of sensitivity, could allow rapid on/off responses with a high degree of regulation at the post-synaptic membrane, akin to synaptic release at the pre-synaptic membrane. An example physiological system that would benefit from the sensitivity and rapid response of a single-use receptor detection system is the peripheral pain circuitry.

One of the most common pathways for processing pain in our bodies is through the Dorsal Root Ganglion (DRG) of the spinal cord. In this system, noxious pain stimuli are detected by sensory receptors and transduced into electrical signals within the peripheral terminals of unmyelinated C-fibers. This activity is relayed to the dorsal horn of the spinal cord, up to the brainstem, and ultimately processed within the cerebral cortex where a pain sensation is realized<sup>3</sup>. From an evolutionary context, one can imagine that in a life threatening situation, succumbing to a painful stimulus would be disadvantageous. Luckily, our bodies have evolved an eloquent response mechanism to acutely dampen pain signals utilizing opioid receptors. Aside from the DRG, opioid receptors are expressed within inhibitory neurons of the medulla, locus coeruleus, periaqueductal gray area, and cortex regions.

The functional implications of opioid receptor expression in neurological systems are exemplified by their G<sub>i</sub>-coupled protein classification. Opioid receptors belong to a family of G<sub>i</sub>-coupled G Protein-Coupled Receptors (GPCRs) that upon activation undergo a conformational change exchanging GDP for GTP allowing the dissociation of the G $\alpha$  from the G $\beta\gamma$  subunit. The activated G $\alpha$  subunit decreases the activation of adenylyl cyclase and cyclic-AMP production

inhibiting signaling pathways within the cell. Additionally, activation of the opioid receptors inhibits calcium channel influx and promotes potassium channel efflux resulting in neuronal hyperpolarization that inhibits action potential initiation. In each cell type, their specific role can vary. In most instances, the opioid receptors are activated by endogenous enkephalin agonists, which can be secreted following a painful stimulus, or by an exogenous pharmacological opioid<sup>4,5</sup>. For these reasons, the front line of defense in severe pain relief is to activate the opioid receptors and inhibit neuronal activity within the analgesic circuit of the spinal cord<sup>6</sup>.

Pain is the most common symptom presented at hospitals. Pain inhibition, or analgesia, is an essential physiological process that our bodies have eloquently evolved utilizing enkephalins and opioid receptors to combat acute injury and persistent pain<sup>4,5</sup>. In conditions of severe and chronic pain, we, as scientists, have hijacked the body's analgesic circuitry through administration of exogenous opiates such as morphine, a  $\mu$ -opioid receptor (MOR) agonist. During infrequent periods of extreme pain, opiates targeting the MOR work extremely well as analgesics; however, in situations of chronic pain, where opiates are repeatedly administered, these opioid receptors undergo changes in their protein trafficking and signaling pathways that result in desensitization and subsequent addiction<sup>7-9</sup>. Our lab hypothesizes that following agonist stimulation, re-using receptors such as MOR via recycling mechanisms back to the cell surface can lead to changes in receptor phosphorylation that drive the desensitization process. For this reason, identifying a receptor that is single-use, and does not recycle back to the cell surface, could minimize the desensitization observed during chronic opioid treatment. While the discovery of morphine has been invaluable in medicine, pharmacological targeting of MOR continues to be highly limited by extensive side effects, including abuse and addiction, that create an enormous burden on the medical industry<sup>10,11</sup>. According to a recent study, over 100 million Americans, and 1.5 billion people worldwide suffer from chronic pain, which is more than the total number of people suffering from diabetes, heart disease, and cancer combined<sup>12,13</sup>. Therefore, finding alternate analgesic targets has high and immediate relevance. One possible avenue for avoiding these negative consequences in chronic pain management could be to selectively target the  $\delta$ -Opioid Receptor (DOR).

The DOR, a  $G_i$ -coupled GPCR, is predominantly expressed in intracellular compartments of nociceptive neurons within periaqueductal gray region of the brain and the dorsal horn of the spinal cord. DOR's activation by enkephalins yields limited addictive properties, possibly due to its single-use characteristics that do not lead to receptor recycling and subsequent desensitization. However, DOR's localization, within intracellular compartments, makes it an unsuitable target for pharmacologic treatment of chronic pain. When DOR is expressed on the

cell surface, the  $\delta$ -selective agonist, DADLE, can activate receptor signaling to mediate pain relief<sup>14</sup>. After DOR activation and endocytosis into the early endosome, it is excluded from the recycling endosome and matures along with the early endosome into a multi vesicular body (MVB) where DOR can incorporate into intraluminal vesicles (ILV). Following ubiquitination, DOR enters the lysosome where it is degraded, exemplifying its single use characteristics<sup>15-17</sup>. In order to increase DOR on the cell surface, newly synthesized receptors must traffic through the biosynthetic pathway. The biosynthetic pathway regulates the delivery of the DOR from stored intracellular pools to allow for quick insertion upon an exocytosis signal (Figure 1)<sup>18</sup>.

In 2003, Kim *et al.* developed a method to study the intracellular retention of DOR using the neuroendocrine cell line pheochromocytoma-12 (PC12) and treatment with a neurotrophin, Nerve Growth Factor (NGF). Upon application of NGF, PC12 cells undergo a neuronal differentiation process that inhibits their proliferative ability and induces neuronal process formation. Following NGF treatment, in PC12 cells expressing a FLAG-tagged DOR, DOR is observed to accumulate intracellularly. Using cycloheximide to inhibit new protein synthesis, the NGF-induced intracellular accumulation of DOR was concluded to be retention of the DOR within the *trans*-Golgi Network (TGN). This phenotype of NGF induced retention closely resembled the DOR localization that had been previously observed in nociceptive neurons. Additionally, the authors concluded that the C-terminal tail of the DOR was sufficient for the internal localization of the receptor by creating a chimeric protein of CD4 and the DOR C-terminal tail. With this chimera, they were able to demonstrate that the specificity for the induction of DOR's intracellular retention by NGF in PC12 cells could be transferred to another protein that would normally not be affected by NGF. After retention, application of a depolarizing solution of 55mM KCl was able to release the retention caused by NGF. While this NGF induced effect is scientifically interesting, one might question if an NGF induced retention mechanism can account for the DOR retention observed in mature nociceptive neurons.

Traditionally, NGF has been shown in mice to be essential for neuronal development and differentiation, but has recently been implicated in the maintenance of sensory neurons, the formation of central pain circuitry, and the activation of the Hypothalamic-Pituitary-Adrenal axis during fight or flight responses<sup>19</sup>. NGF acts through binding to the TrkA receptor activating its downstream signaling pathways to mediate neuronal differentiation and promote cell survival. Interestingly, NGF expression is detectable after development within established DRG, and increased expression has been implicated in hyperalgesia in adult mice<sup>19,20</sup>. Thus, persistent NGF within neuronal environments might explain why the DOR is not basally expressed on the cell surface and confers little analgesic effect at baseline.

Further investigation into the trafficking and manipulation of DOR to the cell surface has been limited; however, the potential for using the DOR as an analgesic target still exists. One can imagine, that by manipulating a protein-protein interaction or kinase phosphorylation site within the C-terminal tail of DOR, the intracellular pool of DOR could be released to allow trafficking to the cell surface<sup>21-24</sup>. This would then allow for selective targeting of DOR in pain remediation with limited desensitization and addictive side effects due to DOR's single use characteristics. The tightly regulated control of DOR trafficking to the cell membrane has many clinical and scientific neurological impacts for drug addiction and understanding the regulation of biosynthetic protein trafficking<sup>25</sup>.

The goals of this thesis are to determine the physiological mechanism regulating DOR retention, and subsequently manipulate the retention mechanism to induce DOR trafficking to the cell surface of nociceptive neurons. If we can find ways to counter the intracellular retention by identifying protein machinery specific to this process, DOR agonists can be used as effective and safe analgesics for chronic pain<sup>26</sup>. Further, a thorough understanding of this regulatory pathway controlling DOR surface delivery, and the required amino acid sequence mediating the NGF-induced retention of DOR, would provide new insights into the evolution of protein trafficking and single-use receptor regulation.

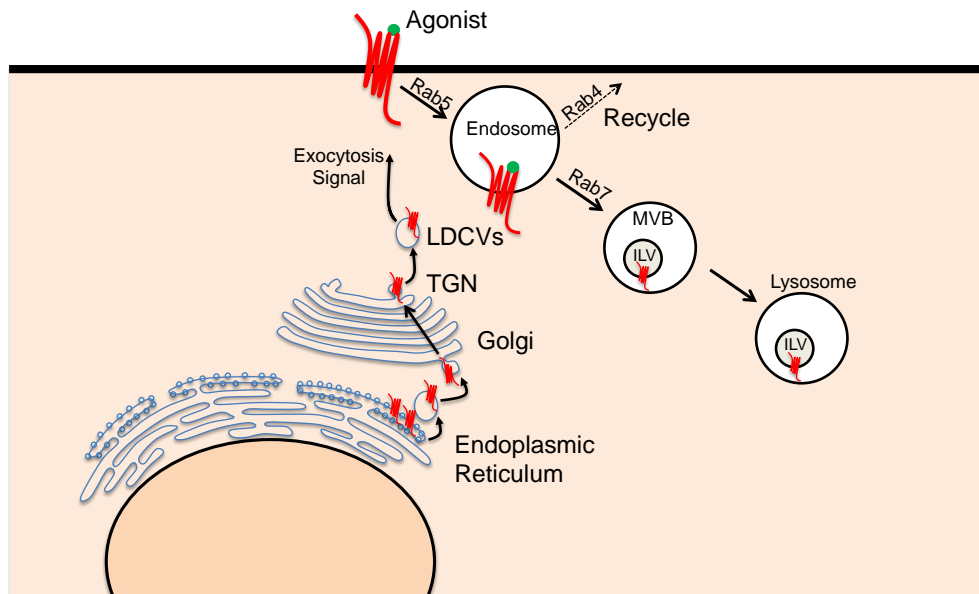


**Figure 1: The  $\delta$ -Opioid Receptor is a Single-Use Receptor that Undergoes Regulated Trafficking to the Cell Surface.** The DOR undergoes N-glycosylation and O-glycosylation within the endoplasmic reticulum. After 2 hours, DOR exits the ER and is transported to the Golgi. Here, it is retained or packaged into vesicles where it awaits a signal for trafficking to the cell surface. Once on the cell surface, DOR can bind to its agonist and is endocytosed. After internalization, the DOR matures along with the early endosome into a multivesicular body (MVB) where it is incorporated into intraluminal vesicles (ILV). Eventually, with assistance from a Ubiquitination signal, DOR is trafficked to the lysosome for degradation.

## References:

1. Lefkowitz, R. J. *et al.* Mechanisms of beta-adrenergic receptor desensitization and resensitization. *Adv. Pharmacol.* **42**, 416–420 (1998).
2. Zastrow, von, M. & Zastrow, von, M. A cell biologist's perspective on physiological adaptation to opiate drugs. *Neuropharmacology* **47 Suppl 1**, 286–292 (2004).
3. Bear, M. F., Connors, B. W. & Paradiso, M. A. Neuroscience: Exploring the Brain. (2012).
4. Bodnar, R. J. & Bodnar, R. J. Endogenous opiates and behavior: 2007. *Peptides* **29**, 2292–2375 (2008).
5. Ignatova, E. G. E., Belcheva, M. M. M., Bohn, L. M. L., Neuman, M. C. M. & Coscia, C. J. C. Requirement of receptor internalization for opioid stimulation of mitogen-activated protein kinase: biochemical and immunofluorescence confocal microscopic evidence. *J. Neurosci.* **19**, 56–63 (1999).
6. Al-Hasani, R. & Bruchas, M. R. Molecular mechanisms of opioid receptor-dependent signaling and behavior. *Anesthesiology* **115**, 1363–1381 (2011).
7. He, L. *et al.* Regulation of opioid receptor trafficking and morphine tolerance by receptor oligomerization. *Cell* **108**, 271–282 (2002).
8. Martini, L., Martini, L., Whistler, J. L. & Whistler, J. L. The role of mu opioid receptor desensitization and endocytosis in morphine tolerance and dependence. *Current Opinion in Neurobiology* **17**, 556–564 (2007).
9. Kim, J. A. *et al.* Morphine-induced receptor endocytosis in a novel knockin mouse reduces tolerance and dependence. *Current Biology* **18**, 129–135 (2008).
10. McLellan, A. T., Lewis, D. C., O'Brien, C. P. & Kleber, H. D. Drug dependence, a chronic medical illness: implications for treatment, insurance, and outcomes evaluation. *JAMA* **284**, 1689–1695 (2000).
11. Hansen, G. R. & Hansen, G. R. The drug-seeking patient in the emergency room. *Emerg. Med. Clin. North Am.* **23**, 349–365 (2005).
12. Committee on Advancing Pain Research, . *Relieving Pain in America: A Blueprint for Transforming Prevention, Care, Education, and Research.* National Academies Press (National Academies Press, 2011).
13. Global Industry Analysts, Inc., Analysts, G. I. & Inc. Global Pain Management Market to Reach US\$60 Billion by 2015, According to a New Report by Global Industry Analysts, Inc. *PRWeb eBooks* 1–3 (2011).
14. Bodnar, R. J. & Bodnar, R. J. Endogenous opiates and behavior: 2011. *Peptides* **38**, 463–522 (2012).
15. Whistler, J. L., Whistler, J. L., Tsao, P. & Zastrow, von, M. A phosphorylation-regulated brake mechanism controls the initial endocytosis of opioid receptors but is not required for post-endocytic sorting to lysosomes. *J. Biol. Chem.* **276**, 34331–34338 (2001).
16. Whistler, J. L. *et al.* Modulation of postendocytic sorting of G protein-coupled receptors. *Science* **297**, 615–620 (2002).
17. Tanowitz, M., Tanowitz, M. & Zastrow, von, M. A novel endocytic recycling signal that distinguishes the membrane trafficking of naturally occurring opioid receptors. *J. Biol. Chem.* **278**, 45978–45986 (2003).
18. Kim, K.-A., Kim, K.-A., Zastrow, von, M. & Zastrow, von, M. Neurotrophin-regulated sorting of opioid receptors in the biosynthetic pathway of neurosecretory cells. *Journal of Neuroscience* **23**, 2075–2085 (2003).
19. Berry, A. *et al.* NGF, brain and behavioral plasticity. *Neural Plast.* **2012**, 784040–9 (2012).
20. Taiwo, Y. O., Levine, J. D., Burch, R. M., Woo, J. E. & Mobley, W. C. Hyperalgesia induced in the rat by the amino-terminal octapeptide of nerve growth factor. *Proc. Natl. Acad. Sci. U.S.A.* **88**, 5144–5148 (1991).

21. Boue-Grabot, E., Archambault, V. & Seguela, P. A protein kinase C site highly conserved in P2X subunits controls the desensitization kinetics of P2X(2) ATP-gated channels. *J. Biol. Chem.* **275**, 10190–10195 (2000).
22. Duvernay, M. T., Duvernay, M. T., Zhou, F. & Wu, G. A conserved motif for the transport of G protein-coupled receptors from the endoplasmic reticulum to the cell surface. *J. Biol. Chem.* **279**, 30741–30750 (2004).
23. Dong, C. *et al.* Regulation of G protein-coupled receptor export trafficking. *Biochim. Biophys. Acta* **1768**, 853–870 (2007).
24. Puthenveedu, M. A. *et al.* Sequence-dependent sorting of recycling proteins by actin-stabilized endosomal microdomains. *Cell* **143**, 761–773 (2010).
25. Pradhan, A. A. A. *et al.* In vivo delta opioid receptor internalization controls behavioral effects of agonists. *PLoS ONE* **4**, e5425 (2009).
26. Pradhan, A. A. A. *et al.* In Vivo Delta Opioid Receptor Internalization Controls Behavioral Effects of Agonists. *PLoS ONE* **4**, e5425 (2009).

## Chapter 2: A Phosphoinositide-regulated Golgi Checkpoint Regulates the Bioavailability of $\delta$ -Opioid Receptors

Daniel J. Shiwarski<sup>1</sup>, Alycia Tipton<sup>2</sup>, Melissa D. Giraldo<sup>3</sup>, Michael S. Gold<sup>3</sup>, Arynah A. Pradhan<sup>2</sup>, Manojkumar A. Puthenveedu<sup>1</sup>

<sup>1</sup>Department of Biological Sciences, The Center for the Neural Basis of Cognition, Carnegie Mellon University, Pittsburgh, PA 15213, USA.

<sup>2</sup>Department of Psychiatry, University of Illinois, Chicago, 1601 West Taylor Street, Chicago, IL 60612, USA.

<sup>3</sup>Department of Anesthesiology, University of Pittsburgh School of Medicine, Pittsburgh, PA 15213, USA; Pittsburgh Center for Pain Research, University of Pittsburgh School of Medicine, Pittsburgh, PA 15213, USA.

### Abstract

Many G protein-coupled receptors (GPCR) are internalized and degraded after activation. For these receptors, cells rely on the surface delivery of newly synthesized receptors for recovery of sensitivity. Whether and how GPCR biosynthetic delivery is regulated, and how this influences receptor physiology *in vivo*, are largely unknown. Here we describe a physiologically relevant neuronal signaling axis that regulates the surface delivery of the delta opioid receptor (DOR), a prototypic GPCR, in peripheral sensory neurons. We define a phosphoinositide-regulated checkpoint that regulates DOR export from the Golgi and retains DOR in intracellular pools in neurons. Further, we provide a proof of concept that manipulating this checkpoint releases DOR from this storage pool, stimulates DOR surface delivery, and allows effective DOR-mediated antinociception *in vivo*. Our results explain why DOR agonists have been largely ineffective *in vivo*, and identify a novel physiologically relevant regulatory system for controlling the surface levels of GPCRs.

## Introduction

G protein-coupled receptors (GPCRs), the largest family of signaling receptors, are highly regulated by membrane trafficking. The interplay between signaling and trafficking has been explored mainly using endocytic and post-endocytic trafficking, which modify the number of receptors on the cell surface (Ferguson et al., 1998; Maxfield and McGraw, 2004; Sorkin and Zastrow, 2002; Zastrow et al., 2003). Activated GPCRs are internalized and trafficked to the endosome. This is associated with a loss of cellular responsiveness to the signal. From the endosome, receptors are either returned to the endosome by recycling, or are degraded in the lysosome (Hanyaloglu and Zastrow, 2008; Marchese and Trejo, 2013). In the latter case, in order for cells to recover signaling, new receptors need to be made and inserted into the cell surface. Compared to endocytic and post-endocytic trafficking, however, little is known about whether and how the delivery of newly synthesized GPCRs is physiologically regulated (Cheng and Filardo, 2012; Dong et al., 2007; Hein et al., 1994).

The delta opioid receptor (DOR) is a prototypical GPCR where regulated delivery of newly synthesized receptors might have a clear physiological and clinical significance (Cahill et al., 2007; Pradhan et al., 2011; Zhang et al., 2006). DOR is expressed in nociceptive neurons, where it can reduce cAMP and open K<sup>+</sup> channels to hyperpolarize and reduce the activity of these neurons (Bardoni et al., 2014; Cahill et al., 2007; Jutkiewicz et al., 2006; Pradhan et al., 2011; Scherrer et al., 2009). Therefore, DOR is an attractive alternative target for managing chronic pain and depression, especially because, in experimental conditions, drugs that activate DOR do not show the adverse effects that severely limit the use of current opioid analgesics (Cahill et al., 2003; Pradhan et al., 2011). Although drugs that activate DOR (termed agonists) work well *in vitro*, the *in vivo* analgesic efficacy of DOR agonists has been equivocal at best. Following tissue injury in experimental mouse and rat models, DOR agonists can have limited analgesic efficacy, but this requires high doses that cause serious adverse effects like convulsions. This poor *in vivo* efficacy has been the critical limiting factor in developing DOR as an analgesic target (Bardoni et al., 2014; Cahill et al., 2007; Danielsson et al., 2006; Gavériaux-Ruff et al., 2011; Jutkiewicz et al., 2006; Scherrer et al., 2009).

A potential explanation for this poor agonist efficacy is that DOR is predominantly localized to intracellular structures in neurons with limited surface expression (Bao et al., 2003; Cahill et al., 2001a; 2001b; Gendron et al., 2014; Kim et al., 2003; Petaja-Repo et al., 2000; Wang et al., 2001; Zhang et al., 1998). This raises the simple and transformative possibility that relocating the intracellular pool of DOR to the cell surface would increase the efficacy of existing DOR agonists. The key limitation relocating the intracellular pool of DOR to the cell surface is that the

mechanisms of DOR retention and surface trafficking are largely unknown. Initial evidence suggested that DOR localizes in vesicles with neurotransmitters, but recent evidence suggests that this might not be the case (Cahill et al., 2007; Pradhan et al., 2011; Zhang et al., 2006). As of now, no specific methods to release the intracellular pool of DOR to the surface in neurons are known.

Here we define an endogenous checkpoint at the trans-Golgi network that limits DOR export from the Golgi and decreases its surface delivery in sensory neurons. This checkpoint is not a general block of exocytic trafficking, and is driven by phosphoinositide conversion of PI(4)P to PI(3,4)P via phosphoinositide 3 kinase (PI3K) activity in the Golgi. Pharmacological manipulation of this phosphoinositide conversion bypasses this checkpoint and drives DOR export from the Golgi, delivering functional DOR to the cell surface. Relocating DOR to the cell surface increases the antinociceptive efficacy of DOR agonists in a mouse model of chronic pain, without causing noticeable side effects. Together, our results describe a checkpoint in the Golgi, controlled by a neuronal-specific signaling axis, that regulates GPCR delivery to the surface. In the case of DOR, this explains why DOR agonists are ineffective when targeting DOR for antinociception *in vivo*. We provide a proof of mechanism for overcoming the low efficacy of existing DOR agonists by bypassing this checkpoint and engineering DOR delivery to the cell surface.

## Results

### PI3K activity is required for DOR export from the Golgi

When an N-terminally FLAG-tagged DOR was expressed in cultured adult mouse trigeminal ganglia (TG) neurons, DOR was localized predominantly in intracellular structures that overlapped with the Golgi apparatus (Fig 1A). This expression system has been highly useful to study many GPCRs including DOR, and we and others have confirmed that tagged receptors are functional (Arttamangkul et al., 2008; Bowman et al., 2015; Guan et al., 1992; Kim et al., 2003; Puthenveedu et al., 2010; Soohoo and Puthenveedu, 2013; Vistein and Puthenveedu, 2013). As an experimental system to start addressing DOR retention mechanistically, we used neuroendocrine PC12 cells expressing N-terminally FLAG-tagged DOR. Consistent with previous observations, DOR expressed in PC12 cells showed predominantly surface expression (Fig 1B). Following Nerve Growth Factor (NGF) treatment for 1 hour, DOR is retained in an intracellular compartment broadly overlapping with the *trans*-Golgi Network (TGN) marker TGN-38 (Fig 1B, C) (Kim et al., 2003).

To establish that this was a transport block of newly synthesized receptors, we first accumulated DOR in the TGN by treating cells with NGF for 1 hour to induce Golgi retention, and then chased this accumulated pool by blocking the synthesis of new DOR with cycloheximide. This chase was performed either in the presence of continued NGF, or after NGF was removed. In the presence of NGF, the intracellular pool persisted even when the synthesis of new DOR was blocked (Fig 1C). In contrast, the intracellular pool was rapidly lost in the absence of NGF. We next directly visualized the NGF-mediated switch to DOR retention by expressing an N-terminally GFP-tagged DOR and imaging DOR using live-cell confocal fluorescence microscopy. When exposed to NGF and imaged live, NGF caused robust intracellular DOR accumulation within one hour (Movie S1). Together, our results indicate that, in PC12 cells, NGF signaling actively blocks DOR export from the Golgi, and recapitulates the intracellular DOR retention seen in neurons.

Considering that DOR is retained in neurons potentially in the absence of NGF (Bao et al., 2003; Cahill et al., 2001a; 2001b; Gendron et al., 2014; Kim et al., 2003; Zhang et al., 1998), we next attempted to identify additional signaling factors that caused retention under physiological conditions in neurons. We focused on factors downstream of the TrkA receptor, the primary target of NGF in PC12 cells, as it is required for the retention of DOR (Kim et al., 2003). Inhibitors of the main TrkA effectors ROCK (Y-27632), MEK (U0126), Akt (Akt1/2 Kinase Inhibitor), PLC (U73122), PKC (Chelerythrine), and c-Src (PP2) did not reduce the NGF-induced retention of DOR. However, inhibition of PI3K by Wortmannin increased NGF-mediated DOR retention (Fig 1C).

Strikingly, PI3K inhibition by either Wortmannin or LY294002 was sufficient to cause DOR retention in the absence of NGF, as measured by the percentage of cells with intracellular DOR (Fig 1D,E). To quantitate the fraction of total cellular DOR that was retained, we used TGN-38 fluorescence as a mask to measure the DOR that co-localized with the Golgi (Fig 1 Supplement 1). NGF treatment or PI3K inhibition significantly increased the fraction of Golgi-localized DOR (Fig 1F), indicating that PI3K activity was required for DOR export. We next directly visualized the switch to DOR retention by PI3K inhibition, by imaging retention of GFP-DOR in live cells as above (Movie S2).

To determine whether PI3K acted through the known downstream kinase targets, we tested whether inhibition of the main targets Akt, PKC, or cSrc, was sufficient to induce DOR retention. In PC12 cells expressing FLAG-tagged DOR, treatment with the Akt inhibitor (Akt 1/2 inhibitor), PKC inhibitor (Chelerythrine), or cSrc inhibitor (PP2), were not sufficient to induce intracellular retention of DOR (Fig 1 Supplement 2A). On quantitation, neither the percentage of cells with Golgi localized DOR nor the percentage of DOR localized to the Golgi increased following inhibition of PKC, Akt, or cSrc (Fig 1 Supplement 2B-C), indicating that these kinases were not required for DOR export.

We next tested whether NGF or PI3K inhibition would induce retention of the related MOR, to differentiate whether this was specific to DOR, or a general block in surface trafficking. In PC12 cells expressing FLAG-tagged MOR, neither NGF treatment, nor inhibition of PI3K by Wortmannin or LY294002, altered the localization of MOR (Fig 2A). Upon quantitation, the percentage of cells showing intracellular retention of MOR did not change with any treatments (Fig 2A,B). The fraction of MOR in the Golgi, calculated as in Fig 1, also did not change upon these treatments (Fig 2C). This suggested that the NGF and PI3K-regulated retention of DOR was not due to a general block in surface trafficking.

To ensure that the intracellular pool of DOR was not derived from receptors internalized from the cell surface, we pre-labeled surface DOR with Alexa647-conjugated anti-FLAG antibodies and followed the surface pool after NGF, Wortmannin, or LY294002 addition. None of these treatments redistributed surface DOR to intracellular compartments (Fig 3A). As a positive control, the DOR agonist DADLE caused robust internalization and redistribution to endosomes (Fig 3A). To quantitate the amount of internalization, we incubated the cells with Alexa488-conjugated secondary antibodies at the end of the treatment. This allowed us to specifically detect the remaining surface pool of labeled DOR, and to quantitatively estimate the fraction of the surface pool that colocalized with the total pool of DOR. The surface and the total pools of DOR

showed robust colocalization in cells treated with NGF, Wortmannin, or LY294002, comparable to control, indicating that these treatments do not induce any noticeable redistribution of surface DOR to intracellular compartments (Fig 3A-B). DADLE, as expected, caused low surface fluorescence and a significant loss of colocalization, consistent with internalization. This shows that the intracellular DOR pool induced by NGF or PI3K inhibition is not due to receptor endocytosis. Blocking new protein synthesis prior to NGF treatment, in contrast, abolished the intracellular pool of DOR, as reported previously (Kim et al., 2003). Together, our results suggest that PI3K activity is required for DOR export from the Golgi, and that NGF inhibits this export, causes DOR retention, and limits surface DOR delivery.

### PTEN inhibition drives DOR surface trafficking in TG neurons

To understand the mechanism of DOR retention and to identify further potential targets to drive DOR surface delivery, we focused on the lipid kinase activity of PI3K. Because phosphoinositide conversion is a dynamic and reversible process, we hypothesized that inhibition of the phosphatase that opposes PI3K, Phosphatase and tensin homolog (PTEN), will relieve intracellular DOR retention and drive DOR to the cell surface. Consistent with this, in PC12 cells expressing FLAG-tagged DOR, three different PTEN inhibitors - SF1670, bpV(HOptic), and bpV(Phen) - abolished NGF-induced DOR retention and induced surface DOR delivery in a dose-dependent manner (Fig 4A-C).

Importantly, we next tested if PTEN inhibition could drive the intracellular pool of DOR to the cell surface in physiologically relevant TG neurons. In cultured TG neurons isolated from adult mice, DOR was predominantly seen in intracellular compartments that overlapped with the Golgi (Fig 4D). As anticipated, NGF did not significantly modify this localization. Treatment with the PTEN inhibitor SF1670 for 1 hour caused a loss of intracellular DOR localization, as measured by the percentage of total DOR overlapping with the Golgi, irrespective of whether NGF was present or not (Fig 4D-F). This loss corresponded with a significantly higher fraction of neurons that showed surface DOR fluorescence (Control = 28.57% +/- 12.53; PTEN IH = 92.86% +/- 7.14,  $p < 0.001$ ), indicating that PTEN inhibition released intracellular DOR in physiologically relevant adult mouse TG neurons. We next directly visualized the redistribution of DOR in neurons following PTEN inhibition, by live cell confocal microscopy of TG neurons expressing GFP-DOR. In TG neurons, GFP-DOR was primarily localized in intracellular pools (Fig 4G). Following PTEN inhibition by bpV(Phen), the intracellular DOR pool was largely lost (Fig 4G). A radial profile analysis for each time point showed, quantitatively, that the fluorescence intensity for the

intracellular pool (smaller radii) decreases and the plasma membrane (larger radii) increased (Fig 4H and I). Quantitation of intracellular DOR fluorescence in multiple neurons showed a significant decrease in the intracellular DOR pool after PTEN inhibition (Fig 4J). These data demonstrate that PTEN inhibition reduced intracellular DOR retention and stimulates DOR surface trafficking in PC12 cells and in TG neurons.

#### Phosphoinositide conversion provides a checkpoint for DOR export from the Golgi

We next attempted to determine the phosphoinositide species that was altered by the PI3K/PTEN balance to regulate DOR export. The predominant lipid species on the Golgi is PI(4)P, and we hypothesized that the likely phospholipid driving Golgi export of DOR was PI(3,4)P<sub>2</sub>. An alternate possibility was that PI(4,5)P<sub>2</sub> conversion to PI(3,4,5)P<sub>3</sub> drove DOR export (See phosphoinositide conversion wheel, Fig 5 Supplement 1) (Di Paolo and De Camilli, 2006; Mayinger, 2012). To distinguish between these possibilities, we tested whether inhibition of SHIP2, a 5' lipid phosphatase (Aoki et al., 2007; Erneux et al., 2011), causes DOR retention. If PI(3,4,5)P<sub>3</sub> was the key lipid species driving Golgi export of DOR, the prediction was that SHIP2 inhibition would be similar to PTEN inhibition, and would increase DOR export even in the presence of NGF by increasing PI(3,4,5)P<sub>3</sub>. In PC12 cells expressing FLAG-tagged DOR, SHIP2 inhibition did not reduce NGF-induced DOR retention. Instead, SHIP2 inhibition was sufficient to induce DOR accumulation on its own (Fig 5A-C). This result is consistent with SHIP2 inhibition decreasing PI(3,4)P<sub>2</sub> levels by enhancing the stability of 5' phosphorylated PI species. Together, the manipulations (summarized in Fig 5 Supplement 1) suggest that PI(3,4)P<sub>2</sub>, and not PI(3,4,5)P<sub>3</sub>, is the main PI species driving DOR export from the Golgi.

#### Phosphoinositide conversion promotes surface delivery of functional DOR

To test whether PTEN inhibition increased functional DOR on the surface, we measured cAMP inhibition by DOR as a primary readout of Gi-coupling. Dynamic changes in cAMP levels were detected using the EPAC Förster Resonance Energy Transfer (FRET) sensor (DiPilato et al., 2004), simultaneously with activation and endocytosis of DOR (Fig 6A, Fig 6 Supplement 1, and Movie S3). DOR activation was measured as attenuation of forskolin-stimulated cAMP (Fig 6B and Fig 6 Supplement 1C-E). In NGF-treated PC12 cells, PTEN inhibition caused a stronger inhibition of cAMP in response to DADLE, consistent with increased availability of DOR on the surface. To directly test whether the increase in activity was due to release of NGF-retained DOR

by PTEN inhibition, we blocked pre-existing surface DOR with the irreversible antagonist chlornaltrexamine (CNA). This allowed us to isolate signaling from newly delivered receptors in a defined period of time (schematic in Fig 6C). Following NGF-induced DOR retention, pre-treatment with CNA significantly reduced DADLE-mediated cAMP inhibition and DOR endocytosis. Following the NGF-induced DOR retention and CNA blockade of surface DOR, PTEN inhibition was sufficient to recover agonist-induced DOR signaling (Fig 6D, time series in Fig 6E-J). Together, our data indicate that the DOR delivered to the surface from intracellular pools by PTEN inhibition was competent to bind agonists and induce signaling.

To test whether PTEN inhibition induced an increase in the levels of endogenous functional DOR in neurons, we evaluated the ability of PTEN inhibition to increase the DOR-mediated inhibition of evoked calcium channel transients in TG neurons. Following pre-treatment of isolated TG neurons with the PTEN inhibitor bpV(Phen) for 30 minutes, agonist-induced (SNC-80) activation of DOR caused a robust inhibition of Ca<sup>2+</sup> transients (Fig 7A-B). To better quantitate the effect of PTEN inhibition, we used the calcium indicator dye Fura 2AM to measure high K<sup>+</sup> evoked responses in neurons before and after DOR activation. KCl-induced Ca<sup>2+</sup> transients were observed as a brief increase in fluorescence intensity followed by decay over time (Fig 7C). Neurons were then characterized as either non-responsive (Fig 7D) or responsive (Fig 7E) based on the decrease in evoked KCl-induced Ca<sup>2+</sup> transients following SNC80 (calculated as more than twice the standard deviation of the initial responses). The percentage of neurons that responded to the DOR agonist SNC80 increased significantly following pre-treatment with the PTEN inhibitor bpV(Phen), compared to control neurons (~52% responders following PTEN inhibition compared to ~13% in control) (Fig 7F). As a control for specificity, PTEN inhibition did not increase the fraction of neurons that responded to capsaicin. These results demonstrate that by driving endogenous DOR to the surface through PTEN inhibition, we can increase the percentage of neurons that functionally respond to DOR agonists.

#### Stimulated DOR delivery increases antinociceptive efficacy of SNC80 in mice.

Because DOR is an attractive target for managing pain, we next tested whether stimulated DOR delivery increases receptor availability enough to increase the efficacy of DOR agonists and allow antinociception at doses that do not cause adverse effects. We chose the Complete Freund's Adjuvant (CFA) model of chronic inflammatory pain in mice to test our model, because it is a well-accepted and commonly used paradigm for chronic inflammatory pain, and one in which DOR agonists have shown partial effects at high doses. In addition, previous studies using

conditional knockout mice have shown that DOR-expressing neurons in peripheral ganglia are critical for the pain-relieving effects of the DOR agonist SNC80 within the CFA model (Gavériaux-Ruff et al., 2011). To test antinociception, mice were injected with CFA in the left hindpaw, and the experiments were performed 72 hours later. Mechanical threshold analysis was performed using von Frey filaments 45min after the final treatment condition, as described previously (Fig 8A) (Pradhan et al., 2013). We first tested multiple doses of the PTEN inhibitor bpV(Phen) pre-treatment to evaluate any possible non-specific affect of PTEN inhibition altering the CFA-induced mechanical hyperalgesia. A PTEN inhibitor concentration of 3mg/kg (subcutaneous, SC) did not alter the CFA-induced mechanical hyperalgesia, and was chosen as an appropriate dose for further studies. In CFA-injected mice, neither bpv(Phen) alone, nor the dose of SNC80 tested (2mg/kg intraperitoneal, IP), relieved CFA-induced mechanical hyperalgesia (Fig 8B). To test whether bpv(Phen) pre-treatment improves SNC80 efficacy, we selected 4 hours after PTEN inhibition as the optimal time point, because our experiments in naïve mice suggested that 4 hours was the optimal time point for SNC80 effectiveness. Pre-administration of bpv(Phen) 4 hours prior to testing significantly increased the efficacy of this dose of SNC80 (Fig 8B). Importantly, in these conditions, robust antinociception was observed without noticeable adverse effects such as convulsions.

We used two controls to establish that the antinociceptive effect induced by PTEN inhibition was caused by increased activation of DOR. First, we tested whether naltrindole, a DOR-selective antagonist, could block the effect of SNC80 in these conditions. We followed a similar paradigm as in Fig 8A, with an additional injection of vehicle or naltrindole (10mg/kg) 1 hour before SNC80 (Fig 8C). bpV(Phen)-treated animals injected with vehicle before SNC80 showed a significantly increased antinociceptive response, comparable to what was seen in Fig 8B. Strikingly, the SNC80-mediated antinociception caused by bpv(Phen) was completely abolished by naltrindole, indicating that this antinociception was likely DOR-mediated (Fig 8D). Animals treated with naltrindole, without bpV(Phen), also did not show antinociception with SNC80. Together, our data support the physiological relevance of our model that phosphoinositide conversion provides a Golgi checkpoint limiting the availability of DOR on the neuronal surface. PTEN inhibition bypasses this checkpoint to drive the intracellular pool of DOR to the neuronal surface and increase the antinociceptive efficacy of DOR agonists (Fig 8E).

## Discussion

This study uses a physiologically relevant prototype, the delta opioid receptor, to investigate how the delivery of newly synthesized GPCRs to the neuronal surface is regulated, and how this modulates receptor signaling *in vivo*. It is well established that controlling the number of surface receptors, by removal or delivery, is a critical method to control the strength and specificity of signals. Our understanding of this process has largely been limited to studies of receptor endocytosis and recycling, where many mechanisms and pathways of regulation have been described (Marchese and Trejo, 2013; Sorkin and Zastrow, 2002). The current results identify a regulated mechanism that controls the delivery of newly synthesized DOR. Because DOR is predominantly degraded after agonist-mediated endocytosis, delivery of newly synthesized DOR is critical for determining the sensitivity of neurons to opioids. Regulation of GPCR export from the Golgi by extracellular signals, as with the NGF-PI3K signaling axis identified here, could be a mechanism to provide control over this delivery and therefore resensitization, akin to the regulation of postendocytic sorting seen with recycling receptors (Bowman et al., 2015; Hanyaloglu and Zastrow, 2008; Vistein and Puthenveedu, 2013; 2014).

A cargo export checkpoint in the Golgi is intriguing, as the prevalent model for cargo transport through the Golgi postulates that compartments containing cargo mature into the next, and that resident enzymes are constantly retrieved by vesicles that travel backwards (Papanikou and Glick, 2014). When receptor cargo reaches the TGN, the expected outcome is that they are packaged into export vesicles, unlike resident proteins that are retrieved to earlier compartments. The retention we observe likely reflects the sorting of DOR between regulated export and retrieval pathways, with 3' phosphorylation of phosphoinositides (PI) switching DOR between these two pathways. PI4P, the predominant PI species in the Golgi, could bias the sorting of DOR to the retrieval pathway in neurons, while an increase in PI(3,4)P<sub>2</sub>, by either activation of PI3K or inhibition of PTEN, could actively sort DOR into a specialized exocytic pathway. In this manuscript, we implicate PI3K inhibition as the mechanism for NGF-induced retention of DOR; however, it is also possible that NGF could indirectly increase PTEN activity to reduce PI(3,4)P<sub>2</sub>. A possible mechanism of NGF-increased PTEN activity is through ROCK activation. Activated ROCK has been shown to phosphorylate PTEN resulting in increased phosphatase stability and activity. In our experiments, this explanation seems unlikely because inhibition of ROCK in the presence of NGF did not alter the NGF-induced retention of DOR (Figure 1). It is further possible that NGF could alter the transcriptional regulation of PTEN or protein stability; however, given the short time frame for NGF-induced retention of DOR (1 hour), and the known ability for NGF to

downregulate PI3K activity within this time frame, we believe that it is NGF's control over PI3K that mediates the intracellular retention.

The exact pathway that DOR takes to the surface is still under debate. DOR has been immunolocalized to large dense core vesicles (LDCVs) in DRGs and in cells overexpressing chromogranin-A and pre-protachykinin-A (PPT-A) (Guan et al., 2005; Zhang et al., 1998). The LDCV localization was lost in mice without PPT-A, suggested a potential mechanism for intracellular storage by interactions of the luminal domain of DOR with the substance P (SP) domain of protachykinin (Guan et al., 2005). The C-terminal 27 amino acids of DOR have also been reported to be sufficient for intracellular DOR retention in PC12 cells and in neurons, suggesting that multiple interactions contribute to regulation of DOR exocytosis (Kim et al., 2003). In this context, a mouse knock-in of a C-terminally GFP-tagged DOR showed surface expression of DOR, independent of SP (Scherrer et al., 2009). It is possible that the surface expression seen in this mouse reflects the C-terminal GFP, which might interfere with intracellular interactions required for normal regulation of DOR trafficking (Gendron et al., 2016; Kim et al., 2003). Consistent with this, exogenous expression of a C-terminally tagged DOR was localized to the surface in neurons, in contrast to an N-terminally tagged DOR which showed intracellular retention comparable to endogenous DOR (Wang et al., 2008).

While pathways that mediate TGN export of proteins, including GPCRs, have been described previously (Bonifacino, 2014; Guo et al., 2013; Malhotra and Campelo, 2011; Wu et al., 2015), it is not readily apparent whether DOR can access any of these pathways. The C-terminal tail of DOR does not contain any identified export motifs, such as the tyrosine-based motifs that bind clathrin adapter proteins (Bonifacino, 2014), the DXXLL motif that binds GGA proteins (Puertollano et al., 2001; Zhu et al., 2001) the triple Arg motif that binds GGA3 (Zhang et al., 2016), or the YYXXF motif used in Arfrp1/AP-1 mediated export (Guo et al., 2013). It is possible that the DOR tail contains a novel export sequence determined by its secondary structure, like a hydrophobic signaling patch found in Kir channels (Li et al., 2016). Similarly, the PKD-Arfaptin-dependent pathway is a well-described pathway that mediates TGN export of a subset of proteins (Cruz-Garcia et al., 2013; Wakana et al., 2012). It is possible that the "default" export pathway that leads to surface delivery of DOR in non-neuronal cells could use this mechanism. This pathway, however, depends on PI4P, which is in contrast to the requirement for PI(3,4)P that we observe in NGF-regulated DOR export. NGF signaling or a neuronal fate possibly switches DOR into a novel pathway based on as yet unidentified interactions of the C-terminal tail of DOR.

Interestingly, in mature neurons, DOR is localized primarily to intracellular structures even without specific NGF signaling (Fig 1A and (Bao et al., 2003; Cahill et al., 2001b; 2007; Gendron et al., 2014; Kim et al., 2003; Walwyn et al., 2005; Zhang et al., 1998). This suggests that neuronal differentiation causes persistent changes that maintain the checkpoint. In contrast to this, NGF and neuronal differentiation can also stimulate the surface delivery of glutamate receptors and secreted cargo like the human Growth Hormone, via a complex of proteins associated with ARMS/Kidins220 (Arévalo et al., 2010; López-Benito et al., 2016), suggesting that multiple downstream targets of NGF can have different effects on Golgi export of different cargo. NGF exerts a time-dependent biphasic response on PI3K activity, where acute NGF treatment upregulates PI3K activity at the plasma membrane, but persistent NGF downregulates PI3K activity (Chen et al., 2012). Consistent with this, short-term NGF treatment might increase the coupling of DOR to channels in brainstem slices (Bie et al., 2010), while persistent NGF induces intracellular retention of newly synthesized DOR by inhibiting PI3K as shown in this study. In addition, DOR activation itself might also serve as a cue for increasing DOR responses. When coupling to voltage-dependent calcium channels was used as a functional readout for DOR, a ROCK-LIMK pathway was found to regulate agonist-dependent export of DOR (Mittal et al., 2013). It is possible that these identified mechanisms might play redundant or overlapping roles in DOR function on the cell surface.

The neuron-specific intracellular retention and limited surface expression could provide an explanation for why DOR has been difficult to target clinically. Previous attempts at targeting DOR to manage pain have mainly focused on developing better DOR agonists (Bardoni et al., 2014; Gavériaux-Ruff et al., 2011; Scherrer et al., 2009). However, these efforts have largely been unsuccessful, as available agonists show poor *in vivo* efficacy, necessitating the use of high doses that cause adverse effects. Attempts to activate intracellular DOR using agonists that are membrane permeable also have been largely unsuccessful, indicating that the intracellular DOR is not competent to induce analgesia, likely because it is lacking the necessary downstream components. Pathological conditions such as chronic inflammation, or pharmacological chaperones, which increase total DOR mRNA and protein expression, cause a proportional increase in surface DOR and enhance the potency of DOR agonists (Bao et al., 2003; Cahill et al., 2003; 2007; Kim et al., 2003; Patwardhan et al., 2005; Pettinger et al., 2013). It is important to note that our study is distinct from these reports. We provide a specific method to increase surface delivery of DOR independent of upregulating DOR synthesis. Engineering the surface delivery of DOR by PTEN inhibition increases surface DOR delivery in physiologically relevant neurons and improves the antinociceptive potency of SNC80. This provides a critical proof of

concept on which to base further strategies to improve the bioavailability of DOR and increase the potency of the many DOR agonists already developed. With emerging data on the importance of the location of signal origin in downstream effects of GPCR signaling (Tsvetanova and Zastrow, 2014), such engineered relocation of receptors as we show here may provide a general blueprint to precisely manipulate the physiology of GPCRs.

## Materials and Methods:

### *Cell Lines and DNA Constructs*

The primary cell line used in this investigation was the pheochromocytoma-12 (PC12) cell line isolated from rat adrenal medulla tissue. This cell line was purchase and verified by ATCC (PC-12 ATCC CRL-1721). These cells were cultured in F12K medium (Invitrogen) supplemented with 10% horse serum and 5% fetal bovine serum. Stable and transient PC12 cell lines expressing the full length DOR with an N-terminal signal sequence Flag epitope (SSF-DOR) have been created to study the intracellular retention of DOR upon NGF (100ng/ml) treatment in a fixed cell assay. The full-length mu opioid receptor (MOR) with an N-terminal signal sequence Flag epitope (SSF-MOR) was used to control for receptor specific effects. For transfection and maintenance of a stable cell lines, the lipofection reagent Lipofectamine 2000 (Invitrogen) and the selection antibiotic Geneticin were used.

### *Pharmacological Experimental Details:*

For all fixed cell pharmacological experiments, the treatments were conducted for one hour followed by fixation and immunofluorescence microscopy that is detailed in additional methods. The concentrations and usage specifications are listed below.

<u>Compound Name</u>	<u>Protein Target</u>	<u>Concentration</u>	<u>Supplier</u>	<u>Catalog #</u>
Y-27632	ROCK Inhibitor	5 $\mu$ M	Cayman	10005583
U0126	MEK Inhibitor	10 $\mu$ M	Cayman	70970
Akt1/2 Kinase IH	Akt 1/2 Inhibitor	500nM	Sigma-Aldrich	A6730-5MG
SC-79	Akt Activator	4 $\mu$ g/mL	Tocris	4635
API-1	Akt Inhibitor	10 $\mu$ M	Tocris	3897
U73122	PLC Inhibitor	10 $\mu$ M	Enzo Life	BML-ST391-
Chelerythrine	PKC Inhibitor	10 $\mu$ M	Sigma-Aldrich	C2932-1MG
PP2	cSrc Inhibitor	500nM	EMD Millipore	529573-1MG
Wortmannin	PI3K Inhibitor	10 $\mu$ M	Enzo Life	BML-ST415-
LY294002	PI3K Inhibitor	10 $\mu$ M	Tocris	1130
Nerve Growth Factor	TrkA	100ng/ $\mu$ L	BD Biosciences	356004
SF1670	PTEN Inhibitor	10 $\mu$ M	Echelon	B-0350
bpV (Phen)	PTEN Inhibitor	10 $\mu$ M	Enzo Life	ALX-270-204-
bpV (HOptic)	PTEN Inhibitor	10 $\mu$ M	Enzo Life	ALX-270-206-
AS1938909	SHIP2 Inhibitor	5 $\mu$ M	EMD Millipore	565840-10MG

Forskolin	AC Activator	5 $\mu$ M	Tocris	1099
$\beta$ -chlornaltrexamine	$\delta$ -Opioid	1 $\mu$ M	Sigma-Aldrich	A00055
DADLE	DOR agonist	10 $\mu$ M	Tocris	3790
SNC80	DOR agonist	2mg/kg	Tocris	0764
DAMGO	MOR agonist	10 $\mu$ M	Tocris	1171

#### *Primary Trigeminal Ganglion Cell Isolation:*

Glass coverslips (Corning) were placed into 6-well plates and pre-coated with poly D-lysine and Laminin to enhance neuron adhesion and promote cell survival before plating. Adult mice (p9-15) were obtained from the animal facility and euthanized via CO<sub>2</sub> asphyxiation. Using large scissors, the head is removed. With small scissors, the skin covering the skull is removed. Cutting away the top of the skull then exposes the brain. The brain is removed by lifting towards the posterior and by cutting Cranial Nerve V. With the brain removed, the Trigeminal Ganglia (TG) is visible as longitudinal bundles of tissue. These bundles are cut into small pieces and placed into ice cold HBSS. A sterile filtered papain solution is applied and incubated for 12 minutes at 37°C. The papain solution is removed, and a dispase/collagenase is applied for 15-20 minutes at 37°C. Upon completion of digestion, the TG tissue is triturated with a fire polished pasture pipet 3-5 times, or until the neurons appear visual dissociated. The TG cells are then plated onto the poly D-lysine coated coverslip within a cloning ring to create a more densely populated cell area. After 5 hours, the cloning ring can be removed, and fresh neural basal media (Invitrogen) can be added to each well.

#### *Transfection of Primary Neurons:*

Lipofectamine 2000 lipofection reagent (Invitrogen) was used per manufactures instructions for DNA transfections. Briefly, 2 $\mu$ g of DNA Plasmid and 5-7 $\mu$ l of Lipofectamine reagent were incubated in 250 $\mu$ l of Opti-MEM (Invitrogen) for 5 minutes at room temperature. These mixtures were then combined and let to complex for 25 minutes. The neuronal growth media was removed, but saved, and the DNA-Lipofectamine solution was added dropwise to the cells containing 1ml of additional Opti-MEM and let to incubate at 37°C for 4-5 hours. Upon completion of the transfection, the reagent-containing medium was removed and replaced with saved neuronal growth medium. Identical conditions and protocol were performed for PC12 cell transfections; however, after transfection F12K + 10% horse serum and 5% fetal bovine serum containing medium was used.

#### *Immunofluorescence and Fluorescence Microscopy:*

Cells were plated on poly-D-lysine coated glass coverslips (Corning) and grown for 24-48 hours. For PC12 SSF-DOR intracellular retention experiments, cells were treated with NGF (100ng/ml) for 1 hour followed by fixation in 4% paraformaldehyde, pH 7.4. The cells were blocked in calcium magnesium containing phospho buffered saline (PBS) with 5% fetal bovine serum, 5% 1M Glycine, and 0.75% Triton X-100. The SSF-DOR was labeled with anti-FLAG M1 antibody (1:1000) conjugated with Alexa-647 (Molecular Probes), and a trans-Golgi marker, anti-TGN-38 (1:2000, Sigma-Aldrich cat#: T9826) rabbit polyclonal for 1 hour in the blocking buffer. The coverslips were washed thrice in calcium magnesium PBS followed by addition of Alexa-568 Goat anti-rabbit secondary (1:1000) antibody in blocking buffer for 1 hour. The coverslips were again washed thrice in calcium magnesium PBS and mounted onto coverslips in calcium magnesium containing anti-fade mounting medium. Following mounting, confocal imaging was performed at 60X magnification using a Nikon TE-2000 inverted microscope with live cell imaging capabilities. Images of representative fields were taken. For all fixed-cell imaging experiments, a minimum of the average fluorescence ratios of 100 cells were quantified to ensure a representative population. Additionally, a minimum of three biological replicates were performed to confirm all results.

#### *Cycloheximide Assay:*

PC12 SSF-DOR cells were plated onto poly-D-lysine coated coverslips in a 24-well plate and incubated overnight at 37°C. NGF (100ng/ml) was added to all appropriate samples for 2 hours to achieve complete intracellular retention of DOR. The media was changed to Opti-MEM + Glutamax (Invitrogen) with cycloheximide (3µg/ml) for 1 additional hour with NGF +/- various pharmacologic inhibitors and activators. The cells were then fixed in 4% paraformaldehyde, and blocked in the immunofluorescence-blocking buffer. Immunofluorescence of SSF-DOR and intracellular compartmental markers were performed as described previously.

#### *DOR Internalization Surface Control Assay:*

Cells were incubated with Alexa-647 M1 antibody for 15min at room temperature (1:500). The antibody was removed, and the cells were washed with Calcium-Magnesium PBS to remove residual antibody. Pharmacologic treatments were added for 1 hour at concentrations used during the pharmacological experiments. After 1 hour, a secondary Alexa-568 antibody to the Flag-M1 was applied at 4°C for 15min (1:1000) to reduce the amount of potential internalization from that

point on. Cells were washed twice with PBS  $\text{Ca}^{2+}$   $\text{Mg}^{2+}$  and fixed in 4% PFA pH 7.4 for 30min. Cells were again washed 3x with PBS  $\text{Ca}^{2+}$   $\text{Mg}^{2+}$  and mounted to coverslips for imaging. Confocal stacks were taken of the cells for no treatment, NGF (100ng/ml), Wortmannin (10 $\mu$ M), LY294002 (10 $\mu$ M), and DADLE (10 $\mu$ M, [D-Ala<sup>2</sup>, D-Leu<sup>5</sup>]-Enkephalin) treatments.

*Live-Cell Imaging of NGF-induced Retention and PTEN IH Release of DOR:*

To visualize DOR in live cells, eGFP was N-terminally tagged to DOR in place of the FLAG-tag previously described. PC12 cells or TG neurons were transfected with eGFP-DOR using Lipofectamine 2000 (Invitrogen) as described previously. Before imaging, cells were transferred to poly-D-lysine coated coverslips. Cells were imaged at 60X magnification using a Nikon TE-2000 inverted microscope with a 37 degree heated enclosure and 5%  $\text{CO}_2$  environment. Images were acquired every minute for 1.5-2 hours. Following 5 min of baseline imaging, pharmacological treatment was added to the coverslip. The images were analyzed and quantified using Image J analysis software. In live cell analysis, due to enhanced consistency from internal controls within a cell, a minimum of 10 cells were quantified from three or more biological replicates to provide sufficient statistical power.

*Immunoblotting and detection:*

PC12 cells expressing SSF-DOR were plated onto 6-well dishes and incubated overnight at 37°C. NGF (100ng/ml), PTEN, Akt, and SHIP2 inhibitors were added to all appropriate samples alone or in combination for 1 hour to recapitulate the experimental conditions used in our imaging experiments looking at intracellular retention of DOR. Cells were scrape harvested and collected by centrifugation. Cell lysis was carried out with lysis buffer containing 2% SDS, 60mM Tris-HCL pH 6.8, Complete Mini EDTA-free (Roche T00004), and PhosStop Tab (Roche A00173). Cell lysate was heated to 95°C to achieve complete lysis, and spun to clarify the supernatant. The protein lysate was combined with 4x Laemmli Sample Buffer from BioRad (cat no. 1610747) with fresh BME and DTT added. The samples were heated to 95°C and electrophoresed using the Mini-PROTEAN system and 4-15% Mini-PROTEAN TGX Stain-free Protein Gels (BioRad cat no. 4568083). Phosphorylation of Akt was assed via immunoblotting with pAkt S473 (cat no. 4060S) and pAkt T308 (cat no. 13038S) primary antibodies from Cell Signaling, and secondary goat-anti rabbit IgG antibody (BioRad cat no. L00019). Detection was achieved using the Clarity Western ECL Substrate (BioRad cat no. 1705601) and the BioRad ChemiDoc Touch imager. Immunoblot

densitometry was performed using the ImageLab 5.2.1 software from BioRad with total protein normalization performed using the BioRad Stain-Free technology according to BioRad protocol (<http://www.bio-rad.com/webroot/web/pdf/lsr/literature/10040758.pdf>, (Gürtler et al., 2013)).

#### *Live-Cell Imaging of cAMP Activity:*

We evaluated activation of DOR by its specific agonist DADLE with a live cell Förster resonance energy transfer (FRET) reporter of cAMP, EPAC (Ponsioen et al., 2004; de Rooji et al., 1998). The EPAC sensor contains a CFP (405nm excitation, 470nm emission) and YFP (515nm excitation, 530nm emission) fluorescent protein linked by a cAMP binding domain. When cAMP binds to the sensor, a decrease in the FRET signal (CFP excitation at 405nm and YFP emission at 530nm) is observed. Experiments followed a validated paradigm for cAMP measurements (Sneddon et al., 2000; Bin et al., 2013). Baseline cAMP was stimulated with Forskolin (5 $\mu$ M) and subsequent inhibition following DOR agonist addition was calculated via the EPAC CFP/FRET ratio. Additionally, blocking the pool of surface receptors with the irreversible DOR antagonist, CNA (1 $\mu$ M), can prevent the basal surface pool of DOR from signaling to isolate the response induced following forced surface trafficking of DOR. As an unbiased method of quantifying DOR functional activity, we have designed an ImageJ plugin to quantify the % of DOR-induced cAMP inhibition and DOR agonist-induced endocytosis in the same cells. These analysis methods are explained in Figure S3.

#### *Ca<sup>2+</sup> Imaging and Electrophysiology:*

TG neurons were prepared from adult rats as previously described (Vaughn and Gold, 2010). Two hours after plating, neurons were transferred to an L-15 based media (Vaughn and Gold, 2010) (Harriott et al., 2012), where they were stored at room temperature for no more than 8 hrs. For Ca<sup>2+</sup> imaging, neurons were loaded with Fura-2 AM in pluronic F127 as previously described (Lu et al., 2006). They were then transferred to bath solution containing vehicle or bpV(Phen) (10 $\mu$ M) where they were incubated at 35°C for 30 minutes prior to study. Depolarization-induced Ca<sup>2+</sup> transients were evoked with high K<sup>+</sup> (30mM, 800ms) every 2 minutes. SNC80 (1 $\mu$ M) was then applied 1 minute prior to the application of SNC80 with high K<sup>+</sup>. The variance around the mean baseline response of all neurons studied in each group was used to identify neurons responsive to SNC80, where a decrease > 2 standard deviations from the mean change observed at baseline was considered a response to SNC80. At the end of each experiment, neurons were

challenged with capsaicin (500nM for 500ms). Neurons used for voltage-clamp experiments were processed in the same way as those used for Ca<sup>2+</sup> imaging, except they were not loaded with fura-2. Inclusion/exclusion criteria were pre-established and were based on the resting Ca<sup>2+</sup> levels, which in healthy neurons is below 150 nM, the stability of the magnitude of the evoked Ca<sup>2+</sup> transient, which in healthy neurons, is neither consistently increasing, nor consistently decreasing over at least 3 applications of high K<sup>+</sup> at an inter-stimulus interval of 3 minutes, and the rate at which intracellular Ca<sup>2+</sup> level returns to baseline after each depolarizing evoked transient, where the recovery is complete within 4 minutes in healthy neurons. Voltage-gated Ca<sup>2+</sup> currents were recorded with bath and electrode solutions composed to minimize voltage-gated Na<sup>+</sup> and K<sup>+</sup> currents, as previously described (Vaughn and Gold, 2010). Currents were evoked from a holding potential of -60 mV, to a test potential of -5 mV every 5 seconds. When currents stabilized after obtaining whole cell access, SNC80 (1μM) was applied via a gravity perfusion system. A decrease > 2 x the standard deviation from the mean baseline current was considered a response to SNC80.

#### *In Vivo PTEN IH and Surface Receptor Quantification:*

To establish a time point in mice for PTEN IH induced surface trafficking of DOR, and visualize newly trafficked receptors, we subcutaneously injected a saline control, or the PTEN IH bpV(Phen) at 3mg/kg and returned the mice to their home cage. At two hour intervals (2hr, 4hr, 6hr) TG neurons were dissociated following the aforementioned protocol. Instead of plating onto coverslips for *in vitro* culturing, we isolated the dissociated neurons and incubated them with Deltorphin II Cy3 (100nM) and Hoechst stain for 10min on ice. The neurons were then centrifuged at 5x gravity and washed with PBS. The labeled neuron suspension was then transferred to a coverslip for live-cell confocal imaging performed at 37°C and 20X magnification using a Nikon TE-2000 inverted microscope. The % of Hoechst positive Deltorphin II Cy3 expressing cells was determined at each time point.

#### *In Vivo Analgesia Assay:*

All experiments were done in accordance with IACUC-approved protocols at the University Illinois at Chicago. Subjects were male C57BL6/J mice, between 9-12 weeks old. Mechanical hyperalgesia was tested using the manual von Frey test following standard protocols established by the Pradhan lab (Pradhan et al. 2013). Baseline mechanical responses were determined, and

inflammatory pain was induced by injecting 13 $\mu$ L of Complete Freund's Adjuvant into the plantar surface of the left hindpaw. On the test day, mice were randomly allocated to different test groups, and injected with vehicle or bpV (Phen) (3 mg/kg Subcutaneous, SC), and returned to their home cages. Four hours post-injection, mice were injected with vehicle or SNC80 (2 mg/kg Intraperitoneal, IP) and mechanical hyperalgesia was assessed 45 minutes later. To confirm specificity to DOR, we treated mice with naltrindole (10mg/kg Subcutaneous, SC), a DOR-selective antagonist, 1 hour before SNC80. The investigator was partially blinded, and was not aware if animals received bpV (Phen) or vehicle.

#### *Statistics and Data Analysis:*

Statistical analyses were performed using GraphPad Prism 5 software, and appropriate statistical tests were chosen based on sample size and distribution. For statistical analysis of the quantified imaging data, two-tailed unpaired t-tests were performed between the different experimental conditions and controls. For calcium imaging in neurons, sample size was based on a preliminary analysis of control neurons in which we determined the proportion of neurons in three fields of view from each of two animals, that were responsive to SNC80, where a neuron was considered responsive to SNC80 if the depolarization evoked Ca<sup>2+</sup> transient in the presence of SNC80 was reduced by more than 2 standard deviations from the mean of at least 3 transients evoked prior to the application of SNC80. These preliminary results were used in a power analysis in which we estimated the number of neurons needed to detect a significant increase in the proportion of SNC80 responsive neurons. To compare the population changes in DOR positive neurons, a two-tailed Fisher's Exact test was performed. For the animal data, a power analysis was performed based upon our initial experiment, and a sample size of >5 was estimated to be adequate. We choose to have our minimum sample size be 10 to exceed concerns due to limited sample size. To analyze the significance of the *in vivo* animal data, a one-way non-parametric ANOVA was performed followed by a Kruskal-Wallis posttest comparing all columns. A p-value of < 0.05 was considered statistically significant. All images were quantified using macros contained within the ImageJ software package. Figures were constructed with ImageJ and Adobe Photoshop CS6.

**Acknowledgements:**

The authors would like to thank Claudia Almaguer, Zara Weinberg, and Drs. Rachel Vistein, Amanda Soohoo, Shanna Bowman, and Cary Shiwarski for technical help and comments. We thank Dr. Alison Barth, Joanne Steinmiller, Jen Dry-Henich, Dr. Rebecca Seal, and Adam Goldring for providing help with isolation of TG neurons. We thank Drs. Nathan Urban, Adam Linstedt, Tina Lee, Peter Friedman, Guillermo Romero, Jean-Pierre Vildardaga, and Alessandro Bisello, for reagents, comments and suggestions. We also thank Drs. Mark von Zastrow, John Williams, and Seksiri Arttamangkul for helpful discussions and reagents. A.A.P. was supported by NIH DA031243, and M.A.P. was supported by NIH DA024698 and DA036086.

## Figures and Figure Legends:

### Figure 1

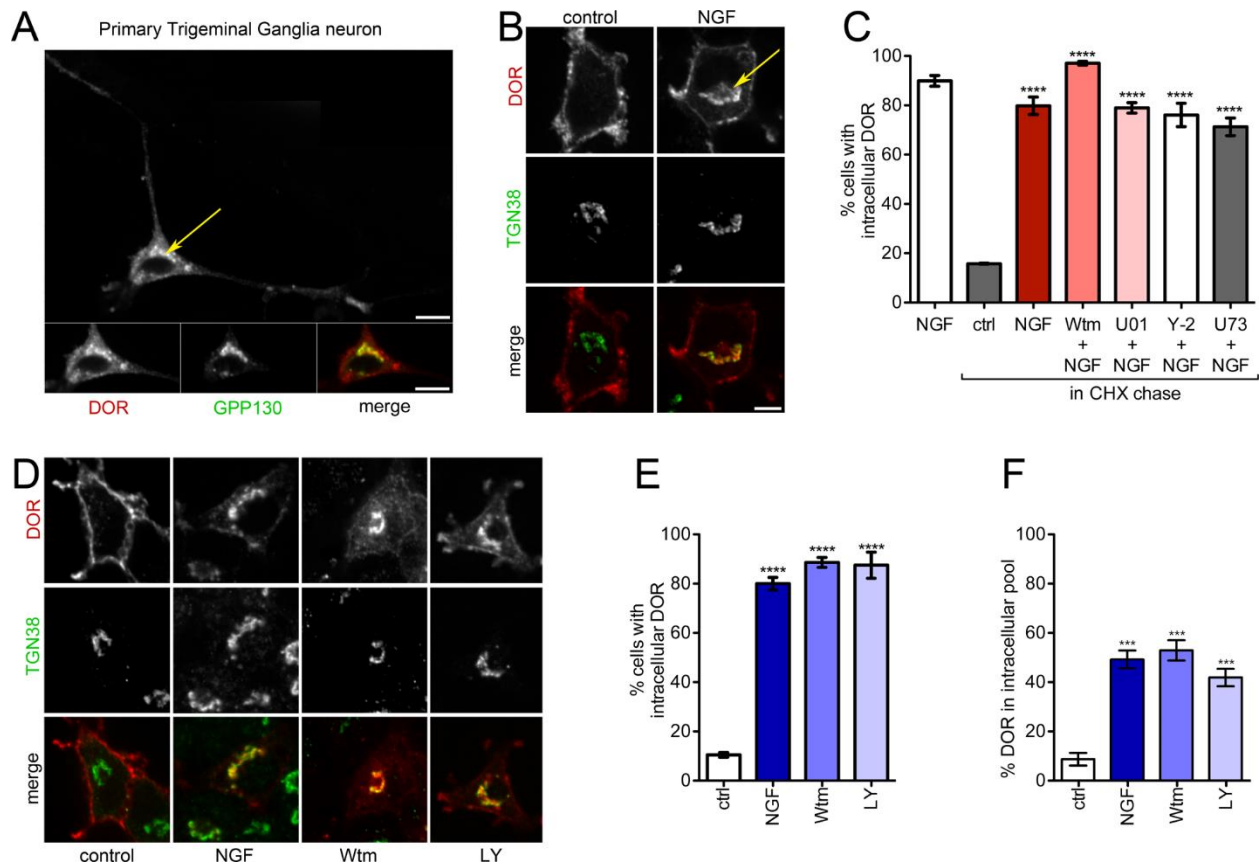


**Figure 1: PI3K is required for DOR delivery to the surface from intracellular pools that overlap with the Golgi.** **A.** Representative confocal image from a fixed primary cultured TG neuron expressing a FLAG-tagged DOR. Internal DOR (red in merge) colocalizes with the Golgi marker GPP130 (green in merge). **B.** Example image of a PC12 cell showing surface DOR. NGF treatment (60 min at 100ng/ $\mu$ L) causes internal DOR accumulation (arrow), colocalizing with TGN-38 (green). **C.** NGF-treated PC12 cells, chased with cycloheximide (CHX) for 1 hour to prevent additional DOR delivery, in the presence of inhibitors of MEK (10 $\mu$ M U0126, noted as U01), ROCK (5 $\mu$ M Y-27632, noted as Y-2), PLC (10 $\mu$ M U73122, noted as U73). The percentage of cells with Golgi-localized DOR is shown ( $n > 100$  cells in each condition; mean  $\pm$  s.e.m.; \*\*\*\* $P < 0.0001$ ). None of the inhibitors prevented NGF-mediated DOR retention. **D.** Representative images showing that inhibition of PI3K with 10 $\mu$ M Wortmannin (Wtm) or LY294002 (LY) is sufficient to cause DOR retention, comparable to NGF. **E.** Quantitation of percentage of cells with DOR Golgi

localization, showing that PI3K inhibition with Wtm or LY is sufficient for DOR retention ( $n > 100$  cells each; mean  $\pm$  s.e.m.; \*\*\*\* $P < 0.0001$ ). **F.** The percentage of total DOR in intracellular pool, calculated by image analysis and quantification as explained in Figure supplement 1, increases upon inhibition of PI3K with Wortmannin (10 $\mu$ M) or LY294002 (10 $\mu$ M) similar to NGF ( $n=47, 73, 45,$  and  $80$  cells for control, NGF, Wtm, and LY; mean  $\pm$  s.e.m., \*\*\* $P < 0.001$ ; by two-sided t-test vs. control).

**Figure 1 Supplement 1: Workflow of quantitative image analysis for determining the percentage of total DOR retained in intracellular pools.**

**Figure 1 Supplement 2. Inhibition of PKC, Akt, or Src do not cause DOR retention in intracellular pools.**

**Figure 2**

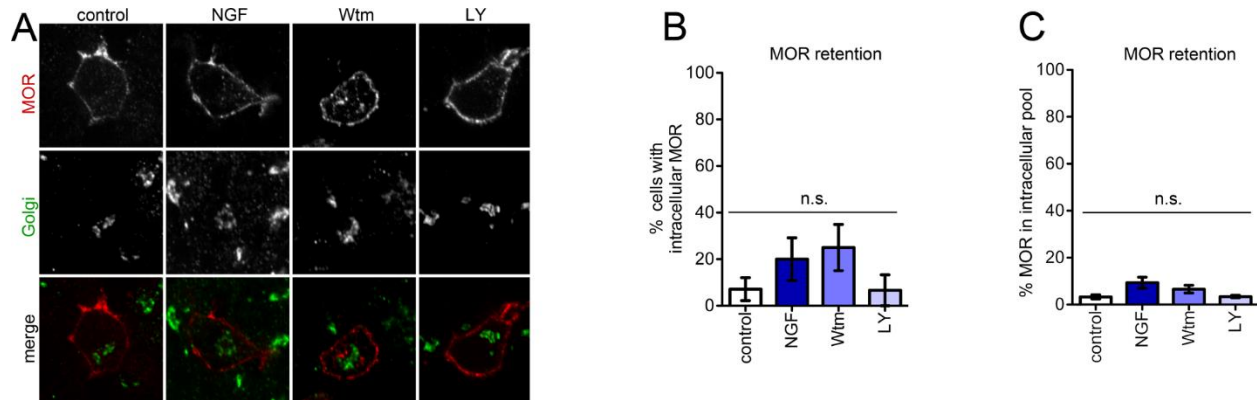


**Figure 2: PI3K inhibition does not induce MOR retention.** **A.** Representative images from PC12 cells expressing MOR, treated with NGF or the PI3K inhibitors Wortmannin (Wtm) or LY294002 (LY). Unlike with DOR, neither NGF treatment nor PI3K inhibition caused MOR retention. **B.** Quantitation of the percentage of cells showing MOR retention ( $n > 50$  cells each; mean  $\pm$  s.e.m.; n.s. denotes not significant). **C.** The percentage of total MOR in intracellular pool, calculated by image analysis and quantification as explained in Figure supplement 1. The percentage does not increase significantly upon addition of NGF or the PI3K inhibitors. ( $n=81, 43, 136,$  and  $111$  cells for control, NGF, Wtm, and LY; mean  $\pm$  s.e.m., n.s = no significance ( $P > 0.05$ ) by two-sided t-test vs. control).

**Figure 3**

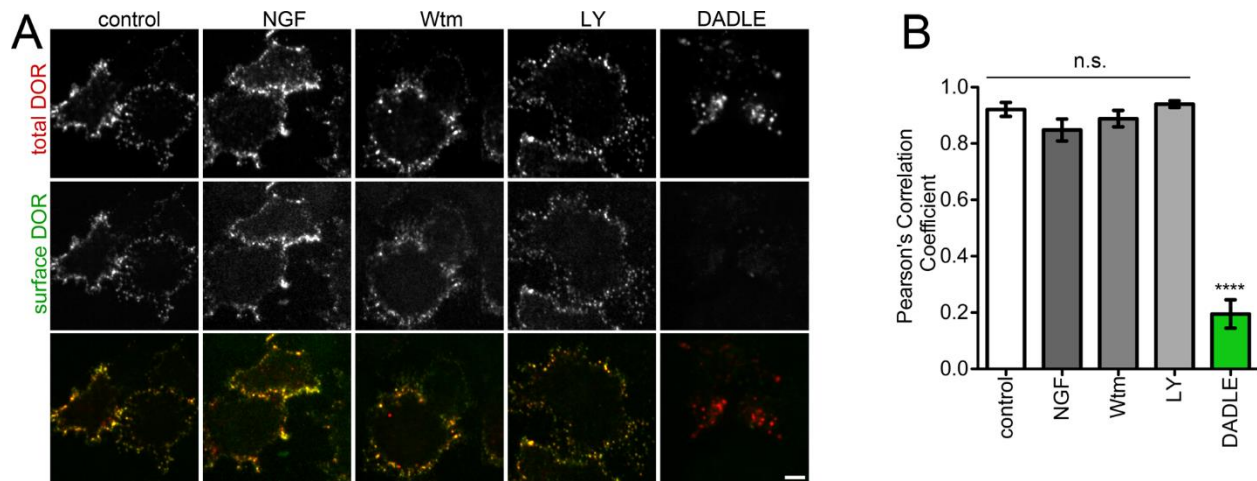


**Figure 3: NGF treatment or PI3K inhibition do not cause endocytosis of surface DOR. A.** Representative images from two-color assay for DOR endocytosis, by selectively labeling the surface vs. total pool of DOR, as described in Methods. Neither NGF nor PI3K inhibition caused endocytosis of pre-labeled surface DOR. The DOR agonist DADLE, as a control, caused robust endocytosis with little remaining surface DOR. **B.** Pearson's Correlation Coefficients of colocalization of the primary and secondary antibody. High correlation denotes minimal endocytosis. DADLE significantly reduced the correlation, consistent with endocytosis ( $n > 50$  cells each; mean  $\pm$  s.e.m.; \*\*\*\* $P < 0.0001$ ). Scale bars are  $5\mu\text{m}$ .

**Figure 4**

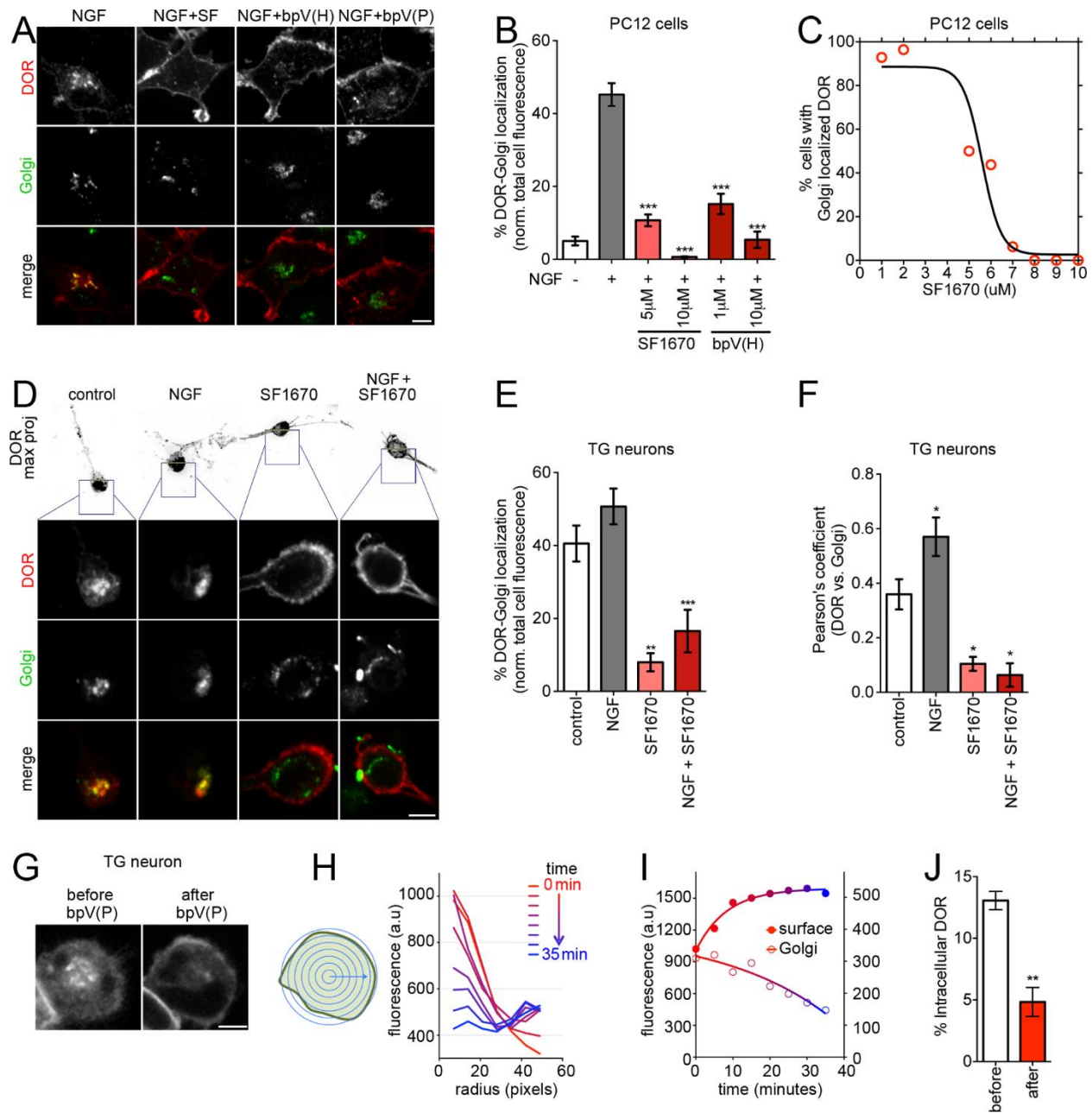


**Figure 4: PTEN inhibition releases Golgi-retained DOR and promotes surface delivery in PC12 cells and TG neurons.** **A.** Example images for PC12 cells expressing FLAG-tagged DOR, treated with NGF, with inhibition of PTEN by 10 $\mu$ M of either SF1670 (SF), bpV HOptic (bpV(H)), or bpV (Phen) (bpV(P)). PTEN inhibition abolishes Golgi retention of DOR. **B.** Image analysis and quantification shows a significant reduction in the percentage of total DOR fluorescence that overlaps with the Golgi upon PTEN inhibition ( $n > 100$  cells each; mean  $\pm$  s.e.m.; \*\*\* $P < 0.001$ ). **C.** A dose response curve for SF1670-mediated loss of Golgi-localized DOR in NGF-treated PC12

cells. **D.** Localization of expressed DOR in TG neurons with or without NGF, with and without the PTEN inhibitor (SF1670, 10 $\mu$ M). PTEN inhibition drives DOR to the surface. **E.** The fraction of Golgi-localized DOR in primary TG neurons, calculated as in B, decreased significantly upon PTEN inhibition (SF1670, 10 $\mu$ M) ( $n > 10$  neurons each; mean  $\pm$  s.e.m.; \*\* $P < 0.01$ , \*\*\* $P < 0.001$ ). **F.** Pearson's Correlation Coefficients show decreased colocalization between DOR and the Golgi upon SF1670 addition ( $n > 10$  neurons each; mean  $\pm$  s.e.m.; \* $P < 0.05$ ). **G.** Example images from TG neurons expressing GFP-DOR imaged live before and after addition of PTEN inhibitor bpV(Phen) (10 $\mu$ M). **H.** Radial profile analysis of the images (schematic) revealed a decrease in the fluorescence intensity of the centre and an increase in the periphery over time following PTEN inhibition (added at  $t = 1$ min). Time is depicted as a color gradient from red to blue. **I.** PTEN inhibition causes an increase in DOR fluorescence in the surface and a decrease in fluorescence in Golgi regions. **J.** Quantitation across multiple neurons show a decrease in the percentage of intracellular DOR normalized to the total cell fluorescence ( $n = 10$ ; mean  $\pm$  s.e.m.; \*\* $P < 0.01$ ). Scale bars are 5 $\mu$ m.

**Figure 5**

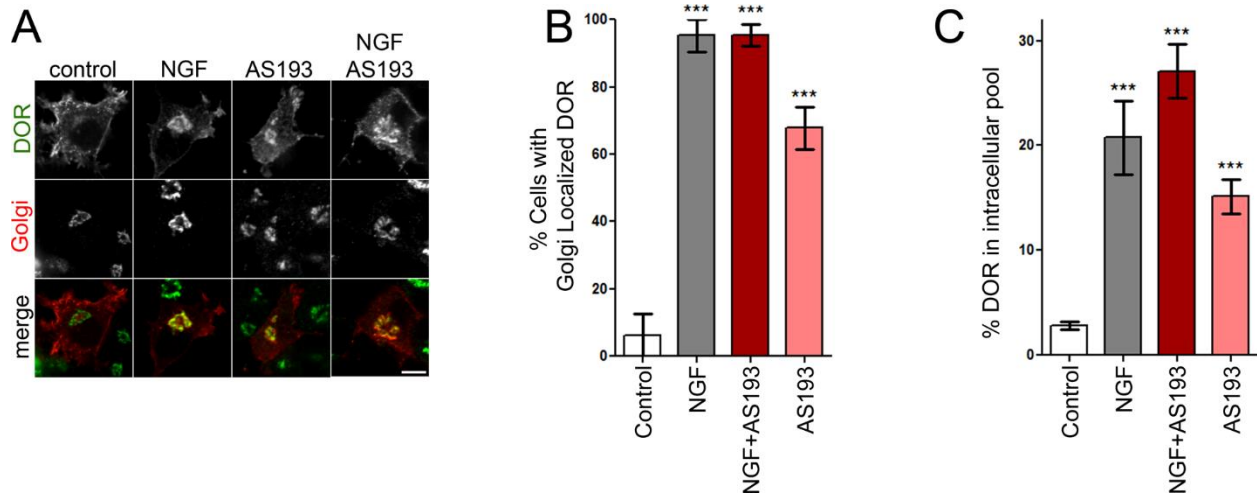


**Figure 5: SHIP2 inhibition causes intracellular accumulation of DOR, similar to NGF. A.** Example images for NGF-treated PC12 cells expressing FLAG-tagged DOR with inhibition of SHIP2 by AS1938909 (AS193, 5 $\mu$ m). AS193 causes DOR retention in the absence of NGF. **B.** Quantitation shows a significant increase in the percentage of cells with Golgi localized DOR after AS193 compared to control treatment (n >100 cells each; mean  $\pm$  s.e.m.; \*\*\* $P$ <0.001). **C.** Similar to NGF treatment, the percentage of total DOR fluorescence in the Golgi increases upon AS193 compared to control treated cells (n >100 cells each; mean  $\pm$  s.e.m.; \*\*\* $P$ <0.001).

**Figure 5 Supplement 1: Schematic of phosphoinositide conversion and summary of results of manipulation.**

**Figure 6**

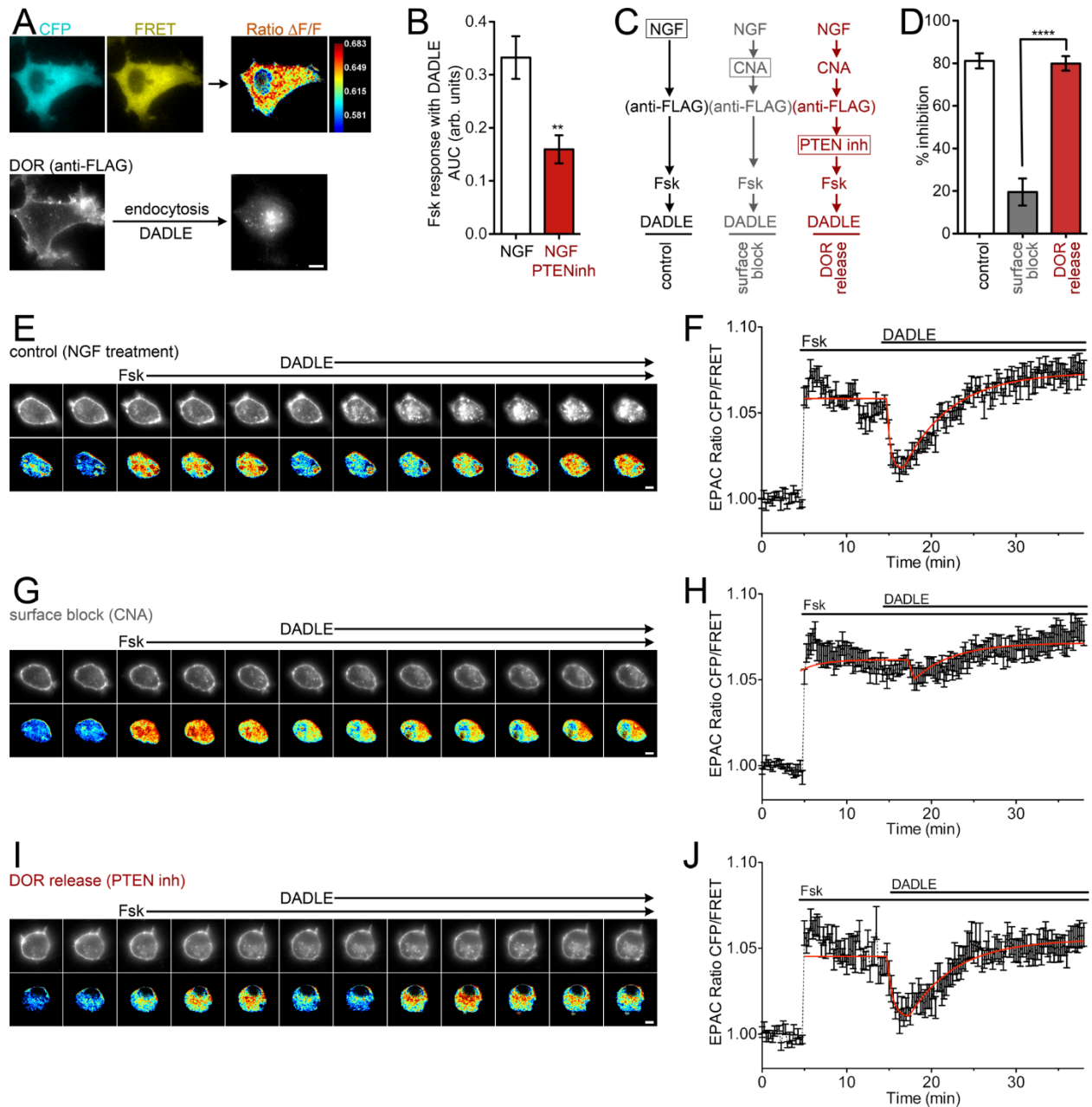


**Figure 6: The pool of DOR delivered to the surface by phosphoinositide conversion is functional.** **A.** Schematic of ratiometric analysis for cAMP measurement using the Epac sensor. The CFP, FRET, and DOR were imaged and followed live in the same cells. FRET ratio image is mapped to blue for low cAMP and red for high cAMP. **B.** Inhibition of Fsk-mediated increases in cAMP by DADLE was measured as an index of the activity of surface DOR. In NGF-treated PC12 cells, DADLE-mediated inhibition was significantly enhanced by PTEN inhibition (SF1670, 10 $\mu$ M), as seen by a lower Fsk response ( $n > 15$  each; mean  $\pm$  s.e.m.;  $**P < 0.01$ ). **C.** Schematic of

experiments to isolate the functional effect of DOR delivery by PTEN inhibition after surface DOR is blocked by CNA (1 $\mu$ M). **D.** The percentage of inhibition of cAMP response under the three conditions show recovery of DADLE-mediated inhibition by PTEN inhibition after surface DOR is blocked by CNA (n >20 cells each; mean  $\pm$  s.e.m.; \*\*\*\* $P$ <0.0001). **E - J.** Example images (E, G, I) from a time lapse movie showing FRET changes and DOR localization after DADLE in the three experimental conditions. The average FRET change (F, H, J) over time from multiple cells (n>20 in each condition) for each experimental condition is shown. Red lines show curve fits for the Fsk response, DADLE response, and desensitization, over time. Error bars are s.e.m. Scale bars are 5 $\mu$ m.

**Figure 6 Supplement 1: Validation of live-cell Epac sensor imaging assay for evaluating DOR activity following agonist administration.**

**Figure 7**

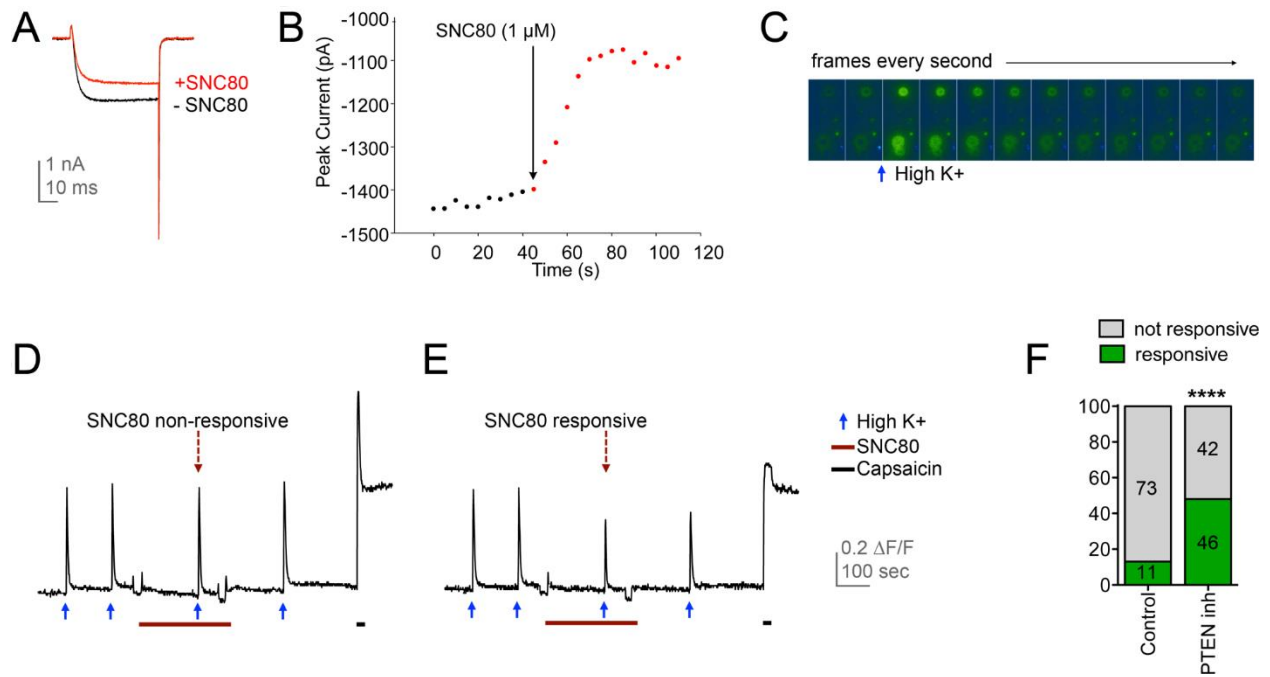


**Figure 7: Phosphoinositide conversion delivers a functional pool of endogenous DOR in TG neurons.** **A.** Example calcium current traces from a voltage-clamped TG neuron after PTEN inhibition, before and after SNC80, showing robust decrease in current after SNC80. **B.** Time course of decrease in current after SNC80 bath application to a TG neuron after PTEN inhibition. **C.** Live imaging of calcium transients of TG neurons in response to high K, detected by Fura-2AM loading. **D-E.** Example traces of Fura-2AM responses showing a neuron that is non-responsive to SNC80 (D) and one that is responsive (E). **F.** Quantification of the fraction of neurons that respond to SNC80 with and without pretreatment with bpV(Phen). The number of cells in each condition is noted. PTEN inhibition induced a significant increase in the fraction of neurons that respond to SNC80 (\*\*\*\* $P < 0.0001$ ).

**Figure 8**

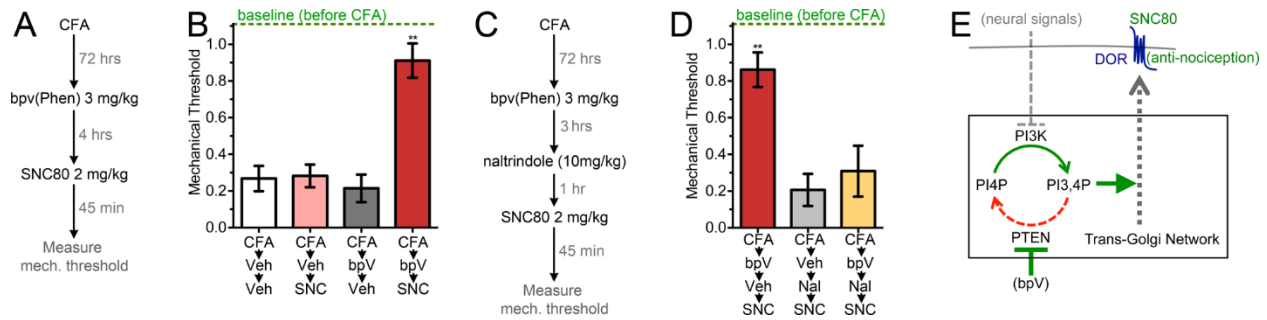


**Figure 8. Stimulated DOR delivery enhances the antinociceptive efficacy of the DOR agonist SNC80.** **A.** The threshold for mechanical hyperalgesia was determined using a manual von Frey hair, in mice after intraplantar injection of CFA. A schematic shows the timeline and doses used in our experiments. **B.** Mechanical responses in mice show that pre-treatment with PTEN inhibitor significantly increased the pain-relieving effects of SNC80 (mean  $\pm$  s.e.m.; \*\* $P < 0.01$ ). SNC80 or bpv (Phen) on their own did not show antinociception compared to control vehicle-injected mice. The mechanical threshold before CFA treatment was used as baseline (green dashed line). **C.** A schematic showing the timeline and doses used in testing whether naltrindole blocks the bpV(Phen)-mediated increase in SNC80 efficacy. **D.** Naltrindole abolishes the increase in SNC80-mediated antinociception caused by PTEN inhibition (mean  $\pm$  s.e.m.; \*\* $P < 0.01$ ). **E.** Proposed model for how phosphoinositide conversion provides a Golgi checkpoint to regulate DOR export and surface availability. Stimulated surface delivery by PTEN inhibition increases pain-relieving effects of SNC80, and provides a proof of mechanism for this strategy to improve the efficacy of existing DOR agonists.

Supplemental Figures:

**Figure 1 Supplement 1**

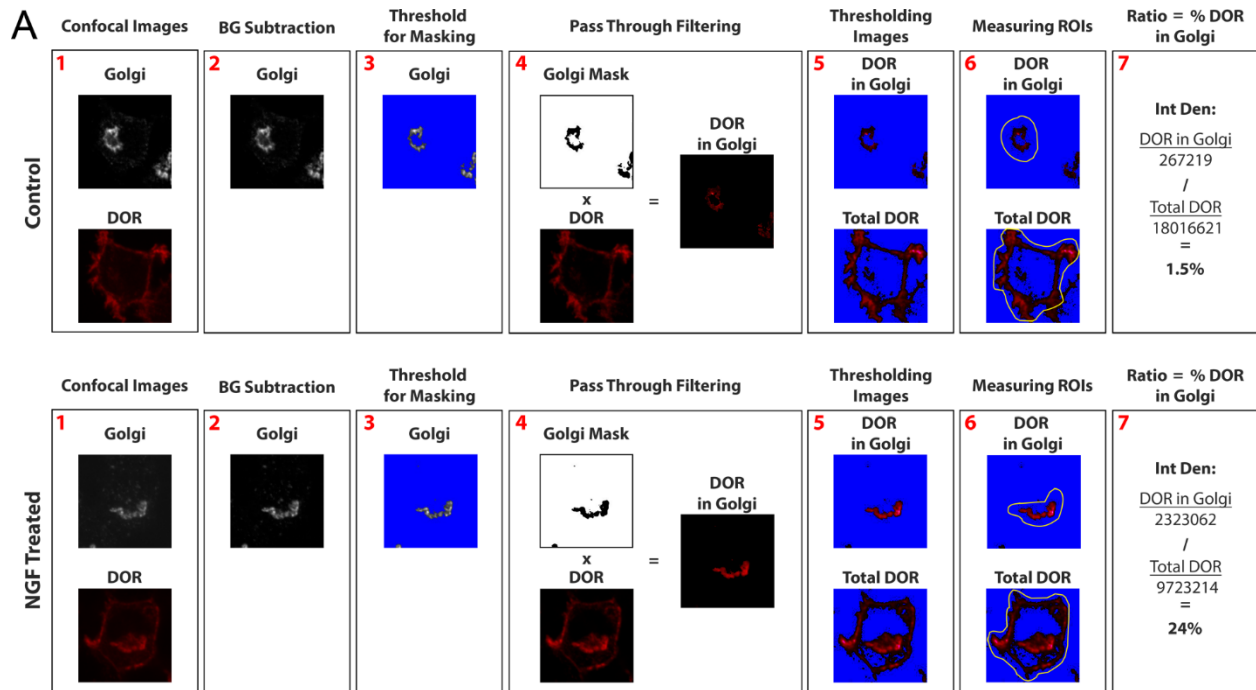


**Figure 1 Supplement 1. Workflow of quantitative image analysis for determining the percentage of total DOR retained in intracellular pools. A.** Analysis method for the fixed-cell quantification of the % of DOR within the Golgi compared to the total cell fluorescence. 1) Confocal images of fluorescently labeled DOR and the Golgi marker (TGN-38) were acquired. 2) The background fluorescence was subtracted from the Golgi channel. 3) The Golgi channel was thresholded to construct a mask of the Golgi region. 4) The Golgi mask was used as a pass through filter by converting the Golgi mask to a binary image and multiplying it by the DOR image. This allows for the measurement of the amount of DOR fluorescence within the Golgi region. 5) The DOR within the Golgi and total DOR images were thresholded to remove bias from background zero pixels. 6) Regions of interest (ROIs) were drawn for the Golgi region and the total DOR signal. Measurements were then made in ImageJ to calculate the total fluorescence within these two regions. 7) The fluorescence signal for DOR within the Golgi was then divided by the total DOR fluorescence signal to get a ratio of the % of DOR within the Golgi compared to the total expression of DOR. An example is shown for this analysis and calculation for a control treated cell where there is little to no Golgi DOR, and an NGF treated cell where there is an apparent Golgi pool of DOR.

## Figure 1 Supplement 2

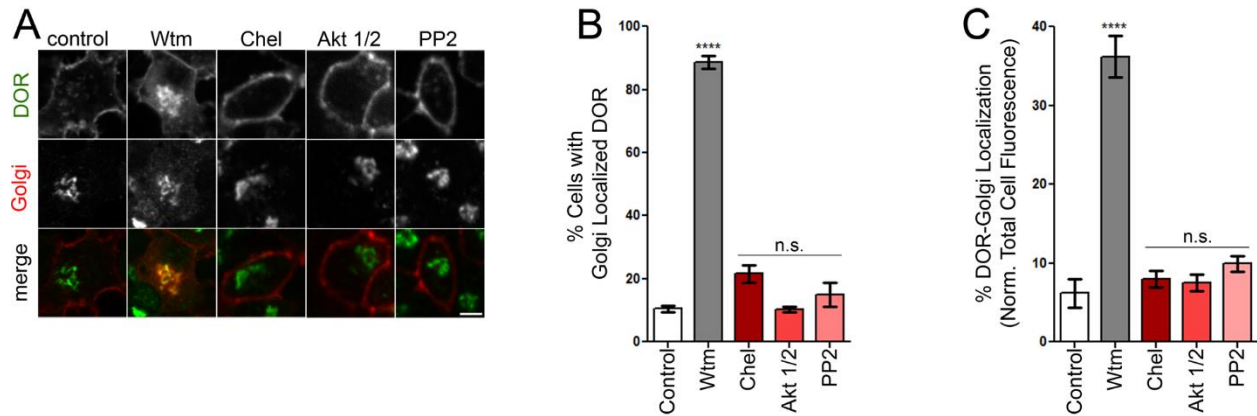


**Figure 1 Supplement 2. Inhibition of PKC, Akt, or Src do not cause DOR retention in intracellular pools. A.** Example images for PC12 cells expressing FLAG-tagged DOR treated with inhibitors of PKC by Chelerythrine (Chel, 10 $\mu$ M), Akt by Akt1/2 Kinase Inhibitor (Akt1/2, 500nM), or cSrc by PP2 (500nM). PI3K inhibition by Wortmannin (Wtm, 10 $\mu$ M) was used as a positive control. **B-C.** Unlike Wtm, inhibition of PI3K downstream targets PKC, Akt, and cSrc do not cause a significant increase in the percentage of cells with intracellular DOR (B), nor the percentage of total DOR fluorescence localized to the Golgi compared to control (C) (n >100 cells each; mean  $\pm$  s.e.m.; \*\*\*\* $P$ <0.0001, n.s. = not significant compared to control).

Figure 5 Supplement 1

Interconversion of Phosphoinositide Species by Kinases and Phosphatases

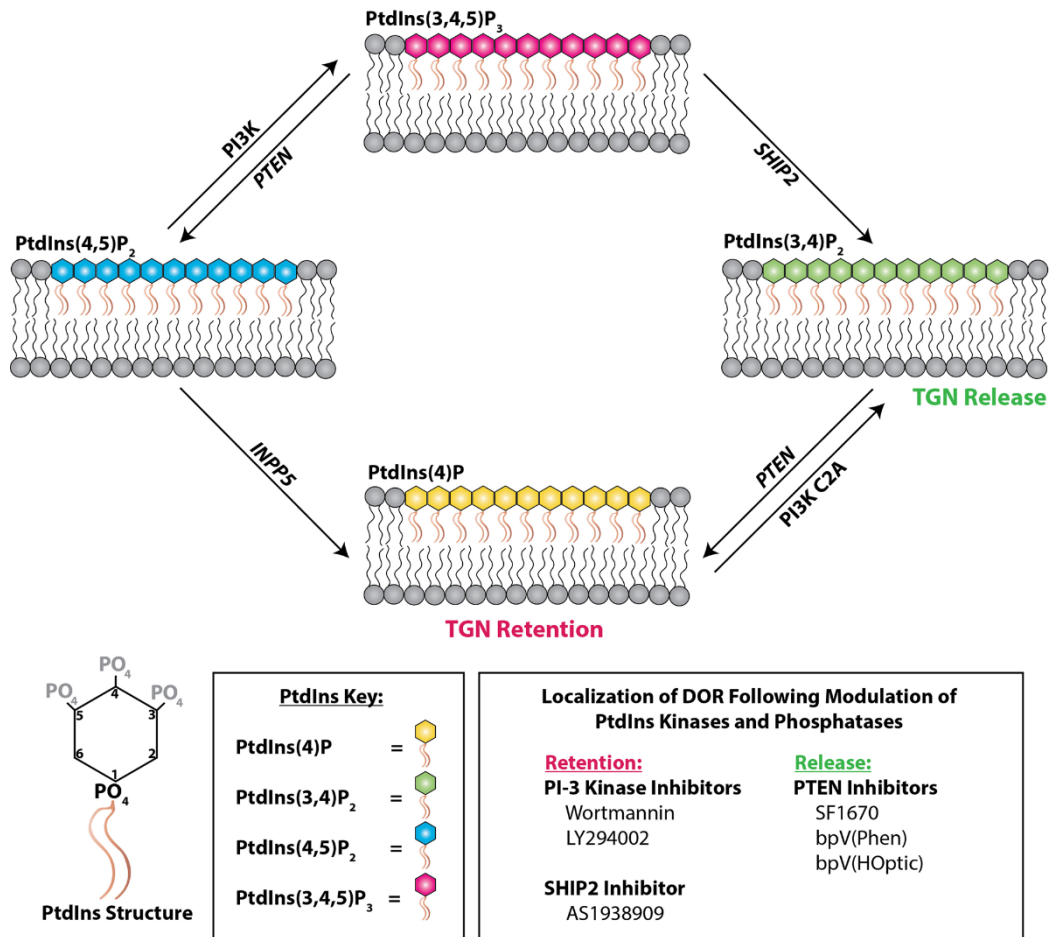
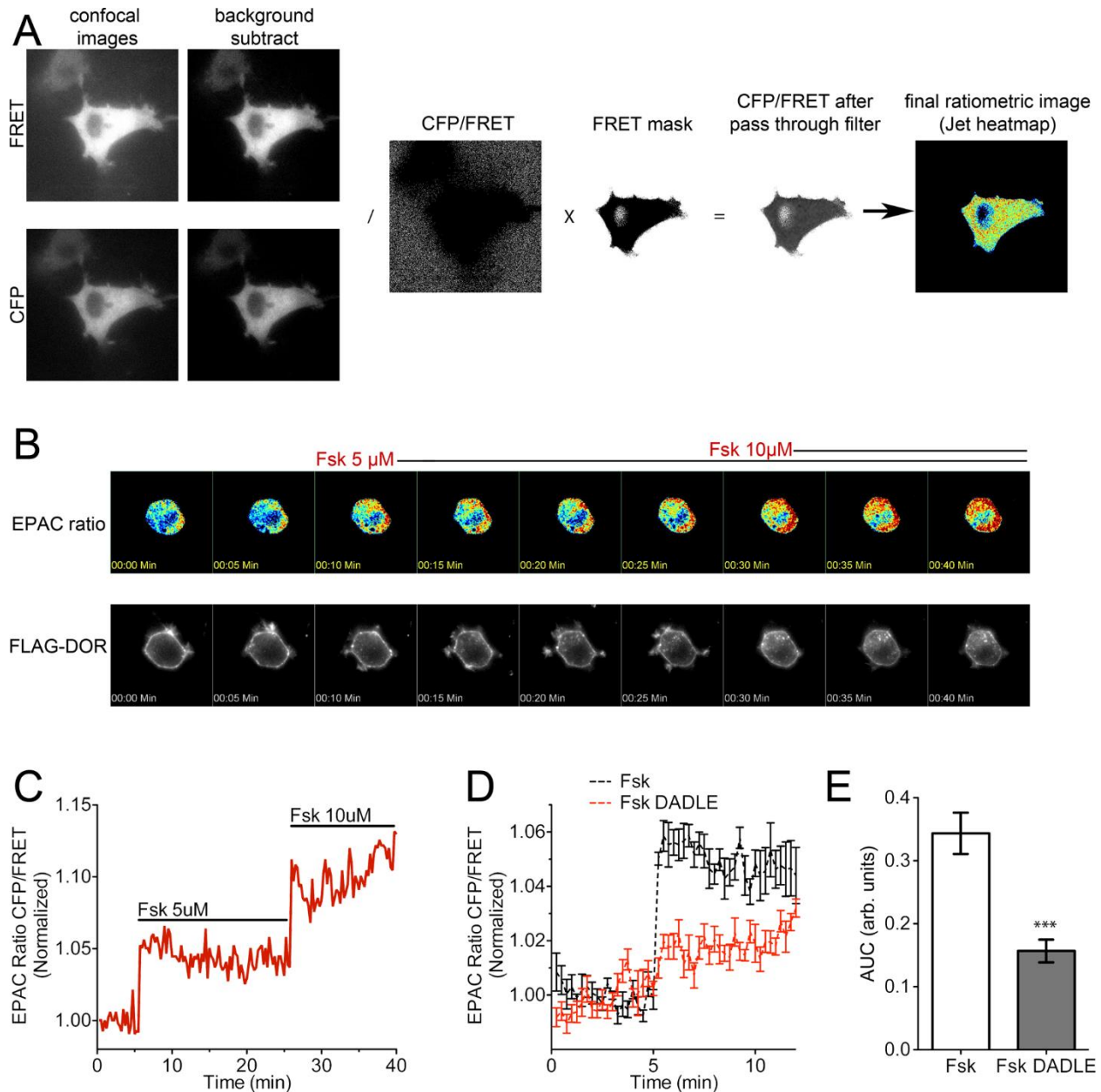


Figure 5 Supplement 1. Schematic of phosphoinositide conversion and summary of results of manipulation. A summary of the regulation of the interconversion of phosphoinositide species and their effects on DOR retention and trafficking is depicted. A reductionist approach suggests that PI(3,4)P2 is the lipid species required for trafficking of DOR to the surface.

**Figure 6 Supplement 1.**



**Figure 6 Supplement 1. A. Validation of live-cell Epac sensor imaging assay for evaluating DOR activity following agonist administration. A.** Relative quantification of the cAMP level was achieved by acquiring a confocal microscopy FRET image (405nm excitation, 540nm emission) and a CFP image (405nm excitation, 470nm emission). Following background subtraction, the ratio of the CFP image to the FRET image allows for the relative determination of the change in cAMP over time. To isolate the cell specific signal, a binary mask was made of the FRET channel and multiplied by the CFP/FRET ratio to be used as a pass through filter. A custom

Jet heatmap was then applied to visualize the change in cAMP signal over time. These images were acquired in live cells at 37°C to provide an appropriate physiological environment. **B.** In order to reproducibly quantify the decrease in cAMP following DOR agonist addition, we increased the baseline cAMP through addition of a sub-maximal dosage of Forskolin (Fsk, 5µM). A stepwise increase in cAMP can be observed following 5µM and 10µM Forskolin addition. Additionally, to visualize the surface pool of receptors we pre-incubated the cells with an Alexa-647 M1 (FLAG) antibody to recognize the surface DOR. Example images of the EPAC ratio signal and surface DOR following the additions of Forskolin are shown. **C.** Quantification of the EPAC ratio signal reveals 5µM Forskolin addition to be a sub-maximal stimulation of cAMP in PC12 cells. **D.** Upon addition of the DOR agonist DADLE (10µM) and Forskolin (5µM) an inhibition in the Forskolin induced cAMP response was observed ( $n = 3$  independent experiments; Fsk,  $n=7$  cells; Fsk DADLE,  $n=17$  cells; plotted as mean  $\pm$  s.e.m). **E.** Further data analysis reveal that the amount of cAMP produced, as measured by quantifying the area under the curve (AUC), following DADLE and Forskolin coadministration is significantly reduced compared to the Forskolin only control ( $n = 3$  independent experiments; Fsk,  $n=15$  cells; Fsk DADLE,  $n=15$  cells; mean  $\pm$  s.e.m.; \*\*\* $P=0.0001$ ; by two-sided t-test vs. Fsk).

## **Supplemental Movies.**

**Movie S1: NGF-induced retention of GFP-DOR in PC12 cells.** To directly visualize NGF-mediated intracellular DOR accumulation, we exposed PC12 cells expressing an N-terminally GFP tagged DOR to NGF (100ng/mL) and imaged them live at 37°C for > one hour.

**Movie S2: Wortmannin-induced retention of GFP-DOR in PC12 cells.** To directly visualize Wortmannin-induced intracellular DOR accumulation, we exposed PC12 cells expressing an N-terminally GFP tagged DOR to Wortmannin (10µM) and imaged them live at 37°C for > one hour.

**Movie S3: Addition of DOR agonist DADLE inhibits Forskolin-stimulated cAMP response.** Dynamic changes in cAMP levels in PC12 cells were detected using the EPAC Förster Resonance Energy Transfer (FRET) sensor, simultaneously with activation and endocytosis of DOR. Forskolin (5µM) was added to increase the basal level of cAMP, followed by the DOR agonist DADLE (10µM) addition to activate DOR and inhibit cAMP. This example movie shows the stimulation of cAMP with Forskolin followed by DADLE addition. cAMP increase can be seen as a change in the EPAC Ratio from blue to red (Right). Subsequent DADLE addition results in endocytosis of DOR confirming receptor activation correlates with cAMP inhibition (Left).

## References:

- Aoki, K., Aoki, K., Nakamura, T., Nakamura, T., Inoue, T., Inoue, T., Meyer, T., Meyer, T., Matsuda, M., and Matsuda, M. (2007). An essential role for the SHIP2-dependent negative feedback loop in neuritogenesis of nerve growth factor-stimulated PC12 cells. *The Journal of Cell Biology* 177, 817–827.
- Arévalo, J.C., Wu, S.H., Takahashi, T., Zhang, H., Yu, T., Yano, H., Milner, T.A., Tessarollo, L., Ninan, I., Arancio, O., et al. (2010). The ARMS/Kidins220 scaffold protein modulates synaptic transmission. *Mol. Cell. Neurosci.* 45, 92–100.
- Arttamangkul, S., Quillinan, N., Low, M.J., Zastrow, von, M., Pintar, J., and Williams, J.T. (2008). Differential activation and trafficking of micro-opioid receptors in brain slices. *Molecular Pharmacology* 74, 972–979.
- Bao, L., Jin, S.-X., Zhang, C., Wang, L.-H., Xu, Z.-Z., Zhang, F.-X., Wang, L.-C., Ning, F.-S., Cai, H.-J., Guan, J.-S., et al. (2003). Activation of delta opioid receptors induces receptor insertion and neuropeptide secretion. *Neuron* 37, 121–133.
- Bardoni, R., Tawfik, V.L., Wang, D., François, A., Solorzano, C., Shuster, S.A., Choudhury, P., Betelli, C., Cassidy, C., Smith, K., et al. (2014). Delta opioid receptors presynaptically regulate cutaneous mechanosensory neuron input to the spinal cord dorsal horn. *Neuron* 81, 1312–1327.
- Bie, B., Bie, B., Zhang, Z., Zhang, Z., Cai, Y.Q., Cai, Y.-Q., Zhu, W., Zhu, W., Zhang, Y., Zhang, Y., et al. (2010). Nerve growth factor-regulated emergence of functional delta-opioid receptors. *Journal of Neuroscience* 30, 5617–5628.
- Bonifacino, J.S. (2014). Adaptor proteins involved in polarized sorting. *Jcb* 204, 7–17.
- Bowman, S.L., Soohoo, A.L., Shiwarski, D.J., Schulz, S., Pradhan, A.A., and Puthenveedu, M.A. (2015). Cell-Autonomous Regulation of Mu-Opioid Receptor Recycling by Substance P. *Celrep* 10, 1925–1936.
- Cahill, C.M., Cahill, C.M., Morinville, A., Morinville, A., Hoffert, C., Hoffert, C., O'Donnell, D., O'Donnell, D., Beaudet, A., and Beaudet, A. (2003). Up-regulation and trafficking of delta opioid receptor in a model of chronic inflammation: implications for pain control. *Pain* 101, 199–208.
- Cahill, C.M., McClellan, K.A., Morinville, A., Hoffert, C., Hubatsch, D., O'Donnell, D., and Beaudet, A. (2001a). Immunohistochemical distribution of delta opioid receptors in the rat central nervous system: evidence for somatodendritic labeling and antigen-specific cellular compartmentalization. *J. Comp. Neurol.* 440, 65–84.
- Cahill, C.M., Morinville, A., Lee, M.C., Vincent, J.P., Collier, B., and Beaudet, A. (2001b). Prolonged morphine treatment targets delta opioid receptors to neuronal plasma membranes and enhances delta-mediated antinociception. *Journal of Neuroscience* 21, 7598–7607.
- Cahill, C.M., Cahill, C.M., Holdridge, S.V., Holdridge, S.V., Morinville, A., and Morinville, A. (2007). Trafficking of delta-opioid receptors and other G-protein-coupled receptors: implications for pain and analgesia. *Trends in Pharmacological Sciences* 28, 23–31.
- Chen, J.-Y., Chen, J.-Y., Lin, J.-R., Lin, J.-R., Cimprich, K.A., Cimprich, K.A., Meyer, T., and

- Meyer, T. (2012). A two-dimensional ERK-AKT signaling code for an NGF-triggered cell-fate decision. *Molecular Cell* 45, 196–209.
- Cheng, S.-B., and Filardo, E.J. (2012). Trans-Golgi Network (TGN) as a regulatory node for  $\beta$ 1-adrenergic receptor ( $\beta$ 1AR) down-modulation and recycling. *Journal of Biological Chemistry* 287, 14178–14191.
- Cruz-Garcia, D., Cruz-Garcia, D., Ortega-Bellido, M., Ortega-Bellido, M., Scarpa, M., Scarpa, M., Villeneuve, J., Villeneuve, J., Jovic, M., Jovic, M., et al. (2013). Recruitment of arfaptins to the trans-Golgi network by PI(4)P and their involvement in cargo export. *Embo J.* 32, 1717–1729.
- Danielsson, I., Gasior, M., Stevenson, G.W., Folk, J.E., Rice, K.C., and Negus, S.S. (2006). Electroencephalographic and convulsant effects of the delta opioid agonist SNC80 in rhesus monkeys. *Pharmacol. Biochem. Behav.* 85, 428–434.
- Di Paolo, G., and De Camilli, P. (2006). Phosphoinositides in cell regulation and membrane dynamics. *Nature* 443, 651–657.
- DiPilato, L.M., Cheng, X., and Zhang, J. (2004). Fluorescent indicators of cAMP and Epac activation reveal differential dynamics of cAMP signaling within discrete subcellular compartments. *Proceedings of the National Academy of Sciences* 101, 16513–16518.
- Dong, C., Dong, C., Filipeanu, C.M., Filipeanu, C.M., Duvernay, M.T., Duvernay, M.T., Wu, G., and Wu, G. (2007). Regulation of G protein-coupled receptor export trafficking. *Biochim. Biophys. Acta* 1768, 853–870.
- Erneux, C., Edimo, W.E., Deneubourg, L., and Pirson, I. (2011). SHIP2 multiple functions: a balance between a negative control of PtdIns(3,4,5)P<sub>3</sub> level, a positive control of PtdIns(3,4)P<sub>2</sub> production, and intrinsic docking properties. *J. Cell. Biochem.* 112, 2203–2209.
- Ferguson, S.S.G., Ferguson, S.S., Zhang, J., Zhang, J., Barakt, L.S., Barak, L.S., Caron, M.G., and Caron, M.G. (1998). Molecular mechanisms of G protein-coupled receptor desensitization and resensitization. *Life Sciences* 62, 1561–1565.
- Gavériaux-Ruff, C., Gavériaux-Ruff, C., Kieffer, B.L., and Kieffer, B.L. (2011). Delta opioid receptor analgesia: recent contributions from pharmacology and molecular approaches. *Behav Pharmacol* 22, 405–414.
- Gendron, L., Cahill, C.M., Zastrow, von, M., Schiller, P.W., and Piñeyro, G. (2016). Molecular Pharmacology of  $\delta$ -Opioid Receptors. *Pharmacol. Rev.* 68, 631–700.
- Gendron, L., Mittal, N., Beaudry, H., and Walwyn, W. (2014). Recent advances on the  $\delta$  opioid receptor: from trafficking to function. *British Journal of Pharmacology* n/a–n/a.
- Guan, J.-S., Guan, J.-S., Xu, Z.-Z., Xu, Z.-Z., Gao, H., Gao, H., He, S.-Q., He, S.-Q., Ma, G.-Q., Ma, G.-Q., et al. (2005). Interaction with vesicle luminal protachykinin regulates surface expression of delta-opioid receptors and opioid analgesia. *Cell* 122, 619–631.
- Guan, X.M., Kobilka, T.S., and Kobilka, B.K. (1992). Enhancement of membrane insertion and function in a type IIIb membrane protein following introduction of a cleavable signal peptide. *J.*

Biol. Chem. 267, 21995–21998.

Guo, Y., Zanetti, G., and Schekman, R. (2013). A novel GTP-binding protein-adaptor protein complex responsible for export of Vangl2 from the trans Golgi network. *Elife* 2, e00160.

Gürtler, A., Kunz, N., Gomolka, M., Hornhardt, S., Friedl, A.A., McDonald, K., Kohn, J.E., and Posch, A. (2013). Stain-Free technology as a normalization tool in Western blot analysis. *Anal. Biochem.* 433, 105–111.

Hanyaloglu, A.C., and Zastrow, von, M. (2008). Regulation of GPCRs by endocytic membrane trafficking and its potential implications. *Annu. Rev. Pharmacol. Toxicol.* 48, 537–568.

Harriott, A.M., Scheff, N.N., and Gold, M.S. (2012). The complex actions of sumatriptan on rat dural afferents. *Cephalalgia* 32, 738–749.

Hein, L., Hein, L., Ishii, K., Ishii, K., Coughlin, S.R., Coughlin, S.R., Kobilka, B.K., and Kobilka, B.K. (1994). Intracellular targeting and trafficking of thrombin receptors. A novel mechanism for resensitization of a G protein-coupled receptor. *J. Biol. Chem.* 269, 27719–27726.

Jutkiewicz, E.M., Baladi, M.G., Folk, J.E., Rice, K.C., and Woods, J.H. (2006). The convulsive and electroencephalographic changes produced by nonpeptidic delta-opioid agonists in rats: comparison with pentylene tetrazol. *Journal of Pharmacology and Experimental Therapeutics* 317, 1337–1348.

Kim, K.-A., Kim, K.-A., Zastrow, von, M., and Zastrow, von, M. (2003). Neurotrophin-regulated sorting of opioid receptors in the biosynthetic pathway of neurosecretory cells. *Journal of Neuroscience* 23, 2075–2085.

Li, X., Ortega, B., Kim, B., and Welling, P.A. (2016). A Common Signal Patch Drives AP-1 Protein-dependent Golgi Export of Inwardly Rectifying Potassium Channels. *Journal of Biological Chemistry* 291, 14963–14972.

López-Benito, S., Lillo, C., Hernández-Hernández, Á., Chao, M.V., and Arévalo, J.C. (2016). ARMS/Kidins220 and synembryn-B levels regulate NGF-mediated secretion. *J. Cell. Sci.* 129, 1866–1877.

Lu, S.-G., Zhang, X., and Gold, M.S. (2006). Intracellular calcium regulation among subpopulations of rat dorsal root ganglion neurons. *J. Physiol. (Lond.)* 577, 169–190.

Malhotra, V., and Campelo, F. (2011). PKD regulates membrane fission to generate TGN to cell surface transport carriers. *Cold Spring Harbor Perspectives in Biology* 3.

Marchese, A., and Trejo, J. (2013). Ubiquitin-dependent regulation of G protein-coupled receptor trafficking and signaling. *Cellular Signalling* 25, 707–716.

Maxfield, F.R., and McGraw, T.E. (2004). Endocytic recycling. *Nat Rev Mol Cell Biol* 5, 121–132.

Mayinger, P. (2012). Phosphoinositides and vesicular membrane traffic. *Biochim. Biophys. Acta* 1821, 1104–1113.

- Mittal, N., Roberts, K., Pal, K., Bentolila, L.A., Fultz, E., Minasyan, A., Cahill, C., Pradhan, A., Conner, D., DeFea, K., et al. (2013). Select G-protein-coupled receptors modulate agonist-induced signaling via a ROCK, LIMK, and  $\beta$ -arrestin 1 pathway. *Celrep* 5, 1010–1021.
- Papanikou, E., and Glick, B.S. (2014). Golgi compartmentation and identity. *Current Opinion in Cell Biology* 29, 74–81.
- Patwardhan, A.M., Berg, K.A., Akopain, A.N., Jeske, N.A., Gamper, N., Clarke, W.P., and Hargreaves, K.M. (2005). Bradykinin-induced functional competence and trafficking of the delta-opioid receptor in trigeminal nociceptors. *J. Neurosci.* 25, 8825–8832.
- Petaja-Repo, U.E., Hogue, M., Laperriere, A., Walker, P., and Bouvier, M. (2000). Export from the endoplasmic reticulum represents the limiting step in the maturation and cell surface expression of the human delta opioid receptor. *J. Biol. Chem.* 275, 13727–13736.
- Pettinger, L., Pettinger, L., Gigout, S., Gigout, S., Linley, J.E., Linley, J.E., Gamper, N., and Gamper, N. (2013). Bradykinin controls pool size of sensory neurons expressing functional  $\delta$ -opioid receptors. *Journal of Neuroscience* 33, 10762–10771.
- Pradhan, A.A., Pradhan, A.A., Befort, K., Befort, K., Nozaki, C., Nozaki, C., Gavériaux-Ruff, C., Gavériaux-Ruff, C., Kieffer, B.L., and Kieffer, B.L. (2011). The delta opioid receptor: an evolving target for the treatment of brain disorders. *Trends in Pharmacological Sciences* 32, 581–590.
- Pradhan, A., Smith, M., McGuire, B., Evans, C., and Walwyn, W. (2013). Chronic inflammatory injury results in increased coupling of delta opioid receptors to voltage-gated Ca<sup>2+</sup> channels. *Mol Pain* 9, 8.
- Puertollano, R., Aguilar, R.C., Gorshkova, I., Crouch, R.J., and Bonifacino, J.S. (2001). Sorting of mannose 6-phosphate receptors mediated by the GGAs. *Science* 292, 1712–1716.
- Puthenveedu, M.A., Puthenveedu, M.A., Lauffer, B., Lauffer, B., Temkin, P., Temkin, P., Vistein, R., Vistein, R., Carlton, P., Carlton, P., et al. (2010). Sequence-dependent sorting of recycling proteins by actin-stabilized endosomal microdomains. *Cell* 143, 761–773.
- Scherrer, G., Scherrer, G., Imamachi, N., Imamachi, N., Cao, Y.-Q., Cao, Y.-Q., Contet, C., Contet, C., Mennicken, F., Mennicken, F., et al. (2009). Dissociation of the opioid receptor mechanisms that control mechanical and heat pain. *Cell* 137, 1148–1159.
- Soohee, A.L., and Puthenveedu, M.A. (2013). Divergent modes for cargo-mediated control of clathrin-coated pit dynamics. *Mol. Biol. Cell* 24, 1725–34–S1–12.
- Sorkin, A., and Zastrow, von, M. (2002). Signal transduction and endocytosis: close encounters of many kinds. *Nat Rev Mol Cell Biol* 3, 600–614.
- Tsvetanova, N.G., and Zastrow, von, M. (2014). Spatial encoding of cyclic AMP signaling specificity by GPCR endocytosis. *Nat. Chem. Biol.* 10, 1061–1065.
- Vaughn, A.H., and Gold, M.S. (2010). Ionic mechanisms underlying inflammatory mediator-induced sensitization of dural afferents. *Journal of Neuroscience* 30, 7878–7888.
- Vistein, R., and Puthenveedu, M.A. (2013). Reprogramming of G protein-coupled receptor

- recycling and signaling by a kinase switch. *Proc. Natl. Acad. Sci. U.S.a.* *110*, 15289–15294.
- Vistein, R., and Puthenveedu, M.A. (2014). Src regulates sequence-dependent beta-2 adrenergic receptor recycling via cortactin phosphorylation. *Traffic* *15*, 1195–1205.
- Wakana, Y., Wakana, Y., van Galen, J., van Galen, J., Meissner, F., Meissner, F., Scarpa, M., Scarpa, M., Polishchuk, R.S., Polishchuk, R.S., et al. (2012). A new class of carriers that transport selective cargo from the trans Golgi network to the cell surface. *Embo J.* *31*, 3976–3990.
- Walwyn, W., Maidment, N.T., Sanders, M., Evans, C.J., Kieffer, B.L., and Hales, T.G. (2005). Induction of delta opioid receptor function by up-regulation of membrane receptors in mouse primary afferent neurons. *Molecular Pharmacology* *68*, 1688–1698.
- Wang, H., Wang, H., Pickel, V.M., and Pickel, V.M. (2001). Preferential cytoplasmic localization of delta-opioid receptors in rat striatal patches: comparison with plasmalemmal mu-opioid receptors. *Journal of Neuroscience* *21*, 3242–3250.
- Wang, H.-B., Wang, H.-B., Guan, J.-S., Guan, J.-S., Bao, L., Bao, L., Zhang, X., and Zhang, X. (2008). Distinct subcellular distribution of delta-opioid receptor fused with various tags in PC12 cells. *Neurochem Res* *33*, 2028–2034.
- Wu, G., Davis, J.E., and Zhang, M. (2015). Regulation of  $\alpha$ 2B-Adrenergic Receptor Export Trafficking by Specific Motifs. *Prog Mol Biol Transl Sci* *132*, 227–244.
- Zastrow, von, M., Zastrow, M.V., Svingos, A., Svingos, A., Haberstock-Debic, H., Haberstock-Debic, H., Evans, C., and Evans, C. (2003). Regulated endocytosis of opioid receptors: cellular mechanisms and proposed roles in physiological adaptation to opiate drugs. *Current Opinion in Neurobiology* *13*, 348–353.
- Zhang, M., Davis, J.E., Li, C., Gao, J., Huang, W., Lambert, N.A., Terry, A.V., and Wu, G. (2016). GGA3 Interacts with a G Protein-Coupled Receptor and Modulates Its Cell Surface Export. *Molecular and Cellular Biology* *36*, 1152–1163.
- Zhang, X., Bao, L., Arvidsson, U., Elde, R., and Hökfelt, T. (1998). Localization and regulation of the delta-opioid receptor in dorsal root ganglia and spinal cord of the rat and monkey: evidence for association with the membrane of large dense-core vesicles. *Neuroscience* *82*, 1225–1242.
- Zhang, X., Zhang, X., Bao, L., Bao, L., Guan, J.-S., and Guan, J.-S. (2006). Role of delivery and trafficking of delta-opioid peptide receptors in opioid analgesia and tolerance. *Trends in Pharmacological Sciences* *27*, 324–329.
- Zhu, Y., Doray, B., Poussu, A., Lehto, V.P., and Kornfeld, S. (2001). Binding of GGA2 to the lysosomal enzyme sorting motif of the mannose 6-phosphate receptor. *Science* *292*, 1716–1718.

## Chapter 3: Optogenetic Recruitment of PI3K C2 $\alpha$ to the *trans*-Golgi Network is Sufficient to Promote Surface Trafficking of the $\delta$ -Opioid Receptor

Daniel J. Shiwarski<sup>1</sup>, Marlena Darr<sup>1</sup>, Manojkumar A. Puthenveedu<sup>1</sup>

<sup>1</sup>Department of Biological Sciences, The Center for the Neural Basis of Cognition, Carnegie Mellon University, Pittsburgh, PA 15213, USA.

### Abstract:

Targeting the delta opioid receptor (DOR) for pain management has been ineffective largely due to its limited surface expression in sensory neurons. Recently, a lipid regulated checkpoint at the Golgi has been identified that mediates DOR surface delivery. Here, we show that this neuronal specific Golgi checkpoint is controlled by Class II PI3K  $\alpha$  (PI3K C2A) activity, independent of Class I PI3Ks. Utilizing live cell imaging techniques, we identified PI3K C2A expression as both required and sufficient for Golgi export of DOR. Additionally, we developed a *trans*-Golgi Network (TGN) targeted optogenetic recruitment strategy to evaluate the sufficiency of the PI3K C2A kinase domain to induce spatiotemporal release of Golgi-retained DOR. Following NGF-induced Golgi retention of DOR, recruitment of the PI3K C2A kinase domain to the TGN resulted in stimulated delivery of DOR to the cell surface. Our results identify a key component in the molecular pathway controlling surface delivery of DOR, and present the first evidence for PI3K C2A activity mediating a Golgi specific checkpoint to induce delivery of G-protein Coupled Receptor to the surface.

**Introduction:**

The delta opioid receptor (DOR) is an inhibitory G<sub>i</sub> protein-coupled receptor (GPCR), and a promising alternative target for pain management(1). However, the clinical utility of DOR agonists for pain management is limited by the low efficacy of DOR-specific agonists and convulsive side effects(2-7). Recent work suggests that the low agonist efficacy is largely the result of a neuronal-specific phosphoinositide checkpoint preventing newly synthesized DOR from reaching the cell surface(8) and restricting DOR exposure to extracellular agonists and surface-localized signaling complexes. In neuronal cells, PI3K inhibition is sufficient to cause DOR retention in the Golgi. Through inhibition of phosphatase and tensin homolog (PTEN), the opposing phosphatase to the PI3K pathway, Golgi-retention of DOR was abolished. Further, inhibition of PTEN in a mouse model of chronic pain promoted trafficking of functional DOR to the cell surface, and increased DOR-agonist efficacy resulting in antihyperalgesia.

While the promise of inducing on-demand receptor trafficking to improve DOR agonist efficacy is clinically significant, the treatment of chronic pain would require long-term pharmacologic intervention. For this reason, a more precise understanding of the molecular mechanism controlling DOR Golgi retention and surface trafficking is needed. This would allow for specific control over DOR trafficking without affecting the broader PI3K-PTEN pathway. Specifically, we sought to determine the exact PI3K that was involved in the phosphoinositide checkpoint preventing newly synthesized DOR from reaching the cell surface. PI-3 kinases control the creation of 3' phosphoinositides within lipid membranes to initiate downstream signaling cascades. The precise control over kinase activity and localization is mediated through binding to phosphoinositides, and is a key factor creating and controlling compartmentalization of proteins within membranes(9). Additionally, the interactions between PI-3 kinases, effector molecules, small GTPases, and adaptor complexes can act as molecular switches to control membrane trafficking processes throughout the cell(9-11).

Within the PI3K protein family there are several sub-classes, Class I, II, and III. Class I PI3Ks, consisting of a p85 regulatory subunit and a p110 catalytic subunit, are primarily responsible for production of phosphatidylinositol (3,4,5)-trisphosphate PI(3,4,5)P<sub>3</sub> from PI(4,5)P<sub>2</sub>. Within Class I PI3Ks, there are several variants of the p110 catalytic subunit,  $\alpha$ ,  $\beta$ ,  $\delta$ , and  $\gamma$ . Several reports have implicated specific PI3K Class I subunit activity in membrane trafficking and fission events, independent of its role as an activator of Akt. Inhibition of the PI3K p110 $\delta$  subunit can inhibit the trafficking of Tumor Necrosis Factor Alpha (TNF $\alpha$ ) from the Golgi by preventing the fission of p230 labeled tubules in macrophages(12). When PI3K becomes active in this system, it increases the conversion of PI(4,5)P<sub>2</sub> to PI(3,4,5)P<sub>3</sub> which creates a docking

site for proteins containing the Pleckstrin homology (PH) domain. Class III PI3K, Vps34, is similar to Class I PI3K, but is only able to synthesize PI(3)P, and is thought to regulate endosome recycling and possibly dynamin recruitment (13, 14).

Class II PI3K comprises of  $\alpha$ ,  $\beta$ , and  $\gamma$  isoforms, contain a unique C2 domain, a PX domain, and are single subunit kinases. They possess both a regulatory and catalytic domain within one protein(14-16). These kinases mainly use PI and PI(4)P as substrates to produce phosphatidylinositol 3-phosphate PI(3)P and phosphatidylinositol (3,4)-bisphosphate PI(3,4)P<sub>2</sub>, but have also been suggested to produce phosphatidylinositol (3,4,5)-trisphosphate PI(3,4,5)P<sub>3</sub> from PI(4,5)P<sub>2</sub> at the *trans*-Golgi Network (TGN). Specifically, Class II PI3K  $\alpha$  (PI3K C2A) has been shown to localize to *trans*-Golgi membranes with the AP-1 adaptor protein to recruit clathrin coated vesicles(17). Additionally, work from the Keen lab demonstrated that PI3K C2A can be activated by clathrin through a direct binding interaction within PI3K N-terminal region to result in increased PI3K activity, an upregulation of PI(3,4,5)P<sub>3</sub>, and promotes the formation of the clathrin lattice assembly to aid vesicle trafficking from the Golgi(18, 19).

Based upon our previous data demonstrating the sufficiency for PI3K and SHIP2 inhibition to promote Golgi retention of DOR, and PTEN inhibition to drive DOR surface trafficking, we hypothesize that a specific subclass of PI3K is responsible for stimulating the production of PI(3,4)P<sub>2</sub> at the *trans*-Golgi Network to promote DOR surface trafficking(8). Additionally, since this would propose a Class I PI3K independent mechanism of regulation, and suggest Class II specific activity, the unwanted side effects from pharmacologically targeting Class I PI3Ks in a clinical setting might be avoided. Here, we demonstrate that inhibition of Class I PI3K  $\alpha$ ,  $\delta$ , or  $\gamma$ , is not sufficient for Golgi retention of DOR, and that micromolar concentrations of the pan PI3K inhibitors Wortmannin and LY294002, sufficient for Class II PI3K inhibition, are required for DOR Golgi retention. Further, expression of PI3K C2A is required for complete surface trafficking of DOR, and optorecruitment of the PI3K C2A kinase domain is sufficient to release the NGF-induced Golgi retention of DOR and stimulate exocytosis of DOR from the TGN to the cell surface. These results identify the lipid kinase regulating a checkpoint in the Golgi, controlled by a neuronal-specific signaling axis, that regulates delivery of DOR to the surface. Targeting PI3K C2A may provide a new therapeutic approach for increasing DOR surface expression to increase DOR agonist efficacy in lieu of PTEN inhibition.

## Results:

### **Activation of PI3K by 740Y<sup>PDGFR</sup> is sufficient to reduce the PI3K-inhibition induced retention of DOR.**

We have previously shown that biosynthetic trafficking of the  $\delta$ -Opioid receptor (DOR), and its retention in the Golgi can be controlled via Nerve Growth Factor (NGF) signaling and PI3K inhibition (8, 20). The exact relationship between PI3K inhibition and NGF-induced Golgi retention of DOR was unknown. In PC12 cells exogenously expressing a FLAG-tagged form of the  $\delta$ -Opioid receptor (FLAG-DOR), fixed-cell immunofluorescence detection and confocal microscopy revealed that DOR is primarily localized to the cell surface; however, following a 1-hour treatment with NGF, DOR is retained within the Golgi apparatus and colocalizes with the *trans*-Golgi network marker TGN-38 (Figure 1A) (8). Inhibition of PI3K with either the reversible inhibitor LY294002 (LY) or the irreversible inhibitor Wortmannin (Wort) was sufficient to induce Golgi retention of DOR (Figure 1A, (8, 21, 22)). We next wanted to determine if PI3K activation was sufficient to prevent DOR Golgi retention following NGF, LY294002, and Wortmannin treatment. To activate PI3K in the presence of these compounds, we utilized a PI3K activating peptide, 740Y<sup>PDGFR</sup> (23). Activation of PI3K by the p85 subunit binding peptide 740Y<sup>PDGFR</sup> decreased the Golgi retention phenotype following NGF and LY treatments. The 740Y<sup>PDGFR</sup> peptide was not sufficient to prevent the Golgi retention phenotype following the irreversible PI3K inhibitor Wortmannin. Activation of PI3K by 740Y<sup>PDGFR</sup> had no effect on DOR Golgi retention on its own (Figure 1A-B). Quantification of the immunofluorescence confirmed that NGF, LY294002, and Wortmannin were all sufficient to increase the percentage of DOR colocalized with the Golgi and the percentage of cells exhibiting Golgi-localized DOR (Figure 1B, S1A). The PI3K activating peptide 740Y<sup>PDGFR</sup> significantly decreased the percentage of DOR colocalized with the Golgi and the percentage of cells exhibiting Golgi-localized DOR following NGF and LY294002, but did not reduced the Wortmannin-induced DOR Golgi retention (Figure 1B, S1A). These data taken together suggest that activation of PI3K is sufficient to prevent NGF and LY294002-induced Golgi retention of DOR and that PI3K activity is downstream of NGF in DOR Golgi retention.

### **PI3K activity is required for DOR export from the Golgi in HEK 293 Cells**

Earlier work from our lab has shown that PI3K inhibition and NGF-induced retention of DOR in PC12 cells is specific to DOR, and that neither PI3K inhibition nor NGF treatment results in Golgi retention of the mu-Opioid receptor (MOR) (8). Additionally, work from Kim et al. showed that TrkA receptor expression was required for the NGF-induced DOR retention in PC12 cells(20). Therefore, we wanted to determine if changes in PI3K activity could control the biosynthetic

trafficking of DOR in cell lines not expressing the TrkA receptor, such as HEK 293 cells. FLAG-tagged DOR and MOR were transfected into HEK 293 cells, grown under antibiotic selection to obtain a stable pool of expressing cells, and evaluated for receptor localization via fixed-cell immunofluorescence detection and confocal microscopy. In FLAG-DOR HEK 293 cells under control conditions, DOR was predominantly localized to the cell surface, and did not colocalize with the Golgi marker GPP130 (Figure S1B). When treated with the PI3K inhibitor Wortmannin, there was a dramatic increase in the amount of Golgi-localized DOR (Figure S1B). Quantification of the DOR immunofluorescence confirmed that treatment with Wortmannin increased both the percentage of DOR localized to the Golgi, and the percentage of cells exhibiting Golgi-localized DOR (Figure S1C-D). Identical experiments were performed with the FLAG-MOR HEK 293 cells. Like DOR, MOR was basally localized to the cell surface; however, upon treatment with the PI3K inhibitor Wortmannin or LY294002 there was no change in MOR localization (Figure S1E). Quantification of the MOR immunofluorescence confirmed that neither treatment with Wortmannin nor LY294002 altered the percentage of MOR localized to the Golgi, or the percentage of cells exhibiting Golgi-localized MOR (Figure S1F-G). These data demonstrate that PI3K inhibition is sufficient to induce the Golgi retention of DOR independently of TrkA signaling in receptor specific manner.

### **PI3K activity controls the Golgi export of GFP-VSVG-DORtail**

To test if PI3K activity was directly affecting the biosynthetic trafficking of DOR, and to evaluate the kinetics of DOR retention and release, we utilized the temperature sensitive mutant (ts045) of the vesicular stomatitis virus glycoprotein (VSVG) to visualize dynamic protein trafficking through the secretory pathway. The temperature sensitive VSVG allows for a temperature-controlled release of VSVG from the ER to the Golgi upon transition from 40°C to 32°C, and has widely been used for studying protein trafficking through the secretory pathway (24-26). For our experiments, we created a chimeric protein consisting of the temperature sensitive mutant (ts045) VSVG linked to the last 27 amino acids of the C-terminal tail domain of DOR because the DOR C-terminal tail has previously been shown to be sufficient for NGF-induced Golgi retention(20). To visualize the trafficking in real-time, we C-terminally tagged our chimeric protein with GFP for live cell fluorescence imaging capabilities (VSVG-DORtail-GFP). HEK 293 cells were transfected with VSVG-DORtail-GFP and grown under antibiotic selection for stable expression. To inhibit exit of the VSVG-DORtail-GFP from the ER, the cells were grown at 40°C. At the time of imaging, the cells were transitioned to 32°C and visualized by live cell fluorescence microscopy.

At time zero, all HEK 293 cells expressing the VSVG-DORtail-GFP exhibited a GFP signal resembling ER localization. Under control conditions, trafficking of the VSVG-DORtail-GFP appeared normal, exiting the ER, accumulating within the Golgi, and budding off into vesicle-like structures trafficking towards the membrane. After one hour at 32°C, most of the Golgi accumulated VSVG-DORtail-GFP signal had dissipated, and the cell membrane showed increased surface fluorescence (Figure 1C, Supplemental Movie 1). When treated with the PI3K inhibitor Wortmannin (Wort), trafficking of the VSVG-DORtail-GFP from the ER to the Golgi appeared normal; however, a significant amount of Golgi accumulated fluorescence remained after one hour at 32°C (Figure 1C, Supplemental Movie 2). To quantitatively evaluate the kinetics of VSVG-DORtail-GFP trafficking, we measured the Golgi fluorescence signal accumulation and decay over the course of the experiment. Inhibition of PI3K by Wortmannin delayed the trafficking of the VSVG-DORtail-GFP from the Golgi and resulted in a prolonged Golgi-localized fluorescence intensity compared to control (NT) (Figure 1D). To determine if PI3K activation by the 740Y<sup>PDGFR</sup> peptide was sufficient to prevent the Golgi retention phenotype following PI3K inhibition, we utilized the reversible nature of the PI3K inhibitor LY294002 (LY). Alone, inhibition of PI3K with LY demonstrated strong intracellular and Golgi retention of VSVG-DORtail-GFP (Figure 1E, Supplemental Movie 3). When LY was added in combination with the PI3K activating peptide 740Y<sup>PDGFR</sup> (740YP), the sustained increase in VSVG-DORtail-GFP Golgi fluorescence was abrogated (Figure 1E-F, Supplemental Movie 4). Quantification of the total Golgi-localized fluorescence for VSVG-DORtail-GFP over time was performed by calculating the area under the curve (AUC) for each experimental condition. Inhibition of PI3K by Wort or LY significantly increased the total Golgi-localized DOR (Figure S1H). Activation of PI3K by the activating peptide 740Y<sup>PDGFR</sup> (740YP) in combination with LY completely abrogated the increase in Golgi-localized DOR AUC observed with LY alone (Figure S1H). These data suggest that inhibiting PI3K decreases the rate of trafficking of VSVG-DORtail-GFP from the Golgi to the cell membrane in HEK 293 cells.

### **Inhibition of Class I PI3Ks is not sufficient to retain DOR in the Golgi**

There are several classes of PI3Ks; Class I, II, and III. The most well known and commonly targeted are the Class I PI3Ks, which are made up of a p85 regulatory subunit and a p110 catalytic subunit. These PI3Ks are primarily responsible for the production of Phosphatidylinositol (3,4,5)-trisphosphate PI(3,4,5)P<sub>3</sub>. Within Class I PI3Ks, there are several subtypes of the p110 catalytic subunit,  $\alpha$ ,  $\beta$ ,  $\delta$ , and  $\gamma$ . At nanomolar and low micromolar concentrations, the PI3K inhibitor Wortmannin preferentially inhibits Class I PI3Ks; however, at concentrations at or above 10  $\mu$ M,

Wortmannin can also inhibit the Class II PI3Ks (15). To test whether the Golgi retention of DOR following treatment with Wortmannin was specific to Class I PI3K inhibition, we administered concentrations of 1 $\mu$ M or 10 $\mu$ M Wortmannin to PC12 cells expressing FLAG-DOR. Treatment with 1 $\mu$ M Wortmannin had a small but statistically significant effect on inducing a Golgi-localized pool of DOR, while 10 $\mu$ M Wortmannin demonstrated a large and significant increase in the Golgi-localized pool of DOR (Figure 2A). Quantification and image analysis of these results showed a 2-fold increase in the percentage of DOR fluorescence localized to the Golgi following 1 $\mu$ M Wortmannin, while NGF and 10 $\mu$ M Wortmannin resulted in an increase in the percentage of DOR fluorescence localized to the Golgi of approximately 4-fold (Figure 2B). Similarly, the percentage of cells exhibiting visual Golgi-localized DOR minimally increased following 1 $\mu$ M Wortmannin, while NGF and 10 $\mu$ M Wortmannin resulted in 80% of cells exhibiting visual Golgi localized DOR (Figure 2C).

To rule out inhibition of Class I PI3Ks as the driver of DOR Golgi retention, we utilized the Class I isoform specific PI3K inhibitors PI-103 (PI3K C1,  $\alpha$ ), IC87114 (PI3K C1,  $\delta$ ), and AS605240 (PI3K C1,  $\gamma$ ) (27-29). Using our fixed cell immunofluorescence assay in PC12 cells expressing FLAG-DOR, Wortmannin (10 $\mu$ M) and LY294002 (10 $\mu$ M), both pan Class I and II PI3K inhibitors, resulted in significant Golgi-localized DOR fluorescence; however, the PI3K Class I specific inhibitors did not cause any change in DOR's localization pattern (Figure 2D, S2A). Quantification and image analysis of these data revealed a significant increase in the percentage of DOR fluorescence localized to the Golgi and the percentage of cells with Golgi-localized DOR following 10 $\mu$ M Wortmannin or LY294002 treatment, but no significant change was observed for either measurement following treatment with the PI3K Class I specific inhibitors (Figure 2E, S2B). Therefore, inhibition of Class I PI3Ks is not sufficient to induce Golgi retention of DOR, and a concentration of over 1 $\mu$ M Wortmannin is required to stimulate a large increase in DOR Golgi localization.

### **Class II PI3K C2 $\alpha$ is required for complete surface trafficking of DOR**

Our results suggest that inhibition of Class I PI3Ks are not sufficient to cause the Golgi retention of DOR; however, concentrations of Wortmannin and LY294002 of 10 $\mu$ M, which can inhibit Class II PI3Ks, are sufficient to induce significant retention of DOR. Additionally, while Class I PI3Ks are traditionally thought to be catalytically active at the plasma membrane, Class II PI3Ks have been shown to be active at the *trans*-Golgi Network, and are involved in intracellular trafficking and clathrin recruitment(17-19). For these reasons, we choose to determine the role of the Class II PI3K  $\alpha$  (PI3K C2A) in DOR Golgi retention by knocking down the endogenous PI3K

C2A in PC12 cells. Rat species specific PI3K C2A shRNAs were designed using the RNAi Central shRNA psm2 Design tool from the Hannon Laboratory and from two previously published shRNAs targeting PI3K C2A (30-32). All PI3K C2A shRNAs were cloned into the pENTR-pSM2(CMV)GFP vector and transiently transfected into PC12 cells for initial evaluation of knockdown (table of sequences in Methods). Three of the five sequences tested (#1-3) showed promising knockdown of PI3K C2A and were transferred into the pLenti X1 Puro Dest vector using Gateway cloning, and lentiviral particles were produced following a modified protocol from Campeau *et al.*(33). Stably transduced PC12 cells expressing the PI3K C2A shRNAs were evaluated for PI3K C2A expression via immunoblotting (Figure 3A). The shRNA sequences #2 and #3 produced an approximate 50% knockdown of PI3K C2A (Figure 3B). The PC12 cells expressing PI3K C2A shRNA #3 (PI3K C2A shRNA) was chosen for use in our further studies.

The PC12 PI3K C2A shRNA-expressing cells were transfected with a fusion construct expressing a previously characterized fluorogen-activated peptide (FAP) N-terminally tagged to DOR (FAP-DOR) and imaged live via fluorescence confocal microscopy. The FAP-DOR was chosen for its far-red emission spectra resulting from a malachite green (MG)-based fluorogen (34) (35) (36) (37). In control cells, not expressing the PI3K C2A shRNA, FAP-tagged DOR was localized to the cell surface; however, in the cells stably expressing the PI3K C2A shRNA, a prominent Golgi-localized pool of DOR was observed (Figure 3C). Image analysis and quantification demonstrated a significant increase in the percentage of DOR fluorescence localized to the Golgi and in the percentage of cells that had Golgi-localized DOR in PI3K C2A shRNA expressing cells compared to cells that only expressed the FAP-tagged DOR (Figure 3D-E). This suggests that PI3K C2A expression is required for complete cell surface trafficking of DOR.

### **Expression of Class II PI3K C2 $\alpha$ is sufficient to decrease the NGF-induced Golgi retention of DOR**

Our data show that PI3K C2A is required for proper trafficking of DOR to the surface in PC12 cells; therefore, we next wanted to determine if overexpression of PI3K C2A was sufficient to prevent the NGF-induced retention of DOR. PC12 cells were transfected with FAP-tagged DOR, GFP-PI3K C2A, and imaged via live-cell fluorescence confocal microscopy. In cells expressing only the FAP-tagged DOR, control treated cells expressed predominantly surface-localized DOR, while 1 hour of NGF treatment resulted in the expected Golgi localization of DOR (Figure 3F). For the cells expressing FAP-tagged DOR and GFP-PI3K C2A, DOR was localized to the cell surface with minimal detectable Golgi localization in both control and NGF treated

conditions (Figure 3F). Quantification of these experiments demonstrated an increase in the percentage of DOR fluorescence localized to the Golgi and in the percentage of cells that had Golgi-localized DOR following NGF treatment for cells that only expressed the FAP-tagged DOR. In cells expressing FAP-tagged DOR and GFP-PI3K C2A, a significant decrease in the NGF-induced retention of DOR, measured via the percentage of DOR fluorescence localized to the Golgi and in the percentage of cells that had Golgi-localized DOR, was observed. Taken together, these data suggest that PI3K C2A is involved in the surface trafficking of DOR, and that overexpression of PI3K C2A is sufficient to reduce NGF-induced retention of DOR.

### **Optogenetic recruitment of the PI3K C2A kinase domain to the *trans*-Golgi Network is sufficient to promote DOR surface trafficking and exocytosis**

In order to determine if the kinase activity of PI3K C2A at the TGN is sufficient to acutely induce trafficking of DOR to the cell surface following NGF-induced retention of DOR, we developed a *trans*-Golgi Network targeted optogenetic recruitment strategy. Previously, Idevall-Hagren *et al.* demonstrated that the CRY2 and CIBN optical dimerization system developed by the Tucker Laboratory could be utilized to control phosphoinositide metabolism at the plasma membrane (38, 39). To utilize this strategy for targeting of PI3K C2A to the *trans*-Golgi Network (TGN), we exchanged the plasma membrane targeting domain on the CIBN-GFP for a TGN targeting domain from the N-terminus of 2,6 sialyltransferase (CIBN-GFP-TGN). The PI3K C2A kinase domain (amino acids 863-1405, KD) was cloned onto the C-terminus of an mCherry-CRY2 chimeric construct to make mCherry-CRY2-PI3K-C2A-KD (Figure 4A). The GFP-CIBN-TGN has a basal TGN localization and the mCherry-CRY2-PI3K-C2A-KD is mostly cytoplasmic before recruitment. Optogenetic recruitment and dimerization between the CRY2 and CIBN is activated by blue light stimulation at 488nm driving the mCherry-CRY2-PI3K-C2A-KD to the TGN. This process provides spatiotemporal control over the PI3K-C2A-KD activity on phospholipid conversion at the TGN (Figure 4A).

To confirm functionality and correct localization of the TGN targeted CIBN-GFP-TGN, and to verify proper recruitment of the mCherry-CRY2-PI3K-C2A-KD upon blue light activation, we transfected PC12 cells with CIBN-GFP-TGN, mCherry-CRY2-PI3K-C2A-KD, and a TGN marker PH-FAPP1-GFP that binds to PI(4)P. The cells were then imaged via live cell fluorescence confocal microscopy. Prior to recruitment, the mCherry-CRY2-PI3K-C2A-KD was localized to the cytoplasm, and the CIBN-GFP-TGN localized to the region overlapping with the PH-FAPP1-GFP. Upon stimulation with 488nm blue light, the mCherry-CRY2-PI3K-C2A-KD was rapidly recruited to the CIBN-GFP-TGN within 5 seconds (Figure 4B, Supplemental Movie 5). To evaluate the

colocalization between CIBN-GFP-TGN, mCherry-CRY2-PI3K-C2A-KD, and PH-FAPP1-GFP we performed a line scan analysis for the images over time. Over the course of 5 seconds following 488nm excitation and recruitment, the fluorescence intensity for the mCherry-CRY2-PI3K-C2A-KD increases within a localized region (Figure 4C, Left). Five seconds after recruitment is initiated, the peak fluorescence intensity of the CIBN-GFP-TGN, mCherry-CRY2-PI3K-C2A-KD, and PH-FAPP1-GFP are superimposed with each other suggesting colocalization and effective recruitment of the mCherry-CRY2-PI3K-C2A-KD to the TGN (Figure 4C, Right).

With the ability to spatially and temporally control the recruitment of the kinase domain of PI3K C2A to the TGN, we could now acutely test the sufficiency of PI3K C2A to alleviate DOR Golgi retention. For these experiments, we transfected PC12 cells with FAP-DOR, CIBN-GFP-TGN, and mCherry-CRY2-PI3K-C2A-KD. This allowed for the simultaneous imaging of DOR trafficking and optogenetic recruitment of mCherry-CRY2-PI3K-C2A-KD to the TGN. Prior to PI3K C2A recruitment, the cells were pretreated with NGF for 1 hour to induce Golgi retention of DOR. Once retention of DOR was confirmed, optical recruitment was initiated by activation with 488nm blue light. Over the course of 5 minutes, the internal Golgi pool of DOR decrease in both size and intensity in response to the recruitment of mCherry-CRY2-PI3K-C2A-KD to the TGN (Figure 4D, Supplemental Movie 6). Further examination of the time-lapse images reveals denovo vesicle formation off of the TGN that appear to traffic towards the cell surface (Figure 4E). Quantification of the DOR fluorescence intensity within the TGN region defined by the CIBN-GFP-TGN over time shows a dramatic decrease in Golgi-localized DOR fluorescence intensity following mCherry-CRY2-PI3K-C2A-KD recruitment (Figure 4F). Additionally, analysis of the initial vs. post recruitment membrane and Golgi-localized DOR fluorescence demonstrates a small but significant increase in DOR membrane fluorescence, and a significant decrease in the Golgi-localized DOR fluorescence (Figure 4G). As a whole, these data demonstrate the sufficiency for PI3K C2A to acutely and specifically release the Golgi-retained pool of DOR and stimulate trafficking to the cell surface.

## Discussion:

Previously, work from our lab revealed that DOR was intracellularly retained within the trans-Golgi network of neuronal cells in a manner that required PI3K inhibition. Further, DOR trafficking to the cell surface depended on the production of PI(3,4)P<sub>2</sub>. While PI3K inhibition was alone sufficient to induce Golgi retention of DOR, the exact PI3K subtype involved, and the sufficiency for PI3K activity to stimulate DOR surface trafficking, was unknown. Here, we show that activation of Class I PI3Ks is sufficient to reduce, but not prevent, the NGF and LY294002 induced Golgi retained DOR; however, inhibition of individual Class I PI3Ks are not sufficient to induce Golgi retention of DOR. Further, our data demonstrate that independent of Class I PI3K activity, Class II PI3K  $\alpha$  activity is both required and sufficient for trafficking of DOR to the cell surface. This study provides the first evidence of PI3K C2A playing a required role in biosynthetic trafficking of a G-protein coupled receptor. Additionally, our data implicating the sufficiency of PI3K C2A to drive surface trafficking DOR could serve as an alternative pharmacological targeting strategy for releasing the intracellular pool of DOR to increase DOR agonist efficacy.

Although PI3Ks have been implicated in many cellular signaling and trafficking processes(40-42), the role of specific PI3K subtypes in TGN export has largely been focused on secretory proteins and glucose transporters(12, 43). In most studies, the PI3K inhibitors Wortmannin and LY294002 have been the main tools to dissect the initial involvement of PI3Ks in trafficking processes(44). While the utility of these inhibitors is without question, their use and interpretation must be carefully considered. Initially, Wortmannin was thought to be a broad spectrum PI3K inhibitor, but later it was found to preferentially target Class I PI3Ks by covalently binding to the p110 $\alpha$  subunit at low nanomolar concentrations(15, 21). Interestingly, inhibition of Class II PI3K  $\alpha$  by Wortmannin reveals Wortmannin resistance with an IC<sub>50</sub> value of 420nM, and 80% inhibition at 10 $\mu$ M(15). Therefore, phenotypes observed requiring micromolar concentrations of Wortmannin are unlikely to be dependent upon Class I PI3Ks.

We utilized this distinction between Class I and Class II PI3Ks exhibiting 100-fold sensitivity to Wortmannin to implicate Class II PI3K in DOR trafficking. In our experiments, we observed a partial effect on Golgi retention of DOR following 1 $\mu$ M Wortmannin, and retention comparable to NGF treatment at 10 $\mu$ M concentrations (Figure 2A-C). Further, use of the PI3K activating peptide 740Y<sup>PDGFR</sup>, that binds to the p85 regulatory subunit of Class I PI3Ks, was sufficient to reduce the NGF and LY294002-induced Golgi retention of DOR, but could not revert the Golgi localization of DOR to control levels in PC12 cells (Figure 1A-B). These results, combined with the micromolar concentration of PI3K inhibitors required to induce Golgi retention of DOR, and the inability for Class I specific PI3K inhibitors to promote DOR Golgi retention

(Figure 2D-E), highlight the potential for Class II PI3K involvement, and not Class I PI3Ks. The partial effect observed on reducing the amount of NGF and LY294002-induced retention of DOR following treatment with the Class I PI3K activating peptide might be the result of Class I PI3Ks ability to produce PI(3,4)P<sub>2</sub> when regulatory control by the p85 subunit is removed. Additionally, without subsequent upregulation of the appropriate 3' phosphatases, activating Class I PI3Ks could shift the balance of phosphoinositides within the cell towards 3' phosphorylated species leading to an increase in PI(3,4,5)P<sub>3</sub>, that can be reduced to PI(3,4)P<sub>2</sub> by the SHIP phosphatases (45-47).

While the role of PI(3,4)P<sub>2</sub> in endocytosis from the plasma membrane has been well studied(48), its function at the *trans*-Golgi network is not well defined. Our previous data implicated PI(3,4)P<sub>2</sub> as the required phosphoinositide species driving DOR trafficking from the TGN to the surface. By using a reductionist approach, and inhibitors against the phosphatases PTEN and SHIP2 in combination with NGF treatment, we showed that PTEN inhibition increased DOR surface trafficking while SHIP2 inhibition increased DOR Golgi retention(8). We did not, however, determine the specific PI3K that was likely stimulating PI(3,4)P<sub>2</sub> production and DOR trafficking at the *trans*-Golgi network. The *trans*-Golgi network contains a large pool of the phosphoinositide PI(4)P that can be visualized with fluorescent fusion proteins linked to the Pleckstrin Homology domain of FAPP1(49-52). Interestingly, even though PI(4)P is one of the main substrates for Class II PI3K, and that Class II PI3K has been shown to localize to the *trans*-Golgi network, little has been shown to implicate Class II PI3K in PI(3,4)P<sub>2</sub> production at the TGN to drive exocytic trafficking(14, 17, 53). One possible explanation for PI3K C2A's role at the TGN in DOR trafficking, is that it is functioning similarly to its role in clathrin-mediated endocytosis.

During the process of clathrin-mediated endocytosis, PI(3,4)P<sub>2</sub> is produced by PI3K C2A following clathrin-coated pit formation (48). The specific localization and activity of PI3K C2A acts to spatiotemporally control the process of clathrin-mediated endocytosis by selectively recruiting the BAR domain containing protein SNX9 (48). At the TGN, a similar mechanism analogous to PI3K C2A's role in endocytosis at the cell surface might control the regulated release of DOR. This PI3K C2A dependent pathway might act as receptor selective alternative trafficking route to the more traditional PI4P constitutive export pathway.

It is well established that there are many ways for membrane proteins and cargo to exit the Golgi; however, the most well studied is through activation of PI4KIII and PI4KII to stimulate PI(4)P synthesis within the Golgi complex that can increase the affinity for ARF, AP1, and GGA coat components for the TGN membranes(50, 52, 54-56). Additionally, Protein Kinase D (PKD) activity at the TGN has been shown to further regulate biosynthetic trafficking of the VSVG protein

by controlling synthesis of PI(4)P and PI(4,5)P<sub>2</sub> (55). It is unlikely that the regulated surface delivery of DOR is facilitated through a PI4K-dependent pathway because inhibition of PI4K can be achieved via 150nM Wortmannin(57). To achieve Golgi retention of DOR and to inhibit exocytic trafficking requires micromolar concentrations of Wortmannin (Figure 2B). Furthermore, since PI(4)P at the TGN is in abundance, it is unclear how NGF addition to PC12 cells would inhibit DOR exocytosis in a PI4K dependent manner. For these reasons, we believe our observed effects on retention of DOR within the Golgi might be the result a more specialized PI3K C2A dependent exocytic pathway that requires PI(3,4)P<sub>2</sub> synthesis at the TGN in neuronal cells. More work will need to be done to determine the exact role, if any, that PI4K and PKD play in the regulated surface delivery of DOR.

While the production of PI(3,4)P<sub>2</sub> by PI3K C2A at the TGN has not directly been demonstrated, its localization to the TGN is well documented. Specifically, PI3K C2A has been shown to localize to *trans*-Golgi membranes and clathrin coated vesicles with the AP-1 adaptor protein, and can directly associate with the AP-2 adaptor protein(17, 18). Additionally, PI3K C2A can recruit clathrin through a direct binding interaction within PI3K C2A N-terminal region that activates the enzyme, increases its propensity to produce PI(3,4)P<sub>2</sub> and PI(3,4,5)P<sub>3</sub>, and creates a linkage to the microtubule network (19, 58). In the future, it will be interesting to look at the role clathrin plays in the TGN export of DOR, and to determine which adapter complex is required for its surface delivery in neuronal cells.

Aside from its involvement in clathrin-mediated processes, PI3K C2A activity has also been implicated in exocytosis of neurosecretory granules, cadherin trafficking, and glucose transporter translocation(59-61). The most well studied is the PI3K C2A role in insulin signaling and Glut4 translocation. Observations were made that inhibition of PI3Ks by 1 $\mu$ M Wortmannin could prevent the translocation process of Glut4 and Glut1 downstream of insulin signaling(44). More recent data has shown that Glut4 translocation to the membrane requires PI3K C2A activity. Specifically, 2 min of insulin treatment resulted in a translocation of PI3K C2A to the plasma membrane mediated by the GTPase TC10. This activation stimulated the production of PI(3)P, and was required for the maximal insulin-induced translocation of the glucose transporter Glut4(61, 62). In a similar manner, NGF stimulated Golgi retention of DOR may alter the activity or localization of PI3K C2A associated GTPases like TC10 to mediate export from the TGN. Interestingly, recent studies have shown that the  $\beta$ -1 Adrenergic Receptor (B1AR) is retained intracellularly through an interaction with the PDZ binding protein PIST (Protein Interacting Specifically with TC10) (63), and that the Somatostatin Receptor 5 (SSTR5) is retained in the Golgi through a direct interaction between its C-terminal PDZ ligand and PIST(64). Since the

amino acid sequence of DOR does not harbor a PDZ ligand, it is unlikely that the NGF-induced Golgi retention of DOR is mediated through an interaction with PIST; however, a similar protein-protein interaction dependent on PI3K C2A activity and PI(3,4)P2 synthesis may regulate its TGN export.

In this study, we have directly demonstrated that PI3K C2A is both required and sufficient for complete trafficking of DOR to the cell surface in PC12 cells. Class I PI3K inhibition is not sufficient to cause retention of DOR in the Golgi, and micromolar concentrations of the pan PI3K inhibitors Wortmannin and LY294002, sufficient to inhibit Class II PI3Ks, are necessary for DOR Golgi retention. Finally, optorecruitment of the PI3K C2A kinase domain is sufficient to release the NGF-induced Golgi retention of DOR and stimulate exocytosis from the TGN to the cell surface. These results present the first evidence for PI3K C2A activity mediating a Golgi specific checkpoint controlled by a neuronal-specific signaling axis to induce delivery of GPCR to the surface. In the future, investigations into the sequence specific requirements for entry into this PI3K C2A dependent export pathway could reveal a receptor selective alternative trafficking route to the more traditional PI4P constitutive export pathway.

**Acknowledgements:**

The authors would like to thank Stephanie Crilly, Zara Weinberg, Elena Shuvaeva, Drs. Shanna Bowersox, and Cary Shiwarski for technical help and comments. We thank Drs. Nathan Urban, Adam Linstedt, Tina Lee, Peter Friedman, Guillermo Romero, Jean-Pierre Villardaga, and Alessandro Bisello, for reagents, comments and suggestions. We also thank Drs. Mark von Zastrow, Jim Keen, and Pietro De Camilli for helpful discussions and reagents. M.A.P. was supported by NIH DA024698 and DA036086.

## **Materials and Methods:**

### Cell Lines and Cell Culture

The cell lines used for experimentation were pheochromocytoma-12 (PC12, #CRL-1721), Human Embryonic Kidney 293 (HEK-293, #CRL-1573), and HEK-293T (#CRL-11268) cells. The PC12 cell line is a neuroendocrine cell line isolated from rat adrenal medulla tissue. These cells were grown at 37°C with 5% CO<sub>2</sub> and cultured in F12K medium (Gibco by Life Technologies 21127-022) supplemented with 10% horse serum and 5% fetal bovine serum (FBS). This medium was changed every 3 days to maintain proper pH and nutrient supply. Plastic culture vessels were coated with collagen IV (Sigma #C5533-5MG) to allow PC12 cells to adhere. The standard passage ratio for PC12 cells was 1:4 to ensure sufficient cell-cell contacts are made, facilitating growth. HEK-293 cells were cultured in Dulbecco's Modified Eagle Medium (DMEM) supplemented with 10% FBS at 37°C with 5% CO<sub>2</sub>. Standard passage ratio was 1:10. The HEK-293T cell line is a derivative of HEK-293 cells that contains the SV40 T-antigen to increase replication efficiency of vectors that have a SV40 replication origin. These cells were specifically used for virus production and were maintained in a similar manner to the HEK293 cells.

### DNA Transfection of Cultured Cells:

PC12 cells were plated in collagen IV coated 6-well plates and grown in F12K media containing 10% horse serum and 5% fetal bovine serum for 24 hours before transfection. Lipofectamine 2000 lipofection reagent (Invitrogen 11668-019) was used to transiently transfect PC12 cells with the desired plasmid constructs following the manufacturers recommendations. Briefly, Opti-MEM (100 uL) was added to two 1.7mL microcentrifuge tubes, Lipofectamine 2000 (7.5 uL) (Invitrogen 11668-019) and the appropriate plasmid DNA (1.5 ug) were added to the Opti-MEM containing 1.7mL microcentrifuge tubes and incubated at room temperature for 5 minutes. The Opti-MEM solution containing the DNA was then added to the microcentrifuge tube containing the Lipofectamine 2000, mixed well, and incubated for 20 minutes at room temperature. The growth medium was removed from the cells to be transfected and 1 mL of Opti-MEM was added to each well. Following incubation, the entire transfection mixture was added dropwise to one well. Cells were then incubated with the transfection mixture at 37°C for 5 hours. Subsequently, the transfection solution was aspirated from the wells and replaced with 2 mL of F12K media containing 10% horse serum and 5% fetal bovine serum. Experiments were conducted 48-72 hours following transfection. For HEK 293 cells, similar protocol with was used substituting appropriate cell specific media.

### Fixed Cell Immunofluorescence

HEK 293 and PC12 cells were transfected with either SSF-DOR or SSF-MOR and stable cells were obtained via antibiotic selection. Stably expressing cells were plated on coverslips (Corning) coated with poly-D-lysine (Sigma, #P7280) and grown at 37°C for 24-48 hrs. Following treatments, cells were fixed in 4% paraformaldehyde, pH 7.4. The cells were blocked with calcium magnesium containing phospho buffered saline (PBS) with 5% fetal bovine serum, 5% 1M glycine, and 0.75% Triton X-100. The flag-tagged receptors, Golgi, and trans Golgi network were labeled for one hour in blocking buffer with: anti-FLAG M1 antibody (Sigma, #F3040) (1:1000) conjugated with Alexa-647 (Molecular Probes, #A20186), anti-GPP130 (a gift from Dr. Adam Linstedt), and anti-TGN-38 rabbit polyclonal antibody (1:2000, Sigma-Aldrich cat#: T9826), respectively. Coverslips were washed 3 times in calcium magnesium PBS then labeled with Alexa-568 Goat anti-rabbit secondary (1:1000, #A11011) antibody in blocking buffer for 1 hour. Cover slips were washed 3 more times in calcium magnesium PBS and mounted onto glass slides using Prolong Diamond Reagent (Molecular Probes, #P36962). Confocal imaging of the mounted cells was performed using a confocal imaging system (XDi spinning disk, Andor) at 60X magnification (Nikon CFI APO TIRF) on a Nikon TE-2000 inverted microscope. Additionally, the imaging set-up contained live cell temperature and humidity controlled imaging capabilities, a mechanical Piezo XYZ-stage (Nikon), iXon 897 Ultra back-illuminated camera (Andor), a laser combiner (Andor) containing 405, 488, 515, 568, and 647nm excitation capabilities, a Dell 5400 Workstation optimized for IQ2 imaging software (Andor), and an active isolation air table (TMC). Images of representative fields were taken. Quantification of the fluorescence ratio was taken for a minimum of 50 cells and averaged to ensure results were representative of the population. A minimum of three biological replicates were performed to confirm the results.

### VSVG-Assay

HEK-293 cells were transfected with either VSVG-GFP or VSVG-GFP-DORtail construct, grown under antibiotic selection, and maintained at the restrictive temperature of 40°C in standard culture medium. Cells were plated on 25mm coverslips and imaged live via confocal fluorescence microscopy using a Nikon TE-2000 inverted microscope as described previously. To initiate ER-

exit and trafficking of the VSVG proteins, live cell imaging was performed at 32°C, and confocal images were acquired every 10 seconds for 2 hours. Cells were treated with vehicle controls or with the PI3 kinase inhibitors Wortmannin or LY294002, (+) and (-) the PI3 kinase activating peptide 740Y<sup>PDGFR</sup>. The images were compiled to form a time-lapse movie showing the cellular trafficking of the  $\alpha$  VSVG-GFP or VSVG-GFP-DORTail expressing cells. GFP fluorescence intensity was quantified using Image J software.

#### Inhibitors and Activators

Compound Name	Protein Target	Concentration	Supplier	Catalog #
Nerve Growth Factor	TrkA	100 ng/ $\mu$ L	BD Biosciences	356004
740Y <sup>PDGFR</sup>	PI3K activator	50 $\mu$ g/mL	Tocris Bioscience	1983
LY294002	PI3K inhibitor	10 $\mu$ M	Tocris Bioscience	1130
Wortmannin	PI3K inhibitor	10 $\mu$ M	Enzo Life Sciences	BML-ST415
PI-103	PI3K C1 $\alpha$ inhibitor	50 nM	Echelon Biosciences	B0303
IC87114	PI3K C1 $\delta$ inhibitor	5 $\mu$ M	Echelon Biosciences	B0305
AS605240	PI3K C1 $\gamma$	25 nM	Echelon Biosciences	B0301

#### Lentiviral shRNA Knockdown of PI3 Kinase C2 $\alpha$ :

Knockdown of PI3 kinase C2 $\alpha$  was performed using shRNA constructs targeting the Rat Pik3c2a. The lentiviral vectors pLenti X1 Puro DEST (694-6) and pENTR/pSM2(CMV) GFP (w513-1) were a gift from Eric Campeau vector (Addgene plasmid #19170, #17297) (33), and the shRNA sequences were designed by following an established protocol from the Hannon Lab and entering the target sequence into the web page: [http://cancan.cshl.edu/RNAi\\_central/RNAi.cgi?type=shRNA](http://cancan.cshl.edu/RNAi_central/RNAi.cgi?type=shRNA) (32). This site outputs a 22\_mer sequence as well as a 97 bp sequence. Restriction sites should be added such that the sequences

can be inserted into the pSM2 plasmid: a XhoI site at the 5' end and an EcoR1 site at the 3' end. After addition of the restriction sites, the sequences were ordered as adapter pairs for cost efficiency. These sequences can be found in Supplemental Table 1. Once the sequences were obtained, a double digest of the pSM2 entry vector was performed with EcoR1 (New England Biolabs) and Xho1 (New England Biolabs). The digested product was run on a 1% agarose gel and purified using a Qiagen Gel Extraction Kit (Qiagen 28704). The adapters (purchased from IDT) were annealed then ligated into the linearized entry vector, pENTR/pSM2(CMV) GFP (w513-1). The ligated constructs were transformed into DH5 $\alpha$  cells and multiple colonies from each transformation were chosen to screen for the correct insert. Correct insertion was confirmed via restriction digest and DNA sequencing. Transient transfection of PC12 cells using Lipofectamine 2000 followed by western blotting was used to assess the knockdown efficiency of the shRNA constructs. The shRNA construct which produced the most efficient knockdown, shRNA #3 in figure 3-A, was inserted into the pLenti-X1 destination vector via the Gateway Cloning Method using the LR reaction (Life Technologies 11791-019) to produce the pLenti-X1-puro-PI3K C2 $\alpha$  shRNA construct.

Lentiviral particles were produced using this construct to stably infect and knockdown PI3K C2 $\alpha$  in PC12 cells. HEK 293T cells were transfected with 15  $\mu$ g pLenti-X1-puro-PI3K C2 $\alpha$  shRNA, 15  $\mu$ g of pMDLg/pRRE (Addgene plasmid #12251), 6  $\mu$ g of pRSV-Rev (Addgene plasmid #12253), and 3  $\mu$ g of pMD2.G (Addgene plasmid #12259) as per Campeau et al. These plasmids were a gift from Didier Trono. The media was changed 24 hours post-transfection. A GFP marker in the expression construct was used to determine transfection efficiency. Exactly 64 hours post-transfection, the virus-containing media was removed and centrifuged at 3,000 x g to pellet non-adherent cells and debris. The virus-containing media was further sterile filtered through a 0.45  $\mu$ m sterile filter to remove any remaining cells debris. To achieve maximum infection efficiency, 1.5 mL of the filtered virus solution was added to each well of a 6-well plate containing PC12 cells at 50% confluency. GFP expression was used to assess proper functional viral production and infection efficiency. Approximately 48 hours post-infection, puromycin (Gibco by Life Technologies A11138-03) selection was added to the growth medium at 1  $\mu$ g/ mL. Stable lines expressing the PI3K C2A shRNA were obtained within 1 week from initial infection, and knockdown was confirmed via immunoblotting.

#### Immunoblotting and Densitometry:

The knockdown of PI3 kinase C2 $\alpha$  was assessed by western blotting. The 6-well plates were placed on ice and growth media was removed, then each well was rinsed with 1 mL PBS.

500  $\mu$ L of PBS was added and cells were scraped collected and transferred to 1.7 mL tubes. Cells were pelleted at 1200  $\times$  g for 5 minutes. Supernatant was aspirated and the pellet was resuspended in 30-75  $\mu$ L of lysis buffer containing 2% SDS, 60 mM Tris-HCL pH 6.8 with Complete Mini EDTA-free (Roche T00004) and PhosStop Tab (Roche A00173). Cells were lysed by vortexing for 15 seconds followed by 2 minutes in a 95°C heat block, then pipetting up and down 3-5 times. This lysis process was performed twice. BCA protein estimation (Pierce BCA Assay KIT, Thermo Fisher, #23225) was performed. For each condition, 40  $\mu$ L samples were prepared from the lysates such that protein content and volume was standardized. 10  $\mu$ L of 4X loading dye and fresh BME and 1  $\mu$ L of 1M DTT were added to the samples. To denature the proteins, samples were heated to 95°C for 5 minutes and ran on a 4–15% Mini-PROTEAN® TGX Stain-Free™ Protein Gels (BioRad #4568083). An overnight transfer at 4°C to a nitrocellulose membrane was performed. Following transfer, the blot was blocked with 5%-TBST for one hour on a shaker. Primary antibody for PI3K C2A (Abcam ab154583) was prepared at 1:1000 in 5% milk-TBST and added to the blot. The blot was incubated at room temperature on a shaker for 1 hour or overnight in cold room. The primary antibody solution was removed and the blot was washed 3X for 5 minutes with 5% milk-TBST. The secondary antibody Goat anti-Rabbit (BioRad #1706515) was prepared at 1:3000 in 5% milk-TBST and added to the blot which incubated on a shaker at room temperature for 1 hour. The secondary antibody solution was removed and the blot was washed 2X for 5 min with TBST and once for 5 minutes with TBS. The blot was developed with Clarity™ Western ECL Substrate (BioRad #1705061) and imaged using the ChemiDoc Touch imaging system (BioRad). Densitometry was performed using the built-in Image J plugin to quantify the band intensity in each lane. Values were then normalized and plotted using Microsoft Excel.

#### Live Cell Imaging with a Fluorogen-activated Peptide

PC12 cells and PC12 cells expressing PI3 kinase C2 $\alpha$  shRNA were plated in a 6-well plate. Once confluency reached approximately 50%, these cells were transfected with a DOR construct that is N-terminally tagged with a fluorogen-activated peptide (FAP) using the Lipofectamine 2000. Two days post transfection, cells were plated on 25 mm poly-D lysine-coated coverslips (Electron Microscopy Sciences Micro Coverglass # 1 ½, #72225-01). The FAP-DOR has a far-red emission spectra, resulting from a malachite green (MG)-based fluorogen (34, 65), which can be visualized via fluorescent microscopy. Fifteen minutes prior to imaging, the cell permeable MG-ester based fluorogen (100nM) was added to the cells. Live confocal imaging of was performed at 37°C using a Nikon TE-2000 inverted microscope. FAP-DOR localization was

quantified using Image J software to determine the ratio of internal DOR fluorescence compared to the total fluorescence signal.

#### Optogenetic Recruitment of PI3K C2 $\alpha$ to the TGN and Release of DOR

The CRY2-CIBN optical recruitment system was adapted by cloning the PI3K C2 $\alpha$  kinase domain (amino acids 863-1405, KD) onto the C-terminus of an mCherry-CRY2 chimeric construct (a gift from Pietro De Camilli) to make mCherry-CRY2-PI3K-C2 $\alpha$ -KD(38). GFP-CIBN, a gift from Chandra Tucker (Addgene plasmid # 26867), was adapted for TGN specific recruitment by cloning the N-term of 2,6 sialyltransferase onto the C-terminus of GFP-CIBN to make GFP-CIBN-SialyT(39). PC12 cells were transiently transfected with the FAP-DOR (1 $\mu$ g), mCherry-CRY2-PI3K-C2 $\alpha$ -KD (C2A KD, 2.5 $\mu$ g), GFP-CIBN-SialyT (CIBN-TGN, 1 $\mu$ g), and the TGN localized PI(4)P sensor PH-FAPP1- iRFP (PH-FAPP1, PH-FAPP1-GFP was a gift from Tamas Balla, 0.5 $\mu$ g) for live imaging of the optogenetic recruitment(66). The GFP-CIBN-SialyT has a basal TGN localization and the mCherry-CRY2-PI3K-C2 $\alpha$ -KD is cytoplasmic before recruitment. Optorecruitment is activated by blue light stimulation at 488nm driving the mCherry-CRY2-PI3K-C2 $\alpha$ -KD to the TGN.

For experiments involving the release of Golgi-retained DOR following by C2A KD recruitment to the TGN, PC12 cells expressing the optogenetic recruitment system were plated onto 25mm poly-D lysine coated coverslips and grown for 48 hours. On the day of the experiment, the coverslips were transferred to imaging chambers and treated with NGF (100ng/mL) for 1 hour. The chambers were then moved to the microscope for live cell confocal imaging performed at 37°C using a Nikon TE-2000 inverted microscope. FAP-DOR was labeled with the MG-ester dye (100nM), and baseline images for DOR (640 nm excitation, 700/75 nm emission) and C2A-KD (561 nm excitation, 620/60 nm emission) expression and localization were acquired three times at 5 second intervals. Initial live recruitment of C2A-KD to the CIBN-TGN was performed by dual excitation of 561nm (35% power) and 488nm (10% power) for one minute with a 620/60 nm emission filter to visualize in real-time the recruitment of the C2A-KD. To maintain C2A-KD recruitment and to visualize DOR trafficking over time, subsequent images were acquired for CIBN-TGN (488nm excitation, 525/50 nm emission), C2A-KD (561 nm excitation, 620/60 nm emission), and FAP-DOR (640nm excitation, 700/75nm emission) every 30 seconds for 15 minutes. Quantification of the live imaging recruitment movies was performed using Image J software. Fluorescence intensity of TGN-localized DOR was compared to the total fluorescence

for each cell and expressed as a ratio. When DOR is released from the TGN, the signal within the TGN decreases as the surface signal increases. Thus, the ratio of TGN to total fluorescence decreases as DOR is released from the Golgi.

#### Line Scan Analysis

A line scan analysis was used to confirm colocalization recruitment of the C2A-KD to the CIBN-TGN, and the PH-FAPP1. Using Image J software, the fluorescence intensity was measured over a line that passed through the region of CIBN-TGN fluorescence and the relative spatiotemporal fluorescence intensity over a pixel (px) area was compared between each of the three channels for C2A-KD, CIBN-TGN, and PH-FAPP1. Colocalization and recruitment was confirmed by visualizing overlapping peaks of fluorescence along the length of this line normalized to the maximal fluorescence intensity in each channel over the line area. During recruitment, the C2A-KD peak increases and localizes to the peaks defined by CIBN-TGN and PH-FAPP1. The data was plotted using Graph Pad Prism software.

#### Image Analysis and Quantification

All imaging data was quantified using Image J. This software was used to measure the total DOR fluorescence for each cell and the fluorescence intensity of DOR within the Golgi for fixed and live cell analysis. The values measured using Image J were transferred to Microsoft Excel to calculate the ratio of the Golgi fluorescence to the total cell fluorescence. This ratio was calculated for each cell and all cell ratios were averaged. The average represents the fraction of DOR present in the Golgi compared to the total cell fluorescence. Additionally, a manual binary quantification was performed to determine the percentage of cells that visually displayed Golgi-localized DOR. Based on visual inspection, each cell that had at least half of its DOR present in the Golgi is scored as a 1 and cells which have little or no DOR in the Golgi are scored as a 0. The average of the binary quantification was used to determine the percentage of cells with Golgi-localized DOR.

#### Statistics and Data Analysis

Statistical analyses were performed using GraphPad Prism 5 software, and the appropriate statistical tests were chosen based on sample size, distribution, and experimental

conditions. A minimum of three independent experiments were performed for each set of data. For statistical analysis of the fixed and live cell immunofluorescence imaging data, two-tailed unpaired t-tests were performed between the different experimental conditions and controls. A p-value of < 0.05 was considered statistically significant. All images were quantified using macros constructed from the functions within Image J software package. Figures were constructed with Image J and Adobe Photoshop CS6.

### Supplemental Table 1:

Table of sequences ordered and 22mer targets

	shRNA 22_mer Sequence	Adapter Pairs
#1	GCCACACCATTTTCATCCACAAG	5'- TCGAGTGCTGTTGACAGTGAGCG <b>ACCACACCATTTTCATCCACAAG</b> TAGTGAAGC - 3' 3'- CACGACAAC <b>TGTC</b> ACTCGCT <b>GGTGTGGTAAAGTAGGTGTT</b> CATCACTTCGGGTGC - 5'
		5'- CACAGATGTACT <b>TTGTGGATGAAATGGTGTGG</b> CTGCCTACTGCCTCGGAG - 3' 3'- TACAT <b>GAACACCTACTTTACCACACCG</b> ACGGATGACGGAGCCTCTTAA - 5'
#2	GAAGGTTGGCACATACAAGAAT	5'- TCGAGTGCTGTTGACAGTGAGCG <b>AAAGGTTGGCACATACAAGAAT</b> TAGTGAAGC - 3' 3'- CACGACAAC <b>TGTC</b> ACTCGCT <b>TTCCAACCGTGTATGTTCTTA</b> ATCACTTCGGGTGC - 5'
		5'- CACAGATGTAA <b>TTCTTGTATGTGCCAACCTT</b> CTGCCTACTGCCTCGGAG - 3' 3'- TACAT <b>TAAAGAACATACACGGTTGGAAG</b> ACGGATGACGGAGCCTCTTAA - 5'
#3	AAAGATATTGCTGGATGACAAT	5'- TCGAGTGCTGTTGACAGTGAGCG <b>CAAGATATTGCTGGATGACAAT</b> TAGTGAAGC - 3' 3'- CACGACAAC <b>TGTC</b> ACTCGC <b>GTTCTATAACGACCTACTGTTA</b> ATCACTTCGGGTGC - 5'
		5'- CACAGATGTAA <b>TTGTCATCCAGCAATATCTTTT</b> GCCTACTGCCTCGGAG - 3' 3'- TACAT <b>TAAACAGTAGGTCGTTATAGAAA</b> ACGGATGACGGAGCCTCTTAA - 5'
#4	TCCAGTCACAGTGCAAAGAAAC	5'- TCGAGTGCTGTTGACAGTGAGCG <b>CCCAGTCACAGTGCAAAGAAAC</b> TAGTGAAGC - 3' 3'- CACGACAAC <b>TGTC</b> ACTCGC <b>GGGTCAGTGTACGTTTCTTTG</b> ATCACTTCGGGTGC - 5'
		5'- CACAGATGTAG <b>TTTCTTTGCACTGTGACTGG</b> ATGCCTACTGCCTCGGAG - 3' 3'- TACAT <b>CAAAGAAACGTGACACTGACCT</b> ACGGATGACGGAGCCTCTTAA - 5'
#5	AGCCTACAACCTTGATAAGAAAG	5'- TCGAGTGCTGTTGACAGTGAGCG <b>CGCCTACAACCTTGATAAGAAAG</b> TAGTGAAGC - 3' 3'- CACGACAAC <b>TGTC</b> ACTCGC <b>GCGGATGTTGA</b> ACTAT <b>TTCTTT</b> CATCACTTCGGGTGC - 5'
		5'- CACAGATGTACT <b>TTCTTATCAAGTTGTAGG</b> CTTGCCTACTGCCTCGGAG - 3' 3'- TACAT <b>GAAAGAATAGTTCAACATCCGA</b> ACGGATGACGGAGCCTCTTAA - 5'

## Figure Legends:

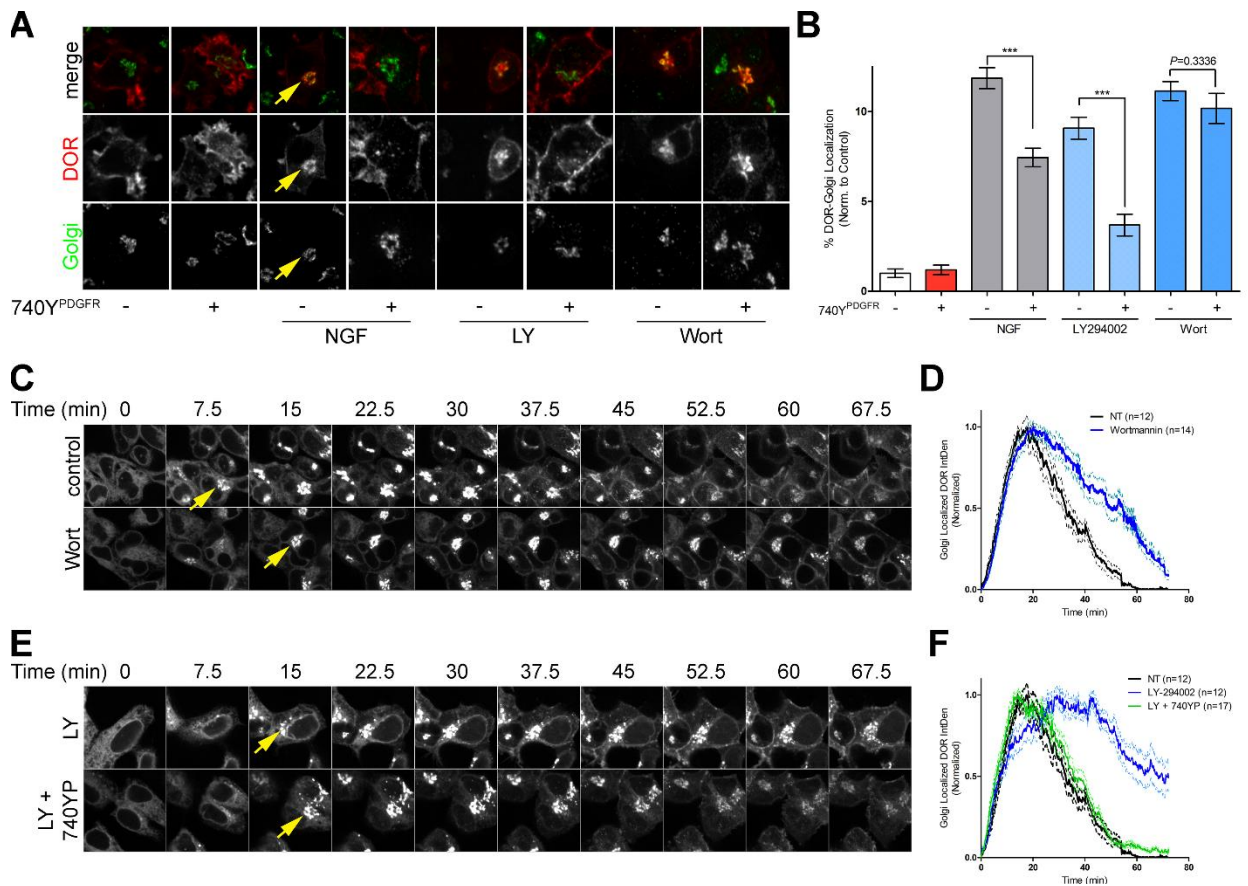


**Figure 1: Activation of PI3K by 740Y-PDGFR is sufficient to reduce the PI3K-inhibition induced retention of DOR.** **A.** Example images (of  $n = 3$  independent experiments) for PC12 cells expressing FLAG-DOR, untreated (first two columns), or treated with Nerve Growth factor (NGF, 100ng/mL) for 1 hour. NGF treatment induces intracellular retention of DOR (Red) that colocalizes with the Golgi (Green). Inhibition of PI3K via LY294002 (LY, 10 $\mu$ M) or Wortmannin (Wort, 10 $\mu$ M) is sufficient to cause an accumulation of DOR in the Golgi. Activation of PI3K by the p85 subunit binding peptide 740Y<sup>PDGFR</sup> (50 $\mu$ g/mL) decreased the NGF and LY294002-induced Golgi localization of DOR, but did not reduce the Wortmannin-induced localization of DOR. Images are shown (-) and (+) 740Y<sup>PDGFR</sup>. **B.** Image analysis and quantification shows a significant reduction in the % of total DOR fluorescence that overlaps with the Golgi in the NGF and LY294002 conditions following addition of the PI3K activating peptide 740Y<sup>PDGFR</sup>. There was no significant reduction in the amount of Wortmannin-induced retention of DOR following the addition of 740Y<sup>PDGFR</sup>. Further, 740Y<sup>PDGFR</sup> had no effect on Golgi localization of DOR on its own (Ctl (-),  $n=108$  cells; NGF (-),  $n=127$  cells; NGF (+),  $n=162$  cells; LY (-),  $n=104$  cells; LY (+),  $n=60$  cells; Wort (-),  $n=119$  cells; Wort (+),  $n=49$  cells; 740Y<sup>PDGFR</sup> (+),  $n=30$  cells; mean  $\pm$  s.e.m.;

\*\*\* $P < 0.001$ ; by one-way ANOVA with Dunn's Multiple Comparison Test). **C.** Example time-lapse images (of  $n = 4$  independent experiments) for HEK 293 cells expressing VSVG-DORtail-GFP imaged at the permissive temperature of 32°C. PI3K inhibition by Wortmannin (Wort, 10 $\mu$ M) resulted in sustained intracellular Golgi signal compared to control. **D.** Quantification of the Golgi associated fluorescence signal revealed a kinetic slowing of trafficking from the Golgi following treatment with Wortmannin (control,  $n=12$  cells; Wortmannin,  $n=14$  cells; mean  $\pm$  s.e.m.). **E.** Example time-lapse images (of  $n = 4$  independent experiments) for HEK 293 cells expressing VSVG-DORtail-GFP imaged at the permissive temperature of 32°C. PI3K inhibition by LY294002 (LY, 10 $\mu$ M) resulted in sustained intracellular Golgi signal compared to control. When LY294002 was combined with the PI3K activating peptide 740Y<sup>PDGFR</sup> (50 $\mu$ g/mL) the sustained fluorescence Golgi signal was abolished. **F.** Quantification of the Golgi associated fluorescence signal revealed a kinetic slowing of trafficking from the Golgi following treatment with LY294002 that was reverted with addition of the PI3K activating peptide 740Y<sup>PDGFR</sup> (control,  $n=12$  cells; LY294002,  $n=12$  cells; LY294002 + 740Y<sup>PDGFR</sup>,  $n=17$  cells; mean  $\pm$  s.e.m.).

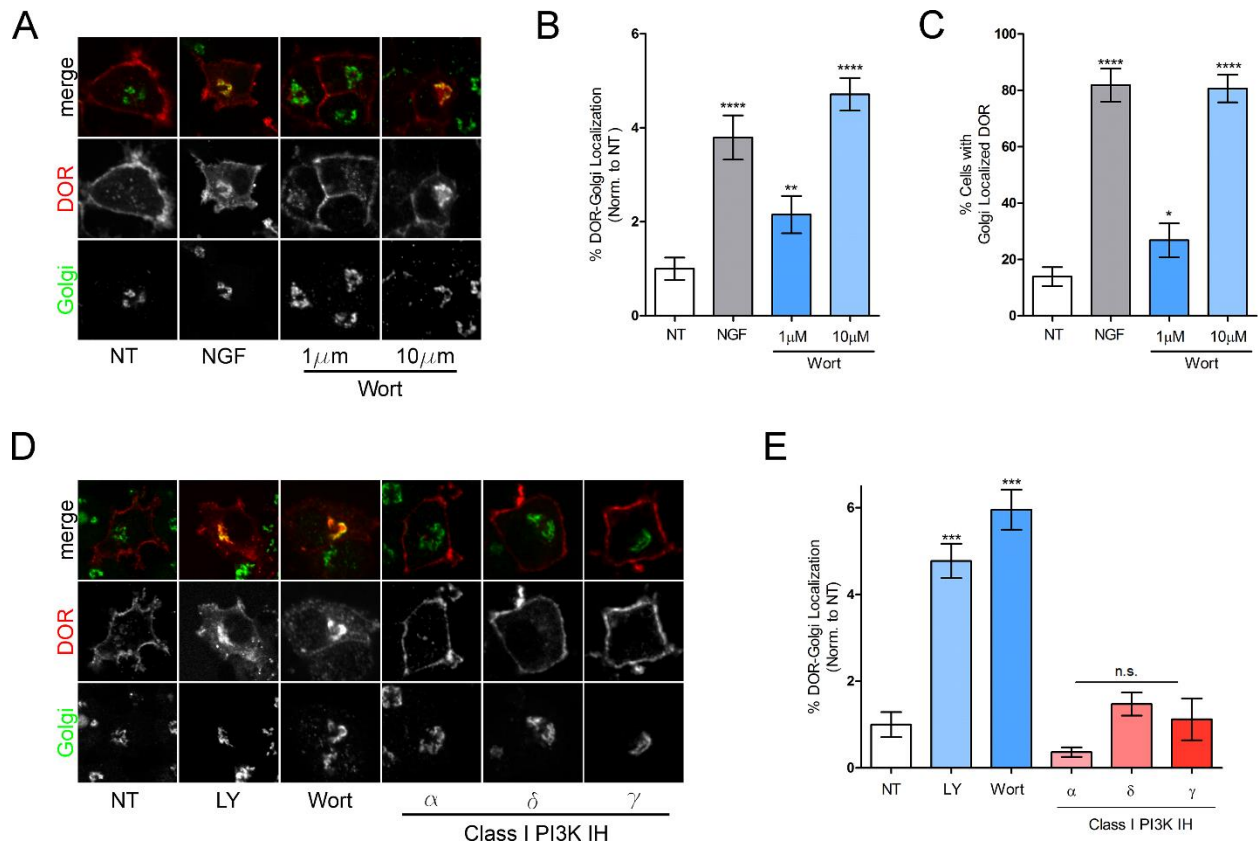


**Figure 2: Class I PI3K is not required for Golgi retention of DOR.** **A.** Example images (of  $n = 3$  independent experiments) for PC12 cells expressing FLAG-DOR, untreated (NT), or treated with Nerve Growth factor (NGF, 100ng/mL) for 1 hour. NGF treatment induces intracellular retention of DOR (Red) that colocalizes with the Golgi (Green). Inhibition of PI3K via Wortmannin (Wort, 1  $\mu$ M) leads to a partial accumulation of DOR in the Golgi. Inhibition of PI3K via Wortmannin (Wort, 10  $\mu$ M) leads to a large accumulation of DOR in the Golgi. **B.** Image analysis and quantification shows a significant increase in the % of total DOR fluorescence that overlaps with the Golgi in the NGF condition, and a dose dependent effect on the % of DOR-Golgi localization for Wortmannin 1  $\mu$ M and 10  $\mu$ M (NT,  $n=105$  cells; NGF,  $n=64$  cells; Wort 1  $\mu$ M,  $n=56$  cells; Wort 10  $\mu$ M,  $n=67$  cells; mean  $\pm$  s.e.m.; \*\* $P<0.01$ , \*\*\*\* $P<0.0001$ ; by two-sided  $t$ -test vs. NT). **C.** Further quantification demonstrated a significant increase in the % cells with Golgi-localized DOR following NGF treatment and PI3K inhibition by Wortmannin 1  $\mu$ M and 10  $\mu$ M (NT,  $n=105$  cells; NGF,  $n=64$  cells; Wort 1  $\mu$ M,  $n=56$  cells; Wort 10  $\mu$ M,  $n=67$  cells; mean  $\pm$  s.e.m.; \*\* $P<0.01$ , \*\*\*\* $P<0.0001$ ; by two-sided  $t$ -test vs. NT). **D.** Example images (of  $n = 3$  independent experiments) for PC12 cells expressing FLAG-DOR, untreated (NT), or treated with Nerve Growth factor (NGF, 100ng/mL), LY294002 (LY, 10  $\mu$ M), or Wortmannin (Wort, 10  $\mu$ M) for 1 hour induces intracellular retention of DOR (Red) that colocalizes with the Golgi (Green). Class I specific PI3K inhibitors PI-

103 (PI3K C1  $\alpha$ , 50nM), IC87114 (PI3K C1  $\delta$ , 5 $\mu$ M), and AS605240 (PI3K C1  $\gamma$ , 25nM) were not sufficient to cause Golgi retention of DOR. **E.** Image analysis and quantification demonstrated a significant increase in the % cells with the Golgi-localized DOR following NGF treatment and PI3K inhibition by LY294002 (LY, 10 $\mu$ M), or Wortmannin (Wort, 10 $\mu$ M), but not following Class I specific PI3K inhibition by PI3K inhibitors PI-103 (PI3K C1  $\alpha$ , 50nM), IC87114 (PI3K C1  $\delta$ , 5 $\mu$ M), and AS605240 (PI3K C1  $\gamma$ , 25nM) (NT,  $n=42$  cells; NGF,  $n=73$  cells; LY,  $n=77$  cells; Wort,  $n=45$  cells;  $\alpha$ ,  $n=82$  cells;  $\delta$ ,  $n=99$  cells;  $\gamma$ ,  $n=28$  cells; mean  $\pm$  s.e.m.; \*\* $P<0.01$ , \*\*\*\* $P<0.0001$ ; by two-sided  $t$ -test vs. NT).

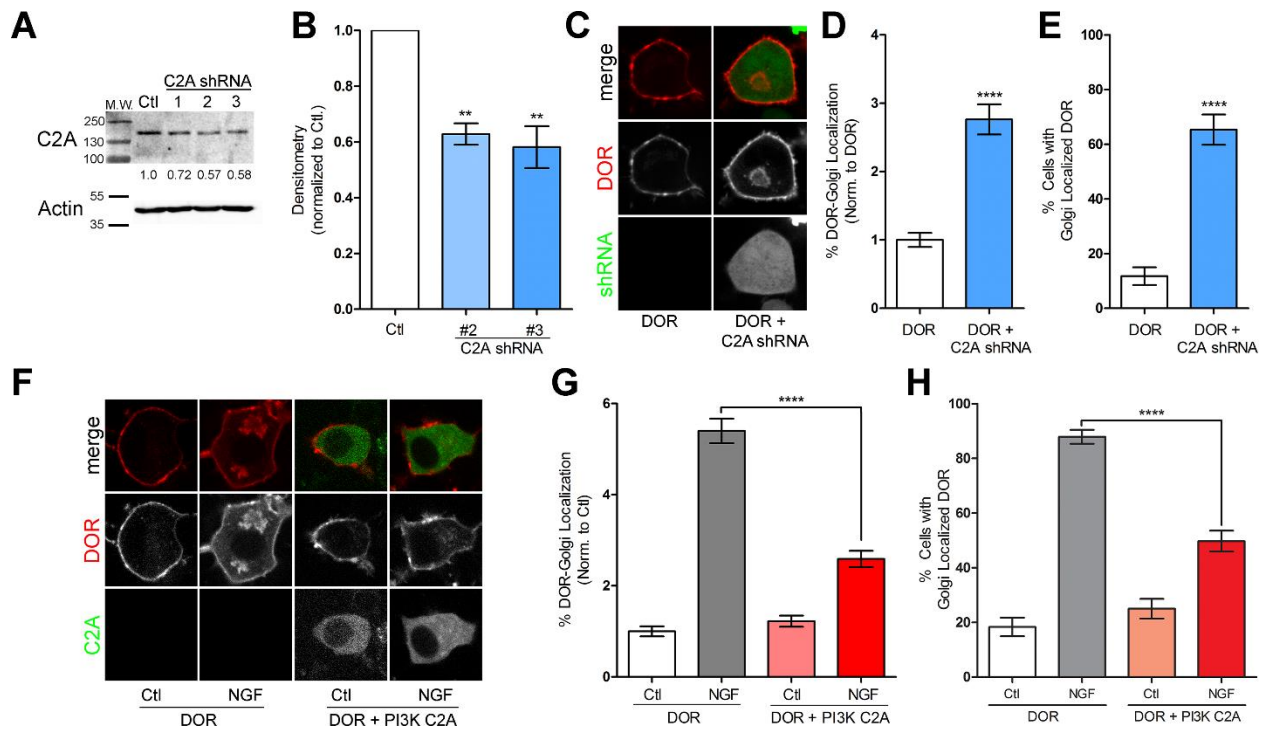


**Figure 3: Class II PI3K C2 $\alpha$  is required for surface trafficking of DOR.** **A.** Immunoblotting for PI3K C2 $\alpha$  (C2A) confirmed knockdown of C2A in PC12 cells stably expressing C2A lentiviral shRNA. Three different shRNA sequences were used to determine the most efficient knockdown. A representative immunoblot is shown, with actin as a loading control. Blot densitometry was performed to quantitate the percentage of knockdown for C2A shRNA sequences #1, #2, and #3 compared to control (Ctl) cells. **B.** Densitometry (of  $n = 3$  independent experiments) revealed C2A shRNA sequences #2 and #3 as providing a significant reduction in C2A protein expression with shRNA #3 providing the best knockdown at 49% ( $n=3$ ; mean  $\pm$  s.e.m.; \*\* $P < 0.01$ ; by two-sided  $t$ -test vs. Ctl). **C.** Example images (of  $n = 3$  independent experiments) for PC12 cells expressing FAP-DOR (DOR) with and without lentiviral PI3K C2 $\alpha$  shRNA #3 (C2A shRNA) with a GFP reporter. Cells stably expressing the PI3K C2 $\alpha$  shRNA were identified via GFP expression, and had increased intracellular DOR. **D.** Image analysis and quantification revealed a significant increase in the % of total DOR fluorescence that overlaps with the Golgi in cells stably expressing the PI3K C2 $\alpha$  shRNA compared to DOR only cells (DOR,  $n=102$  cells; DOR + C2A shRNA,  $n=75$  cells; mean  $\pm$  s.e.m.; \*\*\*\* $P < 0.0001$  by two-sided  $t$ -test vs. DOR). **E.** Further quantification confirmed a significant increase in the % cells with Golgi-localized DOR in cells stably expressing the PI3K C2 $\alpha$  shRNA compared to DOR only cells (DOR,  $n=102$  cells; DOR + C2A shRNA,  $n=75$  cells; mean  $\pm$  s.e.m.; \*\*\*\* $P < 0.0001$  by two-sided  $t$ -test vs. DOR). **F.** Example images (of  $n = 3$  independent experiments) for PC12 cells expressing FAP-DOR (DOR, Red) alone and in combination with overexpression of GFP-PI3K C2 $\alpha$  (PI3K C2A, Green) untreated (Ctl), or treated

with Nerve Growth factor (NGF, 100ng/mL) for 1 hour. Overexpression of GFP-PI3K C2 $\alpha$  was sufficient to prevent the NGF-induced Golgi retention of DOR. **G.** Quantification and image analysis show a significant decrease in the % of total DOR fluorescence that overlaps with the Golgi in cells treated with NGF when overexpressing GFP-PI3K C2 $\alpha$  compared to DOR only cells (DOR Ctl,  $n=131$  cells; DOR NGF,  $n=165$  cells; DOR + PI3K C2A Ctl,  $n=144$  cells; DOR + PI3K C2A NGF,  $n=171$  cells; mean  $\pm$  s.e.m.; \*\*\*\* $P<0.0001$  by two-sided  $t$ -test vs. DOR Ctl). **H.** Further quantification demonstrated a significant decrease in the % cells with Golgi-localized DOR in cells treated with NGF when overexpressing GFP-PI3K C2 $\alpha$  compared to DOR only cells (DOR Ctl,  $n=131$  cells; DOR NGF,  $n=165$  cells; DOR + PI3K C2A Ctl,  $n=144$  cells; DOR + PI3K C2A NGF,  $n=171$  cells; mean  $\pm$  s.e.m.; \*\*\*\* $P<0.0001$  by two-sided  $t$ -test vs. DOR Ctl).

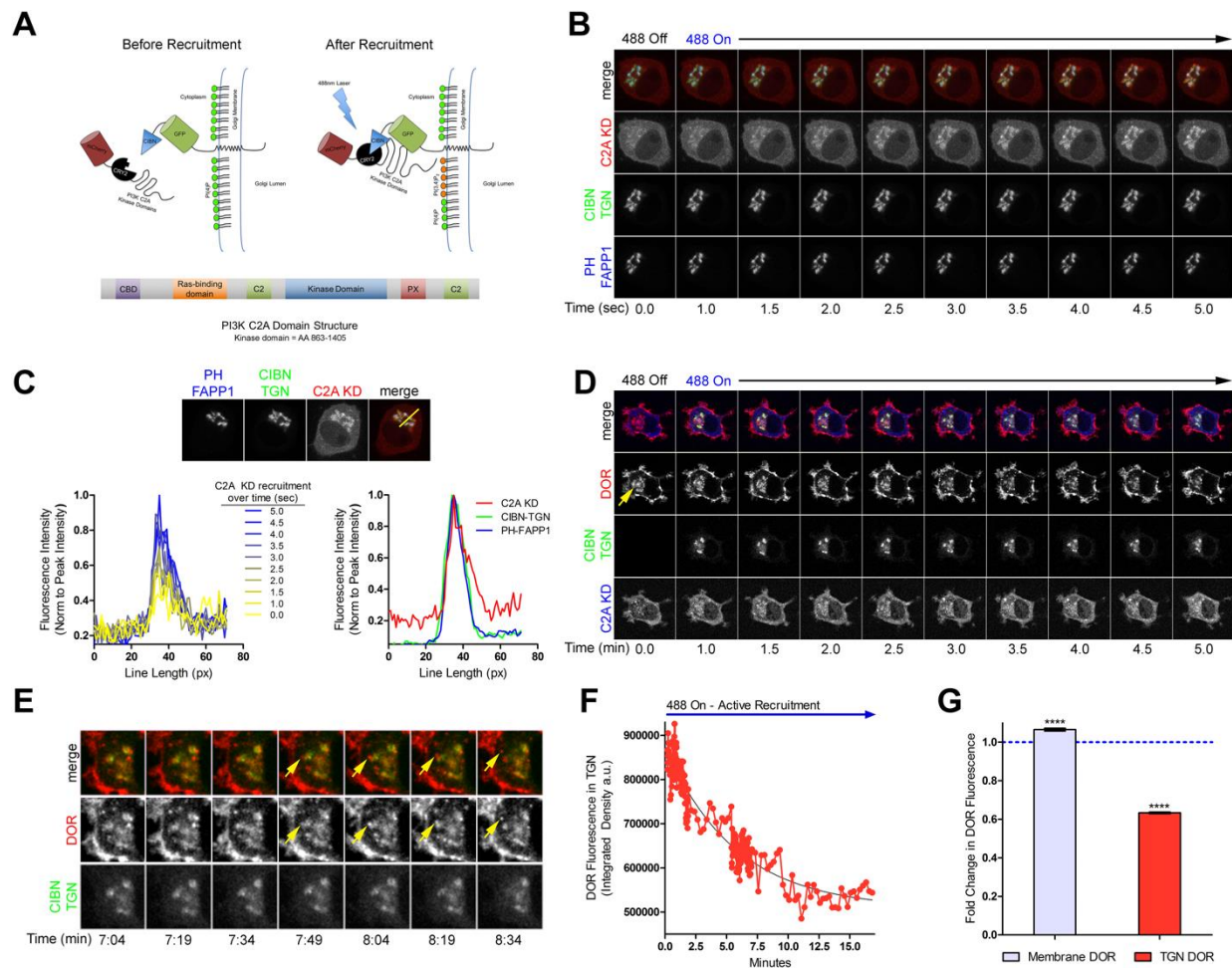


**Figure 4: Optogenetic recruitment of the PI3K C2 $\alpha$  kinase domain to the *trans*-Golgi network is sufficient to induce DOR surface trafficking.** **A.** A schematic showing the optogenetic recruitment strategy for targeting the PI3K C2 $\alpha$  kinase domain to the *trans*-Golgi network (TGN) upon stimulation with blue light. The CRY2-CIBN optical recruitment system was adapted by cloning the PI3K C2 $\alpha$  kinase domain (amino acids 863-1405, KD) onto the C-terminus of an mCherry-CRY2 chimeric construct to make mCherry-CRY2-PI3K-C2 $\alpha$ -KD. Additionally, the GFP-CIBN was adapted for TGN specific recruitment by cloning the N-term of 2,6 sialyltransferase onto the C-terminus of GFP-CIBN to make GFP-CIBN-SialyT. The GFP-CIBN-SialyT has a basal TGN localization and the mCherry-CRY2-PI3K-C2 $\alpha$ -KD is mostly cytoplasmic before recruitment. Optorecruitment is activated by blue light stimulation at 488nm driving the mCherry-CRY2-PI3K-C2 $\alpha$ -KD to the TGN. This process provides spatiotemporal control over the PI3K-C2 $\alpha$ -KD activity on phospholipid conversion at the TGN. **B.** PC12 cells were transiently transfected with the mCherry-CRY2-PI3K-C2 $\alpha$ -KD (C2A KD, Red), GFP-CIBN-SialyT (CIBN-TGN, Green), and the TGN-localized PI(4)P sensor PH-FAPP1- iRFP (PH-FAPP1, Blue) for live

imaging of the optogenetic recruitment. Before stimulation with the 488nm light, CIBN-TGN and PH-FAPP1 were colocalized, and the C2A KD was cytoplasmic. During the live stimulation with 488nm light, recruitment of the C2A KD to the CIBN-TGN and PH-FAPP1 can be observed within 5 seconds. **C.** Analysis of the recruitment and colocalization of the C2A KD to the CIBN-TGN and PH-FAPP1 region was performed via a line scan plot (example line in Yellow) to identify relative spatiotemporal fluorescence intensity over a pixel (px) area. Over time, the fluorescence intensity profile of the C2A KD along the line increased (Left, Yellow to Blue), and the peak fluorescence intensity, and the fluorescence intensity distribution for C2A KD (Red), CIBN-TGN (Green), and PH-FAPP1 (Blue) are all highly overlapping after 5 seconds (Right). **D.** PC12 cells were transiently transfected with the mCherry-CRY2-PI3K-C2 $\alpha$ -KD (C2A KD, Blue), GFP-CIBN-SialyT (CIBN-TGN, Green), and FAP-DOR (DOR, Red) for live imaging of the optogenetic recruitment and induced surface trafficking following NGF-induced retention of DOR. NGF (100ng/mL) was added for 1 hour to cause Golgi retention of DOR (Yellow arrow). Optical recruitment of the mCherry-CRY2-PI3K-C2 $\alpha$ -KD to the TGN was performed to stimulate PI3K C2 $\alpha$  and induce surface trafficking of the retained pool of DOR. Following recruitment, the Golgi pool of DOR decreases and appears to vesiculate. **E.** Analysis of live imaging frames reveal the formation of vesicles containing DOR beginning in the TGN (Yellow arrow), bud off, and appear to be trafficking to the cell surface. **F.** Image analysis and quantification of the complete recruitment movie demonstrate a decrease in the DOR fluorescence intensity within the TGN over time following active and sustained recruitment of the mCherry-CRY2-PI3K-C2 $\alpha$ -KD to the TGN. **G.** Quantification and analysis (of  $n = 8$  independent experiments) show the fold change in DOR membrane and TGN-localized fluorescence normalized to their starting values (dotted blue line) following recruitment of mCherry-CRY2-PI3K-C2 $\alpha$ -KD to the TGN. There is a significant decrease in the fluorescence intensity of DOR within the TGN following recruitment (TGN DOR, 37%), as well as a significant increase in the total DOR membrane fluorescence (Membrane DOR, 7%) (Membrane DOR,  $n=8$  cells; TGN DOR,  $n=8$  cells; mean  $\pm$  s.e.m.; \*\*\*\* $P < 0.0001$  by two-sided  $t$ -test vs. Respective Ctl).

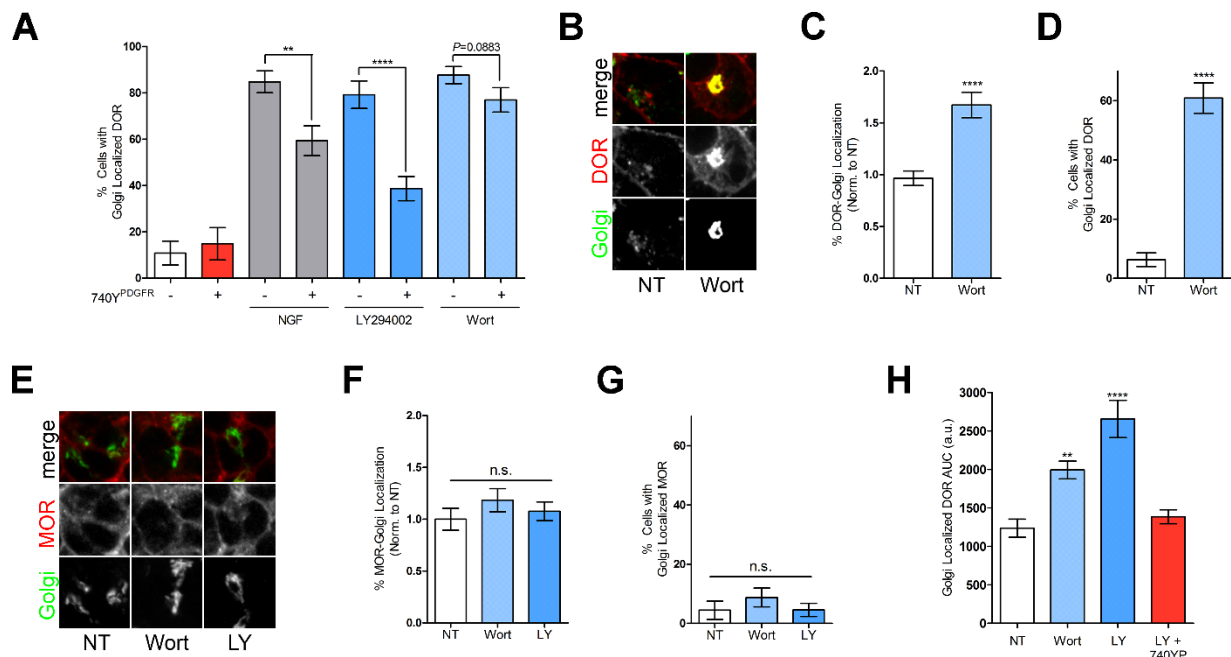


**Figure S1: Activation of PI3K by 740Y-PDGFR is sufficient to reduce the PI3K-inhibition induced retention of DOR.** **A.** Image analysis and quantification shows a significant reduction in the % cells with the Golgi-localized DOR in the NGF and LY294002 conditions following addition of the PI3K activating peptide 740Y<sup>PDGFR</sup>. There was no significant reduction in the amount of Wortmannin-induced retention of DOR following the addition of 740Y<sup>PDGFR</sup>. Further, 740Y<sup>PDGFR</sup> had no effect on Golgi localization of DOR on its own (Ctl (-),  $n=108$  cells; NGF (-),  $n=127$  cells; NGF (+),  $n=162$  cells; LY (-),  $n=104$  cells; LY (+),  $n=60$  cells; Wort (-),  $n=119$  cells; Wort (+),  $n=49$  cells; 740Y<sup>PDGFR</sup> (+),  $n=30$  cells; mean  $\pm$  s.e.m.; \*\* $P<0.01$ , \*\*\* $P<0.001$ ; by one-way ANOVA with Dunn's Multiple Comparison Test). **B.** Example images of HEK 293 cells expressing FLAG-DOR (DOR). In control conditions (NT), DOR is present on the cell surface; however, in HEK 293 cells, PI3K inhibition by Wortmannin (Wort, 10 $\mu$ M) increases the Golgi localization of DOR. **C.** Image analysis and quantification reveal a significant increase in the % of total DOR fluorescence that overlaps with the Golgi following PI3K inhibition by Wortmannin (Wort, 10 $\mu$ M) (NT,  $n=111$ ; Wort,  $n=92$ ; mean  $\pm$  s.e.m.; \*\*\* $P<0.001$ ; by two-sided t-test vs. NT). **D.** Image analysis and quantification shows a significant increase in the % cells with the Golgi-localized DOR following PI3K inhibition by Wortmannin (Wort, 10 $\mu$ M) (NT,  $n=111$ ; Wort,  $n=92$ ; mean  $\pm$  s.e.m.; \*\*\* $P<0.001$ ; by two-sided t-test vs. NT). **E.** Example images of HEK 293 cells expressing FLAG-MOR. In control conditions (NT), MOR is present on the cell surface; however, unlike for DOR, PI3K inhibition by Wortmannin (Wort, 10 $\mu$ M) or LY294002 (LY, 10 $\mu$ M) does not increase the Golgi localization of MOR. **F.** Image analysis and quantification show a non-significant change in the % of total MOR fluorescence that overlaps with the Golgi following PI3K inhibition by Wortmannin or LY294002 (NT,  $n=45$ ; Wort,

$n=80$ ; LY,  $n=88$ ; mean  $\pm$  s.e.m.; not significant; by two-sided t-test vs. NT). **G.** Image analysis and quantification resulted in a non-significant change in the % cells with the Golgi-localized MOR following PI3K inhibition by Wortmannin or LY294002 (NT,  $n=45$ ; Wort,  $n=80$ ; LY,  $n=88$ ; mean  $\pm$  s.e.m.; not significant; by two-sided t-test vs. NT). **H.** Area under the curve analysis of the VSVG-DORtail-GFP experiments revealed that PI3K inhibition by Wortmannin (Wort, 10 $\mu$ M) and LY294002 (LY, 10 $\mu$ M) significantly increased the total Golgi-localized signal. Addition of the PI3K activating peptide 740Y<sup>PDGFR</sup> (50 $\mu$ g/mL) in combination with LY294002 (LY + 740YP) was sufficient to block the effect of LY294002 (control,  $n=12$  cells; LY294002,  $n=12$  cells; LY294002 + 740Y<sup>PDGFR</sup>,  $n=17$  cells; mean  $\pm$  s.e.m.; \*\* $P<0.01$ ; \*\*\* $P<0.001$ ; by two-sided t-test vs. NT).

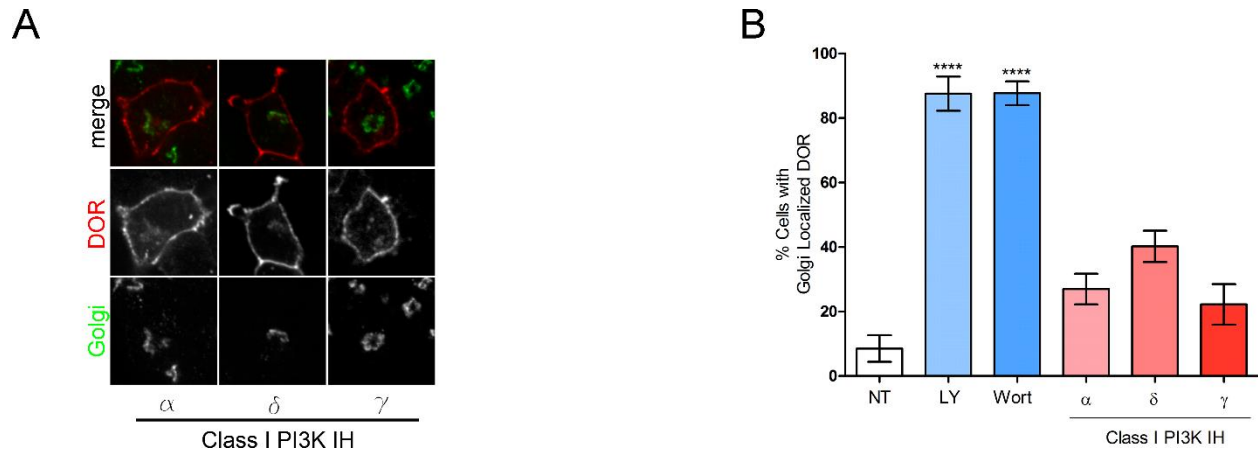


**Figure S2: Class I PI3K is not required for Golgi retention of DOR.** **A.** Example images (of  $n = 3$  independent experiments) for PC12 cells expressing FLAG-DOR, treated for 1 hour with Class I specific PI3K inhibitors PI-103 (PI3K C1  $\alpha$ , 50nM), IC87114 (PI3K C1  $\delta$ , 5 $\mu$ M), and AS605240 (PI3K C1  $\gamma$ , 25nM). **B.** Quantification demonstrated a significant increase in the % cells with Golgi-localized DOR following NGF treatment and PI3K inhibition by LY294002 (LY, 10 $\mu$ M), or Wortmannin (Wort, 10 $\mu$ M), but not following Class I specific PI3K inhibition by PI3K inhibitors PI-103 (PI3K C1  $\alpha$ , 50nM), IC87114 (PI3K C1  $\delta$ , 5 $\mu$ M), and AS605240 (PI3K C1  $\gamma$ , 25nM) (NT,  $n=42$  cells; NGF,  $n=73$  cells; LY,  $n=77$  cells; Wort,  $n=45$  cells;  $\alpha$ ,  $n=82$  cells;  $\delta$ ,  $n=99$  cells;  $\gamma$ ,  $n=28$  cells; mean  $\pm$  s.e.m.; \*\* $P < 0.01$ , \*\*\*\* $P < 0.0001$ ; by two-sided  $t$ -test vs. NT).

## References:

1. Pradhan, A. A., Pradhan, A. A., Befort, K., Befort, K., Nozaki, C., Nozaki, C., Gavériaux-Ruff, C., Gavériaux-Ruff, C., Kieffer, B. L., and Kieffer, B. L. (2011) The delta opioid receptor: an evolving target for the treatment of brain disorders. *Trends in Pharmacological Sciences*. **32**, 581–590
2. Scherrer, G., Scherrer, G., Imamachi, N., Imamachi, N., Cao, Y.-Q., Cao, Y.-Q., Contet, C., Contet, C., Mennicken, F., Mennicken, F., O'Donnell, D., Donnell, D. O., Kieffer, B. L., Kieffer, B. L., Basbaum, A. I., and Basbaum, A. I. (2009) Dissociation of the opioid receptor mechanisms that control mechanical and heat pain. *Cell*. **137**, 1148–1159
3. Jutkiewicz, E. M., Baladi, M. G., Folk, J. E., Rice, K. C., and Woods, J. H. (2006) The convulsive and electroencephalographic changes produced by nonpeptidic delta-opioid agonists in rats: comparison with pentylentetrazol. *Journal of Pharmacology and Experimental Therapeutics*. **317**, 1337–1348
4. Cahill, C. M., Cahill, C. M., Holdridge, S. V., Holdridge, S. V., Morinville, A., and Morinville, A. (2007) Trafficking of delta-opioid receptors and other G-protein-coupled receptors: implications for pain and analgesia. *Trends in Pharmacological Sciences*. **28**, 23–31
5. Bardoni, R., Tawfik, V. L., Wang, D., François, A., Solorzano, C., Shuster, S. A., Choudhury, P., Betelli, C., Cassidy, C., Smith, K., de Nooij, J. C., Mennicken, F., O'Donnell, D., Kieffer, B. L., Woodbury, C. J., Basbaum, A. I., MacDermott, A. B., and Scherrer, G. (2014) Delta opioid receptors presynaptically regulate cutaneous mechanosensory neuron input to the spinal cord dorsal horn. *Neuron*. **81**, 1312–1327
6. Gavériaux-Ruff, C., Gavériaux-Ruff, C., Kieffer, B. L., and Kieffer, B. L. (2011) Delta opioid receptor analgesia: recent contributions from pharmacology and molecular approaches. *Behav Pharmacol*. **22**, 405–414
7. Danielsson, I., Gasiór, M., Stevenson, G. W., Folk, J. E., Rice, K. C., and Negus, S. S. (2006) Electroencephalographic and convulsant effects of the delta opioid agonist SNC80 in rhesus monkeys. *Pharmacol. Biochem. Behav*. **85**, 428–434
8. Shiwarski, D. J., Tipton, A., Schmidt, B. A., Giraldo, M. D., Gold, M. S., Pradhan, A. A., and Puthenveedu, M. A. A phosphoinositide-regulated Golgi checkpoint regulates the bioavailability of delta opioid receptors. *Nat. Med*.
9. De Matteis, M. A., De Matteis, M. A. M., Godi, A. A., and Godi, A. (2004) PI-3-kinase membrane traffic. *JCB*. **6**, 487–492
10. Grosshans, B. L., Ortiz, D., and Novick, P. (2006) Rab and their effectors: achieving specificity in membrane traffic. *Proceedings of the National Academy of Sciences*. **103**, 11821–11827
11. Stenmark, H. (2009) Rab GTPases as coordinators of vesicle traffic. *Nature Publishing Group*. **10**, 513–525
12. Low, P. C., Low, P. C., Misaki, R., Misaki, R., Schroder, K., Schroder, K., Stanley, A. C., Stanley, A. C., Sweet, M. J., Sweet, M. J., Teasdale, R. D., Teasdale, R. D., Vanhaesebroeck, B., Vanhaesebroeck, B., Meunier, F. A., Meunier, F. A., Taguchi, T., Taguchi, T., Stow, J. L., and Stow, J. L. (2010) Phosphoinositide 3-kinase  $\delta$  regulates membrane fission of Golgi carriers for selective cytokine secretion. *The Journal of Cell Biology*. **190**, 1053–1065
13. Carpentier, S., Carpentier, S., N'Kuli, F., N'Kuli, F., Grieco, G., Grieco, G., Van Der Smissen, P., Van Der Smissen, P., Janssens, V., Janssens, V., Emonard, H., Emonard, H., Bilanges, B., Bilanges, B., Vanhaesebroeck, B., Vanhaesebroeck, B., Gaide Chevronnay, H. P., Gaide Chevronnay, H. P., Pierreux, C. E., Pierreux, C. E., Tyteca, D., Tyteca, D., Courtoy, P. J., and Courtoy, P. J. (2013) Class III phosphoinositide 3-

- kinase/VPS34 and dynamin are critical for apical endocytic recycling. *Traffic*. **14**, 933–948
14. Mazza, S., and Maffucci, T. (2011) Class II phosphoinositide 3-kinase C2alpha: what we learned so far. *Int J Biochem Mol Biol*. **2**, 168–182
  15. Domin, J., Pages, F., Volinia, S., Rittenhouse, S. E., Zvelebil, M. J., Stein, R. C., and Waterfield, M. D. (1997) Cloning of a human phosphoinositide 3-kinase with a C2 domain that displays reduced sensitivity to the inhibitor wortmannin. *Biochem. J*. **326**, 139–147
  16. Backer, J. M. (2008) The regulation and function of Class III PI3Ks: novel roles for Vps34. *Biochem. J*. **410**, 1–17
  17. Domin, J., Domin, J., Gaidarov, I., Gaidarov, I., Smith, M. E. K., Smith, M. E., Keen, J. H., Keen, J. H., Waterfield, M. D., and Waterfield, M. D. (2000) The class II phosphoinositide 3-kinase PI3K-C2alpha is concentrated in the trans-Golgi network and present in clathrin-coated vesicles. *J. Biol. Chem*. **275**, 11943–11950
  18. Gaidarov, I., Gaidarov, I., Smith, M. E., Smith, M. E. K., Domin, J., Domin, J., Keen, J. H., and Keen, J. H. (2001) The class II phosphoinositide 3-kinase C2alpha is activated by clathrin and regulates clathrin-mediated membrane trafficking. *Molecular Cell*. **7**, 443–449
  19. Gaidarov, I., Gaidarov, I., Zhao, Y., and Keen, J. H. (2005) Individual phosphoinositide 3-kinase C2alpha domain activities independently regulate clathrin function. *J. Biol. Chem*. **280**, 40766–40772
  20. Kim, K.-A., Kim, K.-A., Zastrow, von, M., and Zastrow, von, M. (2003) Neurotrophin-regulated sorting of opioid receptors in the biosynthetic pathway of neurosecretory cells. *Journal of Neuroscience*. **23**, 2075–2085
  21. Wymann, M. P., Bulgarelli-Leva, G., Zvelebil, M. J., Pirola, L., Vanhaesebroeck, B., Waterfield, M. D., and Panayotou, G. (1996) Wortmannin inactivates phosphoinositide 3-kinase by covalent modification of Lys-802, a residue involved in the phosphate transfer reaction. *Molecular and Cellular Biology*. **16**, 1722–1733
  22. Vlahos, C. J., Matter, W. F., Hui, K. Y., and Brown, R. F. (1994) A specific inhibitor of phosphatidylinositol 3-kinase, 2-(4-morpholinyl)-8-phenyl-4H-1-benzopyran-4-one (LY294002). *J. Biol. Chem*. **269**, 5241–5248
  23. Derossi, D. D., Williams, E. J. E., Green, P. J. P., Dunican, D. J. D., and Doherty, P. P. (1998) Stimulation of Mitogenesis by a Cell-Permeable PI 3-Kinase Binding Peptide. *Biochem Biophys Res Commun*. **251**, 5–5
  24. Scales, S. J., Scales, S. J., Pepperkok, R., Pepperkok, R., Kreis, T. E., and Kreis, T. E. (1997) Visualization of ER-to-Golgi transport in living cells reveals a sequential mode of action for COPII and COPI. *Cell*. **90**, 1137–1148
  25. Nakamura, N., Nilsson, T., Rabouille, C., Hui, N., Slusarewicz, P., Watson, R., Nilsson, T., Kreis, T. E., Hui, N., Slusarewicz, P., Kreis, T. E., and Warren, G. (1995) Characterization of a cis-Golgi matrix protein, GM130. *The Journal of Cell Biology*. **131**, 1715–1726
  26. Kreis, T. E., and Kreis, T. E. (1986) Microinjected antibodies against the cytoplasmic domain of vesicular stomatitis virus glycoprotein block its transport to the cell surface. *EMBO J*. **5**, 931–941
  27. Park, S., Chapuis, N., Bardet, V., Tamburini, J., Gallay, N., Willems, L., Knight, Z. A., Shokat, K. M., Azar, N., Vigiúí, F., Ifrah, N., Dreyfus, F., Mayeux, P., Lacombe, C., and Bouscary, D. (2008) PI-103, a dual inhibitor of Class IA phosphatidylinositide 3-kinase and mTOR, has antileukemic activity in AML. *Leukemia*. **22**, 1698–1706
  28. Sadhu, C., Masinovsky, B., Dick, K., Sowell, C. G., and Staunton, D. E. (2003) Essential role of phosphoinositide 3-kinase delta in neutrophil directional movement. *J. Immunol*. **170**, 2647–2654
  29. Camps, M., Rückle, T., Ji, H., Ardisson, V., Rintelen, F., Shaw, J., Ferrandi, C., Chabert, C., Gillieron, C., Françon, B., Martin, T., Gretener, D., Perrin, D., Leroy, D., Vitte, P.-A., Hirsch, E., Wymann, M. P., Cirillo, R., Schwarz, M. K., and Rommel, C. (2005) Blockade

- of PI3Kgamma suppresses joint inflammation and damage in mouse models of rheumatoid arthritis. *Nat. Med.* **11**, 936–943
30. Bridges, D., Ma, J.-T., Park, S., Inoki, K., Weisman, L. S., and Saltiel, A. R. (2012) Phosphatidylinositol 3,5-bisphosphate plays a role in the activation and subcellular localization of mechanistic target of rapamycin 1. *Mol. Biol. Cell.* **23**, 2955–2962
  31. Wang, Y., Yoshioka, K., Azam, M. A., Takuwa, N., Sakurada, S., Kayaba, Y., Sugimoto, N., Inoki, I., Kimura, T., Kuwaki, T., and Takuwa, Y. (2006) Class II phosphoinositide 3-kinase alpha-isoform regulates Rho, myosin phosphatase and contraction in vascular smooth muscle. *Biochem. J.* **394**, 581–592
  32. Silva, J. M., Li, M. Z., Chang, K., Ge, W., Golding, M. C., Rickles, R. J., Siolas, D., Hu, G., Paddison, P. J., Schlabach, M. R., Sheth, N., Bradshaw, J., Burchard, J., Kulkarni, A., Cavet, G., Sachidanandam, R., McCombie, W. R., Cleary, M. A., Elledge, S. J., and Hannon, G. J. (2005) Second-generation shRNA libraries covering the mouse and human genomes. *Nat. Genet.* **37**, 1281–1288
  33. Campeau, E., Ruhl, V. E., Rodier, F., Smith, C. L., Rahmberg, B. L., Fuss, J. O., Campisi, J., Yaswen, P., Cooper, P. K., and Kaufman, P. D. (2009) A versatile viral system for expression and depletion of proteins in mammalian cells. *PLoS ONE.* **4**, e6529
  34. Pratt, C. P., He, J., Wang, Y., Barth, A. L., and Bruchez, M. P. (2015) Fluorogenic Green-Inside Red-Outside (GIRO) Labeling Approach Reveals Adenylyl Cyclase-Dependent Control of BKα Surface Expression. *Bioconjug. Chem.* **26**, 1963–1971
  35. Szent-Gyorgyi, C., Stanfield, R. L., Andreko, S., Dempsey, A., Ahmed, M., Capek, S., Waggoner, A. S., Wilson, I. A., and Bruchez, M. P. (2013) Malachite green mediates homodimerization of antibody VL domains to form a fluorescent ternary complex with singular symmetric interfaces. *J. Mol. Biol.* **425**, 4595–4613
  36. Szent-Gyorgyi, C., Schmidt, B. F., Schmidt, B. A., Creeger, Y., Fisher, G. W., Zakei, K. L., Adler, S., Fitzpatrick, J. A. J., Woolford, C. A., Yan, Q., Vasilev, K. V., Berget, P. B., Bruchez, M. P., Jarvik, J. W., and Waggoner, A. (2008) Fluorogen-activating single-chain antibodies for imaging cell surface proteins. *Nat. Biotechnol.* **26**, 235–240
  37. Wu, Y., Tapia, P. H., Jarvik, J., Waggoner, A. S., and Sklar, L. A. (2014) Real-time detection of protein trafficking with high-throughput flow cytometry (HTFC) and fluorogen-activating protein (FAP) base biosensor. *Curr Protoc Cytom.* **67**, Unit 9.43.
  38. Idevall-Hagren, O., Idevall-Hagren, O., Dickson, E. J., Dickson, E. J., Hille, B., Hille, B., Toomre, D. K., and Pietro De Camilli (2012) Optogenetic control of phosphoinositide metabolism. *Proceedings of the ...* **109**, E2316–E2323
  39. Kennedy, M. J., Hughes, R. M., Peteya, L. A., Schwartz, J. W., Ehlers, M. D., and Tucker, C. L. (2010) Rapid blue-light-mediated induction of protein interactions in living cells. *Nat Meth.* **7**, 973–975
  40. Houle, S. S., and Marceau, F. F. (2003) Wortmannin alters the intracellular trafficking of the bradykinin B2 receptor: role of phosphoinositide 3-kinase and Rab5. *Biochem. J.* **375**, 151–158
  41. Gaffet, P., Jones, A. T., and Clague, M. J. (1997) Inhibition of calcium-independent mannose 6-phosphate receptor incorporation into trans-Golgi network-derived clathrin-coated vesicles by wortmannin. *J. Biol. Chem.* **272**, 24170–24175
  42. Raiborg, C., Schink, K. O., and Stenmark, H. (2013) Class III phosphatidylinositol 3-kinase and its catalytic product PtdIns3P in regulation of endocytic membrane traffic. *FEBS J.* **280**, 2730–2742
  43. Leto, D., and Saltiel, A. R. (2012) Regulation of glucose transport by insulin: traffic control of GLUT4. *Nat Rev Mol Cell Biol.* **13**, 383–396
  44. Clarke, J. F., Young, P. W., Yonezawa, K., Kasuga, M., and Holman, G. D. (1994) Inhibition of the translocation of GLUT1 and GLUT4 in 3T3-L1 cells by the phosphatidylinositol 3-kinase inhibitor, wortmannin. *Biochem. J.* **300 ( Pt 3)**, 631–635

45. Li, H., and Marshall, A. J. (2015) Phosphatidylinositol (3,4) bisphosphate-specific phosphatases and effector proteins: A distinct branch of PI3K signaling. *Cellular Signalling*. **27**, 1789–1798
46. Dyson, J. M., Dyson, J. M., Kong, A. M., Kong, A. M., Wiradjaja, F., Wiradjaja, F., Astle, M. V., Astle, M. V., Gurung, R., Gurung, R., Mitchell, C. A., and Mitchell, C. A. (2005) The SH2 domain containing inositol polyphosphate 5-phosphatase-2: SHIP2. *Int. J. Biochem. Cell Biol.* **37**, 2260–2265
47. Erneux, C., Edimo, W. E., Deneubourg, L., and Pirson, I. (2011) SHIP2 multiple functions: a balance between a negative control of PtdIns(3,4,5)P<sub>3</sub> level, a positive control of PtdIns(3,4)P<sub>2</sub> production, and intrinsic docking properties. *J. Cell. Biochem.* **112**, 2203–2209
48. Posor, Y., Posor, Y., Eichhorn-Gruenig, M., Eichhorn-Gruenig, M., Puchkov, D., Puchkov, D., Schöneberg, J., Schöneberg, J., Ullrich, A., Ullrich, A., Lampe, A., Lampe, A., Müller, R., Müller, R., Zarbakhsh, S., Zarbakhsh, S., Gulluni, F., Gulluni, F., Hirsch, E., Hirsch, E., Krauss, M., Krauss, M., Schultz, C., Schultz, C., Schmoranzer, J., Schmoranzer, J., Noé, F., Noé, F., Haucke, V., and Haucke, V. (2013) Spatiotemporal control of endocytosis by phosphatidylinositol-3,4-bisphosphate. *Nature*. **499**, 233–237
49. Dowler, S., Currie, R. A., Campbell, D. G., Deak, M., Kular, G., Downes, C. P., and Alessi, D. R. (2000) Identification of pleckstrin-homology-domain-containing proteins with novel phosphoinositide-binding specificities. *Biochem. J.* **351**, 19–31
50. Weixel, K. M., Blumental-Perry, A., Watkins, S. C., Aridor, M., and Weisz, O. A. (2005) Distinct Golgi populations of phosphatidylinositol 4-phosphate regulated by phosphatidylinositol 4-kinases. *J. Biol. Chem.* **280**, 10501–10508
51. Szentpetery, Z., Szentpetery, Z., Balla, A., Balla, A., Kim, Y. J., Kim, Y., Lemmon, M. A., Lemmon, M. A., Balla, T., and Balla, T. (2009) Live cell imaging with protein domains capable of recognizing phosphatidylinositol 4,5-bisphosphate; a comparative study. *BMC Cell Biol.* **10**, 67
52. Cruz-Garcia, D., Cruz-Garcia, D., Ortega-Bellido, M., Ortega-Bellido, M., Scarpa, M., Scarpa, M., Villeneuve, J., Villeneuve, J., Jovic, M., Jovic, M., Porzner, M., Porzner, M., Balla, T., Balla, T., Seufferlein, T., Seufferlein, T., Malhotra, V., and Malhotra, V. (2013) Recruitment of arfaptins to the trans-Golgi network by PI(4)P and their involvement in cargo export. *EMBO J.* **32**, 1717–1729
53. De Matteis, M. A., Wilson, C., and D'Angelo, G. (2013) Phosphatidylinositol-4-phosphate: the Golgi and beyond. *Bioessays*. **35**, 612–622
54. De Matteis, M. A., De Matteis, M. A., Luini, A., and Luini, A. (2008) Exiting the Golgi complex. *Nature Publishing Group*. **9**, 273–284
55. Van Lint, J., Rykx, A., Maeda, Y., Vantus, T., Sturany, S., Malhotra, V., Vandenheede, J. R., and Seufferlein, T. (2002) Protein kinase D: an intracellular traffic regulator on the move. *Trends Cell Biol.* **12**, 193–200
56. Di Paolo, G., and De Camilli, P. (2006) Phosphoinositides in cell regulation and membrane dynamics. *Nature*. **443**, 651–657
57. Meyers, R., and Cantley, L. C. (1997) Cloning and characterization of a wortmannin-sensitive human phosphatidylinositol 4-kinase. *J. Biol. Chem.* **272**, 4384–4390
58. Zhao, Y., Zhao, Y., Gaidarov, I., Gaidarov, I., Keen, J. H., and Keen, J. H. (2007) Phosphoinositide 3-kinase C2alpha links clathrin to microtubule-dependent movement. *J. Biol. Chem.* **282**, 1249–1256
59. Meunier, F. A., Osborne, S. L., Hammond, G. R. V., Cooke, F. T., Parker, P. J., Domin, J., and Schiavo, G. (2005) Phosphatidylinositol 3-kinase C2alpha is essential for ATP-dependent priming of neurosecretory granule exocytosis. *Mol. Biol. Cell.* **16**, 4841–4851
60. Yoshioka, K., Yoshida, K., Cui, H., Wakayama, T., Takuwa, N., Okamoto, Y., Du, W., Qi, X., Asanuma, K., Sugihara, K., Aki, S., Miyazawa, H., Biswas, K., Nagakura, C., Ueno,

- M., Iseki, S., Schwartz, R. J., Okamoto, H., Sasaki, T., Matsui, O., Asano, M., Adams, R. H., Takakura, N., and Takuwa, Y. (2012) Endothelial PI3K-C2 $\alpha$ , a class II PI3K, has an essential role in angiogenesis and vascular barrier function. *Nat. Med.* **18**, 1560–1569
61. Falasca, M., Hughes, W. E., Dominguez, V., Sala, G., Fostira, F., Fang, M. Q., Cazzolli, R., Shepherd, P. R., James, D. E., and Maffucci, T. (2007) The role of phosphoinositide 3-kinase C2 $\alpha$  in insulin signaling. *J. Biol. Chem.* **282**, 28226–28236
62. Leibiger, B., Moede, T., Paschen, M., Yunn, N.-O., Lim, J. H., Ryu, S. H., Pereira, T., Berggren, P.-O., and Leibiger, I. B. (2015) PI3K-C2 $\alpha$  Knockdown Results in Rerouting of Insulin Signaling and Pancreatic Beta Cell Proliferation. *CELREP.* **13**, 15–22
63. Neudauer, C. L., Joberty, G., and Macara, I. G. (2001) PIST: a novel PDZ/coiled-coil domain binding partner for the rho-family GTPase TC10. *Biochem Biophys Res Commun.* **280**, 541–547
64. Bauch, C., Koliwer, J., Buck, F., Hönck, H.-H., and Kreienkamp, H.-J. (2014) Subcellular sorting of the G-protein coupled mouse somatostatin receptor 5 by a network of PDZ-domain containing proteins. *PLoS ONE.* **9**, e88529
65. Szent-Gyorgyi, C., Schmidt, B. F., Schmidt, B. A., Creeger, Y., Fisher, G. W., Zakel, K. L., Adler, S., Fitzpatrick, J. A. J., Woolford, C. A., Yan, Q., Vasilev, K. V., Berget, P. B., Bruchez, M. P., Jarvik, J. W., and Waggoner, A. (2008) Fluorogen-activating single-chain antibodies for imaging cell surface proteins. *Nat. Biotechnol.* **26**, 235–240
66. Balla, T., and Várnai, P. (2002) Visualizing cellular phosphoinositide pools with GFP-fused protein-modules. *Sci. STKE.* **2002**, pl3

## Chapter 4: NGF-induced Golgi Retention of $\delta$ -Opioid Receptors Requires Dual RXR Retention/Retrieval Motifs

Daniel J. Shiwarski<sup>1</sup>, Manojkumar A. Puthenveedu<sup>1</sup>

<sup>1</sup>Department of Biological Sciences, The Center for the Neural Basis of Cognition, Carnegie Mellon University, Pittsburgh, PA 15213, USA.

### **Abstract:**

The delta opioid receptor (DOR) is a single-use G-protein coupled receptor (GPCR) with predominate intracellular localization in neuronal cells. Localization studies have revealed internal storage pools of DOR in neuronal cultures and following NGF treatment in PC12 cells. Previously, it was shown that the last 27 amino acids of DOR are sufficient to confer NGF-induced Golgi retention; however, the amino acid sequence required for this phenotype was unknown. Here, we demonstrate that this neural specific Golgi retention requires dual RXR retention/retrieval motifs within the DOR C-terminal tail. Additionally, deletion of the last 27 amino acids of DOR results in basal ER retention, and limited surface expression. Alanine mutation of potential serine/threonine phosphorylation sites, cysteine modification sites, and partial tail deletions of the last 27 amino acids had no effect on the basal surface expression, or NGF-induced Golgi localization. Our results identify a novel role for RXR retention/retrieval motifs in biosynthetic receptor trafficking from the Golgi complex to the cell surface. Additionally, it suggests a mechanism by which protein-protein interactions, dimerization, and phosphorylation events could reversibly alter the trafficking, localization, and function of DOR.

## Introduction:

For many G protein-coupled receptors (GPCR), the exact amino acid sequence of the C-terminal cytoplasmic tail has been shown to be important for receptor localization and function. Additionally, post-translational modifications and protein-protein interactions provide further regulation of trafficking and sorting. One of the most well studied examples of a GPCR with C-terminal sorting signals has been the beta 2-adrenergic receptor (B2AR). Various phosphorylation events and protein-protein interactions through its C-terminal PDZ ligand provide spatiotemporal control over receptor localization and function (1-5). Interestingly, most of these studies focus on the regulation of GPCRs after agonist induced receptor internalization and recycling of receptors back to the surface. There have been some reports of sequence motifs regulating *de novo* GPCR trafficking to the surface, but limited studies have investigated the required amino acid sequence motifs within the cytoplasmic tail (6, 7). For most GPCRs, the classical view is that once native folding has occurred their transport to the cell surface is constitutive and relatively unregulated. However, for a few receptors, exiting the Endoplasmic Reticulum (ER-export) has been shown to require specific amino acid sequences for proper trafficking to the cell surface. Specifically, COP-II di-acidic binding motifs (DXE), di-hydrophobic phenylalanine motifs (FF), and di-leucine containing motifs (LL), have been the most well studied (8). These sequence motifs are most commonly found within the membrane proximal region of the C-terminus, and their presence within a receptor's primary sequence creates a rate-limiting step for trafficking to the cell surface.

Recently, additional post-ER checkpoints and receptor retrieval signals have been suggested. There are two main sequence motifs that appear to control this regulation, a poly-basic motif, and a multi-arginine containing motif (9-13). The exact position of these sequences within the C-terminus of a receptor appears to control whether they function in ER-exit, ER-retrieval, or Golgi export, but predicting the phenotype from the primary amino acid sequence is difficult (10). Interestingly, the delta-Opioid receptor (DOR), a GPCR with known sequence dependent regulation for ER-export, has recently been shown to undergo an additional neuronal specific sorting step within the trans-Golgi network(14, 15).

Our lab has shown that a phosphoinositide-regulated Golgi checkpoint can limit the surface availability of DOR in neuronal cells(15). Specifically, in the neuroendocrine PC12 cell line, treatment with Nerve Growth Factor (NGF), or inhibition of Class II PI3K alpha results in accumulation of DOR within the *trans*-Golgi network(16). Further, creation of chimeric proteins expressing the last 27 amino acids of the C-terminal DOR tail are sufficient to retain the VSVG, CD4, and the  $\mu$ -Opioid Receptor (MOR) within the *trans*-Golgi network in response to NGF and

PI3 Kinase (PI3K) inhibition (16, 17). These results suggest that there must be a sequence dependent sorting motif that is required for retaining DOR following NGF treatment, PI3K inhibition, or in primary sensory neurons. For this reason, we wanted to determine the required C-terminal sequence motif that prevents newly made DOR from trafficking to the cell surface in the presence of NGF and PI3K inhibition. By determining the sequence required for NGF-induced retention of DOR, we will gain deeper insight into the mechanism of retention, and can establish a retention motif to enable a search for other receptors that might traffic similar to DOR.

To begin this study, we analyzed the last 27 amino acids of the DOR cytoplasmic tail to look for possible sequence motifs that might contribute to the NGF and PI3K inhibition induced retention of DOR. Within this amino acid sequence were potential phosphorylation, palmitoylation, di-acidic, and di-arginine motifs, but no PDZ ligand. Here, we demonstrate that even though the last 27 amino acids of DOR do not contain a traditional ER exit signal (FIL, or LL), they are required for proper ER-exit and trafficking to the cell surface (8). Mutation of the potential phosphorylation, palmitoylation, di-acidic, and di-arginine motifs to alanine has minimal effect on the NGF or PI3K inhibition-induced retention of DOR. Interestingly, mutating both of the dual-arginine containing RXR motifs prevent the NGF or PI3K inhibition-induced retention of DOR. These results demonstrate the first evidence of the requirement for dual RXR motifs in the stimulated retention of a GPCR.

## Results:

### The C-terminal tail of DOR regulates delivery of the receptor to the cell surface

Previously, our data, along with Kim et al., have shown that the C-terminal 27 amino acids of the  $\delta$ -Opioid Receptor (DOR) are sufficient to retain the VSVG, CD4, and  $\mu$ -Opioid Receptor (MOR) within the *trans*-Golgi network of PC12 cells in response to Nerve Growth Factor (NGF) and PI-3 Kinase (PI3K) inhibition (16, 17). However, in the presence of NGF treatment or PI3K inhibition, the requirement of the last 27 amino acids of DOR have not been tested. To investigate this, we created five deletion mutants, a full C-terminal 27 amino acid deletion (345 TGA), and then four segmental deletions ( $\Delta$ 345-352,  $\Delta$ 353-359,  $\Delta$ 360-366,  $\Delta$ 367 TGA) of a FLAG-tagged version of the mouse DOR (Figure 1A). A graphical representation of DOR and the C-terminal deletions are also shown (Figure S1A). PC12 cells were transfected with wild-type or an individual deletion mutant and imaged via fixed-cell confocal fluorescence microscopy to determine DOR localization in normal growth conditions, and following 1 hour of Nerve Growth Factor (NGF) treatment. Wild-type DOR displayed surface localization at baseline and a Golgi-localized pool following NGF treatment (Figure 1A). Interestingly, when the last 27 C-terminal amino acids were deleted, there was a significant pool of Golgi-localized DOR at baseline, and following NGF treatment, a strong pool of intracellular DOR was observed (Figure 1A). For the segmental deletion mutants  $\Delta$ 345-352,  $\Delta$ 353-359,  $\Delta$ 360-366, and  $\Delta$ 367 TGA, all receptors were surface localized in normal growth conditions and became Golgi-localized following NGF treatment (Figure 1A).

To quantitate the differences between WT DOR and the various deletion mutants, image analysis was performed to calculate the percentage of DOR fluorescence that was localized to the Golgi (*trans*-Golgi Network marker, TGN-38), and to determine the percentage of cells imaged for each condition that visually exhibited Golgi-localized DOR. To compare between wild-type and deletion mutants, the data was normalized to the no treatment condition for the wild-type receptor. All deletion mutants of DOR were similar to wild-type at baseline, except for the 345 TGA mutant. This deletion of the entire 27 amino acid C-terminal region showed a 2.7-fold increase in the percentage of DOR fluorescence localized to the Golgi (Figure 1B). Following NGF treatment, a significant increase is observed for wild-type DOR (DOR WT), and all deletion mutants. When compared to DOR wild-type NGF treatment, a partial, but significant decrease in the NGF-induced Golgi localization of DOR was observed for the  $\Delta$ 345-352 and  $\Delta$ 353-359 receptors. Similarly, quantification of the percentage of cells exhibiting Golgi-localized DOR demonstrated increased DOR Golgi localization at baseline for the 345 TGA DOR, and a reduction in the extent of NGF-induced Golgi localization for the  $\Delta$ 345-352 and  $\Delta$ 353-359 receptors (Figure 1C). These data

show that the last 27 amino acids of DOR are required for proper trafficking of the receptor to the cell surface, and that the region between amino acids 345-359 might play a role in the NGF-induced Golgi localization of DOR.

### **DOR C-terminal tail deletions $\Delta$ 345-352 and $\Delta$ 353-359 exhibit a reduction in Golgi retention following PI3K inhibition.**

We further wanted to determine if the  $\Delta$ 345-352 and  $\Delta$ 353-359 deletions mutants of DOR showed reduced Golgi retention following PI3K inhibition. PC12 cells expressing FLAG-tagged DOR wild-type,  $\Delta$ 345-352, and  $\Delta$ 353-359 were treated with the PI3K inhibitor Wortmannin (Wort, 10 $\mu$ M) or LY294002 (LY, 10 $\mu$ M) for 1 hour and imaged via fixed-cell confocal fluorescence microscopy to determine DOR localization. As expected, immunofluorescence images of DOR wild-type (WT) revealed significant Golgi localization following PI3K inhibition compared to the total cell DOR fluorescence (Figure S1B). The  $\Delta$ 345-352 and  $\Delta$ 353-359 DOR deletion mutants appeared to have less Golgi-localized DOR following PI3K inhibition by Wortmannin or LY294002, and also exhibited strong surface localized receptor (Figure S1B).

To quantitatively evaluate the effect of the  $\Delta$ 345-352 and  $\Delta$ 353-359 deletion mutants on PI3K inhibition induced Golgi retention of DOR, image analysis for the percentage of DOR fluorescence localized to the Golgi was normalized to DOR WT Wortmannin treated cells for comparison to the full length DOR WT (Figure S1C). Both the  $\Delta$ 345-352 and  $\Delta$ 353-359 deletion mutants demonstrated a small, but statistically significant, reduction in the percentage of DOR localized to the Golgi after treatment with Wortmannin. Similarly, the  $\Delta$ 345-352 and  $\Delta$ 353-359 deletions resulted in a lower percentage of cells with Golgi-localized DOR after treatment with Wortmannin (Figure S1D). Analysis of DOR Golgi localization following treatment with LY294002 revealed similar results to PI3K inhibition with Wortmannin; however, only the  $\Delta$ 353-359 LY294002 treated cells were significantly reduced compared to the DOR WT (Figure S1C-D). Together, these data suggest that both the NGF-induced and PI3K inhibition-induced retention of DOR requires the C-terminal amino acids 345-359 for a complete effect.

### **Mutating potential phosphorylation sites within the C-terminal tail of DOR does not affect the basal or NGF-induced Golgi retention of DOR**

Since there were no C-terminal deletion mutants that abolished the NGF or PI3K inhibition-induced Golgi retention of DOR, we hypothesized that post-translational modifications of amino acids spanning several deletion segments within the C-terminal DOR tail might contribute to the retention phenotype. Sequence analysis of the last 27 amino acids of DOR revealed five potential

serine/threonine phosphorylation sites. To remove the potential phosphorylation sites, and determine the contribution of each amino acid for NGF-induced DOR retention, we individually mutated each serine or threonine to alanine using site directed mutagenesis (Figure 2A). PC12 cells were transfected with either a wild-type Flag-tagged DOR, or alanine mutated threonine and serine receptors (T352A, T353A, T358A, T361A, S363A), and treated with NGF for 1 hour. Example images from fixed-cell confocal immunofluorescence microscopy show that for all wild-type and mutated receptors, NGF induced a Golgi localized pool of DOR compared to the control no treatment conditions (Figure 2A).

Quantification of the percentage of DOR fluorescence localized to the Golgi was normalized to DOR WT with no treatment to compare the alanine mutants to the full length DOR. There was no statistical difference between the DOR WT no treatment condition and the alanine mutants no treatment condition. Additionally, there was no statistical difference between the DOR WT NGF and the alanine mutants NGF; however, a subtle non-significant decrease in the DOR fluorescence within the Golgi was observed for the T358A, T361A, and S363A alanine mutants. Similar non-significant results were observed for the analysis of the percentage of cells with Golgi-localized DOR. While there is an observed change in the amount of NGF-induced Golgi retention of DOR for the alanine mutants, it seems unlikely that phosphorylation of these residues is required for the retention phenotype.

### **C360 within the C-terminal tail of DOR is not required for NGF-induced Golgi retention of DOR.**

Additional sequence analysis of the last 27 amino acids of DOR identified cysteine 360 (C360) as a potential site for post-translational modification. Cysteine is well known as a target site for many post-translation modifications, and within the DOR tail was identified as a possible palmitoylation site. Since palmitoylation can alter trafficking events and membrane integration of C-terminal tails, we wanted to evaluate the role of C360 in the NGF-mediated retention of DOR through mutation of this residue, in combination with other potential phosphorylation sites. If modification of the C360 was required for NGF-induced DOR retention, mutation of the cysteine to alanine using site directed mutagenesis should drive DOR to the surface even in the presence of NGF. The C360 was positioned within a serine/threonine rich region that spanned several of the initial deletion mutants, therefore, additional combinatorial mutations were made (C360A, C360A-T361A, T358A-C360A-T361A-S363A) (Figure 3A). PC12 cells were transfected with either a wild-type Flag-tagged DOR (DOR WT), or the alanine mutated C360 receptors (C360A, C360A-T361A, T358A-C360A-T361A-S363A), and treated with NGF for 1 hour. Example images

from fixed-cell confocal immunofluorescence microscopy show that for wild-type and C360 mutated receptors, NGF induced a Golgi localized pool of DOR compared to the control no treatment conditions (Figure 3B).

When quantifying the percentage of DOR fluorescence localized to the Golgi to compare the cysteine mutants to the full length DOR, mutation of the C360 to alanine either alone, or in combination with T358, T361, and S363 revealed a small but significant decrease in the DOR fluorescence within the Golgi compared to DOR WT NGF (Figure 3C). Analysis of the percentage of cells with Golgi-localized DOR revealed a similar small but significant decrease between the DOR WT NGF and the cysteine mutants NGF (Figure 3D). Interestingly, the combinatorial mutations of the C360A with the threonine and serine residues did not provide any further quantifiable decrease in DOR-Golgi localization. These partial effect on NGF-induced retention observed for the C360A mutants suggests that C360 may contribute to the degree of NGF-induced Golgi retention of DOR, but that it is not required for the majority of the retention phenotype.

#### **Alanine mutations of single di-arginine containing motifs within the third intracellular loop and C-terminal tail of DOR do not prevent the NGF-induced retention of DOR**

We next became interested in several potential arginine motifs occurring in the C-terminal tail and ICL3. Di-arginine motifs have been reported to facilitate ER retention, and possible COP-I retrieval from the ER and Golgi, so these regions seemed like good candidates mediating the NGF-induced retention of DOR (12, 13, 18). Within the third intracellular loop of DOR, there was a di-arginine amino acid sequence motif (RSLRR) that highly resembled amino acids 344-349 (SLRRPR) of the C-terminal tail, and a less similar arginine containing motif from 352-356 (TTRER) (Figure 4A). We mutated all amino acids within each motif to alanine (SLRRPR to AAAAAA, TTRER to AAAAA, RSLRR to AAAAA), and created a combined mutant with both di-arginine motifs mutated to alanine (RSLRR and SLRRPR to AAAAA and AAAAAA) within a Flag-tagged DOR construct. PC12 cells expressing either a wild-type Flag-tagged DOR, or one of the alanine mutated motif receptors (SLRRPR $\Delta$ Ala, TTRER $\Delta$ Ala, RSLRR $\Delta$ Ala, RSLRR and SLRRPR $\Delta$ Ala), were treated with NGF or the PI3K inhibitor LY294002 for 1 hour. Example images from fixed-cell confocal immunofluorescence microscopy showed that all wild-type and mutated receptors demonstrated primarily surface localization in normal baseline no treatment conditions. NGF and LY294002 treatment increased Golgi-localization of DOR compared to the control no treatment conditions for all DOR constructs (Figure 4B).

To calculate the role of the di-arginine motifs in DOR Golgi localization, image analysis was performed to determine the percentage of DOR fluorescence localized to the Golgi, and the percentage of cells with Golgi-localized DOR. The SLRRPR $\Delta$ Ala, TTRER $\Delta$ Ala, RSLRR $\Delta$ Ala, and RSLRR & SLRRPR $\Delta$ Ala did not significantly affect the NGF-induced DOR-Golgi localization. Mutating the SLRRPR $\Delta$ Ala, TTRER $\Delta$ Ala, and RSLRR $\Delta$ Ala alone resulted in a small, but significant decrease in the DOR fluorescence within the Golgi following PI3K inhibition by LY294002 compared to DOR WT LY294002 (Figure 4C). Similarly, analysis of the percentage of cells with Golgi-localized DOR showed a non-significant decrease for SLRRPR $\Delta$ Ala, TTRER $\Delta$ Ala, and RSLRR $\Delta$ Ala alone following NGF-treatment. A small but significant decrease was observed between the DOR WT LY294002 and the SLRRPR $\Delta$ Ala, TTRER $\Delta$ Ala, and RSLRR $\Delta$ Ala alone (Figure 4D). Taken together, these data indicate that single di-arginine motifs within the third intracellular loop of DOR and the C-terminal tail are not required for the NGF-induced DOR retention.

### **Two RXR motifs within the C-terminal tail of DOR are required for NGF-induced Golgi retention**

Both the individual deletion mutants  $\Delta$ 345-352 and  $\Delta$ 353-359, and the alanine mutations of SLRRPR $\Delta$ Ala and TTRER $\Delta$ Ala resulted in a partial reduction in the NGF-induced retention of DOR. We therefore decided to look for conserved motifs within these regions that might be required for the retention effect. When evaluating the evolutionary conservation of the DOR (OPRD1 gene) C-terminal tail across Human, Mouse, and Rat species, we were able to identify two highly conserved arginine containing, arginine-any amino acid-arginine, or RXR motifs (Figure 5A). Interestingly, these RXR motifs were never mutated at the same time in our previous experiments. For this reason, we decided to mutate all five arginines within the C-terminal 27 amino acids of the DOR tail to alanine, to assess their involvement in the NGF-induced retention. Example images from fixed-cell confocal immunofluorescence imaging of PC12 cells expressing either wild-type Flag-tagged DOR (DORtail SLRRPRQATTRE) or alanine mutated RXR motifs (DORtail SLAAPAQATTAEA) demonstrated primarily surface localization in normal baseline no treatment conditions (Figure 5B). Following NGF treatment, or PI3K inhibition by LY294002 for 1 hour, wild-type DOR exhibited increased Golgi-localization; however, the arginine mutant was almost completely surface localized (Figure 5B).

To quantify the requirement of the dual RXR motifs, we calculated the percentage of DOR fluorescence localized to the Golgi for wild-type and arginine mutant receptors and normalized it to wild-type DOR no treatment control for comparison. While wild-type DOR showed the expected

increase in the percentage of DOR localized to the Golgi following NGF or PI3K inhibition by LY294002, mutating the RXR motifs (DORtail SLAAPAQATTAEA) significantly decreased the NGF and LY-induced DOR-Golgi localization (Figure 5C). Additionally, analysis of the percentage of cells with Golgi-localized DOR for the wild-type DOR NGF and LY294002 compared to the RXR motif mutant demonstrated a large and statistically significant decrease (Figure 5D). These data conclusively show that the arginine residues within the C-terminal tail of DOR are required for the NGF and PI3K inhibition-induced Golgi retention of DOR. Further, it suggests that both RXR motifs are required, and that mutation of either alone is not sufficient to prevent the NGF-induced retention.

## Discussion:

Traditionally, regulated biosynthetic trafficking for GPCRs has largely focused on ER-export. This is similarly true for DOR. It was discovered that the rate limiting step in *de novo* delivery of DOR to the cell surface was proper folding and exit from the ER (7, 14, 19). Additionally, the use of pharmacological chaperones, and agonist induced receptor palmitoylation was able to alter the efficiency for DOR transport to the cell surface (20-22). Receptors that are not folded, processed, or modified properly exit the ER for degradation (19). While these data reveal the basis for DOR transport to the cell surface, all experiments were conducted in HEK 293 cells with an exogenously expressed C-terminally FLAG-tagged  $\delta$ -Opioid receptor. The actual rate-limiting transport processes during DOR's trafficking to the cell surface might vary between cell types, and could require protein-protein interactions that an affinity tag might interfere with. Recently, our lab identified a phosphoinositide-regulated Golgi checkpoint that controls the surface delivery of DOR in neurons (15). Additionally, this checkpoint required the activation of PI3K Class II alpha at the trans-Golgi network for surface trafficking of DOR(16). Further, in PC12 cells exogenously expressing an N-terminal FLAG-tagged DOR, a block in DOR surface trafficking, and retention of DOR within the Golgi, could be achieved via NGF treatment or PI3K inhibition (15, 16). Here, we demonstrate that the NGF-mediated retention of DOR within the Golgi requires dual-arginine containing motifs (RXR) within DOR's C-terminal tail. Similarly, mutation of the RXR motifs to alanine (AXA) is sufficient to prevent the retention of DOR following NGF treatment or PI3K inhibition.

The C-terminal amino acid sequence for GPCRs, and DOR specifically, have been previously implicated in the regulation and control of receptor trafficking; however, primary amino acid sequence motifs controlling the Golgi checkpoint were not known(6). Kim et al. showed that the last 27 amino acids of DOR were sufficient for NGF-mediated retention of DOR in PC12 cells. Interestingly, the requirement for these amino acids in surface trafficking was unknown (17). Deletion of these amino acids, DOR 345 TGA, resulted in incomplete trafficking of DOR to the surface even in the absence of NGF treatment (Figure 1). This was surprising because normally deletion of the entire C-terminal tail, including the transmembrane proximal region, is required for impaired ER-export (6). Interestingly, smaller segmental deletions of DOR did not affect ER-export, nor did they drastically alter the NGF-mediated Golgi retention of DOR. There were minimally significant affects on reducing the NGF-mediated Golgi retention of DOR for the  $\Delta$ 345-352 and  $\Delta$ 353-359 deletion mutants, but neither resulted in prevention of the phenotype (Figure 1).

While C-terminal post-translational modifications such as serine/threonine phosphorylation sites and cysteine palmitoylation had been previously shown to modulate internalization and possibly degradation of DOR, we evaluated their requirement for basal and NGF-induced Golgi retention of DOR (20, 23). Based upon a previous publication showing that phosphorylation of T353 on DOR was important for receptor downregulation, we hypothesized T353 and other serine/threonine phosphorylation sites within the last 27 amino acids could be altering receptor downregulation by changing its ability to traffic to the cell surface (23). All phosphorylation mutants, including T353, when mutated to alanine, displayed normal basal and NGF-treated receptor distribution (Figure 2). Additionally, palmitoylation of DOR has been shown to be required for proper ER-exit and surface trafficking of DOR (20). Therefore, we examined the affect of mutating the potential palmitoylation site C360, along with combinatorial mutants of serine/threonine phosphorylation sites and palmitoylation site C360 to alanine. Again, for all of the mutated receptors evaluated, DOR appeared to traffic to the surface unrestricted in baseline conditions, and showed a significant increase in Golgi retention following NGF treatment (Figure 2 and 3). These data suggest that post-translational modification of serine (363), threonine (352, 353, 358, 361), or cysteine (360) within the last 27 amino acids is not required for basal surface trafficking and NGF-induced Golgi retention of DOR.

Di-arginine sequences have been reported to facilitate ER retention, and possible COP-I retrieval from the ER and Golgi, these regions seemed like good candidates mediating the NGF-induced retention of DOR (12, 13, 18). In individual alanine mutants (RSLRR and SLRRPR and TRER), DOR appeared to traffic and respond to NGF treatment similar to the wild-type receptor (Figure 4). This suggested that the individual arginine motifs within the third intracellular loop and the C-terminal 27 amino acids was not required for the basal surface trafficking and NGF-induced Golgi retention of DOR.

The remaining sequence motif to be tested was the RXR ER and Golgi retrieval or retention motif. Initially we did not think that this would be contributing the the NGF-induced Golgi retention because the RXR motif is thought to provide ER retention at baseline. The first protein shown to require the RXR motif for ER retention and retrieval was the ATP-sensitive potassium channel  $\alpha$  (Kir6.1/2) and  $\beta$  (SUR1) subunits, which contain an RKR motif in their C-terminal sequence. This channel cannot get to the cell surface unless the the subunit complexes can properly form, which mask the RXR retention/retrieval sequence. This sequence motif was found to be sufficient for retention/retrieval when transplanted to other potassium channels and even GPCRs (24). Upon further investigation, Zerangue et al. were able to determine that the actual flanking sequence and amino acid between the two arginine residues can influence the strength

of ER retention/retrieval, and can even alter apparent steady-state localization of the receptor to other compartments, like the Golgi (25). It is likely that the amino acids flanking the DOR RXR motif direct DOR for Golgi retrieval following NGF instead of the ER. Since these initial publications a few observations have been made for variations of this RXR motif contributing to an ER retention/retrieval like affect (13, 18, 26, 27).

The most relevant receptors to the DOR C-terminal tail RXR motifs reported to contain this motif are the Vasopressin V2 receptor (ER/ERGIC retention/retrieval regulated by the protein folding state), GABA receptor (ER retention/retrieval regulated by dimerization), and the NMDA Receptor (ER retention regulated by phosphorylation) (26, 28, 29). All of these receptors require this sequence for quality control of functional receptors and channels, that when masked, allows for export through the secretory pathway and proper trafficking to the cell surface. Interestingly, DOR readily exits the secretory pathway at baseline, but following NGF treatment in PC12 cells, the RXR motifs create a Golgi retention/retrieval signal that can be regulated by PI3K activity (Figure 5). Additionally, we know that the pool of retained DOR following NGF treatment is functional, and can be transported to the surface via PTEN inhibition to provide increased agonist-induced Gi signaling (15). This suggests a novel function for RXR motifs in DOR that allow for exiting the ER, but provide retention/retrieval within the Golgi following cell signaling changes that result from NGF treatment.

For other GPCRs, dimerization has been shown to control ER export and surface trafficking (30, 31). DOR is known to form homodimers, and also heterodimers with other GPCRs, but most of the dimerization has been shown at the cell surface (32, 33). While dimerization could potentially mask the dual RXR retrieval sequences and allow for trafficking of DOR to the surface in normal conditions, it is unclear how NGF would induce the Golgi retention by preventing dimerization. Additionally, when the C-terminal 15 amino acids of DOR were deleted, no agonist induced dimerization occurred; however, some higher order complexes were observed (34). This deletion would leave the RXR motifs intact allowing for retention/retrieval in the absence of dimerization. It would be interesting to see if deletion of the C-terminal 15 amino acids of DOR resulted in any retention/retrieval in normal conditions.

If dimerization is not the primary regulatory mechanism driving the NGF-induced retention of DOR, could protein-protein interactions control DOR's Golgi-retention vs. surface trafficking? There is evidence to suggest that RXR motifs can be masked to facilitate forward biosynthetic trafficking through direct binding interaction with 14-3-3, which may compete for recognition of these motifs by COP-I coat proteins, which presumably play a role in the retention, but they have also been suggested to be masked by other proteins that bind in the vicinity of the RXR C-terminal

motifs (13). One such GPCR relevant example is a PDZ interaction that masks the RXR motif of the NMDA receptor variant NR1.3. DOR does not contain a PDZ ligand; however, it has been shown to interact with several proteins through its C-terminal tail (35). A known DOR interacting partner that would serve as a good candidate for a protein that could mask its RXR motif is  $\beta$ -arrestin 1 (35, 36). For GPCRs,  $\beta$ -arrestins are known to bind to the receptors within the region of the third intracellular loop and the C-terminal tail. Binding to  $\beta$ -arrestin 1 at the Golgi could possibly provide the masking required to prevent retention/retrieval of DOR at baseline, and stimulate the recruitment of proteins such as ROCK, LIMK and Cofilin, known to stimulate agonist-induced DOR surface trafficking (36). In this scenario, NGF treatment would prevent  $\beta$ -arrestin 1 recruitment to the Golgi by altering its localization, allowing for the exposure of the RXR motifs and Golgi retention. In future experiments we plan to test the affect of NGF on  $\beta$ -arrestin 1 localization and recruitment to the Golgi.

Another possible interacting candidate protein complex could be the G-proteins. Both  $\beta$ -arrestins and the G-proteins are known to compete for binding within the region of the third intracellular loop and the C-terminal tail of GPCRs. Intriguingly, one could speculate that both G-protein and  $\beta$ -arrestin binding to the receptor to act as master regulators of alternative interactions. Further, it is possible that G-proteins are pre-loaded onto the receptor in the ER to only allow for ER exit if the receptor and G-protein complex is formed. The G-proteins are known to be present at the ER, and GPCR G-protein complexes have been observed within the Golgi. This binding would mask the RXR motifs and allow export. In order to achieve Golgi retention of DOR following NGF treatment, one could imagine that the GTPase-activating protein (GAP) for  $G\alpha_i$ -proteins, such as RGS4 or GAIP, could get recruited to the Golgi to allow dissociation of the  $G\alpha_i$ -protein and unmasking of the RXR motifs (37). Additionally, this could provide one explanation as to why pharmacological chaperones that mimic agonist binding can induce ER export of DOR. There are many possible hypotheses for the masking and unmasking of the RXR retention/retrieval signal, but without further mechanistic detail, an explanation for how the regulation and coordination of RXR motif affects trafficking through the secretory pathway is speculative at best. Additionally, further confirmation that the RXR motifs required for NGF-induced retention of DOR are those that have been previously implicated in ER retention/retrieval of many of the channel proteins and receptors discussed above is needed.

In conclusion, the  $\delta$ -Opioid receptor is retained within the Golgi following NGF treatment or PI3K inhibition in PC12 cells through a dual RXR motif dependent mechanism. Both RXR motifs are required for the NGF-induced retention of DOR, and effects of phosphorylation and cysteine modification within the last 27 amino acids of the C-terminal tail have minimal regulatory

consequences for retention. These results describe for the first time a Golgi-retention/retrieval mechanism that requires two RXR motifs, and is masked at baseline, but can be triggered through growth factor signaling or PI3K inhibition. The regulation provided by this mechanism is exciting because it allows for a cell type specific on demand delivery of fully folded, modified, and functional receptors to the surface in response to receptor-mediated signaling events. Physiologically, a system such as this is perfectly suited for a single-use, non-recycling, receptor such as DOR. An available pool of ready-to-use receptors can be waiting within the cell and released on demand when the appropriate signal is present by modulating the masking or unmasking of the RXR motif. In future studies, it will be interesting to identify the RXR motif masking partner(s) for DOR, and to look for C-terminal RXR motifs within other GPCRs with known intracellular retention phenotypes. Additionally, identifying the requirement and sufficiency of flanking amino acids that confer Golgi retention/retrieval as opposed to ER or ERGIC retention/retrieval could allow for a better prediction of receptor localization from the primary amino sequence. Finally, by pharmacologically triggering masking of the RXR motifs of DOR, it might be possible to drive fully functional receptors to the cell surface in a receptor specific manner.

**Acknowledgements:**

The authors would like to thank Zara Weinberg, and Drs. Shanna Bowersox, and Cary Shiwarski for technical help and comments. We thank Drs. Nathan Urban, Adam Linstedt, Tina Lee, Peter Friedman, Guillermo Romero, Jean-Pierre Vildardaga, and Alessandro Bisello, for reagents, comments and suggestions. M.A.P. was supported by NIH DA024698 and DA036086.

## Materials and Methods:

### Cell Line and Cell Culture

The cell line used for experimentation was pheochromocytoma-12 (PC12, #CRL-1721) cells. The PC12 cell line is a neuroendocrine cell line isolated from rat adrenal medulla tissue. These cells were grown and cultured in F12K medium (Gibco by Life Technologies 21127-022) supplemented with 10% horse serum and 5% fetal bovine serum (FBS) at 37°C with 5% CO<sub>2</sub>. The media was changed every 3 days to maintain proper cell health. Tissue culture flasks were coated with collagen IV (Sigma #C5533-5MG) to allow PC12 cells to adhere. PC12 cells were passed at a ratio of 1:4 to ensure sufficient seeding density to facilitate growth.

### DNA Transfection of Cultured Cells:

PC12 cells were plated onto collagen IV coated 6-well plates and grown in 10% horse serum and 5% fetal bovine serum F12K media for 24 hours before transfection. Transfection were performed using the Lipofectamine 2000 lipofection reagent (Invitrogen 11668-019) to transiently transfect PC12 cells with the desired DOR plasmid constructs as previously reported

(15, 16). DNA and Lipofectamine ratio were selected from the manufacturers recommendations. We choose to use 7.5 uL of Lipofectamine 2000 and 1.5 ug of the appropriate DOR plasmid DNA. Growth media was removed from the 6-well plate and 1 mL of Opti-MEM was added to each well. Following Lipofectamine-DNA incubation, the transfection mixture was added dropwise to each well. Cells were left to incubate with the transfection mixture for 5 hours at 37°C. Subsequently, the transfection solution was removed from all wells and replaced with 2 mL of growth medium. Experiments were conducted 48-72 hours following transfection.

### DNA plasmids and Mutagenesis:

The wild-type DOR construct consists of an N-terminal Signal Sequence FLAG-tag in the pcDNA3.1 vector. All point mutants and deletion mutants were constructed using a modified QuickChange PCR protocol and confirmed via DNA sequencing. Primer design for the alanine point mutants and deletion mutants was performed using the QuickChange Primer Design Tool from Agilent Technologies. For the DOR 345 TGA, which is a deletion of the last 27 C-terminal amino acids, a TGA loopin reaction was performed using the following primers: Top Primer: 5' CAAGAACCCGGCAGTTGACGTCGTCCCCGCCAGGCC 3'; Bottom Primer: 3' GTTCTTGGGCCGTCAACTGCAGCAGGGGCGGTCCGG 5'. DOR wild-type template (50 ng, 1 uL), Top Primer (125 ng, 1 uL), Bottom Primer (125ng, 1 uL), were mixed with 10x Pfu Turbo

Reaction Buffer (5  $\mu$ L), dNTP Mix (1  $\mu$ L), PfuTurbo (1  $\mu$ L), and H<sub>2</sub>O to 30  $\mu$ L. The PCR reaction was performed as follows: Step 1: 95°C for 2 min, Step 2: 95°C for 30 sec, 55°C for 1 min, 68°C for 14 min, repeated for 18 cycles, Step 3: 72°C for 15min, Step 4: 4°C hold. Following the PCR reaction, a DpnI digest was performed for 1 hour followed by bacterial transformation in DH5 $\alpha$  cells. For the remaining deletion mutants and alanine point mutants, the identical protocol was used with the following primer pairs:

DOR Mutation	Primer Pair	Primer Sequence
$\Delta$ 345-352	Top Primer	5'-CGCCAAGAACCCGGCAGTACGCCTGAGCGTGTCACT-3'
	Bottom Primer	3'-GTCATGCGCACTCGCACAGTGAC-5'
$\Delta$ 353-359	Top Primer	5-CGTCGTCCCCGCCAGGCCACCTGCACCCCCTCCGACGGC-3'
	Bottom Primer	3'-GTGGACGTGGGGGAGGCTGCCG-5'
$\Delta$ 360-366	Top Primer	5'-CGTGAGCGTGTCAGTCCCGGCGGTGGCGCTGCCGCC-3'
	Bottom Primer	3'-GGCCGCCACCGCGACGGCGG-5'
$\Delta$ 367 TGA	Top Primer	5'-ACCCCTCCGACGGCCGTGAGGTGGCGCTGCCGCCTG-3'
	Bottom Primer	3'-TGGGGGAGGCTGCCGGGCACTCCACCGCGACGGCGGAC-5'

#### Fixed Cell Immunofluorescence

PC12 expressing FLAG-DOR and the FLAG-DOR mutants were plated on coverslips (Corning) coated with poly-D-lysine (Sigma, #P7280) and grown at 37°C for 48 hrs. Following treatments with either NGF (100ng/mL) or PI3K inhibition (LY294002, 10 $\mu$ M) for 1 hour, cells were fixed in 4% paraformaldehyde, pH 7.4. The coverslips were blocked with calcium magnesium containing phospho buffered saline (PBS) with 5% fetal bovine serum, 5% 1M glycine, and 0.75% Triton X-100. To conduct the immunofluorescence imaging, DOR and *trans*-Golgi network were labeled for one hour in blocking buffer with anti-FLAG M1 antibody (Sigma, #F3040) (1:1000) conjugated with Alexa-647 (Molecular Probes, #A20186), and anti-TGN-38 rabbit polyclonal antibody (1:2000, Sigma-Aldrich cat#: T9826), respectively. Three washes were performed using calcium magnesium PBS. Alexa-568 Goat anti-rabbit secondary (1:1000, #A11011) antibody in blocking buffer for 1 hour was added to label the anti-TGN-38. Cover slips were again washed in calcium magnesium PBS and mounted to glass slides using Prolong Diamond Reagent (Molecular Probes, #P36962). Spinning-disk confocal immunofluorescence imaging of the was performed using an Andor confocal imaging system (XDi spinning disk, Andor) at 60X magnification (Nikon CFI APO TIRF) on a Nikon TE-2000 inverted microscope with a mechanical Piezo XYZ-stage (Nikon), iXon 897 Ultra back-illuminated camera (Andor), a laser combiner (Andor) containing 405, 488, 515, 568, and 647nm excitation capabilities, IQ2 imaging software

(Andor), and a isolation table (TMC). Images of representative fields were taken. Quantification of the fluorescence ratio was taken for all cells imaged and averaged to ensure results were representative of the population. A minimum of three biological replicates were performed to confirm the results.

#### Growth Factors and Inhibitors

Compound Name	Protein Target	Concentration	Supplier	Catalog #
Nerve Growth Factor	TrkA	100 ng/ $\mu$ L	BD Biosciences	356004
LY294002	PI3K inhibitor	10 $\mu$ M	Tocris Bioscience	1130

#### Image Analysis and Quantification

All imaging analysis and data was quantified using Image J. Custom macros were written to allow unbiased measurements for the total DOR fluorescence for each cell and the fluorescence intensity of DOR within the Golgi for fixed and live cell analysis(15). The ratio of DOR fluorescence within the Golgi to the total cell fluorescence was used to measure the amount of total DOR in the Golgi under each treatment condition. This ratio was calculated for each cell and then averaged across all cells. Further, a binary quantification was performed to manually determine the percentage of cells that visually displayed Golgi-localized DOR. The binary quantification results were averaged to determine the population percentage of cells with Golgi-localized DOR. More detailed procedure and a quantification example can be found in our previous publication(15).

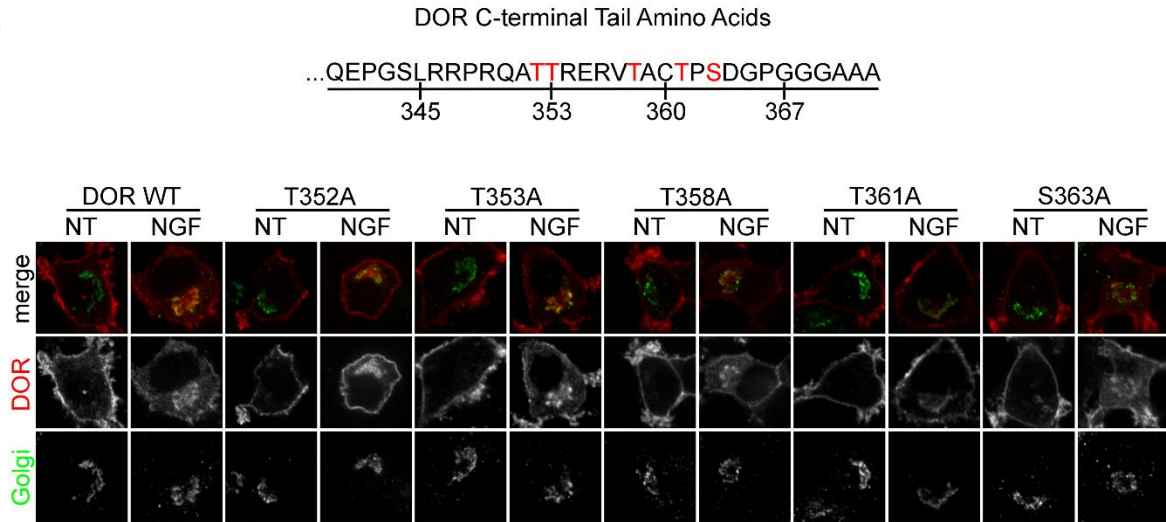
#### Statistics and Data Analysis

Statistical and graphical analyses were performed using GraphPad Prism 5 software. Statistical tests were chosen based on the experimental sample size, distribution, and conditions. Minimally, three independent biological replicates were performed for each data set. For statistical analysis of the fixed cell immunofluorescence imaging data, two-tailed unpaired t-tests and one-way ANOVA were performed when appropriate. A p-value of < 0.05 was considered statistically significant. The figures and visuals were constructed Adobe Photoshop CS6.

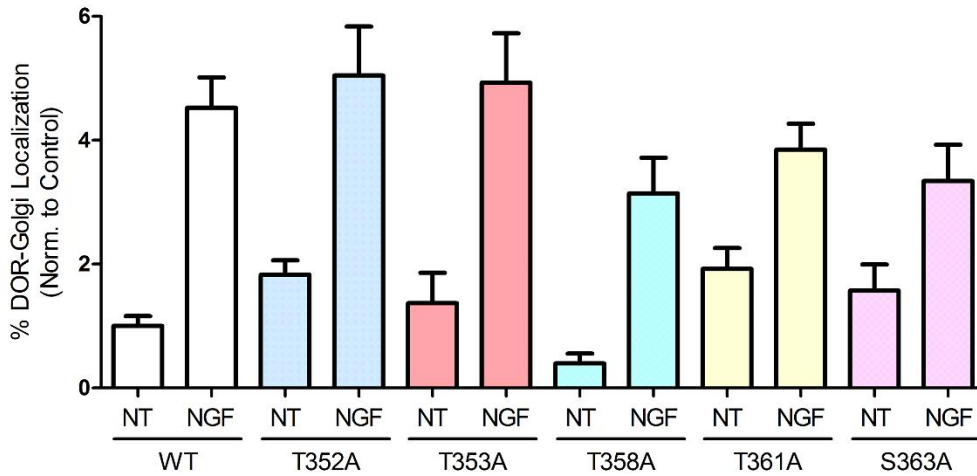


In a Flag-tagged DOR construct, the entire 27 amino acid region was deleted by adding in a stop codon at position 345 (345 TGA). Subsequent deletion mutants were made to determine the region with the DOR C-terminal tail required for the NGF-induced Golgi retention of DOR (345 TGA,  $\Delta$ 345-352,  $\Delta$ 353-359,  $\Delta$ 360-366,  $\Delta$ 367 TGA). In PC12 cells expressing the wild-type Flag-tagged DOR (DOR WT), immunofluorescence images reveal that DOR is highly expressed on the cell surface under control no treatment (NT) conditions, and following 1 hour of Nerve Growth Factor treatment (NGF, 100ng/mL), DOR accumulates in a region that colocalizes with the trans-Golgi Network marker TGN-38 (Golgi, marked by yellow arrow). Removal of the last 27 amino acids of the DOR tail sequence (345 TGA) results in an increase in the basal internal pool of DOR under no treatment conditions, and increases following NGF treatment. Sectional deletions of the regions comprising the 27 amino acids of the C-terminal DOR tail sequence all demonstrate baseline surface localization under control no treatment conditions, and accumulation of DOR within the Golgi region following NGF treatment. **B.** Quantitative analysis of the immunofluorescence images showed an increase in the percentage of DOR fluorescence localized to the Golgi region following NGF treatment for cells expressing DOR WT. The tail deletion mutant, DOR 345 TGA, exhibited an increase in the percentage of DOR fluorescence localized to the Golgi at baseline, that persisted following NGF treatment. Of the individual DOR tail deletion mutants, the  $\Delta$ 345-352, and the  $\Delta$ 353-359 displayed a small, but significant reduction in the percentage of DOR fluorescence localized to the Golgi following NGF treatment compared to DOR WT NGF. The remaining deletion mutants were similar to DOR WT in both NT and NGF treatment conditions (DOR WT NT,  $n=82$  cells; DOR WT NGF,  $n=77$  cells; 345 TGA NT,  $n=37$  cells; 345 TGA NGF,  $n=44$  cells;  $\Delta$ 345-352 NT,  $n=97$  cells;  $\Delta$ 345-352 NGF,  $n=98$  cells;  $\Delta$ 353-359 NT,  $n=77$  cells;  $\Delta$ 353-359 NGF,  $n=105$  cells;  $\Delta$ 360-366 NT,  $n=84$  cells;  $\Delta$ 360-366 NGF,  $n=80$  cells;  $\Delta$ 367 TGA NT,  $n=34$  cells;  $\Delta$ 367 TGA NGF,  $n=39$  cells; mean  $\pm$  s.e.m.; \* $P<0.05$ , \*\* $P<0.01$ ; by two-sided t-test vs. DOR WT NGF). **C.** Additional quantification of the percentage of cells that appeared to have Golgi-localized DOR demonstrated a similar pattern to the fluorescence quantification. DOR 345 TGA tail deletion exhibited an increase in the percentage of cells with Golgi-localized DOR localized at baseline, and the  $\Delta$ 345-352, and the  $\Delta$ 353-359 DOR tail deletions displayed a small, but significant reduction in the percentage of cells with Golgi-localized DOR following NGF treatment compared to DOR WT NGF (DOR WT NT,  $n=82$  cells; DOR WT NGF,  $n=77$  cells; 345 TGA NT,  $n=37$  cells; 345 TGA NGF,  $n=44$  cells;  $\Delta$ 345-352 NT,  $n=97$  cells;  $\Delta$ 345-352 NGF,  $n=98$  cells;  $\Delta$ 353-359 NT,  $n=77$  cells;  $\Delta$ 353-359 NGF,  $n=105$  cells;  $\Delta$ 360-366 NT,  $n=84$  cells;  $\Delta$ 360-366 NGF,  $n=80$  cells;  $\Delta$ 367 TGA NT,  $n=34$  cells;  $\Delta$ 367 TGA NGF,  $n=39$  cells; mean  $\pm$  s.e.m.; \*\* $P<0.01$ , \*\*\* $P<0.001$ ; by two-sided t-test vs. DOR WT NGF).

A



B



C

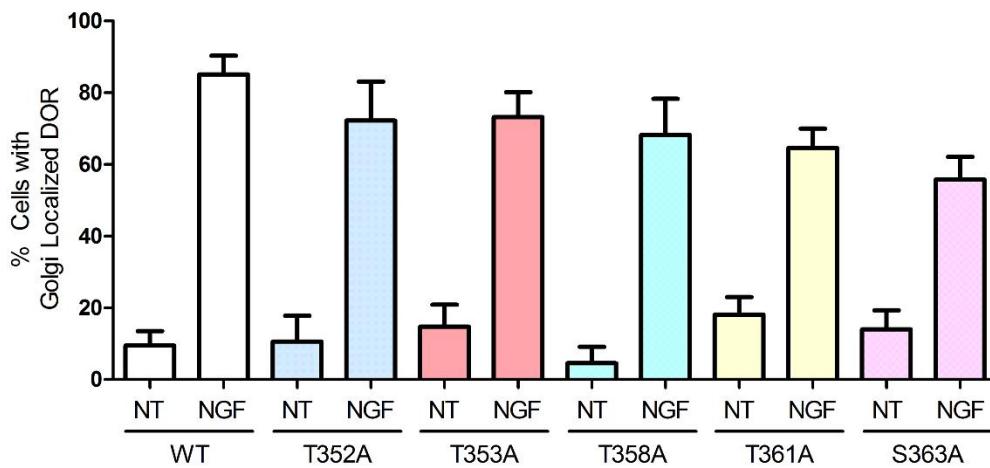


**Figure 2: Mutating the potential phosphorylation sites within the C-terminal tail of DOR to alanine does not significantly affect the basal or NGF-regulated Golgi retention of DOR. A.**

Within the last 27 amino acids of the DOR C-terminal tail there are five potential serine or threonine phosphorylation sites (Red). Immunofluorescence imaging of PC12 cells expressing a wild-type Flag-tagged DOR (DOR WT) or alanine mutated threonine and serine (T352A, T353A, T358A, T361A, S363A) receptors in control conditions (NT) or following 1 hour of Nerve Growth Factor (NGF, 100ng/mL) treatment. For all wild-type and mutated receptors, NGF induced a Golgi localized pool of DOR. **B.** Quantification of the percentage of DOR fluorescence localized to the Golgi was normalized to DOR WT with NGF to compare the alanine mutants to the full length DOR. There was no statistical difference between the DOR WT NT and the alanine mutants NT; however, the T352A, T353A, T361A, and S363A had slightly increased DOR fluorescence within the Golgi at baseline. Additionally, there was no statistical difference between the DOR WT NGF and the alanine mutants NGF; however, a subtle decrease in the DOR fluorescence within the Golgi was observed for the T358A, T361A, and S363A alanine mutants (DOR WT NT,  $n=53$  cells; DOR WT NGF,  $n=50$  cells; T352A NT,  $n=20$  cells; T352A NGF,  $n=20$  cells; T353A NT,  $n=35$  cells; T353A NGF,  $n=41$  cells; T358A NT,  $n=22$  cells; T358A NGF,  $n=22$  cells; T361A NT,  $n=58$  cells; T361A NGF,  $n=71$  cells; S363A NT,  $n=41$  cells; S363A NGF,  $n=61$  cells; mean  $\pm$  s.e.m.; non-significant; by two-sided t-test vs. DOR WT NT and NGF). **C.** Analysis of the percentage of cells with Golgi-localized DOR displayed similar results. In both the baseline (NT) and NGF treated conditions there were no statistically significant changes observed between the DOR WT and the alanine mutants (DOR WT NT,  $n=53$  cells; DOR WT NGF,  $n=50$  cells; T352A NT,  $n=20$  cells; T352A NGF,  $n=20$  cells; T353A NT,  $n=35$  cells; T353A NGF,  $n=41$  cells; T358A NT,  $n=22$  cells; T358A NGF,  $n=22$  cells; T361A NT,  $n=58$  cells; T361A NGF,  $n=71$  cells; S363A NT,  $n=41$  cells; S363A NGF,  $n=61$  cells; mean  $\pm$  s.e.m.; non-significant; by two-sided t-test vs. DOR WT NT and NGF).

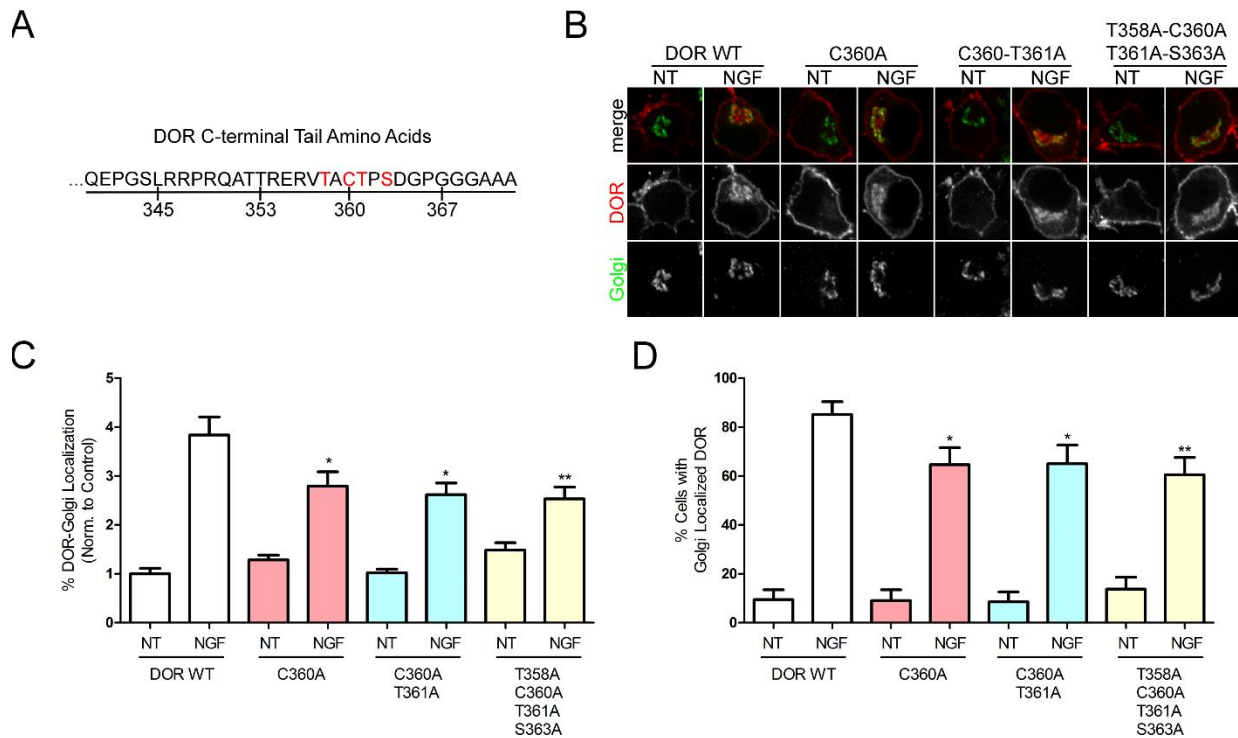


**Figure 3: Eliminating the potential post-translational modification site C360 within the C-terminal tail of DOR to alanine minimally decreases the NGF-induced Golgi retention of DOR.** **A.** Within the last 27 amino acids of the DOR C-terminal tail there is one cysteine residue (C360) that is a potential target for post-translational modifications within a serine/threonine rich region (Red). **B.** Immunofluorescence imaging of PC12 cells expressing a wild-type Flag-tagged DOR (DOR WT) or alanine mutated C360 alone or in combination with threonine and serine mutations (C360A, C360A\_T361A, T358A\_C360A\_T361A\_S363A) in control conditions (NT) or following 1 hour of Nerve Growth Factor (NGF, 100ng/mL) treatment. For all wild-type and mutated receptors, NGF induced a Golgi localized pool of DOR. **C.** Quantification of the percentage of DOR fluorescence localized to the Golgi was normalized to DOR WT with NT to compare the cysteine mutants to the full length DOR. Mutating the C360 to alanine either alone, or in combination with T358, T361, and S363 revealed a small but significant decrease in the DOR fluorescence within the Golgi compared to DOR WT NGF (DOR WT NT,  $n=75$  cells; DOR WT NGF,  $n=61$  cells; C360A NT,  $n=67$  cells; C360A NGF,  $n=65$  cells; C360A\_T361A NT,  $n=47$  cells; C360A\_T361A NGF,  $n=40$  cells; T358A\_C360A\_T361A\_S363A NT,  $n=51$  cells; T358A\_C360A\_T361A\_S363A NGF,  $n=49$  cells; mean  $\pm$  s.e.m.; \* $P<0.05$ , \*\* $P<0.01$ ; by two-sided t-test vs. DOR WT NGF). **D.** Similarly, analysis of the percentage of cells with Golgi-localized DOR revealed a small but significant decrease between the DOR WT NGF and the cysteine mutants NGF. Interestingly, in combination with the C360A mutation, alanine mutations of the

threonine and serine residues did not provide any further decrease in DOR-Golgi localization (DOR WT NT,  $n=75$  cells; DOR WT NGF,  $n=61$  cells; C360A NT,  $n=67$  cells; C360A NGF,  $n=65$  cells; C360A\_T361A NT,  $n=47$  cells; C360A\_T361A NGF,  $n=40$  cells; T358A\_C360A\_T361A\_S363A NT,  $n=51$  cells; T358A\_C360A\_T361A\_S363A NGF,  $n=49$  cells; mean  $\pm$  s.e.m.; \* $P<0.05$ , \*\* $P<0.01$ ; by two-sided t-test vs. DOR WT NGF).

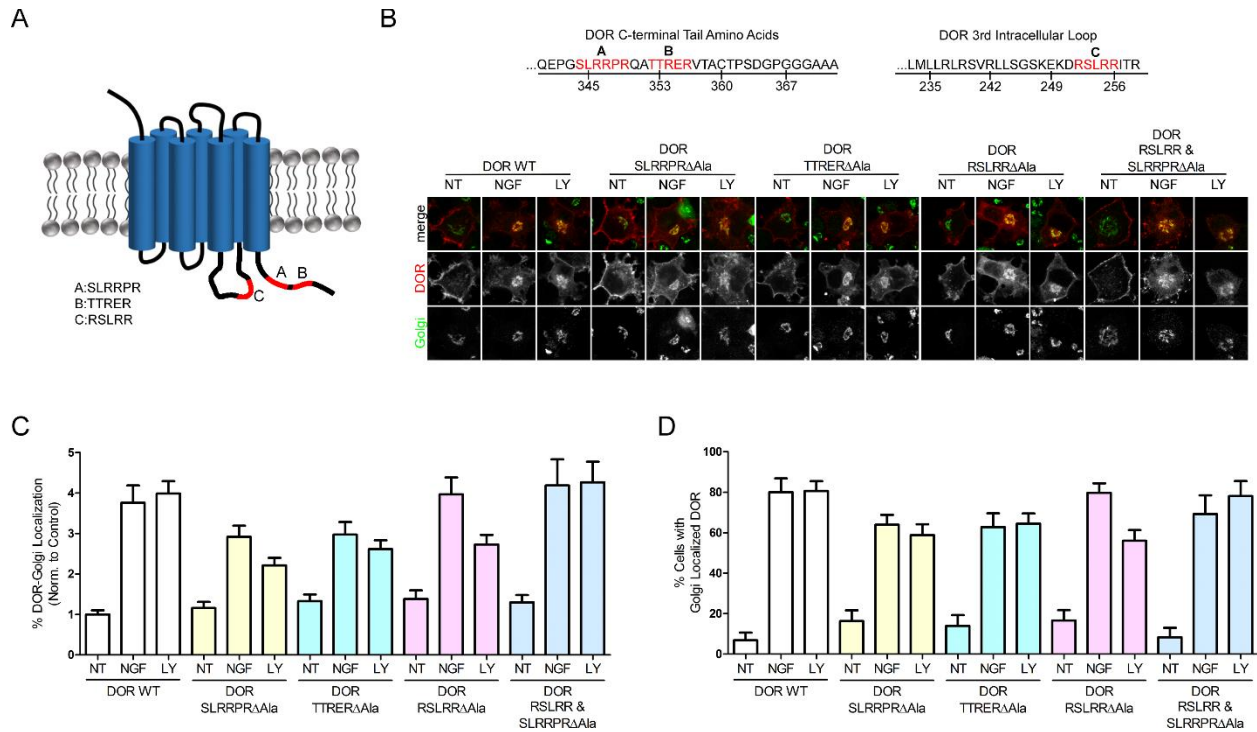


**Figure 4: Alanine mutations of di-arginine containing motifs within the third intracellular loop and C-terminal tail of DOR do not significantly inhibit the NGF-induced retention of DOR.** **A.** Within the third intracellular loop and C-terminal tail of DOR there is a repetitive sequence, SLRR. Alanine mutant versions of a Flag-tagged DOR were made containing the SLRRPR to AAAAAA (A), TTRER to AAAAA (B), RSLRR to AAAAA (C), and both RSLRR and SLRRPR to AAAAA and AAAAAA. **B.** Immunofluorescence imaging of PC12 cells expressing a wild-type Flag-tagged DOR (DOR WT) or alanine mutated di-arginine containing motifs demonstrated primarily surface localization in normal baseline no treatment conditions (NT). Following NGF treatment for 1 hour (NGF, 100ng/mL) or PI3K inhibition by LY294002 (LY, 10μM), all DOR constructs exhibited increased Golgi-localization. **C.** Quantification of the percentage of DOR fluorescence localized to the Golgi was normalized to DOR WT with NT to compare the alanine mutated di-arginine containing motifs to the full length DOR. Mutating the SLRRPRΔAla, TTRERΔAla, RSLRRΔAla, and both RSLRR and SLRRPRΔAla did not significantly affect the NGF-induced DOR-Golgi localization. Mutating the SLRRPRΔAla, TTRERΔAla, and RSLRRΔAla alone resulted in a small, but significant decrease in the DOR fluorescence within the Golgi following PI3K inhibition by LY compared to DOR WT LY (DOR WT NT,  $n=58$  cells; DOR WT NGF,  $n=56$  cells; DOR WT LY,  $n=67$  cells; SLRRPRΔAla NT,  $n=49$  cells; SLRRPRΔAla NGF,  $n=91$  cells; SLRRPRΔAla LY,  $n=85$  cells; TTRERΔAla NT,  $n=43$  cells; TTRERΔAla NGF,  $n=51$  cells; TTRERΔAla LY,  $n=90$  cells; RSLRRΔAla NT,  $n=40$  cells; RSLRRΔAla NGF,  $n=52$  cells;

RSLRR $\Delta$ Ala LY,  $n=91$  cells; SLRRPR $\Delta$ Ala & RSLRR $\Delta$ Ala NT,  $n=36$  cells; SLRRPR $\Delta$ Ala & RSLRR $\Delta$ Ala NGF,  $n=26$  cells; SLRRPR $\Delta$ Ala & RSLRR $\Delta$ Ala LY,  $n=32$  cells; mean  $\pm$  s.e.m.; \*\* $P<0.01$ , \*\*\* $P<0.001$ , \*\*\*\* $P<0.0001$ ; by two-sided t-test vs. DOR WT NGF and LY). **D.** Analysis of the percentage of cells with Golgi-localized DOR showed a small but significant decrease between the DOR WT LY and the SLRRPR $\Delta$ Ala, TTRER $\Delta$ Ala, and RSLRR $\Delta$ Ala alone. A non-significant decrease was observed for SLRRPR $\Delta$ Ala, TTRER $\Delta$ Ala, and RSLRR $\Delta$ Ala alone following NGF-treatment (DOR WT NT,  $n=58$  cells; DOR WT NGF,  $n=56$  cells; DOR WT LY,  $n=67$  cells; SLRRPR $\Delta$ Ala NT,  $n=49$  cells; SLRRPR $\Delta$ Ala NGF,  $n=91$  cells; SLRRPR $\Delta$ Ala LY,  $n=85$  cells; TTRER $\Delta$ Ala NT,  $n=43$  cells; TTRER $\Delta$ Ala NGF,  $n=51$  cells; TTRER $\Delta$ Ala LY,  $n=90$  cells; RSLRR $\Delta$ Ala NT,  $n=40$  cells; RSLRR $\Delta$ Ala NGF,  $n=52$  cells; RSLRR $\Delta$ Ala LY,  $n=91$  cells; SLRRPR $\Delta$ Ala & RSLRR $\Delta$ Ala NT,  $n=36$  cells; SLRRPR $\Delta$ Ala & RSLRR $\Delta$ Ala NGF,  $n=26$  cells; SLRRPR $\Delta$ Ala & RSLRR $\Delta$ Ala LY,  $n=32$  cells; mean  $\pm$  s.e.m.; \*\* $P<0.01$ ; by two-sided t-test vs. DOR WT NGF and LY).

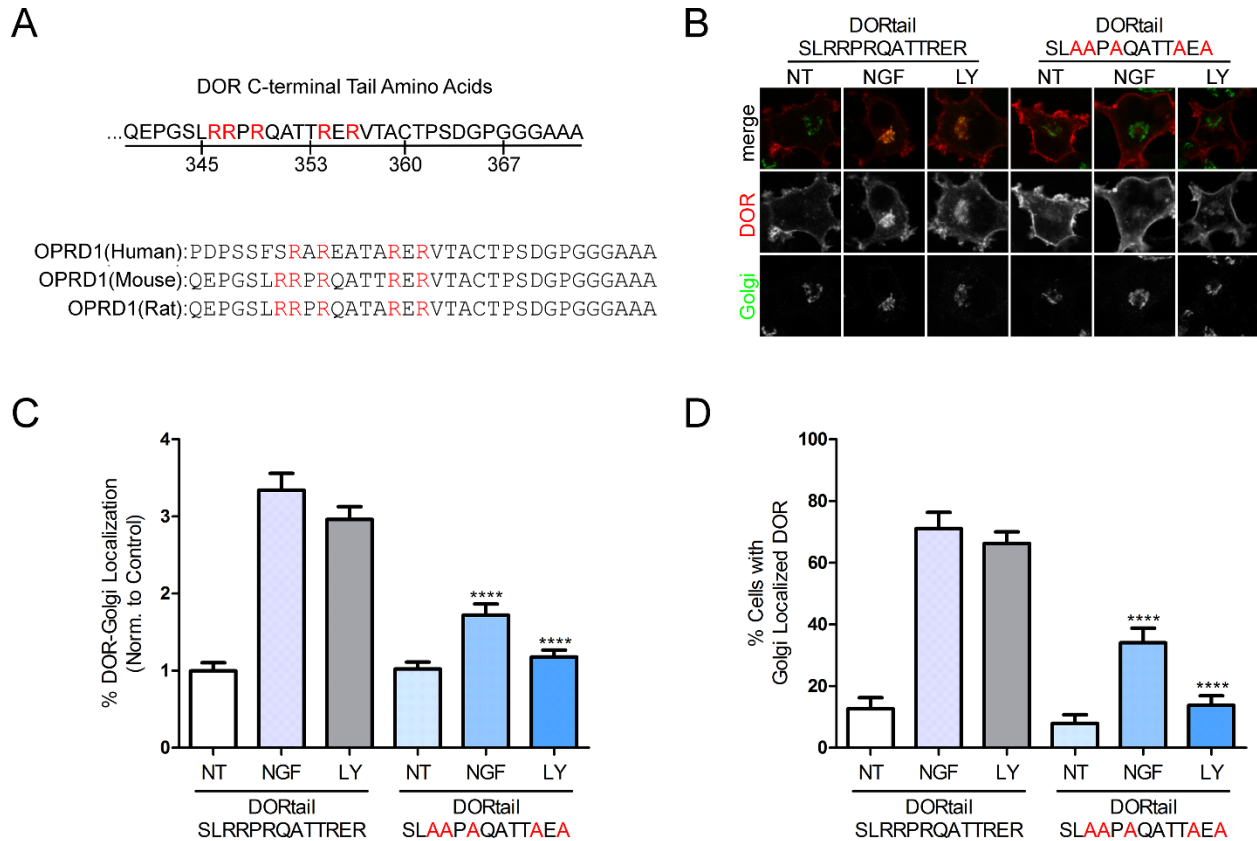


**Figure 5: Two RXR motifs within the C-terminal tail of DOR are required for NGF-induced Golgi retention.** **A.** The C-terminal 27 amino acids of DOR contain two, highly conserved, RXR retention motifs. Sequences comparison between the Human, Mouse, and Rat DOR (OPRD1) C-terminal tail demonstrate the high sequence conservation (Arginine highlighted in Red). All five of the arginine within the mouse C-terminal tail of DOR were mutated to alanine. **B.** Immunofluorescence imaging of PC12 cells expressing a wild-type Flag-tagged DOR (DORtail SLRRPRQATTRE) or alanine mutated RXR motifs (DORtail SLAAPAQATTAE) demonstrated primarily surface localization in normal baseline no treatment conditions (NT). Following NGF treatment for 1 hour (NGF, 100ng/mL), or PI3K inhibition by LY294002 (LY, 10 $\mu$ M), wild-type DOR exhibited increased Golgi-localization; however, the arginine mutant was almost completely surface localized. **C.** Quantification of the percentage of DOR fluorescence localized to the Golgi was normalized to wild-type DOR (DORtail SLRRPRQATTRE) NT to compare the alanine mutated RXR motifs (DORtail SLAAPAQATTAE) to the full length DOR. Mutating the RXR motifs (DORtail SLAAPAQATTAE) significantly decreased the NGF and LY-induced DOR-Golgi localization (DORtail SLRRPRQATTRE NT,  $n=86$  cells; DORtail SLRRPRQATTRE NGF,  $n=75$  cells; DORtail SLRRPRQATTRE LY,  $n=159$  cells; DORtail SLAAPAQATTAE NT,  $n=87$  cells; DORtail SLAAPAQATTAE NGF,  $n=94$  cells; DORtail SLAAPAQATTAE LY,  $n=123$  cells;

mean  $\pm$  s.e.m.; \*\*\*\* $P$ <0.0001; by two-sided t-test vs. DOR WT NGF and LY). **D.** Further analysis of the percentage of cells with Golgi-localized DOR showed a significant decrease between the DOR WT NT and LY and the RXR motifs mutant (DORtail SLAAPAQATTAEA) (DORtail SLRRPRQATTRER NT,  $n=86$  cells; DORtail SLRRPRQATTRER NGF,  $n=75$  cells; DORtail SLRRPRQATTRER LY,  $n=159$  cells; DORtail SLAAPAQATTAEA NT,  $n=87$  cells; DORtail SLAAPAQATTAEA NGF,  $n=94$  cells; DORtail SLAAPAQATTAEA LY,  $n=123$  cells; mean  $\pm$  s.e.m.; \*\*\*\* $P$ <0.0001; by two-sided t-test vs. DOR WT NGF and LY).

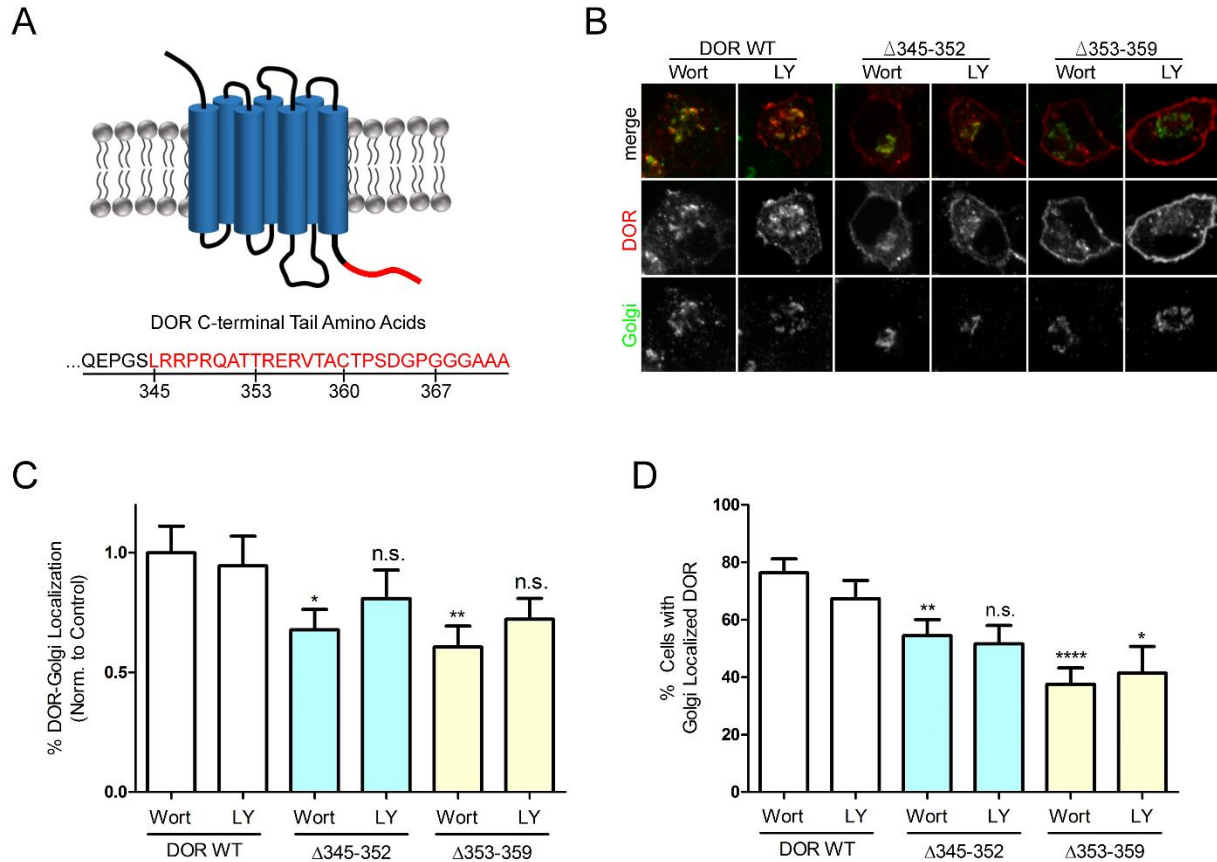


**Figure S1: The DOR C-terminal tail deletions  $\Delta$ 345-352 and  $\Delta$ 353-359 exhibit a reduction in Golgi retention following PI3K inhibition.** **A.** A schematic of the delta-Opioid receptor topology with the last 27 amino acids of the C-terminal tail identified (Red). The amino acid sequence of the C-terminal tail is depicted below. **B.** Immunofluorescence images of the PC12 cells expressing DOR WT,  $\Delta$ 345-352, and  $\Delta$ 353-359 after 1 hour of treatment with the PI3K inhibitor Wortmannin (Wort, 10 $\mu$ M) or LY294002 (LY, 10 $\mu$ M). The  $\Delta$ 345-352 and  $\Delta$ 353-359 deletions mutants both appeared to have less DOR fluorescence localized to the Golgi compared to DOR WT. **C.** Quantification of the percentage of DOR fluorescence localized to the Golgi was normalized to DOR WT with Wortmannin to compare the deletions mutants to the full length DOR. For both the  $\Delta$ 345-352 and  $\Delta$ 353-359 deletions after treatment with Wortmannin, a small, but statistically significant reduction in the percentage of DOR localized to the Golgi was observed (DOR WT Wort,  $n=76$  cells; DOR WT LY,  $n=55$  cells;  $\Delta$ 345-352 Wort,  $n=79$  cells;  $\Delta$ 345-352 LY,  $n=62$  cells;  $\Delta$ 353-359 Wort,  $n=73$  cells;  $\Delta$ 353-359 LY,  $n=50$  cells; mean  $\pm$  s.e.m.; \* $P<0.05$ , \*\* $P<0.01$ ; by two-sided t-test vs. DOR WT Wort or LY). **D.** Similarly, the  $\Delta$ 345-352 and  $\Delta$ 353-359 deletions resulted in a lower percentage of cells with Golgi-localized DOR after treatment with Wortmannin.

Following treatment with LY294002, only the  $\Delta 353-359$  was significantly reduced compared to the DOR WT (DOR WT Wort,  $n=76$  cells; DOR WT LY,  $n=55$  cells;  $\Delta 345-352$  Wort,  $n=79$  cells;  $\Delta 345-352$  LY,  $n=62$  cells;  $\Delta 353-359$  Wort,  $n=73$  cells;  $\Delta 353-359$  LY,  $n=50$  cells; mean  $\pm$  s.e.m.; \* $P<0.05$ , \*\* $P<0.01$ , \*\*\*\* $P<0.0001$ ; by two-sided t-test vs. DOR WT Wort or LY).

## References:

1. Puthenveedu, M. A., Puthenveedu, M. A., Zastrow, von, M., and Zastrow, von, M. (2006) Cargo regulates clathrin-coated pit dynamics. *Cell*. **127**, 113–124
2. Puthenveedu, M. A., Puthenveedu, M. A., Yudowski, G. A., Yudowski, G. A., Zastrow, von, M., and Zastrow, von, M. (2007) Endocytosis of neurotransmitter receptors: location matters. *Cell*. **130**, 988–989
3. Vistein, R., and Puthenveedu, M. A. (2013) Reprogramming of G protein-coupled receptor recycling and signaling by a kinase switch. *Proc. Natl. Acad. Sci. U.S.A.* **110**, 15289–15294
4. Puthenveedu, M. A., Puthenveedu, M. A., Lauffer, B., Lauffer, B., Temkin, P., Temkin, P., Vistein, R., Vistein, R., Carlton, P., Carlton, P., Thorn, K., Thorn, K., Taunton, J., Taunton, J., Weiner, O. D., Weiner, O. D., Parton, R. G., Parton, R. G., Zastrow, von, M., and Zastrow, von, M. (2010) Sequence-dependent sorting of recycling proteins by actin-stabilized endosomal microdomains. *Cell*. **143**, 761–773
5. Magalhaes, A. C., Dunn, H., and Ferguson, S. S. G. (2012) Regulation of GPCR activity, trafficking and localization by GPCR-interacting proteins. *British Journal of Pharmacology*. **165**, 1717–1736
6. Duvernay, M. T., Duvernay, M. T., Zhou, F., and Wu, G. (2004) A conserved motif for the transport of G protein-coupled receptors from the endoplasmic reticulum to the cell surface. *J. Biol. Chem.* **279**, 30741–30750
7. Duvernay, M. T., Dong, C., Zhang, X., Robitaille, M., Hébert, T. E., and Wu, G. (2009) A single conserved leucine residue on the first intracellular loop regulates ER export of G protein-coupled receptors. *Traffic*. **10**, 552–566
8. Dong, C., Dong, C., Filipeanu, C. M., Filipeanu, C. M., Duvernay, M. T., Duvernay, M. T., Wu, G., and Wu, G. (2007) Regulation of G protein-coupled receptor export trafficking. *Biochim. Biophys. Acta*. **1768**, 853–870
9. Gilbert, C., Gilbert, C. E., Zuckerman, D., Zuckerman, D. M., Currier, P., Currier, P. L., Machamer, C., and Machamer, C. E. (2014) Three basic residues of intracellular loop 3 of the beta-1 adrenergic receptor are required for golgin-160-dependent trafficking. *IJMS*. **15**, 2929–2945
10. Parmar, H. B., Barry, C., and Duncan, R. (2014) Polybasic trafficking signal mediates golgi export, ER retention or ER export and retrieval based on membrane-proximity. *PLoS ONE*. **9**, e94194
11. Zhang, X., Dong, C., Wu, Q. J., Balch, W. E., and Wu, G. (2011) Di-acidic motifs in the membrane-distal C termini modulate the transport of angiotensin II receptors from the endoplasmic reticulum to the cell surface. *Journal of Biological Chemistry*. **286**, 20525–20535
12. Schutze, M. P., Peterson, P. A., and Jackson, M. R. (1994) An N-terminal double-arginine motif maintains type II membrane proteins in the endoplasmic reticulum. *EMBO J*. **13**, 1696–1705
13. Michelsen, K., Yuan, H., and Schwappach, B. (2005) Hide and run. Arginine-based endoplasmic-reticulum-sorting motifs in the assembly of heteromultimeric membrane proteins. *EMBO Rep*. **6**, 717–722
14. Petaja-Repo, U. E., Hogue, M., Laperriere, A., Walker, P., and Bouvier, M. (2000) Export from the endoplasmic reticulum represents the limiting step in the maturation and cell surface expression of the human delta opioid receptor. *J. Biol. Chem.* **275**, 13727–13736
15. Shiwarski, D. J., Tipton, A., Schmidt, B. A., Giraldo, M. D., Gold, M. S., Pradhan, A. A., and Puthenveedu, M. A. A phosphoinositide-regulated Golgi checkpoint regulates the bioavailability of delta opioid receptors. *Nat. Med.*
16. Shiwarski, D. J., Darr, M., and Puthenveedu, M. A. Optogenetic Recruitment of PI3K C2α

- to the trans-Golgi Network is Sufficient to Promote Surface Trafficking of the  $\delta$ -Opioid Receptor
17. Kim, K.-A., Kim, K.-A., Zastrow, von, M., and Zastrow, von, M. (2003) Neurotrophin-regulated sorting of opioid receptors in the biosynthetic pathway of neurosecretory cells. *Journal of Neuroscience*. **23**, 2075–2085
  18. Roth, D., Lynes, E., Riemer, J., Hansen, H. G., Althaus, N., Simmen, T., and Ellgaard, L. (2010) A di-arginine motif contributes to the ER localization of the type I transmembrane ER oxidoreductase TMX4. *Biochem. J.* **425**, 195–205
  19. Petaja-Repo, U. E., Petaja-Repo, U. E., Hogue, M., Laperriere, A., Bhalla, S., Walker, P., and Bouvier, M. (2001) Newly synthesized human delta opioid receptors retained in the endoplasmic reticulum are retrotranslocated to the cytosol, deglycosylated, ubiquitinated, and degraded by the proteasome. *J. Biol. Chem.* **276**, 4416–4423
  20. Petaja-Repo, U. E., Petäjä-Repo, U. E., Hogue, M., Hogue, M., Leskelä, T. T., Leskela, T. T., Markkanen, P. M. H., Markkanen, P. M. H., Tuusa, J. T., Tuusa, J. T., Bouvier, M., and Bouvier, M. (2006) Distinct subcellular localization for constitutive and agonist-modulated palmitoylation of the human delta opioid receptor. *J. Biol. Chem.* **281**, 15780–15789
  21. Leskelä, T. T., Leskela, T. T., Markkanen, P. M. H., Markkanen, P. M. H., Pietila, E. M., Pietilä, E. M., Tuusa, J. T., Tuusa, J. T., Petäjä-Repo, U. E., and Petaja-Repo, U. E. (2007) Opioid receptor pharmacological chaperones act by binding and stabilizing newly synthesized receptors in the endoplasmic reticulum. *J. Biol. Chem.* **282**, 23171–23183
  22. Leskelä, T. T., Leskelä, T. T., Markkanen, P. M. H., Markkanen, P. M. H., Alahuhta, I. A., Alahuhta, I. A., Tuusa, J. T., Tuusa, J. T., Petäjä-Repo, U. E., and Petäjä-Repo, U. E. (2009) Phe27Cys polymorphism alters the maturation and subcellular localization of the human delta opioid receptor. *Traffic*. **10**, 116–129
  23. Trapaidze, N., Cvejic, S., Nivarthi, R. N., Abood, M., and Devi, L. A. (2000) Role for C-tail residues in delta opioid receptor downregulation. *DNA Cell Biol.* **19**, 93–101
  24. Ma, D., Zerangue, N., Lin, Y. F., Collins, A., Yu, M., Jan, Y. N., and Jan, L. Y. (2001) Role of ER export signals in controlling surface potassium channel numbers. *Science*. **291**, 316–319
  25. Zerangue, N., Malan, M. J., Fried, S. R., Dazin, P. F., Jan, Y. N., Jan, L. Y., and Schwappach, B. (2001) Analysis of endoplasmic reticulum trafficking signals by combinatorial screening in mammalian cells. *Proceedings of the National Academy of Sciences*. **98**, 2431–2436
  26. Hermosilla, R., Oueslati, M., Donalies, U., Schönenberger, E., Krause, E., Oksche, A., Rosenthal, W., and Schüle, R. (2004) Disease-causing V(2) vasopressin receptors are retained in different compartments of the early secretory pathway. *Traffic*. **5**, 993–1005
  27. Kalandadze, A., Wu, Y., Fournier, K., and Robinson, M. B. (2004) Identification of motifs involved in endoplasmic reticulum retention-forward trafficking of the GLT-1 subtype of glutamate transporter. *Journal of Neuroscience*. **24**, 5183–5192
  28. Scott, D. B., Blanpied, T. A., Swanson, G. T., Zhang, C., and Ehlers, M. D. (2001) An NMDA receptor ER retention signal regulated by phosphorylation and alternative splicing. *Journal of Neuroscience*. **21**, 3063–3072
  29. Margeta-Mitrovic, M., Jan, Y. N., and Jan, L. Y. (2000) A trafficking checkpoint controls GABA(B) receptor heterodimerization. *Neuron*. **27**, 97–106
  30. Salahpour, A., Angers, S., Mercier, J.-F., Lagacé, M., Marullo, S., and Bouvier, M. (2004) Homodimerization of the beta2-adrenergic receptor as a prerequisite for cell surface targeting. *J. Biol. Chem.* **279**, 33390–33397
  31. Wu, G., Zhao, G., and He, Y. (2003) Distinct pathways for the trafficking of angiotensin II and adrenergic receptors from the endoplasmic reticulum to the cell surface: Rab1-independent transport of a G protein-coupled receptor. *J. Biol. Chem.* **278**, 47062–47069

32. Law, P.-Y., Erickson-Herbrandson, L. J., Zha, Q. Q., Solberg, J., Chu, J., Sarre, A., and Loh, H. H. (2005) Heterodimerization of mu- and delta-opioid receptors occurs at the cell surface only and requires receptor-G protein interactions. *J. Biol. Chem.* **280**, 11152–11164
33. Gendron, L., Cahill, C. M., Zastrow, von, M., Schiller, P. W., and Piñeyro, G. (2016) Molecular Pharmacology of  $\delta$ -Opioid Receptors. *Pharmacol. Rev.* **68**, 631–700
34. Cvejic, S., and Devi, L. A. (1997) Dimerization of the delta opioid receptor: implication for a role in receptor internalization. *J. Biol. Chem.* **272**, 26959–26964
35. Georgoussi, Z., Georganta, E.-M., and Milligan, G. (2012) The other side of opioid receptor signalling: regulation by protein-protein interaction. *Curr Drug Targets.* **13**, 80–102
36. Mittal, N., Roberts, K., Pal, K., Bentolila, L. A., Fultz, E., Minasyan, A., Cahill, C., Pradhan, A., Conner, D., DeFea, K., Evans, C., and Walwyn, W. (2013) Select G-protein-coupled receptors modulate agonist-induced signaling via a ROCK, LIMK, and  $\beta$ -arrestin 1 pathway. *CELREP.* **5**, 1010–1021
37. Hepler, J. R., Berman, D. M., Gilman, A. G., and Kozasa, T. (1997) RGS4 and GAIP are GTPase-activating proteins for Gq alpha and block activation of phospholipase C beta by gamma-thio-GTP-Gq alpha. *Proceedings of the National Academy of Sciences.* **94**, 428–432

## Chapter 5: TC10 GTP is Sufficient to Drive Constitutive Surface Trafficking of the $\delta$ -Opioid Receptor

Daniel J. Shiwarski<sup>1</sup>, Stephanie Crilly<sup>1</sup>, Marlena Darr<sup>1</sup>, Manojkumar A. Puthenveedu<sup>1</sup>

<sup>1</sup>Department of Biological Sciences, The Center for the Neural Basis of Cognition, Carnegie Mellon University, Pittsburgh, PA 15213, USA.

### Abstract:

Receptor trafficking and transport of proteins to the cell surface has been heavily studied; however, the role of post-ER receptor sorting and exocytic regulation has been assumed to be largely constitutive. Interestingly, trafficking of the  $\delta$ -Opioid receptor (DOR) proceeds through a novel phosphoinositide-regulated Golgi checkpoint and requires Class II PI3K  $\alpha$  activity for Golgi to surface transport. This trafficking checkpoint appears to be regulated in a neuronal cell-type specific manner. In neuronal culture and NGF-treated PC12 cells, DOR accumulates intracellularly as a result of NGF-induced PI3K C2A inhibition. Here, we demonstrate that following NGF-induced retention of DOR, constitutive activity of the Rho-associated GTPase TC10 is sufficient to drive DOR surface trafficking. Using live cell confocal fluorescence microscopy, we determined that acute NGF treatment in neuroendocrine PC12 cells is sufficient to redistribute TC10 to a perinuclear compartment similar to DOR Golgi retention. Additionally, PTEN inhibition released the NGF-retained pool of DOR and facilitates co-trafficking of DOR and TC10 to the cell surface. Biochemically, TC10 directly co-immunoprecipitates with DOR, and this interaction increases following PTEN inhibition induced co-trafficking to the cell surface. Finally, the TC10 effects on DOR trafficking are upstream of PI3K C2A regulated TGN export. These results reveal the first evidence for TC10 GTP activity stimulating trafficking of a GPCR from the Golgi. Additionally, these data reveal a new Golgi export mechanism for GPCR trafficking that requires activation of the TC10-PI3K C2A pathway.

**Introduction:**

For the  $\delta$ -Opioid receptor (DOR), an inhibitory  $G_i$ -coupled G-protein Receptor (GPCR), biosynthetic trafficking and surface availability have been shown to be highly regulated. Recently, our lab identified a phosphoinositide-regulated Golgi checkpoint that controls DOR's surface availability(1). Additionally, it was identified that following NGF-induced Golgi retention of DOR in neuronal cell lines, which exerts its retention effects through inhibition of PI3K, activation of PI 3-kinase Class II Alpha (PI3K C2A), or inhibition of Phosphatase and tensin homolog (PTEN) can stimulate DOR surface trafficking. Further, by driving DOR to the cell surface through PTEN inhibition, we can increase DOR agonist efficacy in a mouse model of chronic pain(1, 2). While these results emphasize the clinical potential for induced receptor surface trafficking, the mechanism by which NGF treatment in neuronal cells results in inhibition of PI3K C2A at the Golgi remains unclear.

While little work has been done to show regulation of GPCR surface trafficking by PI3K C2A, there is evidence to suggest that PI3K C2A can play an integral role in insulin-stimulated Glut4 receptor trafficking to the surface(3). Downstream of insulin signaling, PI3K C2A can be activated by the Rho family GTPase TC10(3). TC10 is a Rho GTPase with high similarity to Cdc42 and Rac1. Like many Rho-associated GTPases, TC10 is thought to act as a molecular switch to regulate a variety of processes from cytoskeletal rearrangements to cell cycle progression; however, it has many distinct and complex regulatory functions within the cell(4). In basal conditions, the activity of TC10 can be controlled by Guanine nucleotide exchange factors (GEFs), and GTPase activating proteins (GAPs). The most well studied GEF for TC10 is the Crk SH3-domain-binding guanine-nucleotide-releasing factor (C3G). Localization and expression of C3G can directly activate TC10; however, C3G's activity is not specific to TC10 and can associate with other Rho and Ras related GTPases to influence cell differentiation, cytoskeletal rearrangements, and vesicle trafficking(5).

In addition to regulation by GEFs and GAPs, TC10 activity can be controlled through binding interactions with other proteins. In GABAergic neurons, TC10 can act to relieve autoinhibition of the guanine nucleotide exchange factor collybistin to facilitate gephyrin clustering (6). In adipocytes, protein-protein interactions between TC10 and Caveolin 1 can act to inhibit the activity of TC10 until its activation following insulin signaling(7). These examples highlight the breadth of TC10 function; however, the most well studied area of TC10 activity is its role in vesicle trafficking and fusion. TC10 expression and function has been implicated in two main trafficking processes; general exocytic events, and insulin stimulated Glut4 receptor exocytosis. Its more general role has been described in the exocytic fusion of Rab11 vesicles resulting in expansion

of membranes during neurite outgrowth(8, 9).More specifically, TC10 has been shown to play an integral part in the Glut4 trafficking response following insulin signaling(3, 10). The mechanism downstream of insulin signaling is thought to require the recruitment of the GEF C3G to activate TC10, and the production of phosphatidylinositol-3-phosphate (PI3P). The result of both TC10 and subsequent PI3K C2A activation leads to the stimulation of Glut4 receptor trafficking to the cell surface(10-12). Although intracellular retention of DOR occurs at the *trans*-Golgi network, and intracellular Glut4 is thought to be held in post-Golgi storage granules, we hypothesized that TC10 activity might control a shared export pathway upstream of PI3K C2A (13).

In addition to its participation in insulin signaling and Glut4 exocytic trafficking, TC10 localization and activity has been shown to be important for NGF-induced neuronal cell differentiation. In the neuroendocrine PC12 cells, NGF treatment is widely used to study the mechanisms of neuronal cell differentiation, neurite formation, and neurite elongation. Specifically, the formation and process of neurite outgrowth following NGF treatment in PC12 cells has been shown to require TC10 GTP hydrolysis(8). To initiate neurite formation and elongation, TC10 must be recruited to the plasma membrane, and can even be synthesized locally to increase mRNA translation at distal neurite segments (8, 9). While significant work has been done to characterize TC10 activity following insulin signaling, and during neuronal differentiation, little has been done to determine TC10's role in GPCR receptor trafficking or trafficking from the Golgi in general. Based on the known regulation of TC10 by NGF, and the ability for TC10 to stimulate activity of PI3K C2A, we hypothesized that TC10 might play a role in the PI3K C2A dependent surface trafficking of DOR.

Our goal was to characterize the effects of acute NGF treatment on TC10 localization, and to determine if TC10 activity is sufficient to induce surface trafficking of Golgi-retained DOR. Using fixed and live cell confocal fluorescence microscopy, we determined that treatment with NGF in PC12 cells shifts TC10 localization from dispersed cytoplasmic vesicles to a diffuse perinuclear region. Interestingly, this shift in localization paralleled the NGF-induced Golgi retention of DOR in both location and timing. Subsequently, addition of a Phosphatase and tensin homolog (PTEN) inhibitor that is know to drive exocytic trafficking of DOR, promoted a binding interaction between DOR and TC10 and resulted in their co-trafficking to the surface(1). Finally, co-expression of DOR with the dominant-active TC10 Q75L was sufficient to prevent the NGF-induced Golgi retention upstream of PI3K C2A activity. These results demonstrate the first evidence of the Rho-associated GTPase TC10 activity stimulating trafficking of a GPCR from the Golgi. Additionally, these data reveal a new mechanism of GPCR exocytic trafficking requiring activation of the TC10-PI3K C2A pathway.

## Results:

### **NGF treatment in PC12 cells shifts TC10 to a perinuclear compartment overlapping with DOR Golgi retention**

Following NGF treatment in PC12 cells, DOR is retained within the trans-Golgi network (TGN) through inhibition of PI3K C2A activity (1, 2). Here, we wanted to determine how NGF treatment in PC12 cells decreased PI3K C2A activity to induce Golgi retention of DOR. It has been reported that activity of the Rho family GTPase TC10 can affect the activity of PI3K C2A; however, the exact role, if any, that TC10 plays in exocytic trafficking from the Golgi was unknown(3). Therefore, we wanted to determine if the GTPase TC10 was affected by NGF treatment. We hypothesized that if TC10 was participating in the Golgi retention or surface trafficking of DOR that NGF treatment might modulate TC10 localization. PC12 cells were transfected with an N-terminal signal sequence fluorogen-activated peptide (FAP)-tagged DOR and a GFP-TC10(2). The fluorescence properties of the FAP-DOR and GFP-TC10 allowed for live cell confocal fluorescence imaging of both proteins simultaneously to determine the effects on localization following NGF treatment. As expected FAP-DOR was primarily localized to the cell surface at baseline. The GFP-TC10 exhibited some membrane fluorescence and diffuse cytoplasmic punctate localization. Following the addition of NGF for 1 hour, a perinuclear pool of DOR, known to colocalize with the TGN, can be observed. Interestingly, the GFP-TC10 membrane fluorescence remains constant, while the cytoplasmic puncta are no longer observed. A broad perinuclear localization pattern for GFP-TC10 can be seen that partially overlaps with the FAP-DOR retention (Figure 1A).

To evaluate the shift in the GFP-TC10 localization pattern following NGF treatment, we performed time-lapse live cell fluorescence confocal imaging of PC12 cells expressing FAP-DOR and GFP-TC10. A baseline image was acquired to determine the pre-NGF localization patterns. NGF was then added, and the cells were imaged every minute for approximately 1 hour. A montage of FAP-DOR and GFP-TC10 shows the effects of NGF treatment on their localization over time. NGF-induced FAP-DOR retention is observed, and GFP-TC10 can be seen to follow the DOR retention localization. Interestingly, the GFP-TC10 puncta originally observed at baseline appear to migrate to the perinuclear region overlapping with FAP-DOR (Figure 1B, Supplemental Movie 1). Quantification was performed to determine the percentage of DOR retained in the Golgi region normalized to the total DOR fluorescence. As expected, NGF treatment resulted in an increase in DOR-Golgi localization for PC12 cells expressing FAP-DOR only. In cells expressing both FAP-DOR and GFP-TC10, NGF treatment also resulted in an increase in DOR-Golgi

localization (Figure 1C). A similar analysis was performed to determine the percentage of TC10 fluorescence that localized to the region defined by DOR Golgi retention normalized to the total GFP-TC10 fluorescence. In cells expressing both FAP-DOR and GFP-TC10, NGF treatment resulted in an increase in TC10-Golgi localization (Figure 1D).

In order to determine if DOR and TC10 were actually colocalizing to the same area following NGF treatment, we performed a fluorescence line scan analysis. For cells expressing FAP-DOR and GFP-TC10, a line was drawn and the fluorescence intensity was plotted to compare the fluorescence profiles for each protein. Prior to NGF treatment, the fluorescence intensity profile of FAP-DOR displays only peaks at the edges suggesting surface fluorescence localization. The fluorescence profile for GFP-TC10 has similar peaks at the edges overlapping with DOR at the cell surface, but also contained fluorescence peaks within the cytoplasmic space (Figure 1E). After NGF was added for 1 hour, dramatic changes in the fluorescence intensity profiles can be observed. The profile for FAP-DOR still displays peaks at the edges due to surface fluorescence, but now contains a large concentration of fluorescence within the cytoplasmic space due to DOR Golgi retention. Strikingly, the post-NGF fluorescence profile for GFP-TC10 still has strong peaks at the edges overlapping with DOR at the cell surface, but also shows concentrated fluorescence peaks within the cytoplasmic space overlapping with the retained DOR (Figure 1E). These data suggest that NGF treatment not only retains DOR within the TGN, but shifts the localization of TC10 from cytoplasmic puncta to a perinuclear region overlapping with retained DOR.

### **Following NGF-induced DOR retention, inhibition of PTEN is sufficient to drive co-trafficking of DOR and TC10 to the cell surface**

We know from our previous work, that PTEN inhibition can drive DOR to the cell surface following NGF treatment(1). Since NGF appears to alter the localization of TC10 in a similar manner to DOR retention, we next wanted to determine the effects of PTEN inhibition on TC10 localization. Using time-lapse live cell fluorescence confocal microscopy, we imaged PC12 cells expressing FAP-DOR and GFP-TC10 to determine the localization changes following NGF and PTEN inhibition. Imaging began at baseline no treatment conditions, followed by 1-hour treatment with NGF. Following NGF treatment and DOR Golgi retention, the PTEN inhibitor bpV(HOpic) was added. As expected PTEN inhibition decreased the Golgi pool of DOR, and increased DOR surface fluorescence. Interestingly, PTEN inhibition increased the surface fluorescence of TC10, and also appeared to increase the colocalization of DOR and TC10 within punctate structures over time (Figure 2A, Supplemental Movie 2). To quantify the change in surface fluorescence

intensity following PTEN inhibition, we measured the mean surface fluorescence intensity over time and normalized it to the initial surface fluorescence intensity. For both DOR and TC10, PTEN inhibition significantly increased the mean surface fluorescence intensity (Figure 2B).

An interesting observation following PTEN inhibition was the appearance of DOR and TC10 co-localizing vesicles that appeared to traffic from the retained pool towards the cell surface. In this example montage, a vesicle is observed to form that contains both DOR and TC10. Over the course of a few minutes, the DOR-TC10 positive vesicle structure migrates towards the surface and eventually results in a localized increased surface fluorescence intensity, suggestive of fusion (Figure 2C). To quantify and compare the changes in cell surface fluorescence intensity over time, we measured the mean cell surface fluorescence intensity after NGF, but before PTEN inhibition, and again following 1 hour of PTEN inhibition. For most cells, the surface fluorescence intensity of DOR increased following PTEN inhibition, and in every cell, the surface fluorescence intensity of TC10 increased (Figure 2D). Additionally, for both DOR and TC10, analysis of the percent change in surface fluorescence intensity following PTEN inhibition resulted in a significant increase in the mean surface fluorescence intensity compared to baseline (Figure 2E). These results suggest that following NGF treatment, PTEN inhibition is sufficient to drive surface trafficking of DOR and TC10.

### **TC10 co-immunoprecipitates with DOR**

Based upon our imaging experiments, DOR and TC10 appear to colocalize to a perinuclear region following NGF treatment (Figure 1), and subsequently increase their colocalization into vesicular structures following PTEN inhibition. Therefore, we next wanted to determine if DOR and TC10 were directly interacting with one another, and whether or not treatment with NGF or PTEN inhibition altered their interaction. We choose to perform immunoprecipitation experiments in PC12 cells expressing a signal sequence FLAG-tagged DOR and GFP-TC10. PC12 cells were transiently transfected with FLAG-DOR only, or FLAG-DOR and GFP-TC10. Cells were either untreated, NGF treated, or treated with NGF followed by the PTEN inhibitor bpV(HOptic). Immunoprecipitation was performed against FLAG-DOR to pull down the receptor and look for an interaction with GFP-TC10. For all conditions, Immunoblotting confirmed that FLAG-DOR was successfully immunoprecipitated (Figure 3A). Immunoblotting against GFP (GFP-TC10) resulted a specific band corresponding to GFP-TC10 in all treatment conditions in cells expressing the FLAG-DOR and GFP-TC10. Interestingly, NGF followed by PTEN inhibition appeared to increase the the amount of TC10 that immunoprecipitated with DOR (Figure 3A).

Supernatant samples from the immunoprecipitation were immunoblotted for FLAG-DOR and GFP-TC10 to confirm depletion of DOR from the lysate, and to determine the expression of GFP-TC10 for each sample (Figure 3B). Densitometry of each immunoblot was performed for multiple experimental replicates to confirm the effects of PTEN inhibition on increasing the DOR-TC10 interaction. Following normalization to the amount of DOR immunoprecipitated, and to the expression level of GFP-TC10 in each condition, treatment with NGF did not significantly alter the interaction between DOR and TC10; however, NGF followed by PTEN inhibition resulted in a greater than 2-fold increase in the interaction between DOR and TC10 (Figure 3C). These data reveal the first evidence that TC10 can biochemically interact with DOR, and that PTEN inhibition following NGF pre-treatment is sufficient to increase the co-immunoprecipitation of DOR and TC10.

**Dominant-active TC10 Q75L is sufficient to drive DOR surface trafficking in the presence of NGF treatment.**

Our data suggest that the localization of DOR and TC10 is influenced by NGF treatment; however, the role TC10 activity plays in DOR surface trafficking is unknown. To determine if TC10 activity can influence DOR trafficking in the presence of NGF, we utilized the dominant active (TC10 Q75L, GTP-bound) and dominant negative (TC10 T31N, cannot bind GTP) TC10 mutants(10, 14). Using live cell fluorescence confocal microscopy, we imaged PC12 cells expressing FAP-DOR and GFP-TC10 WT, Q75L, and T31N to determine the affects of TC10 mutants on DOR Golgi retention following NGF treatment. Imaging began at baseline no treatment conditions, followed by 1-hour treatment with NGF. As expected NGF treatment increased the Golgi pool of DOR when co-expressed with TC10 WT. Interestingly, NGF treatment did not result in a Golgi localized pool of DOR when co-expressed with the dominant active TC10 Q75L. When co-expressed with the dominant negative TC10 T31N, NGF treatment resulted in a similar increase in Golgi-localized DOR as observed for TC10 WT (Figure 4A).

To quantitate these observed effects, we first chose to evaluate the change in DOR and TC10 surface fluorescence following NGF treatment. In all conditions, FAP-DOR co-expressed with TC10 WT, Q75L, and T31N, there was no significant change in the DOR or TC10 surface fluorescence following treatment with NGF (Figure 4B). As expected, quantification of the percentage of DOR retained in the Golgi region normalized to the total DOR fluorescence following NGF treatment resulted in an increase in DOR-Golgi localization for PC12 cells expressing FAP-DOR and TC10 WT. In cells expressing FAP-DOR and TC10 Q75L, NGF treatment did not significantly increase DOR-Golgi localization (Figure 4C). In fact, there was a

significant decrease the the percentage of DOR retained in the Golgi region following NGF treatment when co-expressed with TC10 Q75L. For the cells expressing FAP-DOR and TC10 T31N, NGF treatment increased DOR-Golgi localization similar to the results obtained when co-expressed with TC10 WT (Figure 4C). Similar quantitation was performed to determine the percentage of TC10 fluorescence that localized to the region defined by DOR Golgi retention normalized to the total GFP-TC10 fluorescence. In cells expressing both FAP-DOR and TC10 WT, NGF treatment resulted in an increase in TC10-Golgi localization as observed previously (Figure 1D, 4D). In cells expressing FAP-DOR and TC10 Q75L, NGF treatment did not significantly increase TC10-Golgi localization (Figure 4D). For the cells expressing FAP-DOR and TC10 T31N, NGF treatment increased TC10-Golgi localization similar to the results obtained for TC10 WT (Figure 4D). Interestingly, the baseline TC10-Golgi localization was higher than for the TC10 WT or Q75L, but the difference was not statistically significant. Together, these results demonstrate that the dominant active TC10 Q75L is sufficient to prevent the NGF-induced Golgi retention of DOR.

#### **Dominant-active TC10 Q75L shows increased co-immunoprecipitation with DOR**

The dominant-active TC10 Q75L was sufficient to prevent the NGF-induced retention of DOR; however, the effect of the nucleotide bound to TC10 on the interaction with DOR was unknown. We choose to again perform co-immunoprecipitation experiments in PC12 cells expressing a signal sequence FLAG-tagged DOR and GFP-TC10 WT, Q75L, or T31N. All cells were NGF treated for 1 hour to mimic the imaging experiments. Immunoprecipitation against FLAG-DOR was performed to pulldown the receptor and look for an interaction with TC10. In all conditions, immunoblotting confirmed that FLAG-DOR was successfully immunoprecipitated (Figure S1A). Immunoblotting against GFP (GFP-TC10 WT, Q75L, T31N) resulted a specific band corresponding to GFP-TC10. Interestingly, compared to TC10 WT, the dominant-active TC10 Q75L showed an increased co-immunoprecipitation with DOR, and the dominant-negative exhibited decreased co-immunoprecipitation (Figure S1A).

The supernatant samples from the immunoprecipitations were run on an SDS-PAGE gel and immunoblotted for FLAG-DOR and GFP-TC10 to confirm depletion of DOR from the lysate, and to determine the expression of the GFP-TC10 WT, Q75L, and T31N for each sample (Figure S1B). Densitometry of each immunoblot was performed for multiple experimental replicates to confirm the affects of TC10 GTP activity on altering the DOR-TC10 interaction. Following normalization to the amount of DOR immunoprecipitated, and to the expression level of TC10 for each sample, the dominant-active TC10 Q75L increased the co-immunoprecipitation with DOR

following NGF treatment, and the dominant-negative TC10 decreased the co-immunoprecipitation between DOR and TC10 compared to TC10 WT (Figure S1C). These data show that following NGF treatment, GTP-bound active state of TC10 interacts more readily with DOR than WT or GDP-bound forms.

### **TC10 activity acts upstream of PI3K C2A in the NGF-induced Golgi retention of DOR**

Our data demonstrate that TC10 localization is altered following NGF treatment in PC12 cells, and that dominant-active TC10 GTP is sufficient to prevent the NGF-induced retention of DOR. Additionally, our previous data showed that downstream of NGF, PI3K Class II alpha inhibition (PI3K C2A) was required and sufficient for Golgi retention of DOR(2). There have been a few reports suggesting regulation of PI3Ks by TC10; however, it was unclear if the effects of TC10 activity were upstream or downstream of PI3K C2A inhibition in our system (3, 12). Since inhibition of PI3K C2A by the PI3K inhibitor LY294002 is sufficient to induce Golgi retention of DOR, we hypothesized that we could determine the requirement of TC10 activity for PI3K C2A-induced retention of DOR by utilizing the dominant-active TC10 Q75L mutant. Using fixed-cell fluorescence confocal microscopy, we imaged PC12 cells expressing FLAG-DOR and GFP-TC10 WT, Q75L, and T31N to determine the effects of TC10 mutants on DOR Golgi retention following PI3K inhibition. Cells were either untreated, or treated with the PI3K inhibitor LY294002 for 1 hour, followed by fixation, immunostaining, and confocal imaging. As expected, PI3K inhibition was sufficient to increase the Golgi pool of DOR when co-expressed with TC10 WT (Figure 5A). When co-expressed with TC10 Q75L or T31N, PI3K inhibition remained sufficient to induce the intracellular pool of DOR (Figure 5A).

Quantification to evaluate the change in the percentage of DOR retained in the Golgi region normalized to the total DOR fluorescence following PI3K inhibition resulted in an increase in DOR-Golgi localization for PC12 cells expressing FLAG-DOR and TC10 WT, Q75L, and T31N (Figure 5B). Similarly, quantification was performed to determine the percentage of cells in each condition that displayed Golgi-localized DOR. In cells expressing FLAG-DOR and either TC10 WT, Q75L, or T31N, PI3K inhibition was sufficient to increase the percentage of cells with an intracellular pool of DOR compared to the untreated control (Figure 5C). Additionally, there was no statistically significant difference between the percentage change from untreated to PI3K inhibition for all TC10 variants. Therefore, within the pathway regulating DOR Golgi retention and surface delivery, TC10 GTPase activity is likely upstream of PI3K C2A activity at the Golgi.

## Discussion:

Receptor trafficking and transport of proteins to the cell surface has been heavily researched in the past; however, the role of post-ER receptor sorting and exocytic regulation has been assumed to be largely constitutive. Interestingly, for the  $\delta$ -Opioid receptor (DOR), a novel phosphoinositide-regulated Golgi checkpoint has been identified that controls DOR's surface availability(1). Work from our lab showed that following NGF-induced Golgi retention of DOR in neuronal cell lines, activation of PI 3-kinase Class II Alpha (PI3K C2A) or inhibition of PTEN can stimulate DOR surface trafficking(1). By driving DOR to the surface of primary sensory neurons through PTEN inhibition, we can increase DOR agonist efficacy in a mouse model of hyperalgesia(1, 2). While these results emphasized the therapeutic potential following stimulated receptor surface trafficking, we did not understand the mechanism by which NGF treatment was inducing the Golgi retention of DOR upstream of PI3K C2A.

Here, our data demonstrate that the Rho-associated GTPase TC10, is a downstream effector following NGF treatment in PC12 cells, and that TC10 GTP is sufficient to prevent the NGF-induced retention of DOR. Specifically, we show that 1) acute NGF treatment is sufficient to redistribute the cellular localization pattern of TC10 to a perinuclear compartment similar to DOR Golgi retention, 2) Following the PTEN inhibition stimulated release of the NGF-retained pool of DOR, DOR and TC10 co-traffic to the cell surface, 3) TC10 directly co-immunoprecipitates with DOR, and this interaction increases following PTEN inhibition induced co-trafficking to the cell surface, 4) The dominant-active TC10 Q75L is sufficient to prevent the NGF-induced retention of DOR, 5) and that TC10 effects on DOR trafficking are upstream of PI3K C2A. These results reveal the first evidence for TC10 GTP activity stimulating trafficking of a GPCR from the Golgi. Additionally, this data reveals a new Golgi export mechanism for GPCR trafficking that requires activation of the TC10-PI3K C2A pathway.

In our study, the utilization of live cell fluorescence microscopy was essential to assess changes in TC10 localization following NGF treatment. Additionally, we were able to simultaneously visualize the dynamics of NGF-induced retention of DOR and its effects on TC10 localization in the same cells. This type of data acquisition allowed for in-depth determination of changes in TC10 and DOR co-localization through time. What was striking about the NGF-induced shift in TC10 distribution throughout the cell, was that cytoplasmic TC10 went from diffuse punctate structures to a more uniformly distributed perinuclear localization (Figure 1). While the NGF-induced perinuclear TC10 largely overlapped the known Golgi retention pattern for DOR, there was also an increase in TC10 fluorescence within the space defined by the Golgi

(1, 2, 15). One possibility is that the shift in TC10 to the perinuclear region defined by DOR Golgi retention represents an inactive or inhibited pool of TC10.

The question that then arises is, does NGF treatment in PC12 cells inhibit TC10 activity at the Golgi, and is the role of TC10 at the Golgi the same as at the cell surface? We know from previous reports that activation of tyrosine kinase receptors such as the Insulin receptor (agonist, Insulin), Epidermal Growth Factor receptor (agonist, EGF), and the TrkA receptor (agonist, NGF) can affect TC10 activity. In Insulin receptor signaling, the addition of Insulin has been shown to activate TC10 to drive the exocytosis of Glut4 storage vesicles (10, 11). Addition of EGF in HeLa cells was found to increase TC10 vesicle fusion events, and required TC10 GTP hydrolysis (16). Following EGF treatment and vesicle fusion, TC10 activity was observed to decrease at the cell surface. Similarly, a 24 hour NGF treatment in PC12 cells resulted in decreased TC10 activity at the cell surface along neurites compared to TC10 positive vesicular structures (8). All of these studies have focused on TC10's role in vesicle fusion at the cell membrane, and Glut4 vesicle release; however, a thorough examination of changes in activity at the Golgi were lacking. One previous report observed a change in basal perinuclear localization of TC10. They found that the dominant-negative TC10 T31N appeared to have a higher degree of perinuclear localized vesicles compared to the primarily membrane localized TC10 WT and dominant-active Q75L (16). From this observation they postulated that TC10 might play distinct roles in both initiation of vesicle trafficking from a perinuclear compartment, and vesicle fusion at the plasma membrane.

Our data suggests that TC10 does play a direct role in receptor trafficking and export from the Golgi, distinct from its role at the cell surface. Through simultaneous imaging of DOR and TC10 we directly show that NGF treatment in PC12 cells shifts the localization of wild-type TC10 to a perinuclear compartment (Figure 1). Further, by demonstrating that expression of the dominant-active TC10 Q75L is sufficient to prevent the NGF-induced Golgi retention of DOR and the perinuclear localization of TC10, our results highlight the requirement for inhibition of TC10 activity downstream of NGF-induced DOR retention (Figure 4). Since TC10 GTP is sufficient to promote Golgi export of DOR in the presence of NGF, TC10-dependent exocytosis from the Golgi is likely to be independent of TC10 GTP hydrolysis. If hydrolysis is required, endogenous TC10 activity might be sufficient in combination with the TC10 Q75L dominant-active mutant. Additionally, our data demonstrating PTEN inhibition induced surface trafficking of retained DOR and TC10 suggests the requirement of downstream exocytic regulation from PI3K C2A (Figure 2). Further, dominant active TC10 Q75L is not sufficient to prevent the PI3K inhibition induced retention of DOR (Figure 5). These data, in conjunction with our published data showing the requirement and sufficiency for PI3K C2A to drive DOR surface trafficking, and based upon the

ability for TC10 to stimulate the activity of PI3K C2A downstream of insulin signaling, begin to construct a mechanistic picture for the role of TC10 and PI3K C2A in the regulated delivery of DOR to the cell surface (2, 3).

There are, however, several questions that remain: How specific is this mechanism to DOR? What events are causing a shift in TC10 localization? Additional work from our lab suggests that a dual C-terminal RXR ER retention/retrieval motif is required for the NGF-induced Golgi retention of DOR(15). It will be interesting to determine the role of these RXR motifs in TC10 stimulated export of DOR, and if other GPCRs known to contain similar C-terminal sequences are trafficked to the surface through a TC10-PI3K C2A dependent pathway. Future work to address the mechanism driving the shift in TC10 localization will focus on known GEFs, GAPs, and binding partners for TC10. It is well known that the localization of a GEF is sufficient to recruit and activate Rho GTPases; therefore, if NGF is altering the localization of a TC10 GEF such as C3G, it could have dramatic effects on TC10 localization. Alternatively, NGF treatment could stimulate the recruitment or activity of a TC10 GAP such as the TCGAP or p50RhoGAP (4, 8, 17). Recruitment of a TGN GAP to the TGN would stimulate local GTP hydrolysis of TC10 and push it towards an inactive state.

Another possible mechanism that could explain a shift in TC10 localization to the TGN and regulate receptor trafficking is its protein-protein interaction with Protein interacting specifically with TC10 (PIST). PIST, a TGN resident protein, contains a PDZ-domain, two coiled-coil domains, and a leucine zipper region. Biochemically, PIST has been shown to interact directly with TC10 GTP, and is specific to TC10, showing low affinity towards other Rho associated GTPases(18). PIST is thought to undergo retrograde transport from the TGN by interacting with Rab6 membranes through its coiled-coil domains(19). Additionally, a protein-protein interaction between the PDZ domain of PIST and the PDZ ligand of the Somatostatin Receptor 5 (SSTR5) and the  $\beta$ -1 Adrenergic receptor (B1AR) has been shown to be required for post-endocytic and biosynthetic TGN retention of these receptors in the presence of PIST overexpression(20, 21). Interestingly, competition in binding between the PDZ ligand of B1AR with PIST can relieve the TGN retention and allow trafficking to the surface(22). Although DOR does not contain a C-terminal PDZ ligand like SSTR5 or B1AR, it will be interesting to investigate the role, if any, that PIST plays in the NGF-induced Golgi retention of DOR. Likewise, evaluation of NGF-induced Golgi retention for SSTR5 and B1AR, and the mechanistic dependence on TC10 and PI3K C2A activity will provide further insight into the specificity and receptor sequence requirement for this regulated TC10-PI3K C2A TGN export pathway.

In conclusion, this manuscript identifies a novel requirement for TC10 GTP activity in the PI3K C2A dependent phosphoinositide-regulated Golgi checkpoint of DOR. Following NGF treatment in PC12 cells, TC10 distribution shifts to a perinuclear region overlapping with the Golgi that resembles the localization pattern for the inactive TC10 T31N mutant. Additionally, we show the first evidence of TC10 binding directly to a GPCR, and stimulation of this interaction following PTEN inhibition induced surface trafficking of DOR. We propose that TC10 GTP is acting to facilitate the TGN export of DOR by promoting the recruitment and activation of PI3K C2A to coordinate association of downstream trafficking components. In future work, we hope to investigate the role of TC10 in TGN export of other GPCRs and receptors, as well as identify the regulatory machinery downstream of NGF controlling TC10 localization and activity at the Golgi.

**Acknowledgements:**

The authors would like to thank Zara Weinberg, Elena Shuvaeva, and Dr. Cary Shiwarski for technical help and comments. We thank Drs. Nathan Urban, Adam Linstedt, Tina Lee, Peter Friedman, Guillermo Romero, Jean-Pierre Vilardaga, and Alessandro Bisello, for reagents, comments and suggestions. M.A.P. was supported by NIH DA024698 and DA036086.

## **Materials and Methods:**

### **Cell Lines and Cell Culture**

Pheochromocytoma-12 (PC12, #CRL-1721) cells were used in all experiments. These cells are neuroendocrine in origin, and were originally isolated from rat adrenal medulla tissue. All cells were grown tissue culture incubators at 37°C with 5% CO<sub>2</sub> and cultured in F12K medium (Gibco by Life Technologies 21127-022) supplemented with 10% horse serum and 5% fetal bovine serum (FBS). The media was changed every third day to maintain a constant nutrient supply, and promote cell health. All tissue culture vessels and plates were coated with collagen IV (Sigma #C5533-5MG) to promote PC12 cell adherence and growth. Standard passage procedures were performed using a split ratio of 1:4 to ensure sufficient cell density to facilitate growth.

### **DNA Transfection of Cultured Cells:**

For all transfections performed, PC12 cells were plated in collagen IV coated 6-well plates and grown in F12K media containing 10% horse serum and 5% fetal bovine serum for 24 hours before transfection. Lipofectamine 2000 lipofection reagent (Invitrogen 11668-019) was used to transiently transfect PC12 cells with DOR and TC10 following the manufacturers recommendations. Briefly, Opti-MEM (100 uL) was added to two 1.7mL microcentrifuge tubes, Lipofectamine 2000 (7.5 uL) (Invitrogen 11668-019) and the appropriate plasmid DNA (1.5 ug for DOR and 2ug for TC10) were added to the Opti-MEM containing 1.7mL microcentrifuge tubes and incubated at room temperature for 5 minutes. The DNA containing solution was then added the Lipofectamine 2000 containing solution, mixed, and incubated for 20 minutes at room temperature. Growth medium was removed and replaced with 1 mL of Opti-MEM for each well. The complete transfection mixture was added dropwise to each well in the 6-well plate. For all transfections, the cells were incubated with the transfection mixture for 5 hours at 37°C. The transfection solution was aspirated from each well and replaced with 2 mL of full serum F12K medium. For immunoprecipitations, live, and fixed-cell imaging, experiments were conducted 48-72 hours following transfection.

### **DNA plasmids and Mutagenesis:**

For live cell imaging, a wild-type DOR construct was used consisting of DOR N-terminally tagged with a signal sequence followed by a fluorogen-activated peptide (FAP) in the pcDNA3.1 vector(2). For fixed cell imaging, a wild-type DOR construct N-terminally tagged with a signal

sequence FLAG-tag (SSF-DOR) in pcDNA3.1 was used. The wild-type GFP-TC10 was a gift from Channing Der (Addgene plasmid # 23232) (23). To create the dominant-active (Q75L) and dominant-negative (T31N) TC10 mutants we performed QuickChange mutagenesis on the GFP-TC10 construct. Construction of both mutants were performed using a modified QuickChange PCR protocol and confirmed via DNA sequencing. Primer design for the mutants was performed using the QuickChange Primer Design Tool from Agilent Technologies. Briefly, the reaction took place as follows: GFP-TC10 wild-type template (50 ng, 1 uL), Top Primer (125 ng, 1 uL), Bottom Primer (125ng, 1 uL), were mixed with 10x Pfu Turbo Reaction Buffer (5 uL), dNTP Mix (1 uL), PfuTurbo (1 uL), and H<sub>2</sub>O to 30 uL. The PCR reaction was: Step 1: 95°C for 2 min, Step 2: 95°C for 30 sec, 55°C for 1 min, 68°C for 14 min, repeated for 18 cycles, Step 3: 72°C for 15min, Step 4: 4°C hold. Following the PCR reaction, a DpnI digest was performed for 1 hour followed by bacterial transformation in DH5α cells.

#### Live Cell Imaging with FAP-DOR and GFP-TC10

PC12 cells were grown to approximately 50% confluency then transfected with a N-terminal fluorogen-activated peptide (FAP)-DOR and GFP-TC10 using the Lipofectamine 2000. Similar procedure was performed for the GFP-TC10 Q75L and T31N. Two days post transfection, cells were plated on 25 mm poly-D lysine- coated coverslips (Electron Microscopy Sciences Micro Coverglass # 1 ½, #72225-01). The FAP-DOR has a far-red emission spectra, resulting from a malachite green (MG)-based fluorogen (24, 25), which can be visualized via fluorescent microscopy. Fifteen minutes prior to imaging, the cell permeable MG-ester based fluorogen (100nM) was added to the cells. Live confocal imaging of FAP-DOR and GFP-TC10 was performed at 37°C using a Nikon TE-2000 inverted microscope. Specifically, the imaging set-up consisted of live cell temperature and humidity controlled imaging capabilities, a mechanical Piezo XYZ-stage (Nikon), iXon 897 Ultra back-illuminated camera (Andor), a laser combiner (Andor) containing 405, 488, 515, 568, and 647nm excitation capabilities, a Dell 5400 Workstation optimized for IQ2 imaging software (Andor), and an active isolation air table (TMC). For most experiments, Nerve Growth Factor (NGF, 100ng/mL) was added to cells at the beginning of imaging. FAP-DOR and GFP-TC10 localization were quantified using Image J software to determine effects of NGF on DOR and TC10 localization, as well as the ratio of Golgi DOR and TC10 fluorescence compared to the total fluorescence signal.

## Line Scan Analysis

A line scan analysis was used to confirm colocalization and visualize localization shifts for DOR and TC10 following NGF treatment in PC12 cells. Using Image J software, the fluorescence intensity was measured over a line that passed through the cell to calculate the relative spatiotemporal fluorescence intensity over a pixel (px) area. Line plots before and after NGF for both DOR and TC10 fluorescence were compared and plotted as a percentage of maximum fluorescence across the line for each channel. Colocalization and fluorescence distribution was assessed by visualizing overlapping peaks of fluorescence along the length of the line normalized to the maximal fluorescence intensity in each channel. The data was plotted using Graph Pad Prism 5 software.

## Surface Fluorescence Analysis:

For live cell imaging experiments, the surface fluorescence intensity for FAP-DOR and GFP-TC10 was measured over time using Image J software. The mean fluorescence surface intensity was then plotted over time following treatment with NGF. Alternatively, surface fluorescence intensity measurements were collected before and after the addition of NGF, or following the addition of the PTEN inhibitor bpV(HOpic) to quantitatively measure induced surface trafficking over a population of cells. Data analysis and graphical representation was performed using Graph Pad Prism 5 software.

## Immunoprecipitation, Immunoblotting, and Densitometry:

PC12 cells were plated onto 10cm Collagen IV coated dishes and transfected with either FLAG-tagged DOR only, or FLAG-DOR and GFP-TC10 WT, Q75L, or T31N. 48 hours after transfection, NGF (100ng/mL) was added to cell when appropriate. Similarly, in conditions where PTEN inhibition was used. The PTEN inhibitor bpV(HOpic) was added to cells for 45min after NGF addition. Following completion of all treatments, the cells were placed on ice and growth media was removed and rinsed with 1 mL phosphor buffered saline (PBS). 500 uL of PBS was added to each dish and the cells were scraped collected and transferred to 1.7 mL tubes. Cells were pelleted at 1200 x g for 5 minutes.

Supernatant was aspirated and the pellet was resuspended in 30-75 uL of lysis buffer containing 2% SDS, 60 mM Tris-HCL pH 6.8 with Complete Mini EDTA-free (Roche T00004) and PhosStop Tab (Roche A00173). Cells were lysed by vortexing for 15 seconds followed by 2 minutes in a 95°C heat block, then pipetting up and down 3-5 times. This lysis process was performed twice. BCA protein estimation (Pierce BCA Assay KIT, Thermo Fisher, #23225) was

performed. For each condition, 40  $\mu$ L samples were prepared from the lysates such that protein content and volume was standardized. 10  $\mu$ L of 4X loading dye and fresh BME and 1  $\mu$ L of 1M DTT were added to the samples.

To denature the proteins, samples were heated to 95°C for 5 minutes and ran on a 4–15% Mini-PROTEAN® TGX Stain-Free™ Protein Gels (BioRad #4568083). An overnight transfer at 4°C to a nitrocellulose membrane was performed. Following transfer, the blot was blocked with 5% milk-TBST for one hour on a shaker. Primary rabbit anti-GFP antibody against GFP-TC10 (Cell Signaling GFP (D5.1) XP® Rabbit mAb #2956) was prepared at 1:1000 in 5% milk-TBST and added to the blot. The blot was placed on a shaker and incubated overnight in cold room. The primary antibody solution was removed and the blot was washed 3X for 5 minutes with 5% milk-TBST. The secondary antibody Goat anti-Rabbit (BioRad #1706515) was prepared at 1:3000 in 5% milk-TBST and added to the blot for incubation on a shaker at room temperature for 1 hour. The secondary antibody solution was removed and the blot was washed 2X for 5 min with TBST and once for 5 minutes with TBS. The blot was developed with Clarity™ Western ECL Substrate (BioRad #1705061) and imaged using the ChemiDoc Touch imaging system (BioRad). To visualize effective immunoprecipitation and expression of DOR, Restore Western Blot Stripping buffer (ThermoFisher Scientific #21059) was used for 30min at room temperature. Following two washes with TBST, the blot was re-block in 5% milk-TBST for 1 hour followed by incubation with primary rabbit anti-FLAG tag antibody against FLAG-DOR for 3 hours at room temperature. Identical procedure as used for developing GFP-TC10 was performed.

Densitometry was performed using the built-in Image J plugin to quantify the band intensity in each lane. To account for variations in DOR and TC10 expression between samples, all lanes were normalized to the their GFP-TC10 expression in the supernatant followed by normalization to the quantified FLAG-DOR detected for each immunoprecipitation sample. Values were then plotted using GraphPad Prism 5 software.

#### Fixed Cell Immunofluorescence

PC12 cells were transfected with SSF-DOR and GFP-TC10 WT, Q75L, or T31N. 48 hours after transfection, cells were plated onto coverslips (Corning) coated with poly-D-lysine (Sigma, #P7280) and grown at 37°C for 24 hours. Following treatments (untreated, or 10  $\mu$ M LY294002 for 1 hour), cells were fixed in 4% paraformaldehyde, pH 7.4. The coverslips were blocked with calcium magnesium containing PBS with 5% fetal bovine serum, 5% 1M glycine, and 0.75% Triton X-100. Primary antibodies against FLAG-tagged DOR and the *trans*-Golgi network were labeled for one hour in blocking buffer with: anti-FLAG M1 antibody (Sigma, #F3040) (1:1000)

conjugated with Alexa-647 (Molecular Probes, #A20186), and anti-TGN-38 rabbit polyclonal antibody (1:2000, Sigma-Aldrich cat#: T9826), respectively. Coverslips were washed 3 times in calcium magnesium PBS then labeled with Alexa-568 Goat anti-rabbit secondary (1:1000, #A11011) antibody in blocking buffer for 1 hour. Cover slips were washed 3 more times in calcium magnesium PBS and mounted onto glass slides using Prolong Diamond Reagent (Molecular Probes, #P36962). Confocal imaging was performed using a XDi spinning disk system (Andor) at 60X magnification (Nikon CFI APO TIRF) on a Nikon TE-2000 inverted microscope. Images of representative fields were taken. Quantification of the fluorescence intensity for each channel was measured and averaged to ensure results were representative of the population. A minimum of three biological replicates were performed to confirm the results. Detailed fluorescence analysis procedure can be found in our previous publication(1).

#### Inhibitors and Activators

Compound Name	Protein Target	Concentration	Supplier	Catalog #
Nerve Growth Factor	TrkA	100 ng/ $\mu$ L	BD Biosciences	356004
LY294002	PI3K inhibitor	10 $\mu$ M	Tocris Bioscience	1130
bpV(HOpic)	PTEN inhibitor	10 $\mu$ M	Enzo Life Sciences	ALX-270-206

#### Image Analysis and Quantification

All imaging data was quantified using Image J. This software was used to measure the total DOR fluorescence for each cell and the fluorescence intensity of DOR within the Golgi for fixed and live cell analysis. The values measured using Image J were transferred to Microsoft Excel to calculate the ratio of the Golgi fluorescence to the total cell fluorescence. This ratio was calculated for each cell and all cell ratios were averaged. The average represents the fraction of DOR present in the Golgi compared to the total cell fluorescence. Additionally, a manual binary quantification was performed to determine the percentage of cells that visually displayed Golgi-localized DOR. Based on visual inspection, each cell that had at least half of its DOR present in the Golgi is scored as a 1 and cells which have little or no DOR in the Golgi are scored as a 0. The average of the binary quantification was used to determine the percentage of cells with Golgi-localized DOR.

#### Statistics and Data Analysis

Statistical analyses were performed using GraphPad Prism 5 software, and the appropriate statistical tests were chosen based on sample size, distribution, and experimental

conditions. A minimum of three independent experiments were performed for each set of data. For statistical analysis of the fixed and live cell immunofluorescence imaging data, two-tailed unpaired t-tests were performed between the different experimental conditions and controls. A p-value of  $< 0.05$  was considered statistically significant. All images were quantified using macros constructed from the functions within Image J software package. Figures were constructed with Image J and Adobe Photoshop CS6.

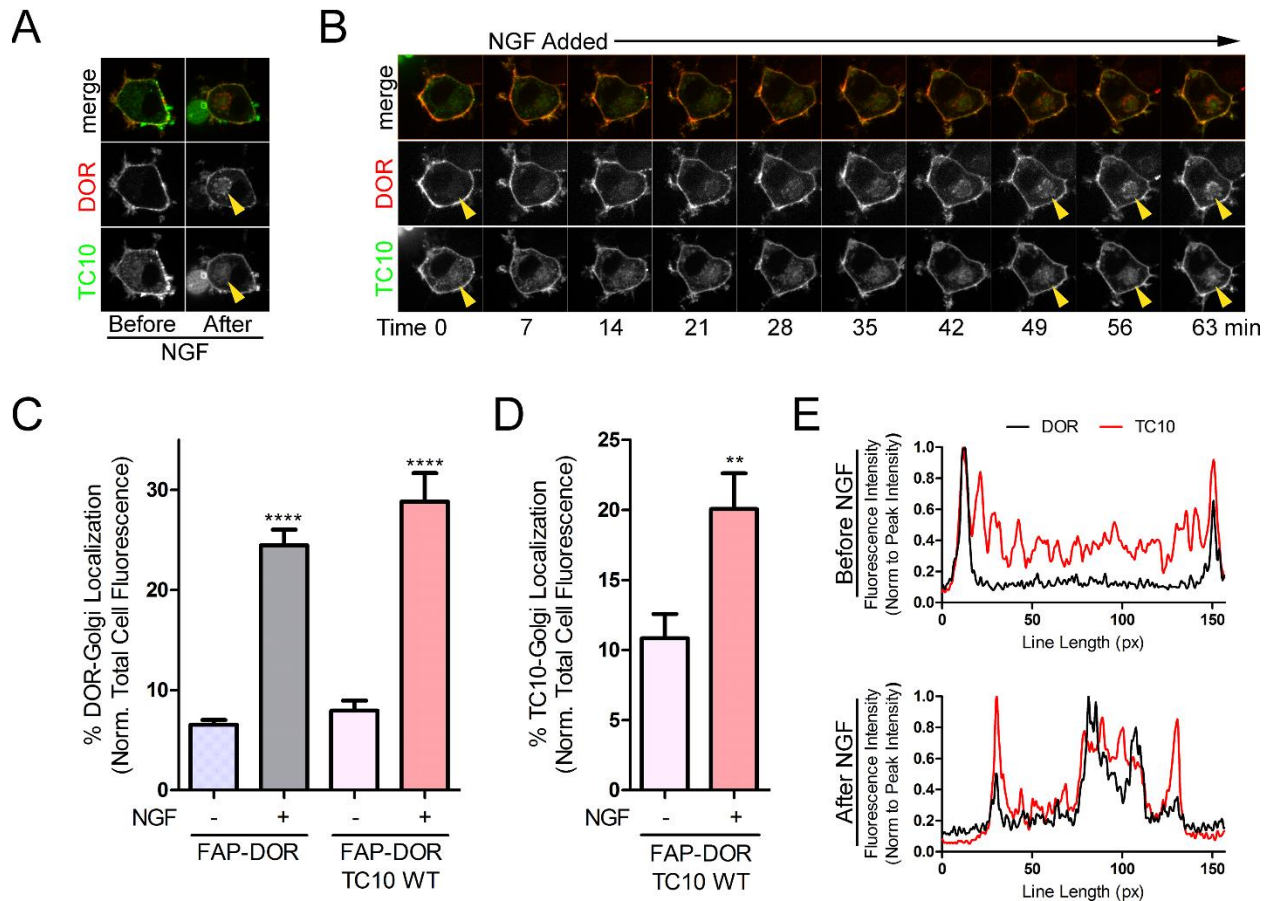


**Figure 1: DOR and TC10 co-localize following NGF treatment.** **A.** In PC12 cells transfected with FAP-DOR (Red) and GFP-TC10 (Green) and imaged via confocal fluorescence microscopy, Nerve Growth Factor (NGF) treatment (100ng/mL) for 1 hour results in intracellular retention of DOR (yellow arrow), and a redistribution of GFP-TC10 to the region of DOR retention (yellow arrow). **B.** Example live cell confocal fluorescence microscopy of cells expressing FAP-DOR (Red) and GFP-TC10 (Green) show the intracellular retention of DOR (yellow arrow), and a redistribution of GFP-TC10 to the region of DOR retention (yellow arrow) over the course of 1 hour following NGF treatment (100ng/mL). **C.** Quantification of the percentage of DOR retained in the Golgi region normalized to the total DOR fluorescence reveal an increase in DOR-Golgi localization following NGF treatment (Before NGF (-), After 1 hour NGF (+)) for PC12 cells expressing FAP-DOR only and FAP-DOR + GFP-TC10 (TC10 WT) (FAP-DOR NGF (-),  $n=16$  cells; FAP-DOR NGF (+),  $n=16$  cells; FAP-DOR TC10 WT NGF (-),  $n=18$  cells; FAP-DOR TC10 WT NGF (+),  $n=18$  cells; mean  $\pm$  s.e.m.; \*\*\*\* $P<0.0001$ ; by two-sided paired t-test vs. FAP-DOR WT NGF (-)). **D.** Similarly, the percentage of TC10 fluorescence that localized to the region defined by DOR Golgi retention normalized to the total GFP-TC10 fluorescence revealed an increase in TC10-Golgi localization following NGF treatment (FAP-DOR TC10 WT NGF (-),  $n=17$

cells; FAP-DOR TC10 WT NGF (+),  $n=17$  cells; mean  $\pm$  s.e.m.;  $**P=0.0019$ ; by two-sided paired t-test vs. FAP-DOR WT NGF (-)). **E.** Analysis of colocalization for the example images in panel B for FAP-DOR and GFP-TC10 was performed via a line scan plot to identify relative spatiotemporal fluorescence intensity over a pixel (px) area. Before NGF treatment (Time = 0 min), the fluorescence intensity profile of FAP-DOR (DOR, Black) shows two peaks at the edges due to surface fluorescence. The GFP-TC10 (TC10, Red) fluorescence profile has peaks at the edges overlapping with DOR at the cell surface, but also exhibits fluorescence peaks within the cytoplasmic space. Following NGF treatment (Time = 60 min), the fluorescence intensity profile of FAP-DOR (DOR, Black) shows two peaks at the edges due to surface fluorescence, and a large concentration of fluorescence within the cytoplasmic space for DOR Golgi retention. The GFP-TC10 (TC10, Red) fluorescence profile has strong peaks at the edges overlapping with DOR at the cell surface, but also exhibits concentrated fluorescence peaks within the cytoplasmic space overlapping with the retained DOR.

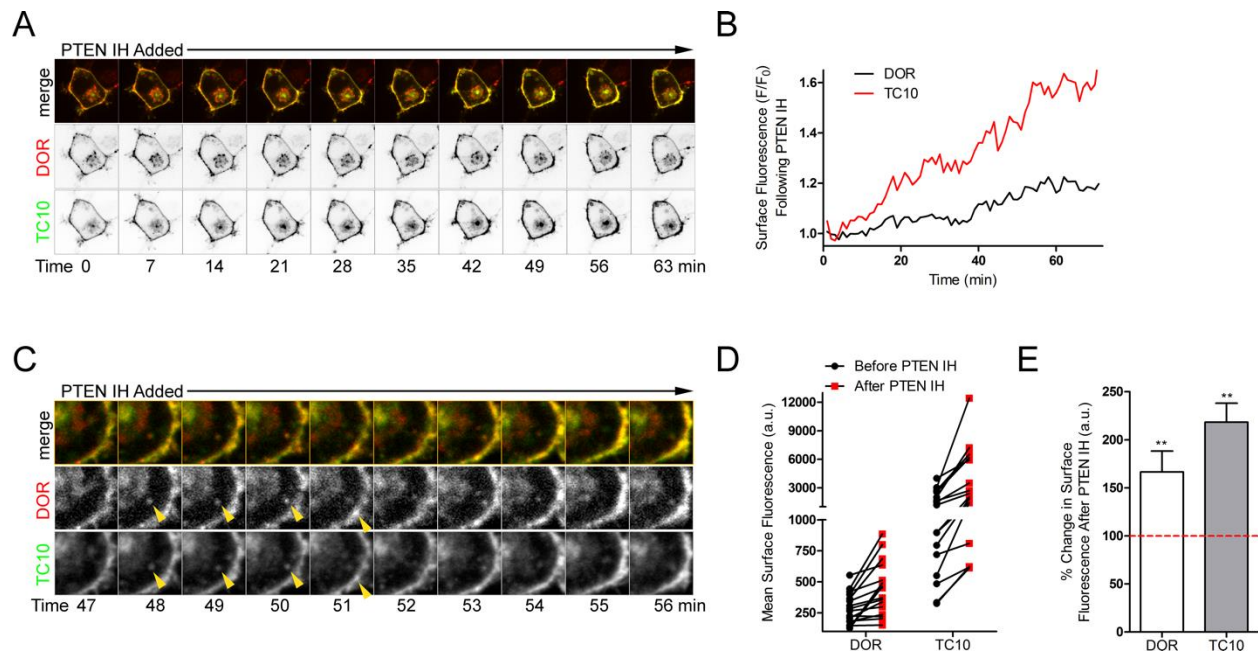


**Figure 2: Following NGF treatment, PTEN inhibition drives DOR and TC10 trafficking to the cell surface.** **A.** After 1 hour of NGF treatment (100ng/mL), the PTEN inhibitor (bpV(HOpic), 10 $\mu$ M) was added to PC12 cells expressing FAP-DOR (Red) and GFP-TC10 (Green). Example live cell confocal fluorescence imaging demonstrates that the retained internal pool of DOR decreases following PTEN inhibition, and the fluorescence intensity of the surface pool increases. The surface fluorescence intensity for TC10 also increases following PTEN inhibition. Additionally, increased surface colocalization (yellow signal in merged channels) between DOR and TC10 is observed following addition of the PTEN inhibitor. **B.** The mean surface fluorescence intensity over time for the experiment in A, was quantified and normalized to the initial surface fluorescence intensity prior to PTEN inhibition ( $F/F_0$ ) for both DOR and TC10. Following PTEN inhibition, both DOR and TC10 surface fluorescence intensity increases above baseline. **C.** Example time-series images show small vesicular structures budding off of the retained DOR compartment and traveling to the cell surface (yellow arrows) following PTEN inhibition. **D.** Quantification of the mean surface fluorescence before and after PTEN inhibition for each cell reveals a significant increasing trend for both DOR and TC10 (DOR,  $n=16$  cells; TC10,  $n=16$  cells; mean  $\pm$  s.e.m.;  $P=0.0012$ ; by two-way RM ANOVA). **E.** There is also a significant increase in the percent change in surface fluorescence after PTEN inhibition for DOR and TC10 compared to baseline surface fluorescence (red dashed line) (DOR,  $n=16$  cells; TC10,  $n=16$  cells; mean  $\pm$  s.e.m.;  $**P<0.01$ ; by two-sided paired t-test vs. DOR or TC10 before PTEN inhibition).

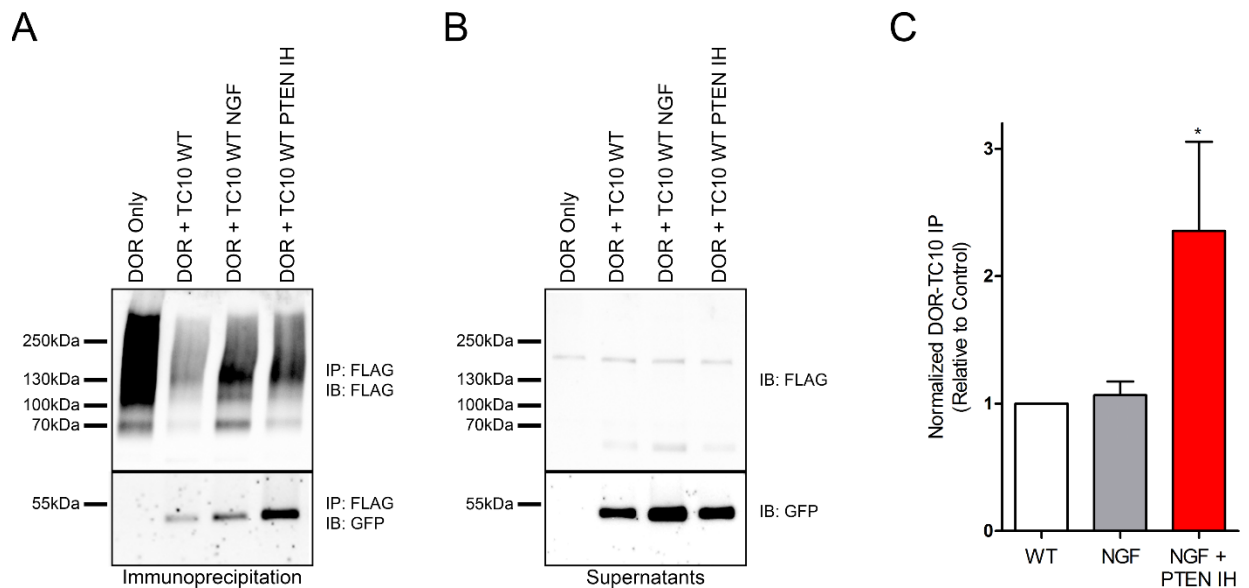


**Figure 3: TC10 co-immunoprecipitates with DOR, and PTEN inhibition increases their interaction.** **A.** PC12 cells expressing FLAG-DOR, or FLAG-DOR and GFP-TC10 were untreated (DOR only, and DOR + TC10 WT), treated with NGF (100ng/mL) for 1 hour (DOR + TC10 WT NGF), or treated with NGF for 1 hour followed by 45 minutes of treatment with a PTEN inhibitor (bpV(HOpic), 10 $\mu$ M) (DOR + TC10 WT PTEN IH). FLAG-DOR was immunoprecipitated (IP) and immunoblots (IB) were performed to detect the FLAG-DOR and GFP-TC10. FLAG-DOR was expressed and detectable in each treatment group of the immunoprecipitation samples (IP: FLAG, IB: FLAG) as a smear between 200 and 70 kDa. The immunoblot for GFP-TC10 (IP: FLAG, IB: GFP) revealed an increased co-immunoprecipitation of TC10 with DOR following NGF and PTEN inhibition (DOR + TC10 WT PTEN IH). **B.** Examination of the supernatant controls reveal depletion of FLAG-DOR from the supernatant (IB: FLAG), and relative expression levels of the GFP-TC10 (IB: GFP) for each condition. **C.** Quantification via densitometry was performed to determine the change in co-immunoprecipitation of TC10 with DOR following NGF and PTEN inhibition. Following normalization to FLAG-DOR and GFP-TC10 expression for each condition, a normalized DOR-TC10 Co-IP ratio revealed a small increase in TC10 Co-IP with DOR following NGF (NGF), and a large significant increase after NGF + PTEN inhibition (NGF + PTEN) (WT,  $n=4$ ; NGF,  $n=3$ ; NGF + PTEN IH,  $n=3$ ; mean  $\pm$  s.e.m.; \* $P<0.05$ ; by two-sided Mann-Whitney test vs. DOR TC10 WT (WT)).

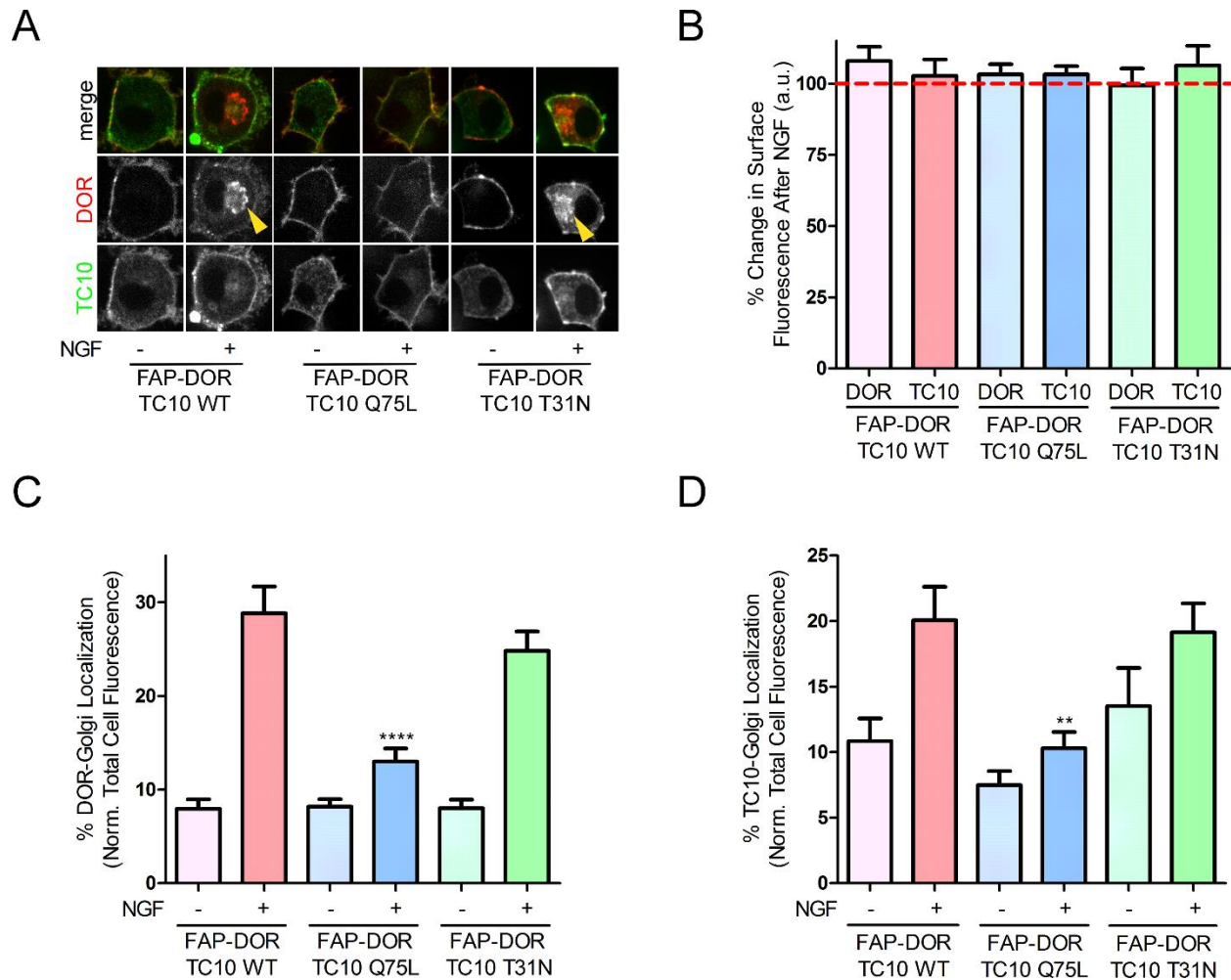


**Figure 4: The dominant-active TC10 Q75L is sufficient for DOR surface trafficking in the presence of NGF treatment. A.** Example live cell confocal fluorescence images for PC12 cells expressing FAP-DOR (Red) and GFP-TC10 (Green), GFP-TC10 Q75L (dominant active mutant), or GFP-TC10 T31N (dominant negative mutant), untreated (-) or treated for 1 hour with with NGF (100ng/ml) (+). NGF-induced Intracellular retention of DOR (yellow arrow) is observed when coexpressed with GFP-TC10 WT and GFP-TC10 T31N, but not GFP-TC10 Q75L. **B.** Quantification of the percent change in surface fluorescence for DOR and TC10 before and after NGF treatment resulted in no significant changes (FAP-DOR + TC10 WT, DOR,  $n=18$  cells; FAP-DOR + TC10 WT, TC10,  $n=18$  cells; FAP-DOR + TC10 Q75L, DOR,  $n=17$  cells; FAP-DOR + TC10 Q75L, TC10,  $n=17$  cells; FAP-DOR + TC10 T31N, DOR,  $n=19$  cells; FAP-DOR + TC10 T31N, TC10,  $n=19$  cells; mean  $\pm$  s.e.m.; \* $P<0.05$ ; by two-sided Wilcoxon matched-pairs signed rank test vs. DOR or TC10 before NGF). **C.** Quantification of the percentage of DOR retained in the Golgi normalized to the total DOR fluorescence reveal a significant increase in DOR-Golgi localization following NGF treatment (Before NGF (-), After 1 hour NGF (+)) for PC12 cells

expressing FAP-DOR + GFP-TC10 (TC10 WT) and FAP-DOR + GFP-TC10 T31N, but not for cells expressing FAP-DOR + GFP-TC10 Q75L. Cells expressing FAP-DOR + GFP-TC10 Q75L had significantly decreased DOR-Golgi localization following NGF treatment compared to TC10 WT expressing cells (FAP-DOR TC10 WT NGF (-),  $n=18$  cells; FAP-DOR TC10 WT NGF (+),  $n=18$  cells; FAP-DOR TC10 Q75L NGF (-),  $n=14$  cells; FAP-DOR TC10 Q75L NGF (+),  $n=14$  cells; FAP-DOR TC10 T31N NGF (-),  $n=17$  cells; FAP-DOR TC10 T31N NGF (+),  $n=17$  cells; mean  $\pm$  s.e.m.; \*\*\*\* $P<0.0001$ ; by two-sided t-test vs. FAP-DOR TC10 WT NGF (+)). **D.** Similarly, the percentage of TC10 fluorescence that localized to the region defined by DOR Golgi retention normalized to the total GFP-TC10 fluorescence revealed an increase in TC10-Golgi localization following NGF treatment for PC12 cells expressing FAP-DOR + GFP-TC10 (TC10 WT) and FAP-DOR + GFP-TC10 T31N, but not for cells expressing FAP-DOR + GFP-TC10 Q75L. Cells expressing FAP-DOR + GFP-TC10 Q75L had significantly decreased TC10-Golgi localization following NGF treatment compared to TC10 WT expressing cells (FAP-DOR TC10 WT NGF (-),  $n=18$  cells; FAP-DOR TC10 WT NGF (+),  $n=18$  cells; FAP-DOR TC10 Q75L NGF (-),  $n=14$  cells; FAP-DOR TC10 Q75L NGF (+),  $n=14$  cells; FAP-DOR TC10 T31N NGF (-),  $n=17$  cells; FAP-DOR TC10 T31N NGF (+),  $n=17$  cells; mean  $\pm$  s.e.m.; \*\*\*\* $P<0.0001$ ; by two-sided paired t-test vs. FAP-DOR TC10 WT NGF (+)).

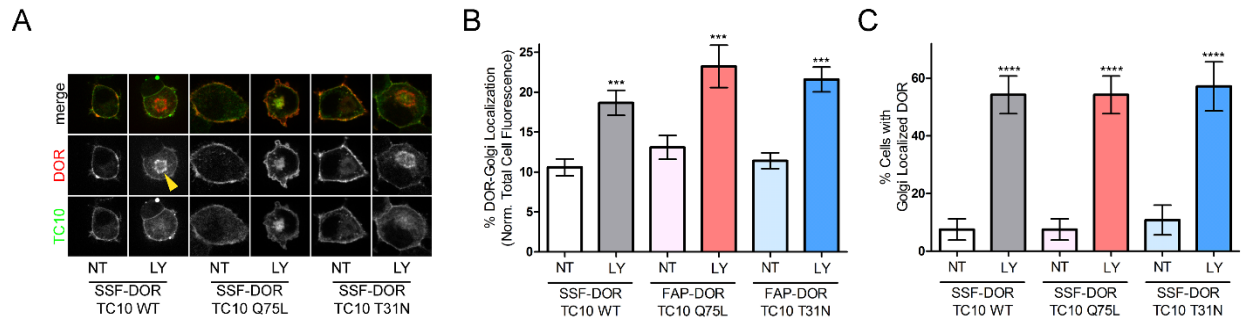


**Figure 5: The dominant-active TC10 Q75L is sufficient for DOR surface trafficking in the presence of PI3K inhibition. A.** Example fixed-cell confocal fluorescence images for PC12 cells expressing a signal sequence FLAG-tagged (SSF) SSF-DOR (Red) + GFP-TC10 WT (Green), FLAG-DOR + GFP-TC10 Q75L (dominant active mutant), and FLAG-DOR + GFP-TC10 T31N (dominant negative mutant) either untreated (NT) or treated for 1 hour with with LY294002 (LY, 10 $\mu$ M). LY-induced intracellular retention of SSF-DOR (yellow arrow) is observed when coexpressed with GFP-TC10 WT, Q75L, and T31N. **B.** Quantification of the percentage of DOR retained in the Golgi normalized to the total DOR fluorescence reveal a significant increase in DOR-Golgi localization following PI3K inhibition for all TC10 variants (SSF-DOR + TC10 WT NT,  $n=53$  cells; SSF-DOR + TC10 WT LY,  $n=59$  cells; SSF-DOR + TC10 Q75L NT,  $n=37$  cells; SSF-DOR + TC10 Q75L LY,  $n=36$  cells; SSF-DOR + TC10 T31N NT,  $n=60$  cells; SSF-DOR + TC10 T31N LY,  $n=60$  cells; mean  $\pm$  s.e.m.; no significance; by two-sided unpaired t-test vs. SSF-DOR LY). **C.** Quantification of the percentage of cells with Golgi-localized DOR fluorescence demonstrates an increase following LY treatment for SSF-DOR when coexpressed with GFP-TC10 WT, Q75L, and T31N. There was no significant change in the percent of cells with Golgi-localized DOR observed for all TC10 variants (SSF-DOR + TC10 WT NT,  $n=53$  cells; SSF-DOR + TC10 WT LY,  $n=59$  cells; SSF-DOR + TC10 Q75L NT,  $n=37$  cells; SSF-DOR + TC10 Q75L LY,  $n=36$  cells; SSF-DOR + TC10 T31N NT,  $n=60$  cells; SSF-DOR + TC10 T31N LY,  $n=60$  cells; mean  $\pm$  s.e.m.; no significance; by two-sided unpaired t-test vs. SSF-DOR LY).

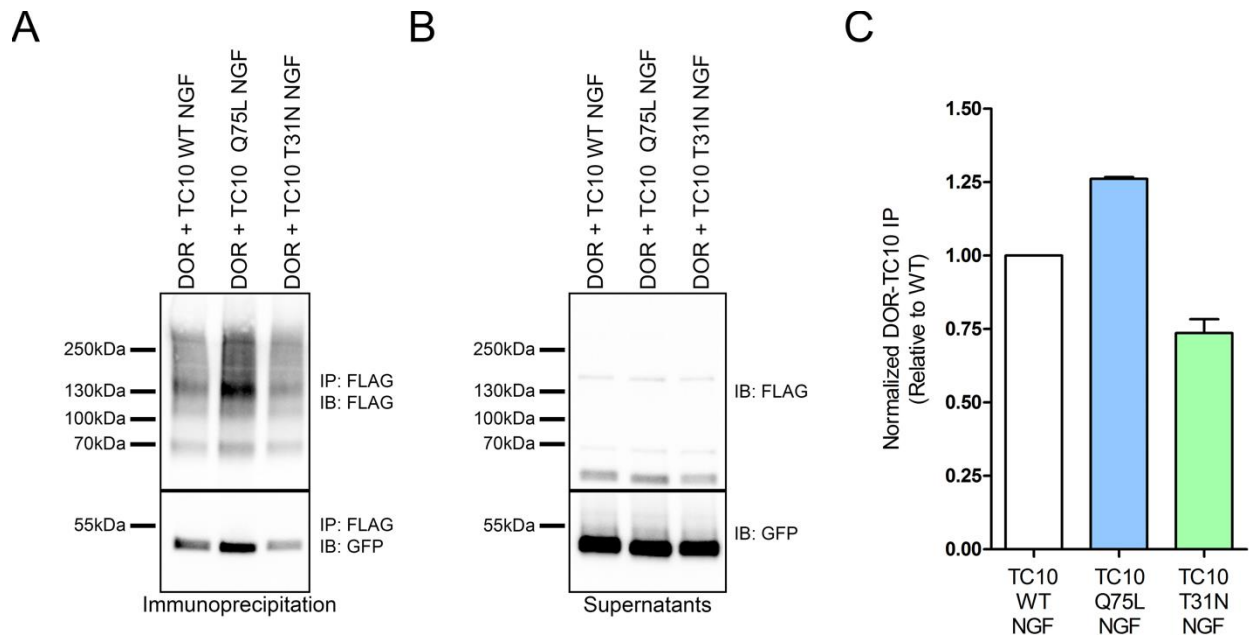


**Figure S1: Dominant-active TC10 Q75L strongly co-immunoprecipitates with DOR, while the dominant-negative TC10 T31N shows decreased co-immunoprecipitation.** **A.** PC12 cells expressing FLAG-DOR, or FLAG-DOR and GFP-TC10 WT, GFP-TC10 Q75L, or GFP-TC10 T31N were treated with NGF (100ng/mL) for 1 hour. FLAG-DOR was immunoprecipitated (IP) and immunoblots (IB) were performed to detect the FLAG-DOR and GFP-TC10. FLAG-DOR was expressed and detectable in each treatment group of the immunoprecipitation samples to similar levels (IP: FLAG, IB: FLAG) as a smear between 200 and 70 kDa. The immunoblot for GFP-TC10 (IP: FLAG, IB: GFP) revealed an increased co-immunoprecipitation of TC10 Q75L with DOR following NGF (DOR + TC10 Q75L NGF), and a decreased co-immunoprecipitation of TC10 T31N with DOR following NGF (DOR + TC10 T31N NGF) compared to TC10 WT expressing cells (DOR + TC10 WT NGF). **B.** Examination of the supernatant controls reveal depletion of FLAG-DOR from the supernatant (IB: FLAG), and relative expression levels of the GFP-TC10 (IB: GFP) for each condition. **C.** Quantification via densitometry was performed to determine the change in co-immunoprecipitation of TC10 with dominant active and dominant negative mutations. Following normalization to FLAG-DOR and GFP-TC10 expression for each condition, a normalized DOR-TC10 Co-IP ratio revealed an increase in TC10 Co-IP with DOR when expressed with the dominant active Q75L mutant, and a decrease in TC10 Co-IP with DOR when expressed with the dominant negative T31N mutant (TC10 WT NGF,  $n=2$ ; TC10 Q75L NGF,  $n=2$ ; TC10 T31N NGF,  $n=2$ ; mean  $\pm$  s.e.m.).

## References:

1. Shiwerski, D. J., Tipton, A., Schmidt, B. A., Giraldo, M. D., Gold, M. S., Pradhan, A. A., and Puthenveedu, M. A. A phosphoinositide-regulated Golgi checkpoint regulates the bioavailability of delta opioid receptors. *Nat. Med.*
2. Shiwerski, D. J., Darr, M., and Puthenveedu, M. A. Optogenetic Recruitment of PI3K C2 $\alpha$  to the trans-Golgi Network is Sufficient to Promote Surface Trafficking of the  $\delta$ -Opioid Receptor
3. Falasca, M., Hughes, W. E., Dominguez, V., Sala, G., Fostira, F., Fang, M. Q., Cazzolli, R., Shepherd, P. R., James, D. E., and Maffucci, T. (2007) The role of phosphoinositide 3-kinase C2 $\alpha$  in insulin signaling. *J. Biol. Chem.* **282**, 28226–28236
4. Neudauer, C. L., Joberty, G., Tatsis, N., and Macara, I. G. (1998) Distinct cellular effects and interactions of the Rho-family GTPase TC10. *Current Biology.* **8**, 1151–1160
5. Radha, V., Mitra, A., Dayma, K., and Sasikumar, K. (2011) Signalling to actin: role of C3G, a multitasking guanine-nucleotide-exchange factor. *Biosci. Rep.* **31**, 231–244
6. Mayer, S., Kumar, R., Jaiswal, M., Soykan, T., Ahmadian, M. R., Brose, N., Betz, H., Rhee, J.-S., and Papadopoulos, T. (2013) Collybistin activation by GTP-TC10 enhances postsynaptic gephyrin clustering and hippocampal GABAergic neurotransmission. *Proc. Natl. Acad. Sci. U.S.A.* **110**, 20795–20800
7. Bridges, D., Chang, L., Lodhi, I. J., Clark, N. A., and Saltiel, A. R. (2012) TC10 is regulated by caveolin in 3T3-L1 adipocytes. *PLoS ONE.* **7**, e42451
8. Fujita, A., Koinuma, S., Yasuda, S., Nagai, H., Kamiguchi, H., Wada, N., and Nakamura, T. (2013) GTP hydrolysis of TC10 promotes neurite outgrowth through exocytic fusion of Rab11- and L1-containing vesicles by releasing exocyst component Exo70. *PLoS ONE.* **8**, e79689
9. Gracias, N. G., Shirkey-Son, N. J., and Hengst, U. (2014) Local translation of TC10 is required for membrane expansion during axon outgrowth. *Nature Communications.* **5**, 3506
10. Chiang, S. H., Baumann, C. A., Kanzaki, M., Thurmond, D. C., Watson, R. T., Neudauer, C. L., Macara, I. G., Pessin, J. E., and Saltiel, A. R. (2001) Insulin-stimulated GLUT4 translocation requires the CAP-dependent activation of TC10. *Nature.* **410**, 944–948
11. Chang, L., Adams, R. D., and Saltiel, A. R. (2002) The TC10-interacting protein CIP4/2 is required for insulin-stimulated Glut4 translocation in 3T3L1 adipocytes. *Proceedings of the National Academy of Sciences.* **99**, 12835–12840
12. Maffucci, T., Brancaccio, A., Piccolo, E., Stein, R. C., and Falasca, M. (2003) Insulin induces phosphatidylinositol-3-phosphate formation through TC10 activation. *EMBO J.* **22**, 4178–4189
13. Leto, D., and Saltiel, A. R. (2012) Regulation of glucose transport by insulin: traffic control of GLUT4. *Nat Rev Mol Cell Biol.* **13**, 383–396
14. Murphy, G. A., Solski, P. A., Jillian, S. A., Pérez de la Ossa, P., D'Eustachio, P., Der, C. J., and Rush, M. G. (1999) Cellular functions of TC10, a Rho family GTPase: regulation of morphology, signal transduction and cell growth. *Oncogene.* **18**, 3831–3845
15. Shiwerski, D. J., and Puthenveedu, M. A. **NGF-induced Golgi Retention of DOR Requires Dual RXR Retention/Retrieval Motifs**
16. Kawase, K., Nakamura, T., Takaya, A., Aoki, K., Namikawa, K., Kiyama, H., Inagaki, S., Takemoto, H., Saltiel, A. R., and Matsuda, M. (2006) GTP hydrolysis by the Rho family GTPase TC10 promotes exocytic vesicle fusion. *Developmental Cell.* **11**, 411–421
17. Chiang, S.-H., Hwang, J., Legendre, M., Zhang, M., Kimura, A., and Saltiel, A. R. (2003) TCGAP, a multidomain Rho GTPase-activating protein involved in insulin-stimulated glucose transport. *EMBO J.* **22**, 2679–2691
18. Neudauer, C. L., Joberty, G., and Macara, I. G. (2001) PIST: a novel PDZ/coiled-coil

- domain binding partner for the rho-family GTPase TC10. *Biochem Biophys Res Commun.* **280**, 541–547
19. Bergbrede, T., Chuky, N., Schoebel, S., Blankenfeldt, W., Geyer, M., Fuchs, E., Goody, R. S., Barr, F., and Alexandrov, K. (2009) Biophysical analysis of the interaction of Rab6a GTPase with its effector domains. *J. Biol. Chem.* **284**, 2628–2635
  20. Wente, W., Efanov, A. M., Treinies, I., Zitzer, H., Gromada, J., Richter, D., and Kreienkamp, H.-J. (2005) The PDZ/coiled-coil domain containing protein PIST modulates insulin secretion in MIN6 insulinoma cells by interacting with somatostatin receptor subtype 5. *FEBS Lett.* **579**, 6305–6310
  21. Bauch, C., Koliwer, J., Buck, F., Hönck, H.-H., and Kreienkamp, H.-J. (2014) Subcellular sorting of the G-protein coupled mouse somatostatin receptor 5 by a network of PDZ-domain containing proteins. *PLoS ONE.* **9**, e88529
  22. Koliwer, J., Park, M., Bauch, C., Zastrow, von, M., and Kreienkamp, H.-J. (2015) The golgi-associated PDZ domain protein PIST/GOPC stabilizes the  $\beta$ 1-adrenergic receptor in intracellular compartments after internalization. *Journal of Biological Chemistry.* **290**, 6120–6129
  23. Roberts, P. J., Mitin, N., Keller, P. J., Chenette, E. J., Madigan, J. P., Currin, R. O., Cox, A. D., Wilson, O., Kirschmeier, P., and Der, C. J. (2008) Rho Family GTPase modification and dependence on CAAX motif-signaled posttranslational modification. *J. Biol. Chem.* **283**, 25150–25163
  24. Szent-Gyorgyi, C., Schmidt, B. F., Schmidt, B. A., Creeger, Y., Fisher, G. W., Zakel, K. L., Adler, S., Fitzpatrick, J. A. J., Woolford, C. A., Yan, Q., Vasilev, K. V., Berget, P. B., Bruchez, M. P., Jarvik, J. W., and Waggoner, A. (2008) Fluorogen-activating single-chain antibodies for imaging cell surface proteins. *Nat. Biotechnol.* **26**, 235–240
  25. Pratt, C. P., He, J., Wang, Y., Barth, A. L., and Bruchez, M. P. (2015) Fluorogenic Green-Inside Red-Outside (GIRO) Labeling Approach Reveals Adenylyl Cyclase-Dependent Control of BK $\alpha$  Surface Expression. *Bioconjug. Chem.* **26**, 1963–1971

## Chapter 6: Conclusions and Future Directions

### Summary:

Collectively, this thesis elucidates the mechanism controlling the regulated surface delivery of DOR in sensory neurons. Specifically, Chapter 2 studies the mechanism controlling surface trafficking of DOR, and shows that a phosphoinositide-regulated Golgi checkpoint regulates the bioavailability of  $\delta$ -opioid receptors. Chapter 3 elaborates on the phosphoinositide-regulated Golgi checkpoint controlling DOR trafficking, and demonstrates that optogenetic recruitment of PI3K C2 $\alpha$  to the *trans*-Golgi network is sufficient to promote surface trafficking of the  $\delta$ -opioid receptor. Chapter 4 explores the amino acid sequence required for Golgi retention of DOR, and reveals that NGF-induced Golgi retention of  $\delta$ -Opioid receptors requires dual RXR retention/retrieval motifs. Chapter 5 investigates the role of the Rho-associated GTPase TC10 in DOR surface trafficking, and shows that TC10 GTP is sufficient overcome the NGF-induced retention of the  $\delta$ -Opioid receptor. Together, these data reveal a novel process for the regulated delivery of Opioid receptors to the cell surface, and establish a proof of principle for the induction of DOR trafficking to the cell surface to provide analgesic relief in the setting of chronic pain.

### **A phosphoinositide-regulated Golgi checkpoint regulates the bioavailability of $\delta$ -opioid receptors**

In Chapter 2, we provide a specific method to increase surface delivery of DOR independent of upregulating DOR synthesis. Because DOR is predominantly degraded after agonist-mediated endocytosis, delivery of newly synthesized DOR is critical for determining the sensitivity of neurons to opioids. Regulation of GPCR export from the Golgi by extracellular signals, as with the NGF-PI3K signaling axis identified here, could act as a mechanism to provide control over receptor delivery and therefore resensitization, akin to the regulation of post-endocytic sorting seen with recycling receptors. By engineering the surface delivery of DOR via PTEN inhibition, we can increase DOR surface trafficking in physiologically relevant neurons and improve the antinociceptive potency of the DOR agonist, SNC80. This provides a critical proof of concept on which to base further strategies to improve the bioavailability of DOR and increase the potency of the many DOR agonists already developed. With emerging data on the importance of the location of signal origin in downstream effects of GPCR signaling, such engineered relocation of receptors as we show here may provide a general blueprint to precisely manipulate the localization of other GPCRs.

In future studies, it will be interesting to evaluate the effects of PTEN induced DOR surface delivery for additional DOR agonists in mouse models of hyperalgesia. Additionally, we would like to determine the role of peripheral vs. central pain circuitry inhibition, and whether a peripherally restricted DOR agonist can provide analgesic benefits when combined with PTEN inhibition pretreatment. We would also like to evaluate receptor desensitization in this model of PTEN inhibition induced DOR trafficking, and perform an in-depth *in vivo* study to rule out adverse side effects of opiate administration such as addiction, dependence, and convulsions.

### **Optogenetic recruitment of PI3K C2 $\alpha$ to the *trans*-Golgi network is sufficient to promote surface trafficking of the $\delta$ -opioid receptor**

In Chapter 3, we have directly demonstrated that PI3K C2A is both required and sufficient for complete trafficking of DOR to the cell surface in PC12 cells. Class I PI3K inhibition is not sufficient to cause retention of DOR in the Golgi, and micromolar concentrations of the pan PI3K inhibitors Wortmannin and LY294002, sufficient to inhibit Class II PI3Ks, are necessary for DOR Golgi retention. Suggesting that trafficking of DOR is dependent on Class II, but not Class I PI3Ks. Finally, optorecruitment of the PI3K C2A kinase domain is sufficient to release the NGF-induced Golgi retention of DOR and stimulate exocytosis from the TGN to the cell surface. These results present the first evidence for PI3K C2A activity mediating a Golgi specific checkpoint controlled by a neuronal-specific signaling axis to induce delivery of a GPCR to the surface.

In the future, investigations into the sequence specific requirements for entry into this PI3K C2A dependent export pathway could reveal a receptor selective alternative trafficking route to the more traditional PI4P constitutive export pathway. Specifically, we would like to look at the role of actin and microtubules in PI3K C2A dependent export of DOR, as well as the requirement of coat proteins and adapter complexes such as AP1, AP2, Clathrin, GGA1, etc. A more detailed mechanistic understanding of the export pathway downstream of PI3K C2A will allow us to define the Golgi-regulated export controlling the surface delivery of receptors such as DOR.

### **NGF-induced Golgi retention of $\delta$ -Opioid receptors requires dual RXR retention/retrieval motifs**

In Chapter 4, we identified that the  $\delta$ -Opioid receptor is retained within the Golgi following NGF treatment or PI3K inhibition through a dual RXR motif dependent mechanism. The dual RXR motifs are required for the NGF-induced retention of DOR, and phosphorylation or cysteine modification within the last 27 amino acids of the C-terminal tail have minimal regulatory consequences for retention. These results describe for the first time a Golgi-retention/retrieval

mechanism that requires two RXR motifs that is masked at baseline, but can be triggered through growth factor signaling or PI3K inhibition. The regulation provided by this mechanism is exciting because it allows for a cell type specific “on demand” delivery of fully folded, modified, and functional receptors to the surface in response to receptor-mediated signaling events. Physiologically, a system such as this is perfectly suited for a single-use, non-recycling, receptor such as DOR. By modulating the masking or unmasking of the RXR motif, an available pool of ready-to-use receptors can be held within the cell and released on demand when the appropriate signal is present. Finally, by pharmacologically masking the RXR motifs of DOR, it might be possible to drive fully functional receptors to the cell surface in a receptor specific manner.

In future studies, it will be interesting identify the RXR motif masking partner(s) for DOR, and to look for C-terminal RXR motifs within other GPCRs with known intracellular retention phenotypes. We have identified several receptors that contain RXR motifs, and are known to exist in intracellular pools; however, the role of NGF in maintaining their retention, and the requirement of their RXR motifs are unknown. For GPCRs that contain RXR motifs, but are not basally retained, one possibility is that G-protein coupling to the receptor could mask the RXR motif. In the absence of G-protein coupling, the RXR motifs would be exposed, allowing for retention/retrieval from the biosynthetic pathway. When G-protein coupling occurs, the motif would then be masked, allowing for export and trafficking of the fully functional GPCR-G-Protein complex to the cell surface. This is an intriguing idea because it allows for multiple points of regulation throughout the trafficking process. Alternatively, proteins such as  $\beta$ -arrestins might similarly associate with the receptor to mask the RXR motifs by binding to the GPCR upon exocytosis in a manner similar to agonist-induced internalization. For these reasons, evaluating the role of both G-proteins and  $\beta$ -arrestins in the masking of these RXR motifs will be of extreme importance. Additionally, we would like to identify the requirement and sufficiency of the RXR motif flanking amino acids that confer Golgi retention/retrieval as opposed to ER or ERGIC retention/retrieval. This could then allow for a better prediction of receptor localization from the primary amino sequence, and help to broaden our understanding of this regulatory mechanism.

### **TC10 GTP is sufficient to prevent the NGF-induced retention of the $\delta$ -Opioid receptor**

In Chapter 5, we revealed a novel requirement for TC10 GTP activity in the Golgi checkpoint of DOR. Following NGF treatment in PC12 cells, TC10 distribution shifts to a perinuclear region overlapping with the Golgi that resembles the localization pattern for the inactive TC10 T31N mutant. Additionally, we show the first evidence of TC10 binding directly to a GPCR, and stimulation of this interaction following PTEN inhibition induced surface trafficking

of DOR. We propose that TC10 GTP is acting to facilitate the TGN export of DOR by promoting the recruitment and activation of PI3K C2A to coordinate association of downstream trafficking components.

In future work, we hope to investigate the role of TC10 in TGN export of other GPCRs and receptors, as well as identify the regulatory machinery controlling TC10 localization and activity at the Golgi. One possible way NGF might directly regulate TC10 activity is through recruitment of the TC10 GEF, C3G. We plan to look at C3G localization following NGF treatment, and assess TC10 activity in the presence and absence of NGF with a TC10 FRET biosensor. Additionally, we have reason to believe that the SSTR5,  $\beta$ 1AR, and Glut4 might be retained similarly to DOR following NGF treatment. Similar experiments as performed here, will be done to evaluate the role of TC10 in their regulated trafficking to the surface. It will be interesting to determine to role of the RXR motifs in coordinating the interaction between DOR and TC10. Preliminary data suggest that the RXR motifs are not required for the DOR-TC10 interaction, but that the last 27 amino acids of DOR are required for ER export and TC10 binding. Additionally, preliminary co-immunoprecipitation experiments with purified TC10 and a chimeric construct containing GST linked to the last 27 amino acids of DOR appear to reveal a direct binding between the two. Further studies will need to be performed to determine the direct binding of TC10 to the last 27 amino acids of DOR, and the sequence requirement of the binding interaction. Finally, we plan to evaluate how DOR is retrieved from the TGN following the NGF-induced retention, and the role TC10 plays in modulating interactions with proteins such as PIST to mediate this retrieval.

### **Conclusion:**

The pathway identified here provides an outline for a quality control mechanism that might regulate single-use receptor trafficking to the cell surface. In general, this pathway is modulated by extracellular signaling molecules such as NGF, and is dependent upon TC10-PI3K C2A activity and the masking of dual RXR retention/retrieval motifs. Our current model suggests that downstream of NGF-TrkA signaling, TC10 and PI3K C2A activity control a Golgi pool of phosphoinositides. Altering the phospholipid composition of the TGN might regulate the masking and unmasking of dual RXR retention/retrieval motifs on DOR to drive surface trafficking or Golgi retention. The potential implications of such a mechanism extending beyond DOR is intriguing, and might reveal a novel neuronal specific or growth factor controlled export pathway out of the TGN that was previously undescribed. One hypothesis is that this regulated trafficking during receptor biogenesis is utilized as a way to test-drive receptor function before transport to the cell surface. One could imagine that for a GPCR, a specific type of G-protein binding such as  $G_q$ -coupling, that could only bind properly folded receptors, may be required to mask retrieval signals

and initiate ER export. Furthermore, during transport and maturation through the Golgi, alternate G-protein coupling such as  $G_i$ -coupling may be required for export. Once the fully functional, and post-translationally modified GPCR-G-protein complex is formed, it could then exit the Golgi and traffic to the surface. Pharmacological intervention into such a pathway could have huge implications across many clinical disciplines. By creating cell permeable peptides to mask the retrieval motifs of retained receptors, we could create a receptor specific mechanism for on-demand release of unresponsive receptors.

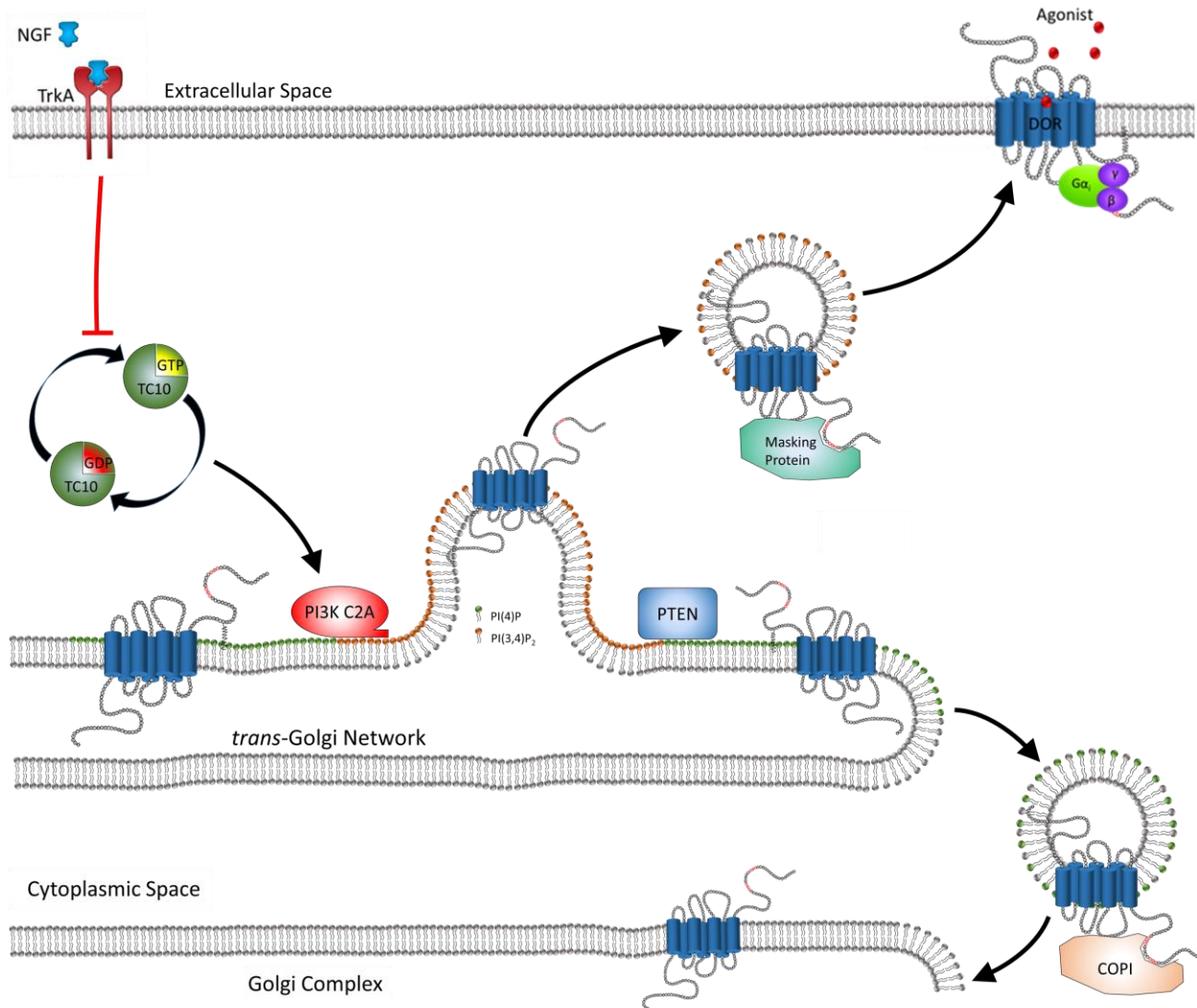


**Figure 1: Working Model of NGF-induced Golgi Retention of DOR.** This cartoon is a graphical representation of the conclusions drawn from this thesis. NGF treatment alters the localization of TC10, resembling the inactive TC10 GDP. TC10 GTP is sufficient to block NGF-induced retention of DOR. TC10 GTP has been shown to stimulate the kinase activity of PI3K C2A, and could activate PI3K C2A at the TGN in our model. PI3K C2A can phosphorylate PI(4)P to make PI(3,4)P<sub>2</sub>. PTEN can work in opposition to PI3K C2A to remove the 3' phosphate of PI(3,4)P<sub>2</sub> to convert it to PI(4)P. At this point, PI(3,4)P<sub>2</sub> might be sufficient to recruit an RXR masking protein, along with the required trafficking components for export to the surface. If this process is inhibited, such as in the case of NGF treatment, the masking protein would not be recruited allowing COPI to bind to the RXR motif to facilitate retrieval of DOR back to an earlier Golgi compartment.

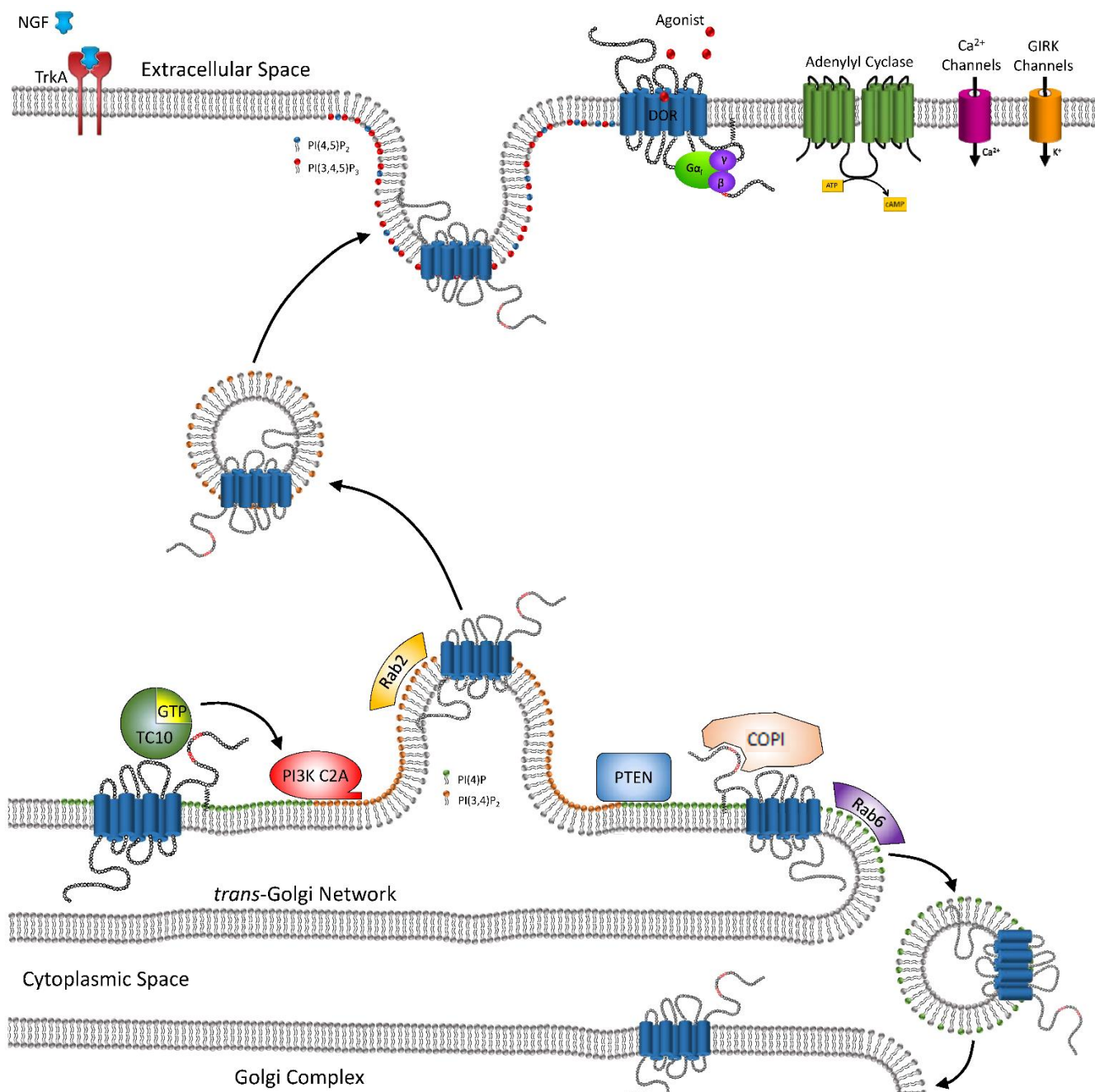


**Figure 2: Proteins implicated in regulated delivery of DOR to the cell surface.** This cartoon is a graphical representation of the potential proteins involved in DOR trafficking to the cell surface and regulated Golgi retention. Additionally, preliminary work from our lab, not shown in this thesis, suggests that Rab2 activity contributes to TGN export of DOR, and that Rab6 activity might promote TGN retention/retrieval.